

**PHYSICALLY BASED MODELING OF WATER INFILTRATION WITH
SOIL PARTICLE PHASE**

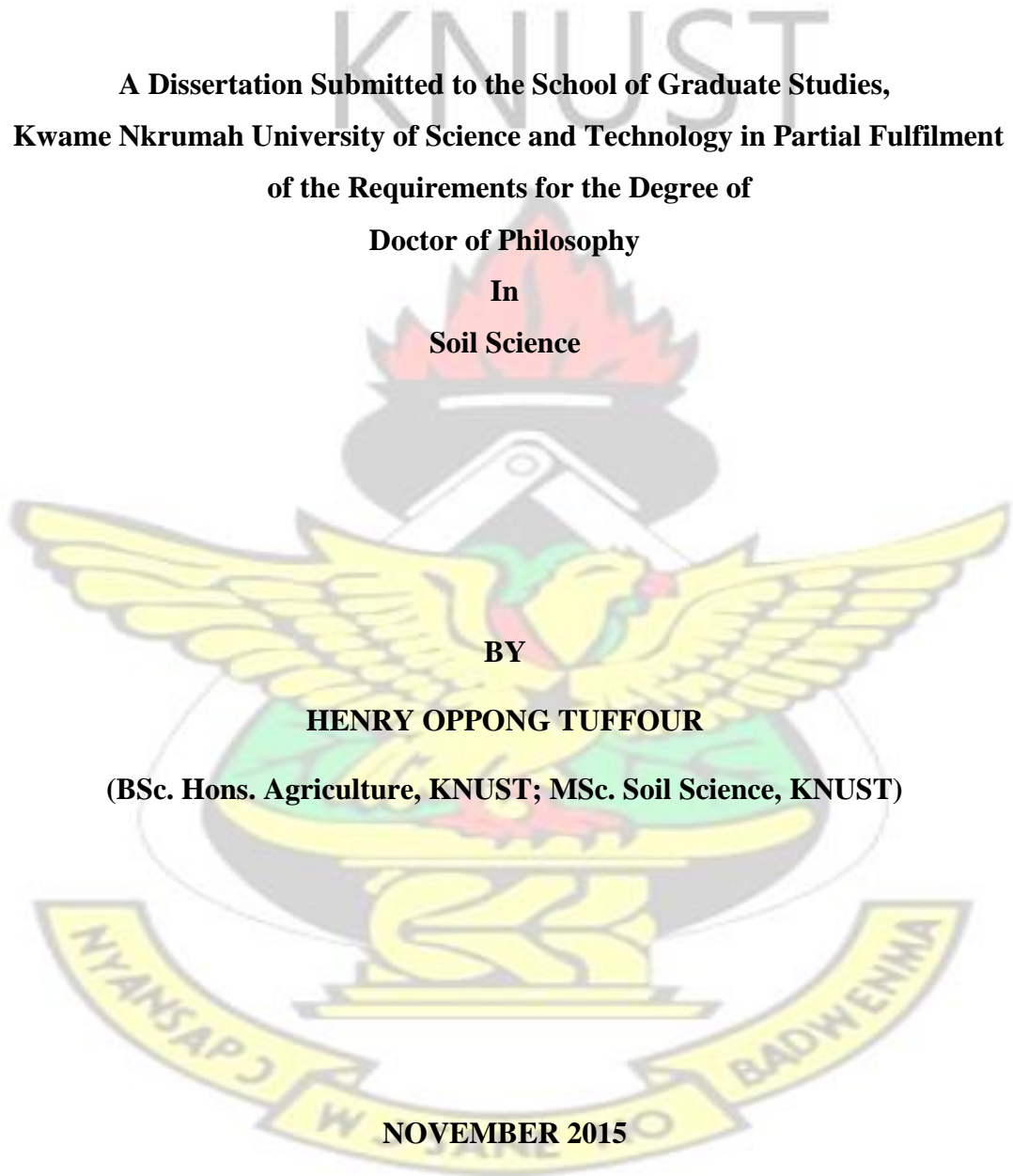
**A Dissertation Submitted to the School of Graduate Studies,
Kwame Nkrumah University of Science and Technology in Partial Fulfilment
of the Requirements for the Degree of
Doctor of Philosophy
In
Soil Science**

BY

HENRY OPPONG TUFFOUR

(BSc. Hons. Agriculture, KNUST; MSc. Soil Science, KNUST)

NOVEMBER 2015



DECLARATION

I certify that this thesis titled, **PHYSICALLY BASED MODELLING OF WATER INFILTRATION WITH SOIL PARTICLE PHASE** does not incorporate, without acknowledgement, any material previously submitted for a degree or diploma in any University. Moreover, to the best of my knowledge and belief, it does not contain any material previously published or written by another person, except where due reference has been made in the text.

.....
HENRY OPPONG TUFFOUR
PG8320512

(Ph.D. CANDIDATE)

.....
DATE

APPROVED BY:

.....
REV. FR. (PROF.) MENSAH BONSU
(PRINCIPAL SUPERVISOR, KNUST)

.....
DATE

.....
PROF. CHARLES QUANSAH
SUPERVISOR, KNUST)

.....
DATE (CO-

.....
DR. ENOCH A. OSEKERE
(HEAD OF DEPARTMENT)

.....
DATE

DEDICATION

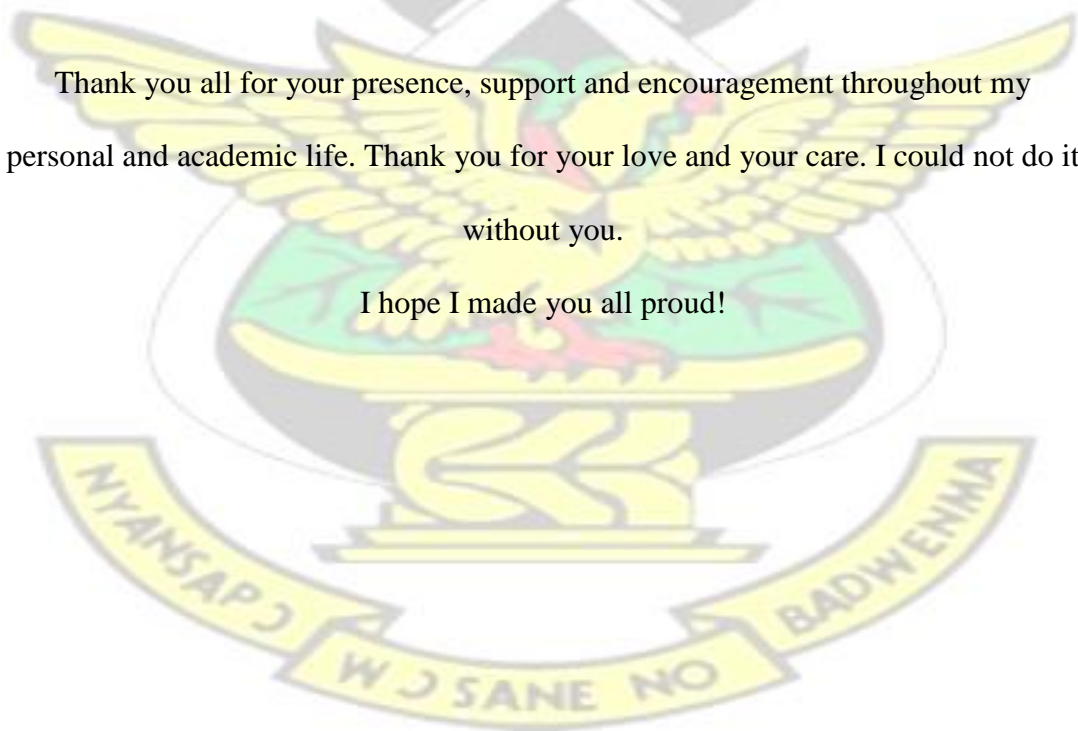
*“All that I am or hope to be, I owe to my Mom and Dad, Who have always Believed in,
Supported and Encouraged me to Knowledge”!*

This work is dedicated to:

- My parents with Love and Gratitude
 - Christiana with Love
- Mary, Livingstone and Jimmy with Appreciation
- Nana Ama Amponsah II and Okatakyie Antwi Agyemang-Tuffour III with Joy
- The Late B.N. Opong Danquah

Thank you all for your presence, support and encouragement throughout my personal and academic life. Thank you for your love and your care. I could not do it without you.

I hope I made you all proud!



ACKNOWLEDGEMENTS

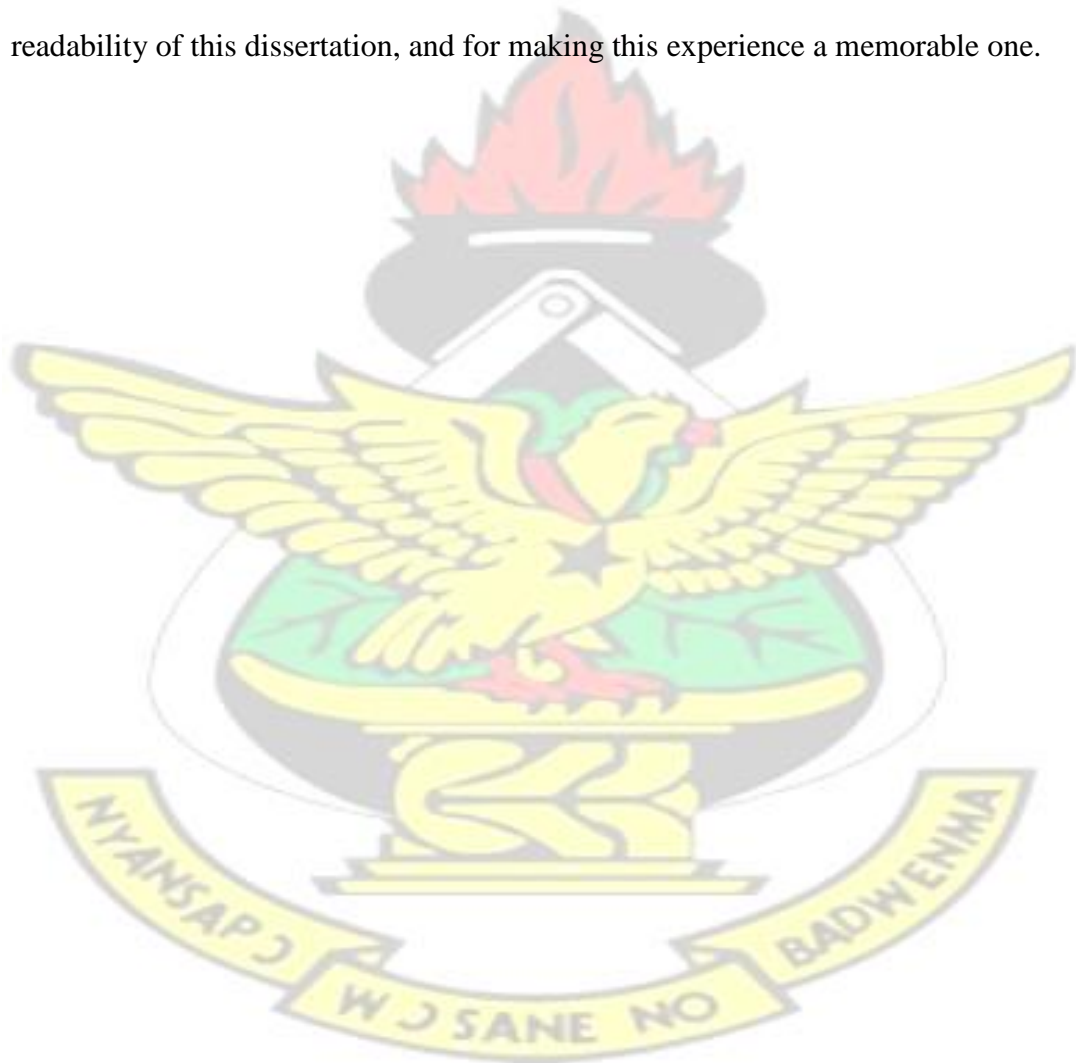
"If I have seen far, it is because I have stood on the shoulders of giants or because I try to work harder". There are two ways of exerting one's strength – pushing down and pulling up. I have had the opportunity of enjoying the latter from countless individuals. Believing in this, it does not matter how far my eyes go, I know that you have been around in your millions, stood firm, supported and encouraged me to this great academic achievement. Although anything I write here is inadequate to express my gratitude, for the most part, I would like to thank my supervisors, Rev. Fr Prof. Mensah Bonsu and Prof. Charles Quansah for their great and sound remarks, and criticisms in making this work possible. I could not complete this research without their greatly appreciated commitment to academic excellence, genuine support, guidance, expertise and patience.

Again, I want to take the opportunity to thank Professors William Oduro, Richard Akromah, Gary W. Parkin, Pieter Groenevelt, Paul Voronin and Dave Elrick (late), and Dr Naresh Thevathasan, for their kind gesture and opportunity they offered me to study at the Ontario College of Agriculture, University of Guelph, Canada.

I am also thankful to have met Messrs Nicholas Osafo Aboagye, Samuel Effah Aboagye and Isaac Kyere Aboagye, and Madam Agnes Abena Akyaa, Madam Cecilia Asiedua and Ms. Dorothea Ama Aboagye, and Mrs Beatrice Mensah Bonsu, whose timely physical and spiritual intercession provided a crucial breakthrough in the development of this work. Many thanks also to Dr Osei Frimpong and Mr Benedict Barnes of the Mathematics Department, KNUST and Mr K.D. Dwomoh of the Department of Biostatistics, University of Ghana, Legon. I would also like to say

a very big thank you to Dr J. Sarkodie-Addo, Dr V. Logah, Dr B.K. Amegashie, Mr T. Adjei-Gyapong, Mr George Nortey and Mr Samuel Joe Acquah.

Many thanks also to my colleagues and friends: Twumasi-Ankrah, Osei-Bonsu, Joseph, Awudu, Paul, Affum, George, Mark, , Caleb, Jake, Aziz, Israel, Murphy, David, Benette, Kyere, Mac Tonto and the company of Tonto Ventures, whose pragmatic suggestions and improvements contributed to the consistency and readability of this dissertation, and for making this experience a memorable one.



ABSTRACT

One of the most important problems of hydrological forecasting in agriculture is to obtain a reliable estimate of effective irrigation. Infiltration is one of the variables which greatly influences the partitioning of irrigation water (especially rainfall) into surface runoff and subsurface flow and continues to occupy the attention of soil physicists and agricultural engineers. It is regarded as a very complex process with several contributing factors. Most infiltration models have been developed for clear water and have limited application to poorly structured soils due to slaking of aggregates and dispersion of clay. In order to address this limitation, an infiltration model was developed to describe the process of infiltration of muddy water into a uniform soil profile based on the Green-Ampt (G-A) flow theory. In addition, it incorporated the concept of surface sealing and allowed for a developing seal with time. The cumulative infiltration amount was found to be related to a constant which is a function of the particle diameter of the sediment, and describes the saturated hydraulic conductivity of seal. Thus, a modified G-A method for infiltration with transient seal formation is proposed that provides improved infiltration, surface sealing, and time-to-incipient ponding predictions during infiltration of muddy water. A laboratory column experiment was conducted to measure the cumulative infiltration amount of clear water (0 g) and soil suspensions made from 10, 20, 30 and 40 g fine sand (= 0.05 mm), silt (= 0.002 mm), and clay (= 0.001 mm) after 60 minutes. The set of the laboratory-measured data were used to evaluate the performance of the infiltration model in simulating cumulative infiltration amount. The model provided good overall agreement with the laboratory-measured data. The result of the study showed that the cumulative infiltration amounts predicted by the infiltration model were very close to the laboratory measurements for the different

fluids and their various concentrations as evidenced by average values of the slope of the regression line between the measured and predicted data, coefficient of determination and root mean square error. The coefficient of determination R^2 ranged from 0.9986 to 0.9998 with RMSE ranging from 0.00814 to 0.0793. The accuracy of the model's prediction capability was in the order of 0 g > 10 g > 20 g > 30 g > 40 g for sand suspension, and 0 g > 10 g > 20 g > 40 g > 30 g for silt and clay suspensions. Overall, the predictability of the model was ranked using the R^2 values in the order: Clear water > Sand suspension > Silt suspension > Clay suspension. The method also provides a good approximation of surface seal thickness, since direct determination of the seal thickness is difficult. Thus, a simple linear equation is proposed for the estimation of seal thickness based on the concentration and settling velocity of the sediment particle. Sand sediments produced thicker seals, even at relatively lower concentrations. Silt and clay sediments produced very thin seals, and their thicknesses showed no significant variations ($P < 0.05$) statistically at equal concentrations and time intervals. Additionally, the major factors responsible for the formation of the surface seals were identified as the size, concentration and settling velocity of the sediment, and the flow velocity of the fluid. The results of the study on saturated hydraulic conductivity were used to predict the relative time-to-incipient ponding of the various sediment surface seals. It was deduced that clear water would take the longest time and clay suspension the shortest time to cause surface ponding. The study showed that the Modified Green and Ampt Surface Sealing (MGASS) infiltration model can be effectively used to predict infiltration under variable moisture conditions and quantitatively analyse the effect of soil texture on surface

sealing and the seal properties, as well as assessing the effect of sediment concentration on infiltration and surface sealing phenomena.

KNUST



PUBLICATIONS FROM THE THESIS

1. Tuffour, H.O. and Bonsu, M. (2015): Applications of Green-Ampt equation to infiltration with soil particle phase. *International Journal of Scientific Research in Agricultural Sciences*, 2(4): 76-88.
2. Tuffour, H.O., Bonsu, M., Quansah, C. and Abubakari, A. (2015): A physicallybased model for estimation of surface seal thickness. *International Journal of Extensive Research*, 4: 60-64.
3. Tuffour, H.O. and Abubakari, A. (2015): Effects of water quality on infiltration rate and surface ponding/runoff. *Applied Research Journal*, 1(3): 108-117.
4. Tuffour, H.O., Adjei-Gyapong, T., Abubakari, A., Melenya, C., Aryee, D. and Khalid A.A. (2015): Assessment of changes in soil hydro-physical properties resulting from infiltration of muddy water. *Applied Research Journal*, 1(3): 137-140.

TABLE OF CONTENTS

DECLARATION	i
DEDICATION	ii
ACKNOWLEDGEMENTS	iii
ABSTRACT	v
PUBLICATIONS FROM THE THESIS	vii
LIST OF FIGURES	xiii
LIST OF ABBREVIATIONS	xviii
LIST OF SYMBOLS	xix
CHAPTER ONE	1
1.0 INTRODUCTION	1
1.1 Objectives	4
1.2 Hypothesis	5
CHAPTER TWO	6
2.0 LITERATURE REVIEW	6
2.1 The process of water movement in soil	6
2.2 Infiltration and its importance	7
2.3 Factors that control infiltration rate	8
2.4 Causes of low infiltration rate	13
2.4.1 Soil compaction	17
2.4.2 Surface sealing and crusting	18
2.5 Principles of water flow	21
2.6 Infiltration modelling	25
2.6.1 Infiltration Models	29

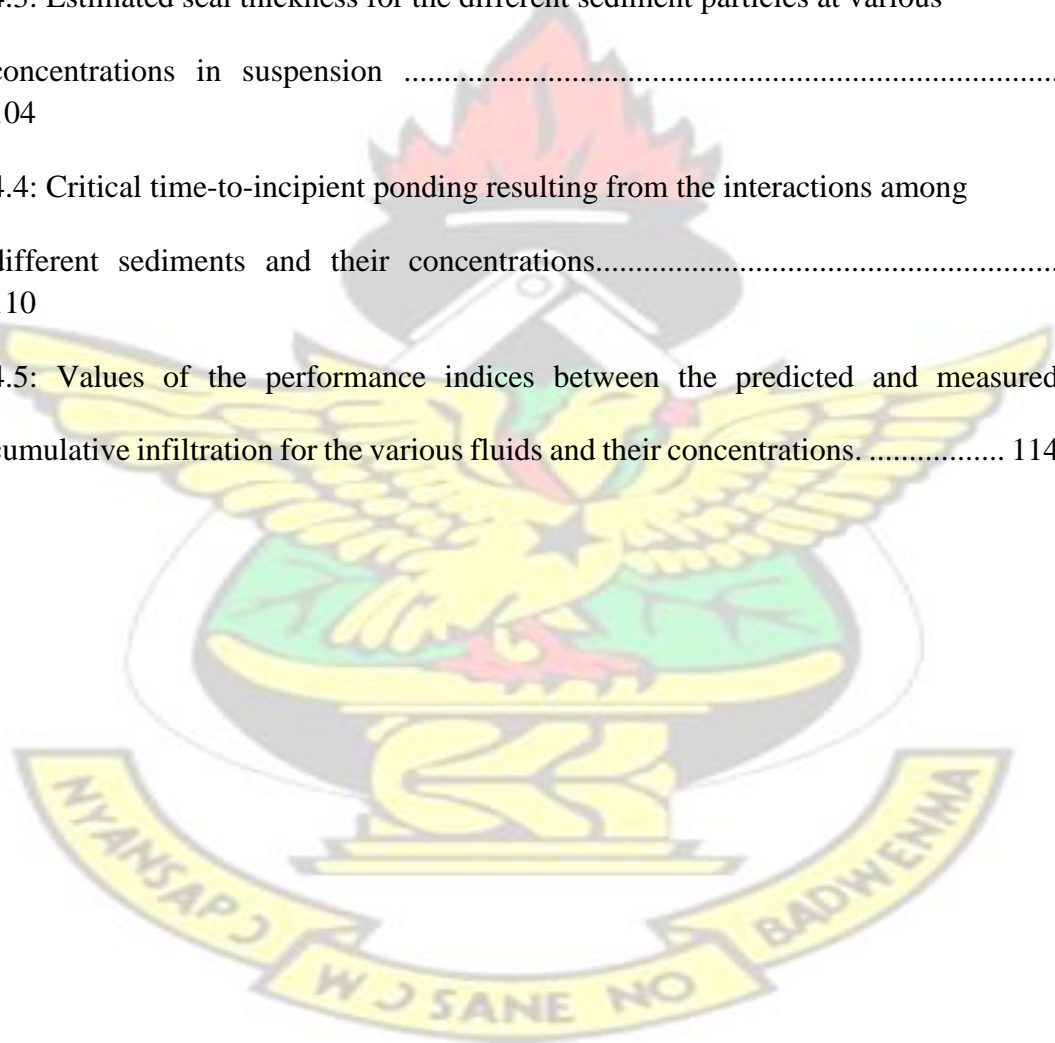
2.6.1.1 Kostiakov Equation	31
2.6.1.2 Horton Equation	33
2.6.1.3 Holtan Equation	37
2.6.1.4 SCS-Model	38
2.6.1.5 Swartzendruber Equation	39
2.6.1.6 Philip Equation	39
2.6.1.7 Smith and Parlange Equation	44
2.6.1.8 Green and Ampt Equation	47
2.7 Infiltration ponds	52
2.8 Hyper-concentrated flows and sediment transport	54
2.9 Sediment transport equations	56
2.9.1 Ackers and White equation	57
2.9.2 Engelund and Hansen	58
2.9.3 Yang's Equation for Sand Transport	59
2.9.4 Yang Equation for Gravel	62
2.9.5 Yang Modification for Water-Sediment Mixtures.....	62
2.10 Model performance evaluation and selection	64
CHAPTER THREE	66
3.0 MATERIALS AND METHODS	66
3.1 Description of soil	66
3.2 Collection of soil cores	66
3.3 Laboratory Measurements	67
3.3.1 Particle size analyses	67

3.3.2 Volumetric soil moisture content and bulk density	68
3.3.3 Saturated hydraulic conductivity (K_s)	70
3.3.4 Separating soil particles	71
3.4 Muddy water infiltration model	72
3.4.1 Model development	72
3.4.2 Theory	73
3.4.2.1 Model assumptions	73
3.4.2.2 Model description.....	74
3.5 Experimental verification of the model	79
3.5.1 Data reduction and presentation	81
3.5.2 Estimation of time-to-incipient ponding (tp)	82
3.6 Model validation	82
3.7 Statistical analysis	84
CHAPTER FOUR	85
4.0 RESULTS AND DISCUSSIONS	85
4.1 Soil physical and hydraulic properties	85
4.2 Infiltration	90
4.2.1 Effect of sediment size on infiltration.....	93
4.2.2 Effect of sediment concentration on infiltration	97
4.3 Surface sealing	101
4.4 Time-to-incipient ponding	109
4.5 Prediction of cumulative infiltration amount by the model	112
4.6 Applications of the proposed model	116

CHAPTER FIVE	
118	
5.0 CONCLUSIONS AND RECOMMENDATIONS	
118	
5.1 Conclusions	
118	
5.2 Recommendations	
121	
REFERENCES	
123 APPENDICES	143
A: Repeated Measures one-way ANOVA analysis with Tukey's Multiple Comparisons test for Hydro-physical properties	143
B: Repeated Measures one-way ANOVA analysis with Tukey's Multiple Comparisons test for infiltration parameters	164
C: Repeated Measures one-way ANOVA analysis with Tukey's Multiple Comparisons test for seal thickness	177
D: One-sample t-test analysis of seal thickness for the different sediments suspensions and concentrations with respect to time	188
E: One sample t-test analysis of time-to-incipient ponding in relation to rainfall rates	192
F: Repeated Measures one-way ANOVA analysis and Tukey's multiple comparisons test of observed and predicted cumulative infiltration amounts	197
G: Paired t-test analysis of measured vs predicted cumulative infiltration amount	

LIST OF TABLES

TABLE	PAGE
4.1a: Summary of initial soil physical and hydraulic properties.....	86
4.1b: Summary of soil physical and hydraulic properties after infiltration.....	87
4.2: Summary of infiltration characteristics following the interactions among the various fluids and their concentrations.....	92
4.3: Estimated seal thickness for the different sediment particles at various concentrations in suspension	104
4.4: Critical time-to-incipient ponding resulting from the interactions among different sediments and their concentrations.....	110
4.5: Values of the performance indices between the predicted and measured cumulative infiltration for the various fluids and their concentrations.	114



LIST OF FIGURES

FIGURE PAGE

2.1: Scheme of soil slaking and sealing processes during infiltration (Greener, 2001)	19
2.2: Illustration of uniform water entry assumption: transmission zone, and sharply defined wetting front.	48
3.1: Sieves arranged in a stack with the mesh size increasing from bottom to top on mechanical shaker	72
3.2: Principles of 3-dimensional throwing motion (left), horizontal sieving (middle) and tap sieving (right).....	72
3.3: A schematic diagram of the apparatus used to test the theory.....	81
4.1a: Cumulative infiltration amount with time for sand suspension at different concentrations	95
4.1b: Cumulative infiltration amount with time for silt suspension at different concentrations	96
4.1c: Cumulative infiltration amount with time for clay suspension at different concentrations	96
4.2a: Cumulative infiltration of clear water and 10 g soil particles in suspension	98

4.2b: Cumulative infiltration of clear water and 20 g soil particles in
suspension
99

4.2c: Cumulative infiltration of clear water and 30 g soil particles in
suspension
99

4.2d: Cumulative infiltration of clear water and 40 g soil particles in
suspension
100

TABLE OF APPENDICES

APPENDIX

A1.1: Repeated Measures one-way ANOVA analyses for Bulk density
.....
144

A1.2: Tukey's multiple comparisons test summary for Bulk density.....
145

A2.1: Repeated Measures one-way ANOVA analyses Total porosity.....
148

A2.2: Tukey's multiple comparisons test summary for Total porosity.....
149

A3.1: Repeated Measures one-way ANOVA analysis for volumetric
moisture content (FC)
152

A3.2: Tukey's multiple comparisons test summary for volumetric moisture
content (FC)
153

A4.1: Repeated Measures one-way ANOVA analyses saturated moisture
content
156

A4.2: Tukey's multiple comparisons test summary for saturated moisture

content	157
A5.1: Repeated Measures one-way ANOVA analysis for saturated hydraulic conductivity	160
A5.2: Tukey's multiple comparisons test summary for saturated hydraulic conductivity	161
B1.1: Repeated measures ANOVA summary for cumulative infiltration amount of different fluids.....	165
B1.2: Tukey's multiple comparisons test summary for cumulative infiltration amount for different fluids	166
B2.1: Repeated measures ANOVA summary for cumulative infiltration rate of different fluids.....	169
B2.2: Tukey's multiple comparisons test summary for cumulative infiltration rate for different fluids	170
B3.1: Repeated measures ANOVA summary for steady state infiltrability of different fluids.....	173
B3.2: Tukey's multiple comparisons test summary for steady state infiltrability for different fluids	174
C1.1: Repeated Measures one-way ANOVA analyses of seal thickness for different concentrations of clay suspension	178
C1.2: Tukey's multiple comparisons test of seal thickness for different	

concentrations of clay suspension	179
C2.1: Repeated Measures one-way ANOVA analyses of seal thickness for different concentrations of silt suspension	180
C2.2: Tukey's multiple comparisons test of seal thickness for different concentrations of silt suspension	181
C3.1: Repeated Measures one-way ANOVA analyses of seal thickness for different concentrations of sand suspension	182
C3.2: Tukey's multiple comparisons test of seal thickness for different concentrations of sand suspension	183
C4.1: Repeated Measures one-way ANOVA analyses of seal thickness for interactions among the different treatments	184
C4.2: Tukey's multiple comparisons test of seal thickness for interactions among the different treatments.....	185
D1: One-sample t-test analysis of variation of seal thickness with time for Clay suspensions	189
D2: One-sample t-test analysis of variation of seal thickness with time for Silt suspensions	190
D3: One-sample t-test analysis of variation of seal thickness with time for Sand suspensions	191
E1: One sample t-test analysis of time-to-incipient ponding for clear water	193

E2: One sample t-test analysis of time-to-incipient ponding for different clay suspensions	194
E3: One sample t-test analysis of time-to-incipient ponding for silt suspensions	195
E4: One sample t-test analysis of time-to-incipient ponding for sand suspensions	196
F1.1: Repeated Measures one-way ANOVA analysis of observed and predicted cumulative infiltration amounts	198
F1.2: Tukey's Multiple Comparisons test of observed and predicted cumulative infiltration amounts	199
G1: Summary of paired t-test analyses of cumulative infiltration amount for observed clear water vs. model predicted value	212
G2: Summary of paired t-test analyses of cumulative infiltration amount for observed 10 g clay suspension vs. model predicted value	213
G3: Summary of paired t-test analyses of cumulative infiltration amount for observed 20 g clay suspension vs. model predicted value	214
G4: Summary of paired t-test analyses of cumulative infiltration amount for observed 30 g clay suspension vs. model predicted value	215
G5: Summary of paired t-test analyses of cumulative infiltration amount for observed 40 g clay suspension vs. model predicted value	216
G6: Summary of paired t-test analyses of cumulative infiltration amount for observed 10 g silt suspension vs. model predicted value	217

G7: Summary of paired t-test analyses of cumulative infiltration amount for observed 20 g silt suspension vs. model predicted value	218
G8: Summary of paired t-test analyses of cumulative infiltration amount for observed 30 g silt suspension vs. model predicted value	219
G9: Summary of paired t-test analyses of cumulative infiltration amount for observed 40 g silt suspension vs. model predicted value	220
G10: Summary of paired t-test analyses of cumulative infiltration amount for observed 10 g sand suspension vs. model predicted value	221
G11: Summary of paired t-test analyses of cumulative infiltration amount for observed 20 g sand suspension vs. model predicted value	222
G12: Summary of paired t-test analyses of cumulative infiltration amount for observed 30 g sand suspension vs. model predicted value	223
G13: Summary of paired t-test analyses of cumulative infiltration amount for observed 40 g sand suspension vs. model predicted value	224

LIST OF ABBREVIATIONS

AMD:	Absolute Mean Difference
AIC:	Akaike Information Criterion
ANOVA:	Analysis of variance
ASTM:	American Society for Testing Materials
ESP:	Exchangeable Sodium Percentage
FAO:	Food and Agriculture Organisation
G-A:	Green and Ampt
GOF:	Goodness-of-fit
MGASS:	Modified Green and Ampt Surface Sealing infiltration model
MRMSE:	Mean Root Mean Square Error

RMSE:	Root Mean Square Error
RMKM:	Revised Modified Kostiakov Model
SAR:	Sodium Absorption Ratio
SSE:	Measure of deviations of observations from predicted data
SST:	Measure of deviations of observations from their mean
UNESCO:	United Nations Educational, Scientific and Cultural Organisation

LIST OF SYMBOLS

Symbol	Definition	Unit
A	Surface/Cross sectional area	L^2
a	Index of surface connected porosity, which is function of the surface conditions and plant roots density	
a	Surface area of cylinder	L^2
A_o	Empirical constant in the Swartzendruber equation	
B	Slope of regression of $\ln(h_o/h_t)$ on t	
b	Constant determined from measured infiltration data in the SCS model	
C	Chézy friction coefficient	$[L^{1/2}/T]$
$C(h)$	Specific water holding capacity	L^{-1}
C_{ppm}	Bed material concentration, excluding wash load	ppm
C_v	Sediment concentration by volume, including wash load	
C_s	Weight concentration of bed material load	
c	Sediment concentration	M/M

$D(\theta)$	Hydraulic diffusivity	L^2/T
d	Depth of the surface layer	L
D	Particle diameter of sediment	L
D_{50}	Diameter of particle larger than 50 weight percent	L
D_m	Median particle diameter	L
d^*	Dimensionless particle diameter	
d_o	Observed data	
d_s	Simulated data	
\bar{d}_o	Mean observed data	
F_g	Mobility number	
f	Total porosity	L^3/L^3
f_f	Darcy-Weisbach friction factor	
F and J	Dimensionless parameters related to flow and sediment characteristics	
GI	Growth index of crop	
G_s	Specific gravity of sediment	
g	Acceleration due to gravity	M/L^3
H	Total hydraulic head	L
h	Pressure head	L
h_p	Water-entry pressure head	L
h_o	Ponding depth	L
h_f	Suction at the wetting front	L
h_t	Hydraulic head at specific time t	L
i	Infiltration rate	L/T
i_f	Final infiltration rate	L/T

i_0	Infiltrability at $t = 0$	L/T
I	Cumulative infiltration amount	L
K	Hydraulic conductivity	L/T
K_s	Saturated hydraulic conductivity	L/T
K_{o1}, K_{o2}	Constants that depend on both soil properties and on θ_i and θ_f	L/T
K_o	Steady state infiltrability or apparent hydraulic conductivity	L/T
$K(h)$	Hydraulic conductivity as a function of both the fluid and porous medium	L/T
$K_x(D)$	Hydraulic conductivity of the surface seal layer	L/T
L	Length of soil column	L
L_f	Depth to wetting front	L
m	Empirical parameter from the van Genuchten-Mualem model	
M_w	Mass of wet soil	M
M_s	Mass of dry soil	M
M_x	Mass of sediments in suspension	M
M_z	Mass of sediments deposited on the soil surface	M
n	Empirical parameter from the van Genuchten-Mualem model	
P	Perimeter of the wetted hydraulic cross section	L

Q	Volumetric flow rate	L^3/T
Q_I	Cumulative volume of water	L^3
q	Flux density (Specific flow rate)	L/T
q_m	Mass flux density	$M/L/T$
q_s	Discharge per unit width of channel	$[L^3/T]$
R	Water application rate/Rainfall rate	L/T
Re	Reynold's number	
Re^*	Shear velocity Reynold's number	
R^2	Coefficient of determination	
R_i	Rainfall intensity	L/T
R_p	Rainfall rate at time-to-ponding	L/T
R_r	Rainfall rate	L/T
R_H	Hydraulic radius	L
r	Radius of cylinder	L
r	Correlation coefficient	
S	Sorptivity – Empirical constant in the Philip and Swartzenruber equations	$L/T^{1/2}$
S_l	Channel slope	
S_E	Energy or water surface slope	
S_{CRE}	Energy or water surface slope at the critical condition	
s	Relative density	
SA	Available storage in the surface layer at a given time	L
t	Time after the start of infiltration	T
t_p	Time-to-incipient ponding	T

U_*	Shear velocity or Friction velocity	L/T
u	Constant determined from measured infiltration data in the SCS model	
V_s	Settling velocity of sediment particle	L/T
V_{sm}	Sediment fall velocity in the water-sediment mixture	L/T
V_t	Total volume of soil	L ³
V_x	Volume of sediments deposited on the soil surface	L ³
V_{CR}	Cross-section velocity at critical condition	L/T
VSE	Unit stream power	
V_{CRSE}	Critical unit stream power at incipient motion	
V_{CR}/V_s	Critical velocity	
y	Flow-resistance characteristics	
z	Vertical distance from datum plane where $H = 0$	L
Z_f	Vertical ordinate at the wetting front	L
Z_x	Thickness of the depositional (surface seal) layer	L
Z_L	Thickness of the soil column including the surface seal layer	L
α and β	Dimensionless constants of the Kostiakov equation	
$\alpha_2, \beta_2, \alpha_3, \beta_3$	Empirically determined parameters for the revised modified Kostiakov model	
λ	Soil parameter that controls the rate of decrease of infiltration and depends on initial water content, θ_i and application rate, R in Horton equation	T-1
θ	Water content	L ³ /L ³
θ_v	Volumetric water content	L ³ /L ³

θ_g	Gravimetric water content	M/M
θ_L	Water content for which hydraulic conductivity is equal to rainfall rate	L^3/L^3
θ_i	Initial water content	L^3/L^3
θ_s	Saturated water content	L^3/L^3
θ_f	Final soil water content	L^3/L^3
θ_r	Residual water content	L^3/L^3
θ	Degree of saturation	
θ_o	Moisture content in dry soils	
$\Delta\theta$	Moisture deficit	L^3/L^3
φ	Correction factor accounting for deviations from sharp wetting front and/or viscous damping depths	
ρ	Density or mass per unit mass	M/L^3
ρ_s	Particle density of soil	M/L^3
ρ_b	Bulk density of soil	M/L^3
ρ_w	Density of water	M/L^3
ρ_γ	Submerged particle density	M/L^3
ρ_f	Fluid density	M/L^3
ρ_m	Density of water-sediment mixture	M/L^3
ω	Dynamic viscosity defined in Poisseulle's law	$M/L/T$
μ	Kinematic viscosity	L^2/T
μ_m	Kinematic viscosity of water-sediment mixture	L^2/T
$\epsilon, \sigma, \vartheta$	Coefficients in the Ackers and White equation	
∇, \emptyset	Parameters related to hydraulic and sediment conditions	

γ	Specific weight	N/L^3
γ_s	Specific weight of sediment	N/L^3
γ_m	Specific weight of water-sediment mixture	N/L^3
τ	Bed shear stress	
τ_0	Tractive force	
τV	Stream power per unit bed load	



CHAPTER ONE

1.0 INTRODUCTION

One most important process in the hydrologic cycle is infiltration, wherein water from precipitation, ice, or irrigation enters the soil through the surface. Water from these sources may also runoff over land and cause erosion, flooding, or flow into streams, lakes, rivers and oceans. Thus, infiltrating water, which constitutes the sole source of water to sustain the growth of vegetation, is filtered by the soil, which removes many contaminants through physical, chemical and biological processes, and replenishes the ground water supply to wells, springs and streams (Rawls *et al.*, 1993; Oram, 2005).

Most recent reports (e.g. Mirzaee *et al.*, 2013; Stewart *et al.*, 2013; Khalid *et al.*, 2014; Parhi, 2014; Tuffour *et al.*, 2014a, b) have shown that the ability to quantify infiltration is of great importance in soil management, especially, in irrigation and drainage designs. Hence, a robust infiltration model, that can correctly predict the actual infiltration, can be quite effective in planning and designing of water resources systems (Parhi, 2014). For example, prediction of flooding, erosion, and pollutant transport depends on the rate of runoff which is directly affected by the rate of infiltration. Quantification of infiltration is also necessary to determine the availability of water for crop growth and to estimate the amount of additional water needed for irrigation. Similarly, by understanding how infiltration rate is affected by surface conditions, measures can be taken to increase it and reduce the erosion and flooding caused by overland flow. However, due to the inherent modelling difficulties, most infiltration equations assume uniform flow of clear water, ignoring

the existence of preferential flow, slaking and dispersion of soil aggregates and clay, and water quality.

An accurate method for predicting the real infiltration process correctly is required for a detailed investigation of soil infiltration characteristics that will help in farm irrigation system modification and new designs. It turns out that the study on the presence of dispersed soil particles in irrigation water will be well fitted to cope with the soil-water flow problems of arid landscapes. It is also necessary to appreciate that the uncritical applications of humid hydrology theories in arid environments where soil dispersion is common can be very misleading. There is, therefore, the need to sharpen the tools for dealing with arid hydrology and for developing the appropriate concepts and intuitions for simple explicit infiltration equations for practical applications.

In agricultural fields, irrigated soils are frequently exposed to sequential periods of rapid wetting followed by drying. Soils that are subjected to these events, in due course, tend to have low aggregate stability (Caron *et al.*, 1992; Rasiah *et al.*, 1992). As a result, when water is applied to these soils, there is slaking of aggregates and/or dispersion of individual clay particles into suspensions. For instance, the impacting force of raindrops causes breakdown and dispersion of soil aggregates. However, during the process of wetting, slaking may predominate over dispersion resulting from the mechanical effect of raindrop impact (Le Bissonais and Bruand, 1993; Loch and Foley, 1994; Le Bissonais *et al.*, 1995; 1998). This is clearly evidenced by the greater proportion of slaked fragments (20 to 60 μm) over clay particles ($< 2 \mu\text{m}$)

(Young and Mullins, 1991). In the event, smaller suspended sediment particles are filtered out at the surface as the water infiltrates and kept in place by the negative water phase pressure below the soil surface (Brown *et al.*, 1988). This may cause the soil to slump, lose porosity and become denser, resulting in surface sealing and hardsetting, which can greatly overshadow other factors affecting infiltration on bare soil surfaces.

Most of the theories and perceptions of soil hydrology refer mostly to standard, wellwatered, clay-rich and organic-rich, fertile soils in the temperate regions. These models have generally worked out for moist environments with water tables near or at the soil surface, but do not always carry over meaningfully over arid and semi-arid regions where soils have poor structure coupled with serious soil erosion. In response to these problems, several researchers (e.g. Bagnold, 1977; Foster *et al.*, 1977; Yalin, 1977; Moss *et al.*, 1980; Abrahams *et al.*, 1988; Jungerius and Van der Meulen, 1988; Witter *et al.*, 1991) have studied the transport of dispersed soil particles in runoffwater. However, their movement with infiltrating water, which frequently occurs under flooded and/or ponded conditions, has not been extensively investigated.

It is evident that most infiltration models (e.g. Green and Ampt, 1911; Philip, 1957a, b, c; Youngs, 1968; Parlange, 1971) have been designed for clear water entering uniform soil profiles and therefore, do not account for the presence and surface deposition of sediments during muddy water infiltration. However, during irrigation, the sediments carried by muddy water are deposited on the soil surface, giving rise to a surface depositional layer (i.e. seal or crust), which has significant effects on infiltration process. A few researchers (e.g. Wang *et al.*, 1999; Fanning *et al.*, 2006)

have attempted to develop infiltration equations involving soil particles in water, however, due to the extensive variation of soil particles' geometry, there has been little success with their applications. This is due to the fact that each of these equations can only be applied to a limited range of sediment and fluid conditions, as well as the bulk soil without giving particular attention to individual soil constituents (i.e. sand, silt and clay).

In consideration of these, infiltration models associated with irrigation in areas prone to soil erosion (i.e. slaking, dispersion, sealing/crusting) should consider the presence of different sediment particles in water in order to understand the mechanisms of muddy water infiltration together with the implications for irrigation recommendations. There is also the need to consider fluid properties in the development of infiltration models. Since infiltration process generally causes changes in soil porosity, they are always accompanied by changes in the soil hydraulic and mechanical parameters. Therefore, knowledge of the infiltration process associated with soil particle phase (muddy water) will serve as base for soil management practices viz., water flux and transport of contaminants in the vadose zone as well as runoff, erosion and flood control.

1.1 Objectives

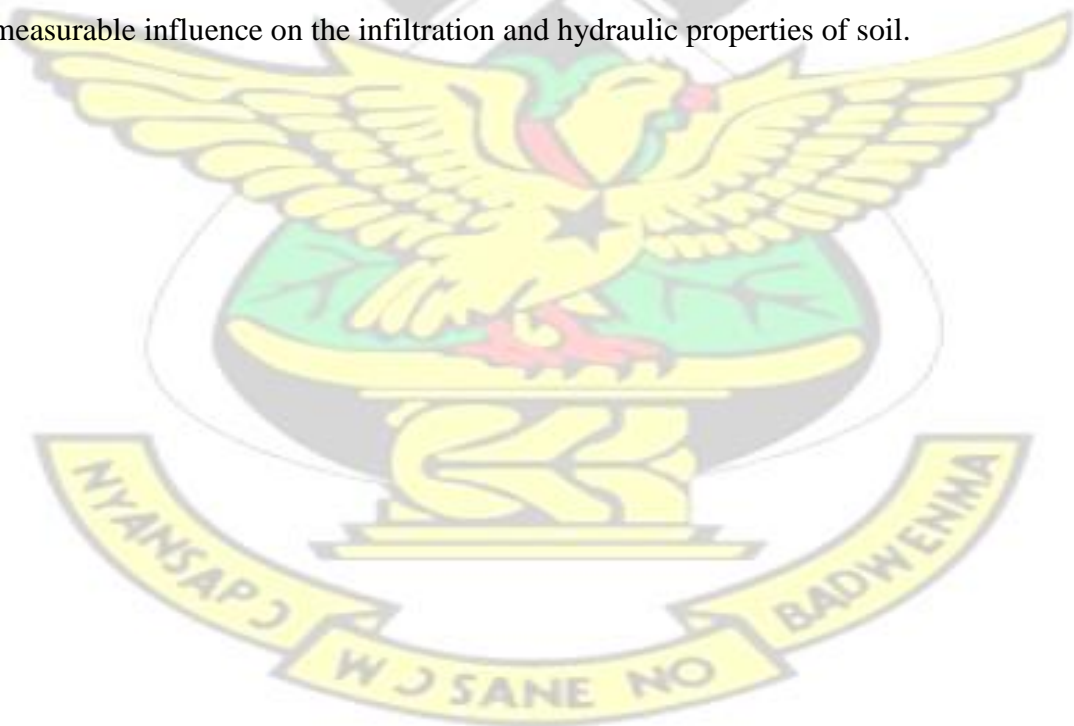
The overall objective of the study was to develop a verified theoretical model to describe the mechanism of muddy water infiltration. The specific objectives were to:

- i. Review available models on infiltration for possible modification for muddy water infiltration.

- ii. Carry out a laboratory test to investigate the effect of different sediment particles at different concentrations in muddy water on infiltration and surface sealing.
- iii. Estimate the time-to-ponding/runoff following the infiltration of muddy water with different sediment particles at different concentrations.
- iv. Highlight the practical importance of the proposed model to soil hydrology.

1.2 Hypothesis

The hypothesis of this study (alternate hypothesis) was that dispersed soil particles in muddy water interact with other soil properties to significantly, influence the infiltration and hydraulic properties of soil. On the other hand, the null hypothesis was that dispersed soil particles in muddy water do not have any meaningful and measurable influence on the infiltration and hydraulic properties of soil.



CHAPTER TWO

2.0 LITERATURE REVIEW

2.1 The process of water movement in soil

Water movement is always from higher energy level to lower energy level and the driving force for the movement is the potential difference between the energy levels. Three important forces are known to affect the movement of water through soil (Hillel, 1998):

- i. The gravitational force or potential difference causes water to flow vertically downward. This is because the gravitational potential energy level of water at a given elevation in the soil profile is higher than that of water at a lower elevation. Similarly, if there is stagnant water on the surface, the weight of the ponded water exerts hydrostatic pressure which increases the rate of infiltration, which is also due to the gravitational force.
- ii. Adhesion or the attraction of the soil matrix to water is responsible for the phenomena of adsorption and capillarity (matric or capillary potential), and to a lesser extent cohesion, which describes the attraction of water molecules to each other. Together, adhesive and cohesive forces produce a suction force which reduces the rate of movement of water below the soil surface. The higher the soil water content, the weaker the suction force and the lower the matric potential difference.
- iii. The attraction of ions and other solutes towards water, resulting in osmotic forces, tends to reduce the energy level in the soil solution.

2.2 Infiltration and its importance

According to Hillel (1998), infiltration can be considered as the process by which water from the surface enters into the soil. Under normal conditions, gravity and

capillarity drive vertical infiltration, whereas capillarity alone drives horizontal infiltration (Philip, 1957b). Redistribution, on the other hand, is the movement of water from point-to-point within the soil profile after the infiltration process. This points out clearly that the two processes are closely related, since the rate of infiltration is always strongly influenced by the rate of water movement within the soil below the surface. After each infiltration event, water movement in the soil continues to redistribute the water below the surface (Rawls *et al.*, 1993). Considering this, many of the factors that control infiltration rate also have a great impact on the redistribution of water below the soil surface during and after infiltration. Hence, understanding how infiltration rate is affected by surface conditions will inform on how measures can be taken to increase it in order to reduce the incidents of erosion and flooding/ponding caused by overland flow.

In addition, quantification of infiltration is considered as a necessary step in determining the availability of water for crop growth and estimation of the amount of additional water needed for irrigation, and in understanding subsurface movement and storage of water (Skaggs and Khaleel, 1982). Thus, the determination of soil infiltrability is of great importance to understanding and describing hydrologic analysis and modelling (Lili *et al.*, 2008). As a ‘rule of thumb’, irrigation systems are designed and managed so that the application rate of water does not exceed the infiltrability of the soil (Bloem and Laker, 1994). Therefore, for optimum performance and management of surface irrigation systems, knowledge of soil infiltration parameters should be well understood (Khatri and Smith, 2005).

However, infiltration is a very complex physical phenomenon, since soil is a very heterogeneous and anisotropic layered porous medium (Tuffour *et al.*, 2014b). As a result, many field workers (e.g. engineers and planners) are uncertain about results from different regions with similar climate and soil conditions. Hence, there is resistance to incorporate design strategies based solely on similarity assumptions. Therefore, researchers, engineers and planners require physics-based solutions as well as geostatistics, scaling and fractal analyses to their design problems.

2.3 Factors that control infiltration rate

Infiltration rate (i) is affected by the inherent properties of the soil profile, especially those that strongly affect hydraulic conductivity, diffusivity and water holding capacity (Turner, 2006). These factors include those that influence soil matric forces and pore-space (such as texture, structure, composition and degree of compaction) and surface sealing which is probably the most significant single factor that affects the process (Moore, 1981a, b; Moore *et al.*, 1981). In this regard, the i actually experienced in a given soil depends on the characteristics of the soil layer (especially, its depth, sorptivity and hydraulic conductivity), rainfall intensity, temperature, vegetation cover, amount and distribution of soil moisture, and availability of water at the surface, and land use (Betson, 1964; Dunne and Leopold, 1978). The process can, therefore, be viewed as a function of the intrinsic permeability of the medium and the fluidity of the penetrating liquid (Hillel, 1980; Siyal *et al.*, 2002; Amin, 2005).

Antecedent water content affects the moisture gradient of the soil at the wetting front, the available pore space to store water and the hydraulic conductivity of the soil. In this regard, initial water content is seen as a critical factor in determining the rate of

infiltration and the rate at which the wetting front proceeds through the soil profile. The drier the soil is initially, the steeper the hydraulic gradient and the greater the available storage capacity; both factors increase infiltration rate (Skaggs and Khaleel, 1982). The wetting front proceeds more slowly in drier soils, because of the greater storage capacity, which fills as the wetting front proceeds (Philip, 1957c).

Critically, the hydraulic conductivity is of greatest importance to infiltration rate since it expresses how easily water flows through soil; it is also a measure of the soil's resistance to flow. By definition, diffusivity is directly proportional to hydraulic conductivity, but, usually only the saturated hydraulic conductivity is used in many of the infiltration equations, since it is easier to determine than either the unsaturated hydraulic conductivity or the diffusivity (SSSA, 1975). The water holding capacity also influences the average suction at the wetting front and sorptivity, as well as some empirical parameters. However, for saturated conditions, the water holding capacity is zero and the hydraulic head is positive (Skaggs and Khaleel, 1982).

Texture also has an enormous influence on the hydraulic conductivity, diffusivity and water holding capacity of soil with respect to pore size distribution. Thus, soils with higher sand percentages have larger pores, higher hydraulic conductivity, diffusivity and infiltration rates, but lower water holding capacity than clay soils, which have smaller pores, because water molecules tend to bind more tightly to their walls. In this way, it does not participate in normal flow process in the soil (Hillel, 1998).

Water in capillary pores (i.e. pores in medium textured soil that range from several micrometres to a few millimetres in width) obeys the laws of capillarity and Darcian flow (Hillel, 1998). Thus, a deep homogeneous soil (containing only capillary pores), as assumed in many infiltration equations is subject to uniform flow in which the infiltration rate decreases as the moisture gradient declines. Conversely, macropores create barriers to water flow in capillary pores when empty, permitting only film flow along their walls; when filled with water, they cause very rapid, often turbulent, downward movement of water to lower layers of the soil profile (Hillel, 1998). This rapid channel drainage that often bypasses much of the soil matrix and can significantly modify infiltration rates is termed “preferential flow” (Šimunek *et al.*, 2003). Even for relatively small earthworm channels, the flow rate in macropores seems to be always higher than the rainfall intensity (Bouma *et al.*, 1982). In this regard, soil structure can be seen to affect the pathway of water movement through the soil (Brady and Weil, 1999).

Soil compaction, which is the result of the application of pressure on the soil surface, destroys soil structure and reduces infiltration rates (Tuffour *et al.*, 2014a), air availability to plant roots and other soil organisms. Rainfall on bare soil can also cause soil compaction. Often where soils have been ploughed continually with heavy equipment there is a hardened and compacted layer below the topsoil called a ploughpan, which may impede redistribution. A naturally hardened layer called a fragipan may also obstruct the vertical movement of water (Brady and Weil, 1999).

Vegetation and other ground covers such as mulches and plant residues reduce soil temperature and evaporation from the soil surface, but vegetation also loses moisture through transpiration. Vegetation also increases infiltration rates by loosening soil

through root growth, and alongside natural mulches and plant residues, intercept rain drops, which compact and damage the structure of bare soil, and cause surface sealing and crusting. Living and dead plant materials also add organic matter to the soil which improves soil structure and water holding capacity and provide habitat for earthworms, which further improve the soil porosity and increase infiltration rates (Brady and Weil, 1999).

Slope also affects infiltration rate. A decrease in water infiltration rate was observed with increase in the slope steepness for grass covered slopes (Haggard *et al.*, 2005; Huat *et al.*, 2006). According to Haggard *et al.* (2005), the slope may have the greatest effect on surface runoff production and infiltration rate when the soil is close to saturation. On the other hand, there is evidence that on bare sloping land, infiltration rates are higher than on bare flat land (Poesen, 1984). This effect is most likely due to reduced seal development on sloping land, as greater runoff velocities maintain a larger proportion of sediment particles in a suspended state resulting in more open pore structure (Römken *et al.*, 1985).

Rainfall intensity is defined as the instantaneous rainfall rate, and for a uniform storm or rainfall simulation, it may be obtained by dividing the depth of rainfall by the duration of rainfall. For non-ponded conditions, the maximal rate of infiltration called the infiltration capacity (Horton, 1940) or infiltrability by (Hillel, 1971) equals or exceeds the rainfall intensity which provides the upper limit for the infiltration rate.

The infiltration rate therefore, equals the rainfall rate until ponding sets in. If the rainfall rate is less than the saturated hydraulic conductivity of the soil, infiltration is likely to continue *ad infinitum* without the incidence of ponding. In this case the water

content of the soil does not reach saturation, but approaches a limiting value (i.e. saturation), which depends on the rainfall intensity. For a given rainfall intensity, R_i , the soil profile approaches a uniform water content θ_L , (the water content at which the hydraulic conductivity, K , is equal to the rainfall rate: $K(\theta_L) = R$). Since unsaturated hydraulic conductivity increases with increasing water content, the higher the rainfall intensity, the higher the value of θ_L (Skaggs and Khaleel, 1982). When the rainfall intensity exceeds the ability of the soil to absorb water, infiltration continues at the infiltrability. At the time of ponding, the infiltrability lags behind the rainfall intensity, depression storage fills up and runoff occurs. If the rainfall intensity is higher, depression storage fills faster and runoff follows sooner after the incidence of ponding.

The infiltration rate (i) after ponding, however, does not depend on R_i for i less than R_i except to the degree that more intense rainfall may cause greater raindrop splash, and greater surface sealing when enough soil particles that splash into the air, land in pore openings, and block them from infiltrating water. Much of the decrease in infiltration rate experienced in unprotected soils is attributed to surface sealing (Shirmohammadi, 1984). When the surface sealed layer dries out and hardens, surface crust forms. This may cause immediate ponding with very low infiltration rate. However, a long soaking rain will tend to soften the crust so that after a time infiltration rate may increase.

When water moves into a soil profile, it displaces air, which is forced out ahead of the wetting front. If there is a barrier to the free movement of air, such as a shallow water table, or when a permeable soil is underlain by a relatively impermeable soil,

the air becomes confined and the pressure becomes greater than atmospheric. Compressed air ahead of the wetting front and the counter flow of escaping air may drastically reduce infiltration rates (Shirmohammadi, 1985). Following this report, Wangemann *et al.* (2000) found that for interrupted flow in dry soils the main retardant to infiltration was entrapped air and reduced aggregate stability, and surface sealing for wet soils. For a two phase flow treatment of infiltration, Le Van Phuc and Morel-Seytoux (1972) reported that infiltration rate after a certain time was well below the saturated hydraulic conductivity, which has been considered as a lower limit by earlier researchers. Infiltration, however, tends to be increased for deeper water tables, since the impedance of the compressed air on infiltration is reduced and the soil profile tends to be drier compared to shallow water table conditions (Shirmohammadi, 1984).

2.4 Causes of low infiltration rate

Many soil properties are known to influence the saturated hydraulic conductivity (K_s) and i of soils. As a result, the effects of organic matter, iron oxides, clay mineralogy, texture and exchangeable cation composition have all been studied. In connection with the latter, the effect of adsorbed potassium on the hydraulic properties of soil is contentious because results from various studies vary, possibly due to differences in clay mineralogy and sample preparation procedures (Levy and Van Der Watt, 1990).

Further, studies by Lado and Ben-Hur (2004) have shown that examination of the differences in texture, exchangeable sodium percentage (ESP), organic matter and pH of various soils could not explain the differences in the final i values between

stable and unstable soil groups. In view of this, it was concluded that the mineralogy of the clay fraction was the critical factor in reduced i between the soils studied. However, slow infiltration can develop in sandy loam soils with low organic matter content (Singer and Oster, 1984) or in medium and coarse textured soils due to restrictive layers at the surface (seals or crusts) or below the surface (compacted layers, hard pans, fine-textured strata or cemented layers) (Ajwa and Trout, 2006; Tuffour *et al.*, 2014a).

Low infiltration rates can also result from dispersion of the fine particles due to sodicity, or lack of sufficient divalent cations such as calcium (Oster *et al.*, 1992). However, according to Agassi *et al.* (1981), when sufficient electrolyte is provided with water, chemical dispersion is low. In this regard, Kazman *et al.* (1983) studied the effect of exchangeable sodium percentage (ESP) on i and seal formation of four (4) smectitic soils of varying textures using distilled water. Infiltration rate was found to be highly sensitive even to low levels of ESP. Baumhardt *et al.* (1992) also showed that field infiltration measurements were dependent on the soil salinity and sodicity, and the salinity of the applied water. This led to the conclusion that the permeability of soil to water depends both on its ESP and on the salt concentration of the percolating solution. In this regard, it can be realised that, deterioration of soil structure is likely to take place even under irrigating non-sodic soils with waters of low sodium absorption ratio (SAR) and salinity. This report upholds an earlier claim made by McNeal *et al.* (1968) that soil permeability decreases with increasing ESP and decreasing salt concentration. However, according to Agassi *et al.* (1981), i is much more sensitive to the ESP of the soil than the hydraulic conductivity.

Another essential soil property affecting i is the structure of the soil and aggregate stability. These two factors are among the most important soil quality indicators because of their relation to i (Doran and Parkin, 1996). Poor soil structure and aggregate stability can lead to a number of problems, most importantly, surface sealing or crusting. Accordingly, Green *et al.* (2000) concluded that the formation of a surface seal caused by the physical breakdown of aggregates and clay dispersion resulted in a decreased i . Due to seal and/or crust formation, the resultant i will tend to decrease to a minimum value irrespective of the initial soil moisture content (Lado and Ben-Hur, 2004).

Again, soil water repellency which describes the inability of water to wet or infiltrate a soil (especially dry soil) spontaneously and, therefore, regarded as a condition that reduces the affinity of soils to water from a few seconds to hours, days or weeks also has a falling impact on i (Feng *et al.*, 2002). In respect of this definition, a positive pressure (water-entry pressure head, h_p) is always required to drive water into the soil. In agreement with this, Contreras *et al.* (2008) emphasized that soil moisture content is an important factor in elucidating this phenomenon. Following this, they further stated that it is likely to be higher in aridic or dry soils than in humid soils.

There are also many other factors that can lower i . Chunye *et al.* (2003) found that the temperature of infiltrating water is related to i because its viscosity changes by ~2% per degree Celsius. This leads to an estimated 40% change of i between summer and winter in arid zones. Abu-Sharar and Salameh (1995) also put emphasis on the sensitive nature of i to any disturbance in surface soil structure. This includes compaction, planting patterns, crop, and cultivation. Mitchell (1986) found that for a

clay soil the final i is not a function of initial i . This indicates that the surface layer is not the zone controlling the i since the specific properties of the clay mineralogy (such as swelling smectite clay) may change with exposure to water, and lower the i . On level surface irrigated fields, low infiltration can result in crop damage due to stagnant water or inadequate aeration in the root zone. This can further result in the growth of algae on the soil surface (biological sealing) that further lowers infiltration. As a result, Oster *et al.* (1992) proposed that irrigation should be stopped when ponding or runoff begins, so as to reduce the damaging effects of low i . This is aimed to prevent erosion and deep pools that will take longer to evaporate.

If the final i increases, the erodibility factors decrease exponentially due to less runoff (Ben-Hur *et al.*, 1992). In this context, Oster *et al.* (1992) reported that, as ‘a rule of thumb’, all water should infiltrate within 24 to 48 hours, since longer periods of ponding increase the potential for poor aeration and disease prevalence. However, for the fact that infiltration varies from place to place within a field, it is recommended that more water be applied than is needed by the crop to ensure adequate irrigation. Application of about 20% more water than is needed by the crop compensates for infiltration variability. Conversely, this increase may cause ponding in areas where i is lowest, constraining and making irrigation expensive (Trout, 1990). This is usually the case when i is slower than sprinkler or drip emitter application rates, resulting in water ponding and reduced application uniformity.

Further, ponded water can increase evaporation losses, weed growth, change in weed species mix, and delay access to the field (Trout, 1990; Ajwa and Trout, 2006).

2.4.1 Soil compaction

Research findings show that almost all tillage practices produce compaction. The bulk density from the soil surface to a foot below, where tillage and tracking occurs is the most definitive measurement of compaction (Oster *et al.*, 1992; Tuffour *et al.*, 2014a). Wheel and track traffic are believed to be the largest contributors to soil compaction (Singer and Oster, 1984; Tuffour *et al.*, 2014a). According to Oster *et al.* (1992), soil compaction results when an applied force or pressure rearranges soil particles and increases soil density. With compaction, the total volume of soil pores decreases (Tuffour *et al.*, 2014a), though, it is possible for the number of small pores to increase while that of the large and continuous conducting pores decreases (Singer and Oster, 1984).

Akram and Kemper (1979) showed that i decreases as compacting forces increase. After nearly two decades of no-tillage, Gomez *et al.* (2001) also observed that, the general compaction of the soil was the main factor, which contributed to reduced K_s and subsequently, i . Tuffour *et al.* (2014a) also observed a significant decrease in i with a subsequent decrease in runoff generation time or time-to-incipient ponding following compaction caused by cattle grazing. In many temperate locations, freezing and thawing are among the most important factors that break compaction in soils. However, in areas devoid of sustained freezing temperatures, this natural amelioration of compaction does not occur and i is consequently reduced (Akram and Kemper, 1979).

Due to water drop impact which triggers soil and clay reorientation that clog soil voids at or near the soil surface, compaction caused by raindrops is regarded as a

dominant factor in crust formation (Hadas and Frenkel, 1982; Ben-Hur *et al.*, 1985). Following this, El-Morsy *et al.* (1991) found that this impact energy from water drops caused a large reduction in i independent of water quality. Undeniably, it is the impact energy that compacts the soil, but not the dispersive properties of the water that reduce i . Thus, compaction from machinery as well as natural forces such as impact energy from rain drops can contribute to the reduction in i since there is a subsequent reduction in pore spaces.

2.4.2 Surface sealing and crusting

Seal and crust formation are very common phenomena in many soils worldwide, especially in arid and semiarid soils where aggregate stability is weak. Rainfall causes a series of interactions between water and soils, viz., compaction, disintegration, detachment, entrainment and deposition. These actions result in the formation of seal and, subsequently, crust. Crust is a thin layer at the soil surface characterized by a greater density, higher shear strength, and lower hydraulic conductivity than the underlying soil (Moss, 1991). The formation of seal and crust depends on many factors, including the texture and stability of the soil, intensity and energy of rainfall, gradients and length of slope, and electrolyte concentration of the soil solution and rainwater (Remley and Bradford, 1989). The extent of surface sealing has been reported to be highly dependent on soil texture, with the silt content being a good indicator of the soil's susceptibility (Norton, 1987).

Surface sealing, as well as most other crust formations, results from three processes (Agassi *et al.*, 1981; Morin *et al.*, 1981):

- 1) Physical disintegration of soil aggregates and their compaction, caused by the impact of raindrops.

- 2) Chemical dispersion of the clay particles. The low electrical conductivity of the rainwater as well as the organo-chemical bonds between the primary particles of the surface aggregates, dictate the rate and degree of dispersion.
- 3) An interface suction force which arranges suspended clay particles into a continuous dense layer. Such almost impermeable layers form right on the surface of the soil or in the immediate subsurface washed-in layer, as discussed by McIntyre (1958).

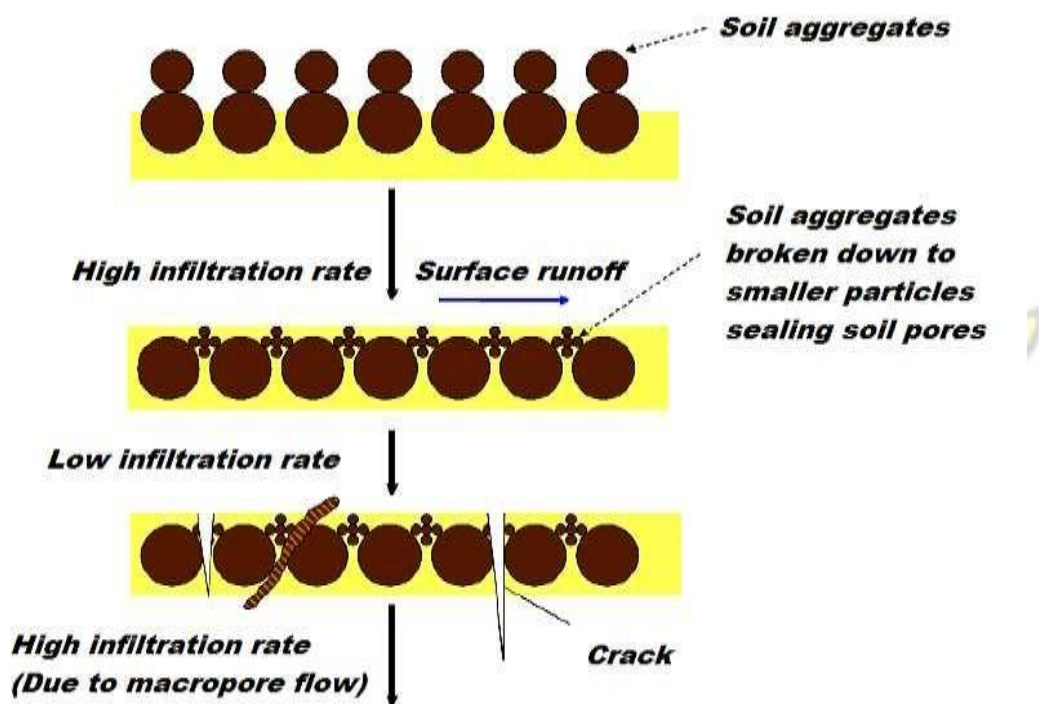


Figure 2.1: Scheme of soil slaking and sealing processes during infiltration (Greener, 2001)

Soil seals and crusts can significantly reduce infiltration rate and subsequently lower the utilization of water resources, and increase runoff, which result in soil erosion. This is so because the K_s of sealed or crusted surface is always lower than that of the subsurface. This, in turn, increases the transport capacity for entraining detached materials from soils (Levy *et al.*, 1994). Much attention has therefore been given to

the formation of seal and crust due to the close relationship they have with surface runoff and/ erosion (both processes involve the detachment of particles and transport processes). Although most erosion models do not recognize this relationship (i.e., effect of crust to erosion), new theories have been presented which comprise a categorical delineation between detachment and transport processes (Bissonris *et al.*, 1998). Therefore, it is suggested that new soil erosion models should take into account the basic concept of sealing and crusting as part of its supporting theories.

Several studies (Einstein, 1968; Brakensiek and Rawls, 1983; Bonsu, 1992) have described different theoretical mechanisms of seals and crusts formation in soils. From these studies, the fundamental descriptive mechanism has been defined to involve two main complementary processes (Cai *et al.*, 1998):

- a. Physical action including disintegration of soil aggregates and compaction of soil particles caused by the impact of raindrop.
- b. Physico-chemical action including dispersion of aggregates, movement of soil particles and exchange of cations that clog the conducting pores to form a less permeable layer at the surface of the soil.

The i values of sealed or crusted soils depend on the K_s of the seal or crust. For this reason, some researchers have tried to measure the K_s of soil surface seals. For instance, McIntyre (1958) found that the K_s of the upper and lower layers of the seal of a sandy loam soil were 2000 and 200 times lower than the K_s values recorded for the undisturbed soils. However, since the seal or crust is a very thin layer, it is very difficult to determine its K_s , hence i value is widely used.

Laboratory studies on the effects of surface sealing on infiltration have commonly simulated single rainfall events of constant intensity and energy on columns or trays of repacked soils. On the contrary, field studies have commonly monitored cumulative infiltration or determined changes in infiltration rate under simulated rainfall events over longer periods of time and related this to indices of rainfall kinetic energy such as cumulative rainfall volume. Consequently, large reductions in infiltration under rainfall observed in both laboratory and field situations have been attributed to the effects of surface sealing (e.g., McIntyre, 1958; Freebairn *et al.*, 1991; Valentin, 1991; Bresson and Cadot, 1992), and these reductions in infiltration can be used as a measure of the rate and degree of surface sealing. Again, Morin and Benyamini (1977) concluded that the hydraulic properties of surface seals control infiltration into bare soils under rainfall, over-riding the effect of hydraulic properties of the bulk soil.

2.5 Principles of water flow

The basic relationship for describing soil water movement was derived from Darcy's experiments in 1856. Following this, equations describing the dynamic and mass conservation for soil water system were first derived by Richards (1931). In consequence, significant efforts have been made to numerically approximate the Richards equation and to derive analytical solutions with fixed boundary conditions. However, these procedures are rarely used in practice because of numerical complications and scarcity of data. Darcy (1856) established that the specific flow rate (i.e. flux density) through porous media is proportional to the hydraulic gradient (Kirkham and Powers, 1972).

$$q = -K(h) \frac{\partial H}{\partial z} \quad (2.1)$$

where,

$H = h + z =$ Total hydraulic head [L] h

$=$ Pressure head [L]

$z =$ Vertical distance from the datum plane where $H = 0$ [L]

$\frac{\partial H}{\partial z} =$ Hydraulic gradient in the z (vertical) direction

$K(h) =$ Hydraulic conductivity which depends on properties of both the fluid and the porous medium [$L T^{-1}$]

$q =$ Specific flow rate (flux density) $= \left(q = \frac{Q}{A} \right)$

$Q =$ Volumetric flow rate [$L^3 T^{-1}$]

$A =$ Area of surface subjected to rainfall or ponding [L^2]

Darcy's equation forms the basis for describing the movement of water through soil.

The equation clearly states that hydraulic conductivity is a function of the soil water content, which in turn, is a function of pressure head (Kirkham and Powers, 1972).

In view of this, Richards (1931) derived two equations that are considered to govern infiltration phenomenon, because they describe the relationships between the soil properties on which infiltration depends, and are based on Darcy's Law and

conservation of mass. The soil properties that characterize infiltration are hydraulic conductivity $K(h)$ [$L T^{-1}$], diffusivity $D(\theta)$ [$L^2 T^{-1}$] and water holding capacity $C(h)$

[L^{-1}]. For layered soils, these properties are characterized for each layer, while for anisotropic soils, they are considered as a function of flow direction (Skaggs and

Khaleel, 1982).

The derivation of the Richards' equation from Darcy's Law and the Law of conservation of mass is instructive in understanding the infiltration process, as well as in understanding many of the other equations used to approximate infiltration (Turner, 2006). Following Darcy's Law from equation (2.1):

$$q = -K(h) \frac{\partial H}{\partial z}$$

Conservation of mass requires that the change in water content relating to time is equal to the change in specific flow rate:

$$\frac{\partial \theta}{\partial t} = -\nabla q \quad (2.2)$$

Assuming a change in flow rate is occurring only in the z direction:

$$\frac{\partial \theta}{\partial t} = -\frac{\partial}{\partial z} [q] \quad (2.3)$$

Substituting equation (2.1) into equation (2.3):

$$\frac{\partial \theta}{\partial t} = \frac{\partial}{\partial z} \left[K(h) \frac{\partial H}{\partial z} \right] \quad (2.4)$$

Substituting for H in terms of h and z :

$$\frac{\partial \theta}{\partial t} = \frac{\partial}{\partial z} \left[K(h) \frac{\partial h}{\partial z} \right] + \frac{\partial}{\partial z} \left[K(h) \frac{\partial z}{\partial z} \right] \quad (2.5)$$

Using the chain rule:

$$\frac{\partial \theta}{\partial t} = \frac{\partial \theta}{\partial h} \frac{\partial h}{\partial t} \quad (2.6)$$

Considering the water holding capacity $C(h)$, which is the slope of the soil-water retention curve given by:

$$C(h) = \frac{\partial \theta}{\partial h} \quad (2.7)$$

By substitution:

$$C(h) \frac{\partial h}{\partial t} = \frac{\partial}{\partial z} \left[K(h) \frac{\partial h}{\partial z} \right] + \frac{\partial K(h)}{\partial z} \quad (2.8)$$

This is the h -based Richards equation, which is valid for unsaturated and saturated conditions. The θ -based form of the equation, stated as:

$$\frac{\partial \theta}{\partial t} = \frac{\partial}{\partial z} \left[D(\theta) \frac{\partial \theta}{\partial z} \right] + \frac{\partial K(\theta)}{\partial z} \quad (2.9)$$

cannot be used to model flow in soils at or near saturation, because $\partial \theta$ tends to approach zero and $D(\theta)$ becomes infinite. It also fails in cases of layered profiles, since discontinuity of θ occurs in situations where abrupt transitions exist between layers (Hillel, 1998). However, equation (2.9) is the same as equation (2.8), where,

$$D(\theta) = K(h) \frac{\partial h}{\partial \theta} \quad (2.10)$$

and $\frac{\partial h}{\partial \theta}$ approaches infinity, when moisture content approaches saturation such that $\partial \theta$ approaches zero. For completely unsaturated flow, the θ -based equation is advantageous because changes in both θ and $D(\theta)$ are typically an order of magnitude less than corresponding changes in h and $C(h)$ for the h -based equation. As a result, round-off errors in numerical solutions of the θ -based equation are less significant than for the h -based equation (Skaggs and Khaleel, 1982). However, the numerical solution of the Richards equation requires numerous measurements to be made to satisfactorily describe variations in soil properties that occur both vertically in the soil profile and from spot-to-spot in the field (Skaggs and Khaleel, 1982), therefore, infiltration models with simplified data requirements are desirable for practical use.

2.6 Infiltration modelling

Throughout the last century and in recent times, infiltration modelling has received a great deal of attention from various researchers (e.g. Green and Ampt, 1911; Kostiaikov, 1932; Philip, 1954; 1957a, b, c; 1969; Mein and Larson, 1973; Smith, 1972; 1976; Smith and Parlange, 1978; Swartzendruber and Hogarth, 1991; Swartzendruber, 1987; 1997; 2000; Argyrokastitis and Kerkides, 2003; Parhi, 2007; 2014). This has led to the development of several infiltration models, which are branded as, physically-, semi-empirically- and empirically-based for its computation (Mishra *et al.*, 1999; Mishra and Singh, 1999). In the face of the availability of these large numbers of infiltration models, new ones are still being either developed, or modified from existing ones for simplicity and ease of application to meet specific

management and environmental conditions. Typical examples include the Soil Conservation Service Curve Number (SCS-CN)-based infiltration model (Mishra and Singh, 2003), Modified Kostiakov equation (Smith, 1972), Revised Kostiakov equation (Parhi *et al.*, 2007) and two-term infiltration equation from the Green and Ampt model (Swartzendruber, 2000).

Physically based models rely on the Law of mass conservation and the Darcy's Law (Swartzendruber, 1968; Bonsu, 1992; Parhi, 2014). Depending on the considerations of flow dynamics, hydraulic conductivity, and the soil water pressure as functions of moisture content for specified boundary conditions, physically based models of varying complexities have been derived (Swartzendruber and Youngs, 1974). Examples include those of Green and Ampt (1911), Philip (1957a, b, c), Philip (1969) and Swartzendruber (1987; 2000). Thus, the physically based models are approximate solutions of the Richards' equation (Shukla *et al.*, 2003). However, solving this equation is extremely difficult for many flow problems requiring detailed data input and use of numerical methods (Rawls *et al.*, 1993).

Semi-empirical models employ simple forms of continuity equation and simple hypothesis on the infiltration rate/cumulative infiltration (Mirzaee *et al.*, 2013; Parhi, 2014). This implies that they are a compromise between empirical and physically based models (Mirzaee *et al.*, 2013), and are based on the systems approach popularly employed in surface water hydrology (Parhi, 2014). Examples include those of Horton (1938), Overton (1964), and Singh and Yu (1990). Empirical models, on the other hand, are derived from data observed either in field or in laboratory. Examples include the models of Kostiakov (1932), Huggins and Monke (1966), modified

Kostiakov (Smith, 1972) and revised modified Kostiakov (Parhi *et al.*, 2007). Usually, when infiltration rate shows a sharp decline with time from the start of water application until a steady-state is approached after a sufficiently large time, it is best described by the equations of Kostiakov (1932) and Horton (1940). However, since these equations and their related experiments are empirical, their coefficients have no physical meaning.

Skaggs and Khaleel (1982) reported that numerical methods that allow the quantification of the vertical percolation of water are critical for assessment of groundwater recharge and in the analysis of contaminant movement through soil. Nevertheless, they are costly, as well as data and time intensive since they require several field measurements. As a result, they are rarely used in practice. From the time that this assertion was made, improvements in computer technology have greatly facilitated the use of numerical techniques. However the large quantity and complexity of the measurements necessary to obtain much of the soil property data required for these numerical solutions impose a severe limitation that has not moderated with time.

For many applications, equations that simplify the concepts involved in the infiltration process are advantageous (Rawls *et al.*, 1993). Simplified approaches include those of Kostiakov (1932), Horton (1939; 1940) and Holtan (1961), and approximate physically based models like those of Green and Ampt (1911) and Philip (1957a). Empirical models tend to be less restricted by assumptions of soil surface and soil profile conditions, but more restricted by the conditions used for their calibration, since their parameters are determined based on actual field-/laboratorymeasured infiltration data (Skaggs and Khaleel, 1982; Hillel, 1998).

However, equations that are physically based approximations use parameters that can be obtained from soil water properties and do not require measured infiltration data.

It has further been noted that these different approximate equations for infiltration result in different predictions for infiltration rate, time to ponding and/or runoff generation even when measurements from the same soil samples are used to derive parameter values. Also, different equations for infiltration require different parameters to be used. All the infiltration equations make use of some of these factors in characterizing infiltration. The more physically based equations rely heavily on the soil hydraulic and physical properties occurring within the profile, such as saturated hydraulic conductivity, soil moisture gradient and suction at the wetting front.

Empirical models, on the other hand, rely more on parameters that are determined by curve fitting or estimated by other means and, thus, may better reflect the effect of differences in surface conditions than the physical models, as long as parameters are calibrated separately for those different conditions (Turner, 2006). Occasionally, the approximate physically based models are used as empirical models with parameters determined in a similar manner. Therefore, the assumptions, form and intent of each equation need to be considered in deciding which equation to use for a particular application.

2.6.1 Infiltration Models

Due to the existence of highly variable initial soil conditions and properties, infiltration process is difficult to characterize. This implies that many factors may

influence the selection of a model, including type of application, desired level of physical-mathematical rigor, and user preference (Clausnitzer *et al.*, 1998). Owing to this, infiltration models vary in their complexity and sophistication (Viessman and Lewis, 2003). In the face of the extensive research carried out in the area of infiltration and storm water runoff, no single equation or mechanism describes all infiltration scenarios (Viessman and Lewis, 2003). No single infiltration model can be expected to best meet all possible requirements simultaneously. Thus to be able to make an informed decision in a given case, knowledge of model performance under different criteria is desirable (Clausnitzer *et al.*, 1998).

The assumptions are the key components in understanding a particular infiltration model. As a result, several equations that simplify the concepts involved in the infiltration process have been developed for field applications. Approximate models such as those of Philip (1957a) and Green and Ampt (1911) apply the physical principles governing infiltration for simplified initial and boundary conditions. They involve ponded surface conditions from time zero onwards (Hillel, 1998), and are based on assumptions of uniform movement of water from the surface down through deep homogenous soil with a well-defined wetting front. However, these assumptions are more valid for sandy soils than for clay soils (Haverkamp *et al.*, 1987). They reduce the amount of physical soil data needed from that of numerical solutions, but also limit their applicability under changing initial and boundary conditions (Haverkamp *et al.*, 1987). Equations that are physically based approximations use parameters that can be obtained from soil water properties and do not require measured infiltration data. Thus, they should be able to produce estimates at lower cost than empirical equations.

Other equations are partially or entirely empirical and parameters must be obtained from measured infiltration data or roughly estimated by other means. Empirical equations such as those of Kostiakov (1932) and Horton (1939; 1940) are less restrictive as to mode of water application because they do not require the assumptions regarding soil surface and soil profile conditions that the physically based equations require (Hillel, 1998). Where soils are heterogeneous, and factors such as macropore flow and entrapped air complicate the infiltration process, empirical equations may potentially provide more accurate predictions, as long as they are used under similar conditions to those under which they were formulated. This is because their initial parameters are determined based on actual field-measured infiltration data (Skaggs and Khaleel, 1982; Rawls *et al.*, 1993). One characteristic of infiltration that all the equations predict is an initially rapid decrease in rate with time for ponded surfaces (Skaggs and Khaleel, 1982).

2.6.1.1 Kostiakov Equation

Kostiakov (1932) proposed a simple empirical infiltration equation based on curve fitting from field data. The equation, thus, describes the measured infiltration curve. Under similar soil and initial water content, it allows prediction of an infiltration curve using the same constants developed for those conditions, and also relates infiltration to time as a power function:

$$i = at^{-\beta} \quad (2.11)$$

where,

i = Infiltration rate [LT^{-1}]

t = Time after infiltration starts [T]

α [L] and β [dimensionless] are constants that depend on the soil type, initial moisture content, rainfall rate and vegetative cover and their values are determined from measured infiltration data, since they have no physical interpretation.

Based on this approach, Criddle *et al.* (1956) developed a logarithmic form of equation (2.11):

$$\log i = \log \alpha - \beta \log t \quad (2.12)$$

to determine the parameter values for α and β by plotting $\log i$ against $\log t$. This results in a straight line if the Kostiakov equation is applicable to the data. The intercept of the equation (infiltration rate at time $t = 1$) is $\log \alpha$ and the slope is $-\beta$. The higher the value of $-\beta$, the steeper the slope and the greater the rate of decline of infiltration. On the other hand, the greater the value of α , the greater the initial infiltration value (Naeth *et al.*, 1991).

This equation is extensively used because of its simplicity, ease of determining the two constants from measured infiltration data and reasonable fit to infiltration data for many soils over short time periods (Clemmens, 1983). The major flaws are that it predicts infiltration rate as infinite at t equals zero and approaches zero for long times, whereas, actual infiltration rates approach a steady value (Philip, 1957a; Haverkamp *et al.*, 1987; Naeth *et al.*, 1991). Also, it cannot be adjusted for different field conditions known to have profound effects on infiltration, such as soil water content (Philip, 1957a). Mezencev (1948) and Smith (1972) have provided a modification to the original Kostiakov equation by adding a constant that represents the term of

ultimate infiltrability (i.e. the infiltration rate reached when the soil becomes saturated after prolonged infiltration). This is given in equation (2.13) as follows:

$$i = \alpha t^{-\beta} + i_f \quad (2.13)$$

where,

i_f = Final infiltration rate [LT^{-1}]

The logic for the inclusion of i_f is that, the infiltration rate decreases as more water infiltrates into the soil until a constant rate known as ultimate infiltrability is attained. Thus, the term “final infiltration rate” signifies that the soil infiltration rate has reached a constant value from which it appears to decrease no more, but not the end of the infiltration process (Hillel, 1980).

Israelson and Hanson (1967) also developed the modified Kostiakov (MK) equation and applied it for estimation of irrigation infiltration. Following this, Mbagwu (1993) recommended the modified Kostiakov equation for routine modelling of the infiltration process on soils with rapid water intake rates. Recently, Parhi *et al.* (2007) and Parhi (2014) introduced the revised modified Kostiakov model (RMKM) expressed as:

$$i = \alpha_2 t^{\beta_2} + \alpha_3 t^{-\beta_3} \quad (2.14)$$

where,

$\alpha_2 t^{\beta_2}$ = The time varying infiltration component which after complete saturation of the soil represents the ultimate infiltrability of the soil

$\alpha_3 t^{-\beta_3}$ = The continuously decaying dynamic infiltration component. When added, the resulting infiltration rate corresponds to the infiltrability curve.

$\alpha_2, \beta_2, \alpha_3, \beta_3$ = Empirically determined parameters from observed data using appropriate optimization techniques, such as the least squares approach (Parhi, 2014).

These equations have proven to be the preferred models used for irrigation infiltration, probably because they are less restrictive on the mode of water application than some other models (Turner, 2006).

2.6.1.2 Horton Equation

The Horton model of infiltration (Horton, 1940) is one of the best-known models in hydrology. It recognizes that infiltration rate (i) decreases with time until it approaches a minimum constant rate (i_f). This decrease in infiltration is primarily attributed to factors operating at the soil surface rather than to flow processes within the soil (Xu, 2003). By definition, an exhaustion process is one in which the rate of work performed is proportional to the work remaining to be performed. This definition relates the infiltration rate to the rate of work performed and the change in infiltrability from i to i_f as the work remaining to be performed, with λ as the constant of proportionality (Horton, 1940). According to Horton (1939; 1940), this equation describes a pattern of exponential decay of infiltration rate from this basic relationship:

$$-\frac{di}{dt} = \lambda(i - i_f) \quad (2.15)$$

Dividing both sides of equation (2.15) by $i - i_f$ and multiplying both sides by dt , it yields:

$$\frac{-di}{i - i_f} = \lambda dt \quad \text{KNUST} \quad (2.16)$$

Integration of equation 2.16 gives:

$$\ln(i - i_f) = -\lambda t + u \quad (2.17)$$

where u , is the integral constant. When $t = 0$, $i = i_o$, $u = \ln(i_o - i_f)$, therefore,

$$\ln \frac{i - i_f}{i_o - i_f} = -\lambda t \quad (2.18)$$

or

$$\frac{i - i_f}{i_o - i_f} = e^{-\lambda t} \quad (2.19)$$

The final form of the Horton equation is obtained when both sides of equation 2.18 are multiplied by the denominator on the left hand side followed by addition of i_f to both sides (Turner, 2006):

$$i = i_f + (i_o - i_f)e^{-\lambda t} \quad (2.20)$$

where,

i = Infiltrability or potential infiltration rate [$L T^{-1}$]

i_f = Final constant infiltration rate [L T⁻¹]

i_o = Infiltrability at $t = 0$ [L T⁻¹]

λ = Soil parameter [T⁻¹] that controls the rate of decrease of infiltration and must depend on initial water content, θ_i [L³ L⁻³] and application rate, R [L T⁻¹] t = Time after start of infiltration [T]

KNUST

The parameters, i_f , λ , and i_o must be evaluated from measured infiltration data.

Subtracting i_f from both sides of equation (2.20) and then taking the natural log of each side gives the following equation for a straight line:

$$\ln(i - i_f) = \ln(i_o - i_f) - \lambda t \quad (2.21)$$

When experimental value for i_f is subtracted from those for i and the natural log of the results are plotted as a function of time, λ can be determined from the slope of the line and i_o , from the intercept. Least squares method is also recommended for estimating parameters (Blake *et al.*, 1968).

Integration of Equation (2.20) yields:

$$I = \int_0^{tp} i dt = i_c + \frac{i_o - i_c}{\lambda} [1 - e^{-\lambda t}] \quad (2.22)$$

Horton's equation has advantages over the Kostiakov equation, in that, at $t = 0$, the infiltrability is not infinite but takes on the finite value i_o . Also, as t approaches infinity, the infiltrability approaches a nonzero constant minimum value of i_f

(Horton, 1940; Hillel, 1998).

Although the equation is empirical, in that, λ , i_f and i_o must be calculated from experimental data, rather than measured in the laboratory, it does reflect the laws and basic equations of soil physics (Chow *et al.*, 1988). As a result, it has been widely used to provide a good fit to data. In contrast, it is cumbersome in practice since it contains three constants that must be evaluated experimentally (Hillel, 1998). A further limitation is that it is applicable only when rainfall intensity exceeds i_f (Rawls *et al.*, 1993). Again, this approach has been criticized because it neglects the role of capillary potential gradients in the decline of infiltrability over time; attributes control almost entirely to surface conditions (Beven, 2004); and assumes that hydraulic conductivity is independent of the soil water content (Novotny and Olem, 1994).

2.6.1.3 Holtan Equation

Holtan (1961) described an empirical equation based on a storage concept in order to provide a means by which infiltration could be estimated using information that is generally available or could be readily obtained for major soils (Holtan and Creitz., 1967). The premise of the equation is that the factors with greatest influence over infiltration rate are soil water storage, surface connected porosity, and the effect of plant root paths (Rawls *et al.*, 1993). After several modifications, the final form of the equation is written as (Holtan and Lopez, 1971):

$$i = GlaSA^{1.4} + i_f \quad (2.23)$$

where,

i = Infiltration rate at given time [$L T^{-1}$]

SA = Available storage in the surface layer (“A” horizon) at a given time [L]

GI = Growth index of crop in percent of maturity a = Index of surface connected porosity (in h^{-1} per $(in)^{1.4}$ of storage). This is a function of surface conditions and density of plant roots

i_f = Constant or steady state infiltration rate [$L T^{-1}$] estimated from the soil hydrologic group in the equation

SA is computed from the relation:

$$SA = (\theta_s - \theta_i)d \quad (2.24)$$

where,

θ_s = Saturated water content of the soil [L^3L^{-3}]

θ_i = Initial volumetric water content of the soil [L^3L^{-3}]

d = Depth of the surface layer [L]

A serious setback to this equation is the determination of the control depth on which to base SA . Considering this, Holtan and Creitz (1967) recommended this depth to be the plough layer or to the first impeding layer or depth of the A horizon provided. However, Smith (1976) argued that infiltration curves are physically much more closely related to moisture gradients and hydraulic conductivity than to soil porosity, therefore, it cannot be expected to adequately describe the infiltration process. However, some studies have shown a strong relationship between infiltration rate and soil porosity (Messing *et al.*, 2005; Kozak and Ahuja, 2005). Also, the equation has also been found to be not directly related to any reference time which makes the

determination of $i(t)$ difficult. In this context, realizing that infiltration rate is a function of the available water storage, the infiltration equation must always be accompanied by a simultaneous solution of the storage equation (Turner, 2006).

2.6.1.4 SCS-Model

The SCS model (1972) is an empirically developed approach to the water infiltration process (Jury *et al.*, 1991), as follows:

$$i = ut^b + 0.6985 \quad (2.25)$$

where,

u and b = constants determined from observed infiltration data.

2.6.1.5 Swartzendruber Equation

Swartzendruber (1987) provided a series solution that holds for small, intermediate and large time, and allows for surface ponding. Its starting point is similar to the GA approach; however, its derivation does not require a step function for the wetted soil profile. In its simplified form, it behaves as a three-parameter infiltration equation given as:

$$I = i_f t + \frac{S}{A_o} [1 - \exp(-A_o t^{0.5})] \quad (2.26)$$

where,

i_f = Final infiltration rate [LT^{-1}]

S and A_o = Empirical constants

The constant A_o is a fitting parameter which value depends on the surface water content. As $A_o \rightarrow \infty$, it reduces to a form of the Philip (1957b) equation with i_f as the coefficient of the linear term, and for which dI/dt approaches i_f as $t \rightarrow \infty$. Concerning the G-A model, the S -term can be corrected using Equation (2.42) to account for ponded conditions.

KNUST

2.6.1.6 Philip Equation

Philip (1957a) developed an infinite-series solution to solve the non-linear partial differential Richards' equation (Richards, 1931), which describes transient fluid flow in a porous medium for both vertical and horizontal directions. This rapidly converging series solves the flow equation for a homogeneous deep soil with uniform initial water content under ponded conditions. For cumulative infiltration, the general form of the infiltration model is expressed in powers of the square-root of time, t , as:

$$I = St^{0.5} + K_{o1}t + K_{o2}t^{3/2} + \dots \quad (2.27)$$

where,

I = Cumulative infiltration [L]

S = Sorptivity [$L T^{-0.5}$], a function of initial and final soil water content (θ_i and θ_f).

K_{o1}, K_{o2} = Constants that depend on both soil properties and on θ_i and θ_f .

For one-dimensional vertical infiltration, K_o is proportional to the soil's saturated hydraulic conductivity (K_s). The ratio K_o/K_s is ≤ 1 , depending on soil type and soil moisture (Philip, 1990), with proposed ranges of $1/3 \leq K_o/K_s \leq 2/3$ (Fuentes *et al.*,

1992) or $0.3 \leq K_o/K_s \leq 0.4$ (Philip, 1990). In the case of three-dimensional infiltration, K_o incorporates both saturated hydraulic conductivity and sorptivity (Smettem *et al.*, 1995; Touma *et al.*, 2007).

Naturally, infiltration occurs over intermediate or transient timescales (neither exclusively early- nor late-time) and is three-dimensional. One such example is infiltration from an axisymmetric single ring source, which can provide a rapid and low-cost measurement of soil hydraulic properties (Braud *et al.*, 2005). However, interpretation of these infiltration tests often requires that the S and K_o terms both be considered (Stewart *et al.*, 2013). Methods to differentiate between sorptivity and saturated hydraulic conductivity for such infiltration conditions have been proposed (e.g. Smiles and Knight, 1976; Smettem *et al.*, 1995; Vandervaere *et al.*, 2000), but may be inadequate for estimating small K_s values (Smettem *et al.*, 1995). With reference to equation (2.27), the time derivative of I (infiltration rate), which is i [L T⁻¹] is given by:

$$i = \frac{1}{2} S t^{-0.5} + K_{o1} + \frac{3}{2} K_{o2} t^{0.5} + \dots \quad (2.28)$$

For horizontal infiltration (i.e. no gravity driven flow), all terms are zero except for the first term on the right side of equations (2.27) and (2.28) and the equations apply to all times greater than zero. For vertical infiltration, (2.27) and (2.28) apply only for a short time when the matric-potential gradient is much greater than the gravity potential gradient (Sullivan *et al.*, 1996). All terms beyond the first two on the righthand side of equations (2.27) and (2.28) are considered to be negligible (Jury *et*

al., 1991). Following this, Philip (1957b) proposed that by shortening the series solution for infiltration from a ponded surface after the first two terms, a concise infiltration rate equation could be obtained as follows:

Under constant head conditions, one- and three-dimensional vertical infiltration into a uniform soil can be adequately described using Philip (1957b) two-term approximation:

$$I = St^{0.5} + K_o t \quad (2.29)$$

Therefore,

$$i = \frac{S}{2} t^{-0.5} + K_o \quad (2.30)$$

where,

i = Infiltration rate [L T⁻¹]

S = Sorptivity [L T^{-0.5}].

t = Time after start of infiltration [T]

K_o = Constant infiltration rate [L T⁻¹] or apparent hydraulic conductivity

This shortened form of the equation is very similar to that of Kostiakov. In actual fact, it is basically the same as the modified Kostiakov equation with $\alpha = 0.5$. The parameters S and K_o , which are dependent on the soil and the initial water content, can be evaluated numerically if the properties of diffusivity and pressure head as functions of soil water content are known. However, this equation predicts values of infiltration rates that are too low for long time periods, because the approximation made is not physically consistent. As t approaches infinity, the infiltration rate should

approach a constant rate (satiated hydraulic conductivity, i.e., $K_s \approx K_o$), but this is impracticable (Philip, 1957b; Youngs, 1968; Skaggs *et al.*, 1969). In view of this, Philip (1957b) and Talsma (1969) proposed that the value of the steady state infiltration rate, K_o , that results from using this equation is approximately $K_s/3$. Again, a comparison of this model with the Green and Ampt equation approximates that, $K_o = 2/3K_s$ (Philip, 1957b; Youngs, 1968).

Philip (1957b) and Touma *et al.* (2007) defined sorptivity (S) as the measurable physical quantity that expresses the capacity of a porous medium for capillary uptake and release of a liquid. Thus, it is a function of the capillarity (the driving force) and the soil's hydraulic conductivity (the dissipation). Considering this, sorptivity is described as an integral property of the soil hydraulic diffusivity (White and Perroux, 1987), and is regarded as constant, provided the water content at the inflow end is constant (Jury *et al.*, 1991). At early times (i.e., $t \ll S^2/K_o^2$), sorptivity dominates the infiltration behaviour, and for very early times ($t \rightarrow 0$), the second term on the right hand side of equation (2.29) may be neglected (White *et al.*, 1992). Conversely, the second term dominates as time increases, subject to the limit of $t = S^2/K_o^2$, when the series expansion from which equation (2.29) was derived is no longer accurate.

Alternate expressions have been developed to describe long-time (steady-state) infiltration behaviour (Philip, 1957a, b; Wooding, 1968; Haverkamp *et al.*, 1994), which lend themselves to estimations of K_s . However, the time required to reach late-time or quasi-steady state conditions may be impractical, particularly for soils with low hydraulic conductivity, and assumptions of homogeneity are typically violated for long infiltration experiments.

A shortcoming of the Philip infiltration model is that the assumptions for which the equation is applicable are rarely found in the field on a large scale. Soil types vary spatially (vertical and horizontal), as do vegetation and surface conditions. Although parameter values can be obtained by making point measurements in the field, variability limits the worth of test results for application to larger areas such as watersheds (Sullivan *et al.*, 1996). Additionally, Whisler and Bouwer (1970) found that determining the values of the parameters S and K_o from soil physical properties was very time consuming and yielded results that were not in agreement with the experimental curve. However, they were able to obtain close agreement with experimental values when the parameters were determined by curve fitting, but the physical significance of the parameters was ignored. Accordingly, Smiles and Knight (1976) suggested that the appropriateness of infiltration data to the 2-parameter Philip equation can be determined by plotting $It^{-0.5}$ as a function of $t^{0.5}$. When both sides of equation (2.29) are divided through by $t^{0.5}$, an equation for a straight line is obtained as:

$$It^{-0.5} = S + K_o t^{0.5} \quad (2.31)$$

The linearity of this curve for early times indicates that equation (2.31) is appropriate for describing the infiltration process and the values for S and K_o can be determined from the y-intercept and slope of the line, respectively. However, when used in this manner, the equation is empirical rather than physically based, although it is derived from physical theory.

2.6.1.7 Smith and Parlange Equation

Smith and Parlange (1978) derived an infiltration equation for arbitrary rainfall rates from the Richards' equation. Both time-to-ponding and infiltrability after ponding can be predicted from this model. It requires only two parameters which may be calculated from measurable soil properties or determined from infiltrometer experiments to make predictions. For soils in which hydraulic conductivity is a function of soil water content and varies slowly near saturation, time-to-ponding may be evaluated by:

$$\int_0^{t_p} R dt = \frac{S^2/2}{R_p - K_s} \quad (2.32)$$

where,

R = Rainfall rate [$L T^{-1}$]

t = Time [T]

R_p = Rainfall rate at time-to-ponding [$L T^{-1}$]

K_s = Saturated hydraulic conductivity [$L T^{-1}$]

θ_i = Initial volumetric soil water content [$L^3 L^{-3}$]

S = Sorptivity [$L T^{-0.5}$] (Philip, 1957a,b)

When hydraulic conductivity varies rapidly near saturation, the equation can be written as:

$$\int_0^{t_p} R dt = \frac{S^2/2}{K_s} \ln \left[\frac{R_p}{R_p - K_s} \right] \quad (2.33)$$

The dual-dependence of sorptivity on capillarity and hydraulic conductivity (Philip, 1957b; Touma *et al.*, 2007) is evident in the exact solution for sorptivity by Parlange (1975):

$$S^2 = (\theta_s - \theta_r)^2 \int_{\theta_o}^{\theta_f} (\theta_f - \theta - 2\theta_o) D(\theta) d\theta \quad (2.34)$$

Haverkamp *et al.* (1990) have given the modified form of equation (2.34) for positive ponded conditions as:

$$S^2 = 2K_s(\theta_s - \theta_r)(1 - \theta_o)h_o + (\theta_s - \theta_r) \int_{h_i}^0 (1 + \theta - 2\theta_o) K(h) dh \quad (2.35)$$

where,

θ_f = Final volumetric soil water content [L^3/L^3]

θ_r = Residual moisture content [L^3/L^3]

θ = Degree of saturation [Dimensionless] given by:

$$\theta = \frac{\theta_i - \theta_r}{\theta_s - \theta_r}$$

h_o = Depth of ponding at the surface [L] h_i

= Initial matric potential [L]

$K(h)$ = Hydraulic conductivity as a function of soil matric potential [L/T]

When diffusivity varies slowly near saturation, the value of S^2 may be estimated as:

θ_s

$$S^2 = 2 \int_{\theta_i}^{\theta_s} (\theta_s - \theta_i) D d\theta \quad (2.36)$$

However, when diffusivity varies rapidly near saturation, the value of S^2 may be estimated as:

$$S^2 = 2(\theta_s - \theta_i) \int_{\theta_i}^{\theta_s} D d\theta \quad (2.37)$$

2.6.1.8 Green and Ampt Equation

The Green-Ampt (1911) theory considers water to move downwards as piston displacement profile or plug flow. The equation was derived for infiltration from a ponded surface into a deep homogeneous soil with uniform initial water content. Subsequently, it has been found to apply best to infiltration into uniform, initially dry, coarse textured soils which exhibit a sharply defined wetting front (Fig. 2) (Hillel and Gardner, 1970). In this context, the transmission zone can be defined as a region of nearly constant water content above the wetting front, which extends as infiltration proceeds. The wetting front, however, is characterized by a constant matric suction, regardless of time or position, and is viewed as a plane of separation between the uniformly wetted infiltrated zone and the as-yet totally uninfiltated zone (Hillel, 1998). These assumptions simplify the flow equation so that it can be solved analytically.

Although measured infiltration data are not required to make predictions using the Green and Ampt (G-A) equation, it is recommended that soil physical properties

should be measured in the field, so that undisturbed field conditions reflect in the resulting data (Green and Ampt, 1911).

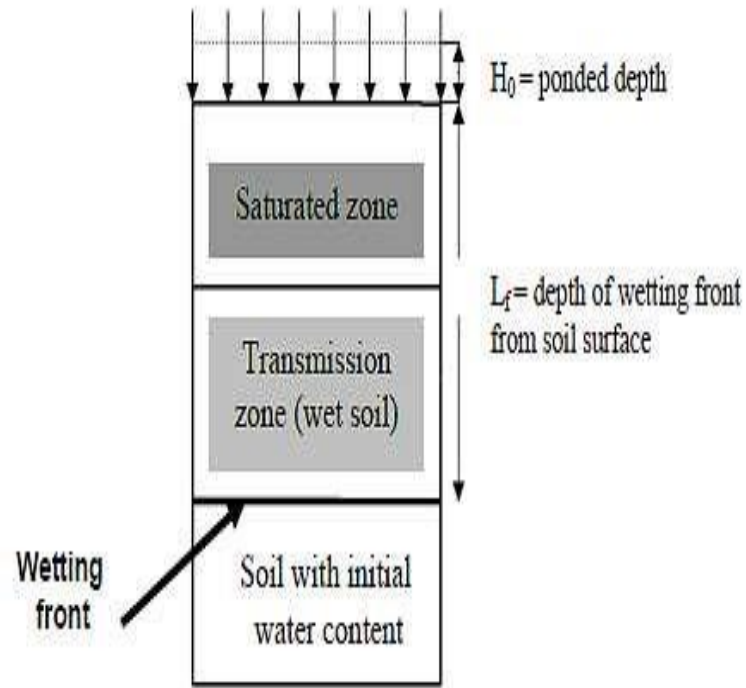


Figure 2.2: Illustration of uniform water entry assumption: transmission zone, and sharply defined wetting front.

From direct application of Darcy's Law, the G-A equation for infiltration rate was formulated as:

$$i = K \left[\frac{h_o + (L_f - h_f)}{L_f} \right] \quad (2.38)$$

where,

i = Infiltration rate [$L T^{-1}$]

K = Hydraulic conductivity of the transmission (wetted) zone [$L T^{-1}$]

h_o = Ponding depth [L] h_f = Suction (negative pressure head) at the

wetting front [L]

L_f = Depth to wetting front [L]

As the wetting front advances with depth, the value of h_f becomes relatively insignificant compared to L_f and the infiltration rate (i) approaches the K value of the transmission zone. In this way, ponding depth is seen to mostly affect infiltration at the beginning when L_f is small. However, as infiltration progresses and L_f increases, the effect of ponding depth decreases and eventually becomes negligible when L_f is sufficiently deep (Bouwer, 1976). Again, due to air entrapment in the soil pores, the hydraulic conductivity parameter is not the conductivity at full saturation, but is instead the conductivity at residual air saturation (Bouwer, 1966; 1969), also referred to as 're-saturated hydraulic conductivity' (Whisler and Bouwer, 1970). In this regard, measurement of K in the field has been described by air-entry permeametry, however, when field measurements are not feasible, an approximation of $K = 0.5K_s$ has been proposed (Bouwer, 1966), where K_s is the laboratory value for saturated hydraulic conductivity.

From the continuity equation, the cumulative infiltration amount, I [L] could be expressed as:

$$I = (\theta_s - \theta_i)L_f = \Delta\theta L_f \quad (2.39)$$

where,

θ_s = saturated moisture content of the soil [$L^3 L^{-3}$]

θ_i = actual volumetric moisture content of the soil (initial water content before infiltration began) [$L^3 L^{-3}$]

$\Delta\theta$ = Moisture deficit (or the difference between saturated and initial volumetric water contents) [$L^3 L^{-3}$] and assuming a very shallow depth of ponding so that $h_o \approx 0$, equation (2.39) may be rewritten as:

$$i = K + \frac{K\Delta\theta h_f}{I} \quad (2.40)$$

Although the G-A model assumes total saturation behind the wetting front, Philip (1954) detected that it is not a necessary requirement and, therefore, suggested that θ_s should be constant, but not necessarily equal to the total porosity, and also, K should be slightly less than K_s . When $i = \frac{dI}{dt}$ is substituted into Equation (2.40) and integrated with the assumption that $I = 0$ at $t = 0$:

$$Kt = I - \Delta\theta h_f \ln \left(1 + \frac{I}{\Delta\theta h_f} \right) \quad (2.41)$$

This form of the equation relates infiltration volume to time from start of infiltration, which is convenient for some applications. Regardless of the many assumptions under which the G-A equation was originally formulated, it has been adapted for use under a much wider variety of conditions (Turner, 2006). For instance, it has produced reasonably good predictions for non-uniform soil profiles that become denser with depth (Childs and Bybordi, 1969), for profiles where hydraulic conductivity decreases with depth or increases with depth (Bouwer, 1969; 1976), and for soils with partially sealed surfaces (Hillel and Gardner, 1970). Bouwer (1969;

1976) described a tabular procedure for calculating the G-A relationship between cumulative infiltration and time for soils with non-uniform initial water contents and hydraulic conductivities. The results showed that the soil profile could be split into layers, each with its own water content, moisture deficit, and hydraulic conductivity from which the G-A approach could be used to calculate cumulative infiltration and time intervals.

The G-A (1911) equation has also provided a simpler definition of sorptivity (Stewart *et al.*, 2013):

$$S^2 = \frac{2K_s(\theta_s - \theta_r)(1 - \theta_o)(h_f - h_o)}{\varphi} \quad (2.42)$$

where, h_f = Wetting front potential, which is also referred to as the effective capillary drive (Morel-Seytoux *et al.*, 1996), capillary pull, or macroscopic capillary length (White and Sully, 1987).

h_o = Ponding depth [L]

θ_o = Zero moisture content (dry conditions)

φ = Correction factor, which accounts for deviations from a sharp wetting front and/or viscous damping effects. For example, $\varphi = 1$ for a G-A (1911) solution, 1.11.7 for the Morel-Seytoux and Khanji (1974) solution and 1.1 for the White and Sully (1987) solution.

Sorptivity measurements can be used to quantify hydraulic conductivity since the latter is embedded in the former (Stewart *et al.*, 2013). One such approach is to utilize field-based sorptivity measurements in conjunction with variations of the traditional

sorptivity model equation (2.42) to quantify K_s (White and Perroux, 1987; 1989). Stewart *et al.* (2013) have also developed a relation (equation 2.43), which allows for early-time infiltration data, typical of measurements obtained from single-ring tests, to be used to estimate K_s :

$$K_s = \left(\frac{S^2 \alpha \varphi}{(\theta_s - \theta_r)(1 - \gamma \theta_o)} \right) \left(\frac{1 + 4.7m + 16m^2}{0.092m + 4.14m^2 + 39m^3} \right) \quad (2.43)$$

where,

m = Subject to the constraint $m = 1 - 1/n$ (i.e., the van Genuchten-Maulem model).

The initial and boundary conditions were set as $\theta = \theta_s$ and no flux, respectively. For early times, when the water content of the final boundary varied by $< 1\%$, sorptivity was calculated from the water flux (i), through the origin by using $S = 2i(t^{0.5})$. The scaling parameter φ was assumed to be 1 and γ was assumed to be 1.025. However, estimates of initial soil moisture and the soil's wetting front potential are essential for this approach. Solutions exist to quantify wetting front potential in dry soils ($\theta_o = 0$) (e.g. Rawls *et al.*, 1992; Morel-Seytoux *et al.*, 1996), given that the parameters of a water retention function are known.

2.7 Infiltration ponds

Storm water infiltration facilities are designed and built to reduce the hydrologic impacts of residential and commercial development. These facilities, which include ponds, dry wells, infiltration galleries and swales are intended to capture and retain runoff and allow it to infiltrate rather than to discharge directly to surface water (Massmann, 2003). Increased runoff resulting from impermeable surfaces may result in the destabilization of stream channels and degradation of fish and wildlife habitat

(Massmann, 2003). Additionally, impervious surfaces prevent rainwater from seeping into the ground and recharging streams, wetlands, and aquifers (Ferguson, 1994). Thus, important benefits of groundwater infiltration facilities include reducing surface runoff volume, reducing pollutant discharge, reducing thermal impacts on fisheries, increasing groundwater recharge, and enhancing low-flow stream conditions (Duchene *et al.*, 1992).

The formation of a clogging layer on the surface of infiltration ponds is a common occurrence within the wetted perimeter. This may be caused by the accumulation of silt, clay, or other fine material that was suspended in the water entering the recharge basin. Additionally, growth of algae on the bottom or in the water, precipitation of calcium carbonate in the water due to increases in pH caused by algae activity, and biological activity on the wetted perimeter (McDowell-Boyer *et al.*, 1986; Bouwer and Rice, 1989; Bouwer, 2002). With the occurrence of deep penetration of particles, the effectiveness of surface cleaning can be greatly reduced, which can result in irrecoverable losses in infiltration capacities (Rehg, 2005). Additional suspended solids can be introduced to a spreading facility by erosion, wave action, and windborne dust. When suspended solids in the influent water are relatively high, the clogging caused by these additional factors is secondary to the clogging caused by the accumulation of solids in the influent water.

When recharging water with low suspended solids, these factors dominate physical clogging processes. To address this problem, it is recommended to design recharge facilities to minimize the impact of erosion or wave action (Bouwer, 2002).

Furthermore, Massmann (2003) recommended that infiltration ponds are constructed well above the water table.

2.8 Hyper-concentrated flows and sediment transport

Different definitions of hyper-concentrated flow have been presented by different researchers. For instance, Pierson (2005) defined hyper-concentrated flows to occur between two limits. At the lower limit, water transports sediment in such quantities that the sediment has negligible effect on flow behaviour and the fluid remains Newtonian. However, at the higher limit, high-discharge debris flows and mudflows transport much more sediment than water can carry. For such cases sediment concentrations are often in excess of 60% by volume and 80% by weight. Morris and Fan (1998) also defined hyper-concentrated flows as sediment-water mixtures having a sediment concentration high enough that the particles interact with one another to create a structural lattice within the fluid of sufficient strength to affect characteristics such as velocity distribution within the flow and particle settling rates. The behaviour of the mixture departs significantly from that of clear water, a Newtonian fluid, and is usually described based on the characteristics of a Bingham fluid. High concentrations of cohesive sediments can significantly affect the behaviour of the sediment-water mixture as it flows in rivers and enters or exits reservoirs (Yang et al., 1996; Morris and Fan, 1998).

For the reason that the hyper-concentration threshold depends on factors including grain size distribution and mineralogy, the threshold concentration will not necessarily be the same in other river systems. Hyper-concentrated flows may be generated during reservoir flushing in river systems that otherwise never experience

hyper-concentration (Morris and Fan, 1998). High concentration flows can produce extremely rapid and large changes in the configuration of erodible channels in rivers and reservoirs. Hyper-concentrated floods cause the cross section to become narrower and deeper with the creation of lateral berms. Because of the high sediment concentration, they can also cause rapid channel aggradation.

Over the past six (6) decades, there has been increased technological development in agriculture in terms of yields, use of agrochemicals and machinery. Combined with this development are the negative side effects such as increased eutrophication, erosion and/or sediment delivery into streams (Krammer and Strauss, 2014). Thus, streams in intensively used agricultural catchments are frequently characterised by increased transport of suspended sediments during rainfall events, which may significantly affect the water quality (Bečvář, 2006; Eder *et al.*, 2010; Krammer and Strauss, 2014). As a result, sediments and nutrients washed out from farmed lands into rivers and reservoirs are one of the major environmental problems worldwide (Zumr *et al.*, 2014). Sediment concentrations are event based and they vary considerably between events, which makes the evaluation of land use change on sediment behaviour difficult (Lewis, 1996; Ulaga, 2005; Krammer and Strauss, 2014). Additionally, measurements of sediment concentrations are rare, however, understanding the routing of the precipitated water and sediment, its pathways and residence time on the surface and in the subsurface are important prerequisites for soil and water management, floods and nutrient control (Krammer and Strauss, 2014; Zumr *et al.*, 2014).

2.9 Sediment transport equations

Bed material load consists of coarse material in the streambed which is mobilized by flowing water, and may be transported either in suspension or as bed load. Bed material transport for selected grain sizes may be supply limited when transport energy exceeds the supply of material of a transportable size (Morris and Fan, 1998). However, when there is an ample supply of transportable material on the streambed, the rate of sediment movement is transport-limited and is determined by the available hydraulic energy in the stream (Morris and Fan, 1998).

Equations describing the capacity of flowing water to transport bed material are categorised into two broad groups – Bed load equations, which describe the amount of material transported as bed load, and total load equations, which actually describe the "total bed material load," which includes bed material transported in suspension plus the bed load (Simons and Senturk, 1992; Yang, 1996; Morris and Fan, 1998). The total bed material load is normally the measure of interest in stream transport studies. Wash load concentration and transport rate cannot be predicted from hydraulic conditions in the stream, but depend on the rate of erosion in source areas and delivery rate of fine sediment to stream channels (ASCE, 1982; Morris and Fan, 1998). Unlike hydraulic equations (e.g., Chezy, Manning and Darcy-Weisbach) which give approximately equivalent results, the application of different sediment transport equations to the same dataset can generate estimates of transport rates ranging over more than 2 orders of magnitude (Morris and Fan, 1998).

2.9.1 Ackers and White equation

Ackers and White related the weight concentration of bed material load C_s to the mobility function F_g by the equation:

$$C_s = \sigma G_s \frac{d}{R_H} \left(\frac{V}{U_o} \right)^\epsilon \left(\frac{F_g}{\epsilon} - 1 \right)^\vartheta \quad (2.44)$$

where,

G_s = Specific gravity of sediment

ϵ , σ , and ϑ are coefficients

V = Mean flow velocity within a single vertical or across an entire cross section, in

which case:

$$V = Q/A \text{ [L/T]}$$

A = Area of the wetted hydraulic cross section [L^2]

Q = Total discharge [L^3/T]

The mobility number F_g is computed as:

$$F_g = \frac{U_o^\epsilon}{[gD(G_s - 1)]^{1/2}} \left[\frac{V}{(32)^{1/2} \log(10R_H/D)} \right]^{1-\epsilon} \quad (2.45)$$

Sediment size is expressed by a dimensionless grain diameter d_* .

where,

g = Gravitational constant, 9.81 m/s^2

D = Particle diameter [L]. When subscripted, it refers to the size on the grain size curve. Thus, D_{90} refers to the diameter of the particle larger than 90 weight-percent of the particles in the mixture

R_H = Hydraulic radius [L] computed as:

$$R_H = A/P$$

It may be conceptualized as the average depth of flow over the frictional boundary.

In a channel which is much wider than deep, the hydraulic radius is closely approximated by the water depth and the assumption that $R_H = d$ is made frequently

P = Perimeter of the wetted hydraulic cross section [L]

U° = Shear velocity or friction velocity, is a measure of the intensity of turbulent fluctuations [L/T], given as (Morris and Fan, 1998):

$$U^\circ = (gR_H S^E)^{1/2} = (\tau/\rho)^{1/2} \quad (2.46)$$

2.9.2 Engelund and Hansen

The equation developed by Engelund and Hansen may be expressed in the following form (Vanoni, 1975; Morris and Fan, 1998):

$$q_s = 0.05\gamma_s V^2 \left[\frac{D_{50}}{g(\gamma_s/\gamma - 1)} \right]^{1/2} \left[\frac{\tau_0}{(\gamma_s - \gamma)D_{50}} \right]^{3/2} \quad (2.47)$$

where,

q_s = Discharge per unit width of channel [L^3/T]

γ = Specific weight [N/L^3], given as:

$$\gamma = \rho g$$

γ_s = Specific weight of sediment [N/L^3]

$\tau_0 = \gamma R_H$ = Tractive force

ρ = Density or mass per unit mass [M/L^3]

D_{50} = Diameter of the particle larger than 50 weight-percent of the particles in the mixture [L]

This equation is dimensionally homogeneous and can be solved using any set of homogeneous units.

2.9.3 Yang's Equation for Sand Transport

Yang (1983) observed that most sediment transport equations for bed load or total bed material load are based on correlating sediment transport to a single hydraulic variable using one of the following basic forms (Yang, 1996):

$$q_s = \forall(Q - Q_{CR})^\phi \quad (2.48)$$

$$q_s = \forall(V - V_{CR})^\phi \quad (2.49)$$

$$q_s = \forall(S^E - S_{CR}^E)^\phi \quad (2.50)$$

$$q_s = \forall(\tau - \tau_{CR})^\phi \quad (2.51)$$

$$q_s = \forall(\tau V - \tau_{CR} V_{CR})^\phi \quad (2.52)$$

$$q_s = \forall(V S^E - V_{CR} S_{CR}^E)^\phi \quad (2.53)$$

where,

q_s = Discharge per unit width of channel [L^3/T]

S^E = Energy or water surface slope

τ = Bed shear stress

$\tau V = (\gamma D S^E) V$ = Stream power per unit bed load

V_{CR} = Cross-section velocity at the critical condition

S_{CR}^E = Energy or water surface slope at the critical condition

VS^E = Unit stream power, defined as the time rate of energy dissipation per unit weight of water computed as the product of mean velocity and slope.

∇ and \emptyset = Parameters related to hydraulic and sediment conditions and having different values in each equation.

A transport relation was developed based on the rate of energy expenditure per unit weight of water, which is defined as the unit stream power and is computed as the product of velocity and slope, VS^E . The equation has the basic form:

$$\log C_{ppm} = F + J \log \left(\frac{VS^E}{V_s} - \frac{V_{CR}}{V_s} \right) \quad (2.54)$$

where,

C_{ppm} = Bed material sediment concentration, excluding wash load (in ppm)

F and J = Dimensionless parameters related to flow and sediment characteristics

V_s = Terminal fall velocity of a sediment particle in a quiescent fluid [L/T]

Subscript 's' = Sediment

Subscript 'CR' = Critical condition of incipient motion

Using regression analysis, Yang (1973) developed the following equation for sand transport:

$$\log C_{ppm} = 5.435 - 0.286 \log \frac{V_s D_m}{\mu} - 0.457 \log \frac{U_o}{V_s} + \left(1.799 - 0.409 \log \frac{V_s D_m}{\mu} - 0.314 \log \frac{U_o}{V_s} \right) \log \left(\frac{VS^E}{V_s} - \frac{V_{CR} S^E}{V_s} \right) \quad (2.55)$$

where,

C_{ppm} = Total sand concentration (ppm by weight)

D_m = Median particle diameter

μ = Kinematic viscosity [L^2/T], defined as:

$$\mu = \omega / \rho$$

ω = Dynamic viscosity of fluid [NT/L^2]

$V_{CR}S^E$ = Critical unit stream power at incipient motion computed from Yang (1973; 1996) as follows:

$$\frac{V_{CR}}{V_s} = \frac{2.5}{\log(V_*d/\mu) - 0.06} + 0.06 \quad (2.56)$$

where,

V_{CR}/V_s = Dimensionless critical velocity defined as the ratio of the average cross-section velocity at the critical condition to the terminal particle fall velocity for the grain size of interest. This ratio was then related to Re^* , the shear velocity Reynolds number (dimensionless), by experimental data to obtain Equation (2.56) for the hydraulically smooth and transition zones. For the hydraulically rough region, on the other hand, the relationship is:

$$\frac{V_{CR}}{V_s} = 2.05 \quad (2.57)$$

Equation (2.57) states that in the turbulent range, for $Re^* > 70$, particles on a bed will begin moving when the average velocity is twice the particle settling velocity. For sediment concentrations more than 100 ppm by weight, the incipient motion criteria can be eliminated without affecting the accuracy of the equation, resulting in (Yang, 1979):

$$\log C_{ppm} = 5.165 - 0.153 \log \frac{V_s D_m}{\mu} - 0.297 \log \frac{U_o}{V_s} + \left(1.780 - 0.60 \log \frac{V_s D_m}{\mu} - 0.480 \log \frac{U_o}{V_s} \right) \log \left(\frac{V S^E}{V_s} \right) \quad (2.58)$$

2.9.4 Yang Equation for Gravel

A gravel transport equation was proposed by Yang (1984) and is given as:

$$\log C_{ppm} = 6.681 - 0.633 \log \frac{V_s D_m}{\mu} - 4.816 \log \frac{U_o}{V_s} + \left(2.784 - 0.305 \log \frac{V_s D_m}{\mu} - 0.282 \log \frac{U_o}{V_s} \right) \log \left(\frac{V S}{V_s} - \frac{V_{CR}}{V_s} \right) \quad (2.59)$$

where,

C_{ppm} = Total gravel concentration (ppm by weight)

D_m = Median particle diameter

2.9.5 Yang Modification for Water-Sediment Mixtures

The previous equations have been derived for sediment transport in essentially clear water, however, these equations must be modified for use with other fluids, or for conditions in which there is an extremely high sediment concentration in the water which requires the modification of fall velocity, kinematic viscosity and relative specific weight. Extremely high suspended-sediment concentrations and hyperconcentrated flows can occur in some river systems and can also occur during reservoir flushing (Morris and Fan, 1998). Based on this, Yang (1996) introduced a modification of the sand transport equation to include the characteristics of the watersediment mixture, using the Yellow River in China as an example. The effect

of sediment concentration on fall velocity of fine sands in the Yellow River was therefore, estimated from (Yang, 1996):

$$V_{sm} = V_s(1 - C_v)^7 \quad (2.60)$$

where,

C_v = Sediment concentration by volume, including wash load

V_{sm} and V_s = Sediment fall velocity in the mixture and in clear water, respectively

The kinematic viscosity is a function of temperature, sediment concentration and size distribution. The expression for the kinematic viscosity of water-sediment mixtures for the grain size distribution is (Morris and Fan, 1998):

$$\mu_m = \frac{\rho_w}{\rho_m} e^{5.06C_v} \quad (2.61)$$

where,

ρ_w and ρ_m = Densities of clear water and water-sediment mixture, respectively
[M/L³]

μ_m = Kinematic viscosity of the mixture [L²/T]

The density of the mixture is expressed as:

$$\rho_m = \rho + (\rho_s - \rho)C_v \quad (2.62)$$

When modified to integrate these effects, Yang (1979) equation for sand transport (Equation 2.58) is expressed as:

$$\log C_{ppm} = 5.165 - 0.153 \log \frac{V_{sm} D_m}{\mu_m} - 0.297 \log \frac{U_o}{V_{sm}} + \left(1.780 - 0.360 \log \frac{V_{sm} D_m}{\mu_m} - \right.$$

$$0.480 \log \left(\frac{U_o}{V_{sm}} \right) \log \left(\frac{\gamma_m}{\gamma_s - \gamma_m} \frac{V_{SE}}{V_{sm}} \right) \quad (2.63)$$

where,

γ_m = Specific weight of water-sediment mixture [N/L³]

2.10 Model performance evaluation and selection

A great number of statistical measures are available for evaluating the performance of a model. Thus, several approaches exist for the selection of a suitable model. Among the common forms such as correlation coefficient, relative error and standard error (Nash and Sutcliffe, 1970), efficiency is most frequently used (Mishra and Singh, 2003; Parhi *et al.*, 2014). Among the simplest approaches is the minimisation of the difference between observed and predicted data to find the best model. For example, a model with higher coefficient of determination (R^2) may be preferred more than one with smaller R^2 . In view of this, Gifford (1976), Davidroff and Selims (1986) and Machiwal *et al.* (2006) used the R^2 to compare infiltration models. Mishra *et al.* (2003) on the other hand, examined the suitability of infiltration models with the coefficient of efficiency. Turner (2006), Igbadun and Idris (2007), Ghorbani Dashtaki *et al.* (2009) and Zolfaghari *et al.* (2012) used R^2 , Absolute Mean Difference (AMD) and the Mean Root Mean Square Error (MRMSE) to select the best infiltration model.

According to Mirzaee *et al.* (2013), increasing the number of parameters generally improves the model performance. This occurs at the expense of a corresponding increase in the possibility of over-parameterization. The infiltration models described herein require between two and four fitting parameters. Hence, a better approach would be to define the optimum model as the model that fits data well with the least

number of fitting parameters at the same conditions. In this regard, additional criteria for model comparison that have a penalty for additional fitting parameters is required.

As a result, several researchers have used this kind of criteria for selecting the best model. For instance, the F-statistic (Green and Carroll, 1978) was used to compare model goodness-of-fit to soil moisture characteristic data by Vereecken *et al.* (1989). Buchan *et al.* (1993) also applied the F-statistic and the Cp statistic of Mallows (1973) to find the best-fit particle-size distribution model. Minasny *et al.* (1999) and Chen *et al.* (1999) used the Akaike Information Criterion (AIC) (Carrera and Neuman 1986) to select the best predictive function of soil-moisture characteristic and the best soil hydraulic function, respectively. Hwang *et al.* (2002) used the F-, Cp and AIC statistics to compare model fit to particle-size distribution data. Recently, Mirzaee *et al.* (2013) used five goodness-of-fit statistics (R^2 , F, Cp, AIC and RMSE) to evaluate model performance.

CHAPTER THREE

3.0 MATERIALS AND METHODS

3.1 Description of soil

Nta series or Gleyic Arenosol (FAO-UNESCO, 1988) obtained from the Department of Horticulture, KNUST was used for the study. The high proportion of large pores owing to their coarse texture account for their good aeration, rapid drainage slow runoff and low moisture holding capacity (Adu, 1992). Though Arenosols have relatively high bulk density values that are typically between 1.5 and 1.7 g/cm³, the

low bulk density of 1.34 g/cm^3 found in the experimental field (Table 4.1) was not an uncommon situation. This could be attributed to soil management strategies including tillage and organic matter management in the field.

3.2 Collection of soil cores

Random sampling technique was employed and 25 core samples from 0-20 cm soil depth were collected from 25 different spots. Undisturbed soil cores were collected from the field site using a 10 cm diameter PVC sewer pipe cut to a length of 30 cm and bevelled at the outer part of the lower end to provide a cutting edge to facilitate the insertion of the core. Field cores were collected by first digging a circular trench around an intact “pillar” of undisturbed soil which was taller and had a slightly larger diameter than the core sampler. The core sampler was then inserted directly into the pillar of soil by striking a wooden plank positioned across the top of the ring, with a mallet. By this, the edges of the pillar were allowed to fall away from the core as it was inserted.

Following complete insertion the core was excavated by hand. When taking the soil core the inner ring created an air filled annulus, hence a sealant was used to ensure good contact between the soil and core and thereby minimised any edge flow down the core. Therefore, the air gaps between the soil and inner surface of the core were filled with melted petroleum jelly (Vaseline was used in this case).

3.3 Laboratory Measurements

3.3.1 Particle size analyses

The hydrometer method (ASTM, 1985) was used in the determination of the particle size distribution. This method was used because it allows for the non-destructive

sampling of suspensions undergoing settling. It also provides for multiple measurements on the same suspension so that detailed particle-size distribution can be obtained with minimum effort. Fifty-one grams (51 g) of air-dried soil from each of the 25 plots were weighed into milk-shake cup bottles. Ten millilitres (10 ml) of 5% Calgon (Sodium hexametaphosphate) alongside with 100 ml of distilled water were added to the soil. The Calgon served as a dispersing agent for the soil particles.

The mixture was shaken with a mechanical shaker for twenty (20) minutes and the content was poured into a 1000 ml measuring cylinder, the milk-shake bottle cap was rinsed with distilled water and added to the content to reach the 1000 ml mark. The cylinder with the content was shaken to distribute the particles equally throughout the suspension and first hydrometer and temperature readings were taken after 40 seconds. The suspension was left to stand for three (3) hours to allow the soil particles to settle. Hydrometer and temperature readings were taken after three hours and the percent fractions of each soil component was calculated as follows:

$$\% \text{ Sand} = 100 - [H_1 + 0.2 (T_1 - 20) - 2] \times 2 \quad (3.0)$$

$$\% \text{ Clay} = H_2 + [0.2 (T_2 - 20) - 2] \times 2 \quad (3.1)$$

$$\% \text{ Silt} = 100 - (\% \text{ Sand} + \% \text{ Clay}) \quad (3.2)$$

where,

H_1 = first hydrometer reading after 40 seconds

H_2 = second hydrometer reading after three hours

T_1 = first temperature reading after 40 seconds

T_2 = the second temperature reading after three hours

The textural class was determined using the textural triangle.

3.3.2 Volumetric soil moisture content and bulk density

Soil water content was determined on volume basis before and after the laboratory infiltration tests. Moist soil samples were taken from the field two days after a heavy rainfall when the soil was assumed to be at or near field capacity, defined as the amount of water held in the soil after the excess gravitational water has drained away and after the rate of downward movement of water has materially ceased, which is attained in the field after 48–72 hours of saturation (Motsara and Roy, 2008). The gravimetric method as described by Gardner (1986) was used to establish initial soil water content for the different soil samples. Wet samples were weighed and oven-dried at 105°C for 24 hours, and then weighed again. Gravimetric soil water content was then determined by the following equation (Gardner, 1986):

$$\theta_g = \frac{M_w - M_s}{M_s} \quad (3.3)$$

where,

M_w = Mass of wet soil

M_s = Mass of dry soil

To convert to volumetric soil water content, the bulk density of the soil was obtained.

The length and diameter of the soil rings were measured and the volume was calculated by:

$$V = \pi r^2 h \quad (3.4)$$

Bulk density was calculated by:

$$\rho_b = \frac{M_s}{V_t} \quad (3.5)$$

Total porosity (f) was calculated from bulk density as:

$$f = 1 - \frac{\rho_b}{\rho_s} \quad (3.6)$$

where, ρ_s is the particle density (assumed to be 2.65 g/cm^3)

Volumetric water content was then calculated by the equation:

$$\theta_v = \theta_g \times \left(\frac{\rho_b}{\rho_w} \right) \quad (3.7)$$

where,

ρ_w = density of water (assumed to be 1.0 g/cm^3)

3.3.3 Saturated hydraulic conductivity (K_s)

The saturated hydraulic conductivity (K_s) measurements were made on the cores in the laboratory using the modified falling head permeameter method similar to that described by Bonsu and Laryea (1989). In the measurement, core samples were obtained from the 0–20 cm depth. The cores were soaked for 24 hours in water until they were completely saturated. A large empty can with perforated bottom was filled with fine gravel. The core was placed on the gravel supported by a plastic sieve. The whole system was placed over a sink in the laboratory and water was gently added to

give hydraulic head in the extended cylinder. The fall of the hydraulic head h_t at the soil surface was measured as a function of time t using a water manometer with a 5 meter scale.

Saturated hydraulic conductivity was calculated by the standard falling head equation as:

$$K_s = \left(\frac{aL}{At}\right) \ln\left(\frac{h_o}{h_t}\right); \quad (3.8)$$

where, a = Surface area of the

cylinder [L^2] A = Surface area of

the soil [L^2] h_o = Initial hydraulic

head [L]

L = Length of the soil column [L]

h_t = Hydraulic head after a given time t [L]

By rewriting equation (3.8), a regression of $\ln\left(\frac{h_o}{h_t}\right)$ on t with slope $b = K_s \left(\frac{A}{La}\right)$ was obtained. Since $a = A$ in this particular case, K_s was simply calculated as:

$$K_s = bL \quad (3.9)$$

3.3.4 Separating soil particles

The different soil particles were obtained by dry sieving through a series of graduated sieves with different mesh sizes. The sample was shaken over nested sieves (in a decreasing order from top to bottom) which were selected to furnish the information required by specification. During sieving, the sample was subjected to a tap mechanism (i.e., both vertical movement or vibratory sieving and horizontal motion

or horizontal sieving) for approximately 120 minutes to provide complete separation of the fine (i.e. dispersible) soil particles of the order 0.05 mm for fine sand, 0.02 mm for silt and < 0.002 mm (assumed herein as 0.001 mm) for clay, according to FAO classification.



Figure 3.1: Sieves arranged in a stack with the mesh size increasing from bottom to top on mechanical shaker



Figure 3.2: Principles of 3-dimensional throwing motion (left), horizontal sieving (middle) and tap sieving (right)

3.4 Muddy water infiltration model

3.4.1 Model development

The model formulation was considered as two distinct processes. The first involved model development and the second was application of model for flow purposes. The model was most efficiently developed in a logical sequence. The modelling process began with a conceptual understanding of the physical phenomenon. The next step involved translating the physical system into mathematical terms. The result was familiar with the Green and Ampt equation for vertical flow. An understanding of this equation and its associated boundary and initial conditions was made necessary before the model was formulated. The basic process that was considered was infiltration of water in the vertical direction. The modelling studies were conducted using deterministic models, based on precise description of cause-and-effect or input-response relationships. The objective of the modelling process was to simulate the effects of soil particles in infiltrating water on cumulative infiltration amount.

3.4.2 Theory

3.4.2.1 Model assumptions

The fundamental assumptions governing the development of the infiltration equation were based on those of Green and Ampt (1911). In addition to these assumptions, the physical model was propounded based on the following assumptions:

- 1) The suspension reaches the soil surface by mass flow with significant sedimentation of particles. In view of this assumption, it is clear that the concentration of the suspension remains constant for a particular sediment particle during the infiltration process, and it obeys Darcy's Law.

- 2) Suspended particles in water are deposited unceasingly on the soil surface, which results in the development of a seal. In this regard, the length of the flow path changes with time.
- 3) Sediment particles are spherically shaped with Reynolds number (Re) less than one (i.e. sediment settling is laminar). Thus, settling of sediments obeys Stoke's law.
- 4) The seal does not form instantly, but upon formation, it is assumed to be saturated with a constant hydraulic conductivity, which is a function of the particle diameter of the sediment.
- 5) The surface seal changes only the saturated hydraulic conductivity and not the saturated water content of the soil column.

3.4.2.2 Model description

Consider a homogeneous soil profile that is saturated with a soil suspension on the inflow side. The vertical ordinate L is assumed positively upwards, $L = 0$ at the soil surface and $L = -Z_f$ at the wetting front. The saturated hydraulic conductivity is K_s . The hydraulic head at the surface is h_o and $h_f - Z_f$ at the wetting front. Since K_s is constant in the entire wetted zone, the infiltration rate i can be obtained from Darcy's Law as follows:

$$q = K_s \left(1 + \frac{h_f}{Z_f} \right) \quad (3.10)$$

Assuming that at time t , a depositional layer of thickness Z_x with conductivity $K_x(D)$ begins to form as the suspension reaches the soil surface and the filtrate moves

through the soil in response to a variable hydraulic gradient. Again, under steady state downward flow, the pressure head remains constant through a considerable depth, starting at the interface of both the seal and sub-seal layers. Therefore, we consider gravitational gradient as the only effective force for water flow at this stage, a very thin depositional layer of low and constant conductivity, and the whole soil profile with the depositional layer, which affects the soil water suction at the wetting front. Consequently, the system can be seen to behave as a constant-head permeameter (Klute and Dirksen, 1986; Bonsu and Laryea, 1989), therefore, Darcy's

Law (Equation 3.10) can be written as:

$$q = K_x(D) \left(1 + \frac{h_f}{Z_f + Z_x} \right) = K_x(D) \left(1 + \frac{h_f}{Z_L} \right) \quad (3.11)$$

where,

$Z_L = Z_f + Z_x$ is the thickness of the soil column together with the depositional layer [L]

$K_x(D)$ = Hydraulic conductivity of the surface seal layer [L/T]

If δM_x is the elemental mass of sediments that accumulate as the surface deposition layer in time δt , and δM_z is the elemental mass of sediments lost from the suspension in time δt , then by the principle of conservation of mass (Bonsu, 1992):

$$q_m = \frac{dM_z}{dt} Z_x = \frac{dM_x}{dt} Z_x \quad (3.12)$$

where,

q_m = Mass flux density of sediments in suspension [M/L/T]

However, mass flux can refer to an alternate form of flux in Darcy's law to describe volumetric flux density (Potter and Wiggart, 2008), therefore, equation (3.12) can be converted to volumetric bases and related to infiltration rate, which is equal to the time rate change of muddy water storage in the soil. Equation (3.12) can therefore, be equally expressed as:

$$q_m = \frac{dM_x}{dt} Z_x = c \frac{dV_x}{dt} Z_x = c \Delta\theta \frac{d}{dt} Z_L \quad (3.13)$$

where,

c = Concentration of sediments in suspension [MM^{-1}]

Combining (3.11) and (3.13) gives:

$$\Delta\theta \frac{d}{dt} Z_L = \frac{K_s}{c} \left(\frac{Z_L + h_f}{Z_L} \right) \quad (3.14)$$

Integrating equation (3.14) by separation of variables for the initial condition $t = 0$:

$$\Delta\theta \int_0^{Z_L} \frac{Z_L dZ_L}{h_f + Z_L} = K_x(D) \int_0^t dt \quad (3.15)$$

$$Z_L \Delta\theta - h_f \ln \left(1 + \frac{Z_L}{h_f} \right) = \frac{K_x(D)}{\Delta\theta} t \quad (3.16)$$

$$I = K_x(D)t + h_f \Delta\theta \ln \left(1 + \frac{I}{h_f \Delta\theta} \right) \quad (3.17)$$

where,

$$K_x(D) = \frac{K_s}{c} d_*$$

$I = Z_1 \Delta \theta$, the cumulative infiltration amount or cumulative quantity of downward infiltration (volume of water per unit bulk soil cross-sectional area) after time t of ponded water application to the soil surface [L]

D = Particle diameter [L]

c = Sediment concentration [MM^{-1}]

d_* = Dimensionless particle diameter, defined by Dietrich (1982) as:

$$d_* = D \left[\sqrt[3]{\frac{\rho_f g \rho_\gamma}{\omega^2}} \right] \quad (3.18)$$

where,

ρ_γ = Submerged particle density [ML^{-3}], expressed as: $\rho_s - \rho$

ρ_f = Fluid density [ML^{-3}]

g = Acceleration due to gravity [LT^{-2}]

ω = Dynamic viscosity [$\text{ML}^{-1}\text{T}^{-1}$]

Equation (3.17) is a nonlinear equation representing the modified Green and Ampt Surface Sealing (MGASS) infiltration model. Due to the non-linearity (i.e. presence of a natural logarithm component), it can be solved for cumulative infiltration for successive increments of time using the Bisection iterative solution. Since the total increase in pathway length is small, it has little impact on the process. The seal is thus, viewed as a self-adjusting system with physical properties which have very strong impact on the whole column.

It is imperative to note that the deposition of sediment particles is a function of particle diameter and concentration of the sediment. Hence, the rate of sediment

deposition varies directly with the hydraulic conductivity of the medium (K_s) plus the constant settling velocity (V_s) of the sediment particle. With a theoretical outcome from probabilistic considerations, a simple formula was proposed in this study to relate the thickness of seal layer (Z_x) to V_s as follows:

$$\frac{dZ_x}{dt} \propto K_s + V_s \quad (3.19)$$

$$\frac{dZ_x}{dt} = cK_s + cV_s \quad (3.20)$$

Integrating (3.20) at $t = 0$,

$$\int_0^{Z_x} dZ_x = \int_0^t [cK_s + cV_s] dt \quad (3.21)$$

$$Z_x = c \int_0^t K_s dt + cV_s \int_0^t dt \quad (3.22)$$

Equation (3.22) becomes:

$$Z_x = ct(K_s + V_s) \quad (3.23)$$

where,

V_s = the settling velocity of sediment particle [L/T], defined as the downward velocity in a low dense fluid at equilibrium in which the sum of the gravity force, buoyancy force and fluid drag force are equal to zero (She *et al.*, 2005; Wu and Wang,

2006; Sadat-Helbar *et al.*, 2009). According to Stokes' law, the fall velocity of spherical particles with Reynolds number (Re) less than 1, can be calculated from (Cheng 1997):

$$c = \text{Concentration of sediments in suspension [MM}^{-1}]$$

$$V_s = \frac{1}{18} \frac{g(s-1)D^2}{\mu} \quad (3.24)$$

where,

g = Acceleration due to gravity [L/T²]

s = Relative density (ρ_s/ρ)

μ = Kinematic viscosity [L²/T]

3.5 Experimental verification of the model

The performance of the proposed model was verified with a series of ponded infiltration tests with clear and muddy water. The experiments were designed to test predictions by investigating a range of saturated hydraulic conductivities, initial and saturated water contents, sediment concentrations (c) and particle diameters which have not been extensively examined in previous infiltration studies. The infiltrating liquids were made of clear water, and suspensions of different soil particle diameters, viz., fine-sand, clay and silt, at different concentrations. The different concentrations were made by adding clean (distilled) water to, 10 (T1), 20 (T2), 30 (T3) and 40 g (T4) of soil to make a total of 400 cm³ and dispersed in a mechanical shaker for 60 minutes. Additionally, an infiltration test was conducted with distilled water (T5), which served as a reference for the study.

Infiltration rates and cumulative infiltration amounts were determined by onedimensional absorption into vertical soil columns of loamy sand texture in five

replications. The bottom of each column was supported with cotton cloth and was wetted from below to expel any entrapped air. Excess water on top of the soil was siphoned out at zero hydraulic head difference. The ponded infiltration experiments were conducted with a surface ponded thickness of 5 cm. A plastic sheet was used to cover the surface of the soil as the suspension was being added, in order to prevent disturbance of the surface. The plastic sheet was removed and a flexible tubing, which had already been filled with water, was used to connect the surface of the suspension to a constant head device. A piezometer in the form of a flexible tubing was connected to a manometer and allowed measurement of the cumulative volume of infiltration.

There was a slight mixing of the water and the suspension at the initial stage but, after a while, as the suspension flowed into the column, there was a clear separation between the water above and the suspension below. All the clamps were removed. Measurements were made for a range of values of concentrations, each on a new soil column. The vertical infiltration was measured in the soil column for 60 minutes. The initial infiltration was measured at 30 seconds interval for the first five minutes after which the interval was increased to 60, 180 and 300 seconds, respectively, as the process slowed down towards the steady state.

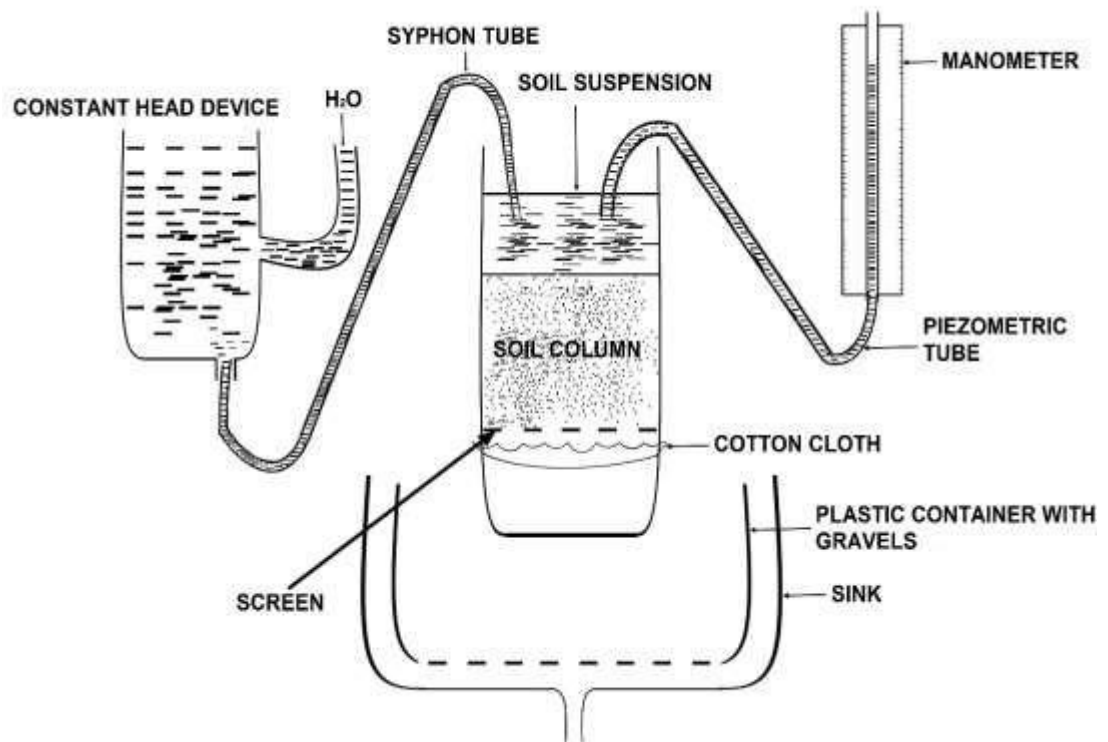


Figure 3.3: A schematic diagram of the apparatus used to test the theory

3.5.1 Data reduction and presentation

To compute the cumulative infiltration amount (I) from the experiment, the volume of water was converted to depth from the relation:

$$I = \frac{Q_I}{A} \quad (3.25)$$

where,

Q_I = Cumulative volume of water (ml); 1 ml = 1 cm³

A = Surface area of the ring, given by:

$$A = \pi r^2$$

$r = \frac{1}{2}$ Ring diameter

The cumulative infiltration amounts (I) were plotted as a function of time for each run on a linear scale with GraphPad Prism 6.0. The slopes of the cumulative infiltration amounts taken at different time scales represented the infiltration rates (i), which were plotted against time and the steady state infiltrability (K_o) was obtained at the point where the infiltration rate curve became almost parallel to the time axis (Khalid *et al.*, 2014; Tuffour *et al.*, 2014a, b).

3.5.2 Estimation of time-to-incipient ponding (t_p)

Analysis of Time-to-incipient ponding (t_p) or runoff initiation was conducted based on the relation modified from Mein and Larson (1973):

$$t_p = \frac{K_x(D)h_f\Delta\theta}{R_r[R_r - K_x(D)]} \quad (3.26)$$

where,

R_r = Rainfall rate [L/T]

Hypothetical R_r values ranging from 5 mm/h (0.0014 mm/s) to 30 mm/h (0.0083 mm/s) were employed in estimation of t_p . The other parameters are as already defined.

3.6 Model validation

In order to compare the infiltration rates for the measured and predicted curves, parameter values were determined for the proposed equation and the results were evaluated quantitatively. The parameters for the experimental infiltration curves were used to predict infiltration parameter values for the models. From each prediction, the output was evaluated by the Root Mean Square Error ($RMSE$) to assess the goodness-of-fit (GOF) of the model. This was done in order to compare values of

infiltration rate evaluated at each time interval, to determine how closely the equation predicted the measured infiltration. The *RMSE* was calculated as follows:

$$RMSE = \left[\frac{1}{n} \sum_{i=1}^n (d_s - d_o)_i^2 \right]^{1/2} \quad (3.27)$$

where,

n = Number of observations

d_o = Observed data

d_s = Simulated data

In general, a lower *RMSE* value was expected to result in a higher agreement between the measured and the predicted data. The predicted values of infiltration were also plotted against experimental values and the coefficient of determination (R^2), which is the square of the coefficient of correlation (r) was determined as follows:

$$R^2 = 1 - \frac{SSE}{SST} \quad (3.28)$$

where, *SSE* measures the deviations of observations from their predicted values as follows:

$$SSE = \sum_i (d_o - d_s)^2 \quad (3.29)$$

SST measures the deviations of the observations from their mean as follows:

$$SST = \sum_i (d_o - \bar{d}_o)^2 \quad (3.30)$$

3.7 Statistical analysis

The accuracy of the equation for predicting the cumulative infiltration was evaluated by comparing the observed values of measurement in the laboratory with the predicted values based on the fitted equation. The data were then subjected to Analysis of variance (ANOVA) and paired t-test analysis using GraphPad Prism version 6.0 to compare the effect of the different sediment particles at different concentrations on the infiltration.



CHAPTER FOUR

4.0 RESULTS AND DISCUSSIONS

The results from the experiment are presented and discussed in Chapter four. The measurement data obtained from the experiment are presented in Tables 4.1a, 4.1b, 4.2, 4.3, 4.4 and 4.5, and Figures 4.1a, 4.1b and 4.1c, and 4.2a, 4.2b, 4.2c, and 4.2d, respectively. Detailed results of statistical analyses, viz., Repeated measures one-way ANOVA ($P < 0.05$), Tukey's multiple comparisons test ($\alpha = 0.05$), Paired samples t-test ($P < 0.05$) and One sample t-test ($P < 0.05$) are provided in the Appendices. The results revealed both significant and insignificant differences among treatment combinations for the various soil properties investigated.

4.1 Soil physical and hydraulic properties

The results of initial analysis of soil physical and hydraulic properties of the study area are presented in Table 4.1a. The results showed that the texture of the field surface (0 - 20 cm) was loamy sand, with sand, silt and clay fractions of 84%, 4.30% and 11.70%, respectively. The average bulk density was 1.34 g/cm^3 with total porosity of 49.43%. The average antecedent and saturated moisture contents were 23.58% and 47.70%, respectively. The average saturated hydraulic conductivity was $2.5 \times 10^{-3} \text{ mm/s}$.

Table 4.1a: Summary of initial soil physical and hydraulic properties

Soil property	Number of samples	Mean value
Saturated hydraulic conductivity (mm s^{-1})	5	2.50E-03
Bulk density (g cm^{-3})	5	1.34
Total porosity (%)	5	49.43
Volumetric moisture content (%)	5	23.58

Saturated moisture content (%)	5	47.70
Moisture deficit (%)	5	24.12
Sand (%)	5	84.00
Silt (%)	5	4.30
Clay (%)	5	11.70
Texture	5	Loamy sand

Table 4.1b presents the summary of the results of the measured physical and hydraulic properties after the infiltration experiment. Comparison of Tables 4.1a and 4.1b indicated substantial changes in the soil properties after the infiltration experiment. Repeated measures one-way ANOVA and Tukey's multiple comparisons test (Appendix A) also showed significant differences among the means of the measured parameters under the different treatments. Therefore, the observed changes could not have arisen by chance.

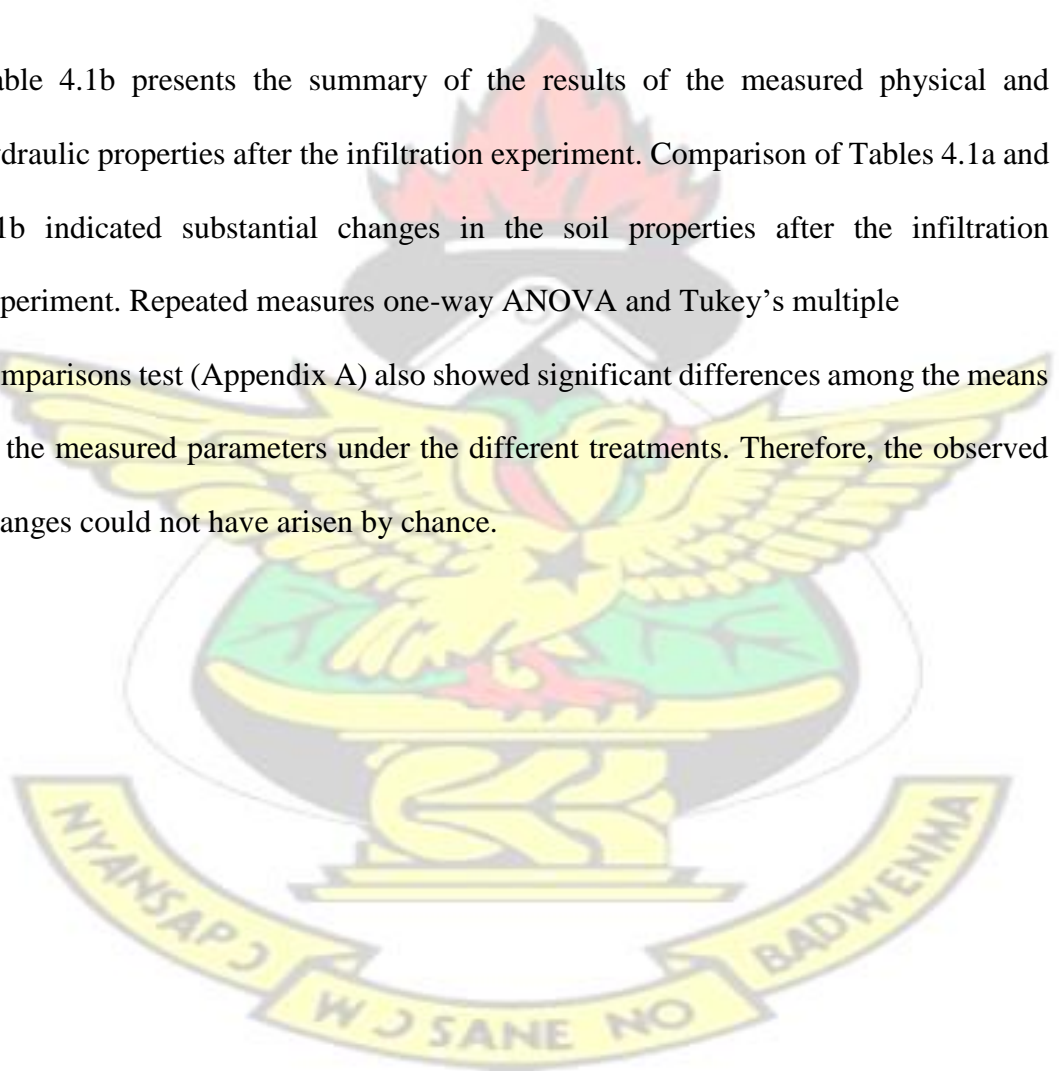


Table 4.1b: Summary of soil physical and hydraulic properties after infiltration

Soil property	Fluid												
	Clear water	Clay suspension†				Silt suspension†				Fine sand suspension†			
		10	20	30	40	10	20	30	40	10	20	30	40
K_s (mm s ⁻¹)	2.5E-3	1.0E-4	5.0E-5	3.3E-5	2.5E-5	2.0E-3	1.0E-3	6.7E-4	5.0E-4	5.0E-3	2.5E-3	1.7E-3	1.3E-3
ρ_b (g cm ⁻³)	1.34	1.37	1.45	1.53	1.55	1.37	1.43	1.48	1.52	1.36	1.41	1.45	1.47
f (%)	49.43	48.30	45.28	42.26	41.51	48.30	46.04	44.15	42.64	48.67	46.79	45.28	44.53
θ_v (%)	23.58	21.01	19.28	17.28	16.65	21.74	20.44	19.21	18.04	22.53	21.38	19.61	18.97
θ_s (%)	47.70	43.50	42.60	40.90	40.10	45.00	44.40	43.50	42.30	46.30	45.70	43.30	42.60

†Mass of sediment particles in suspension (g); θ_v (%) = Volumetric water content at field capacity; ρ_b (g cm⁻³) = Bulk density;
 f (%) = Total porosity; θ_s (%) = Saturated water content; K_s (mm s⁻¹) = Saturated hydraulic conductivity

As expected, differences were observed in the soil properties after the infiltration tests, however, no change could be observed in respect of suspensions with 10 g sediment particles and clear water, except for the K_s of the surface layer formed from the deposition (surface seal) of soil sediments. Final conductivity of the surface seals ranged from 96% to 99% and 20% to 98% less than that of the layer below the surface arising from the deposition of clay and silt sediments, respectively. However, for the sand particles, 10 g sediment suspension increased the final seal conductivity by 100% that of the sub-seal soil. At 20 g sediment concentration, the K_s was similar to the initial value. Upon increasing the sediment concentrations to 30 and 40 g, the K_s dropped by 32% and 48%, respectively. The lower saturated hydraulic conductivity of the clay and silt seals were primarily a result of the thinner measured seal thickness (Table 4.3; Appendices C and D) rather than lower seal resistance. By this, the phenomenon that fine soil particles are capable of clogging soil pore spaces was clearly demonstrated.

Another point to be emphasized is that the bulk density, 1.34 g cm^{-3} , was the same after infiltration with clear water since the soil was a well aggregated stable soil which did not show any clear sign of sediment settlement during the flow process. However, from the results, significant increase in bulk density and reduction in total porosity, moisture content, and saturated hydraulic conductivity were observed after the infiltration of muddy water (with special emphasis on clay and silt suspensions). The reduction in porosity (or increased bulk density) of the soil columns was dependent on the particle diameter and concentration of the suspension. In comparing the results obtained for the different sediment materials, it was realised that

deposition of clay resulted in the maximum reduction in porosity and permeability, followed by silt and sand, respectively. This result led to the conclusion that fine grains at higher concentrations provide more likelihood of clogging the pore system of porous media than coarse grains.

The reduction in porosity operated mainly at top layer of the soil column, leading to clogging of pores, and thus, the drastic reduction in permeability. Thus, the decrease was mainly observed at the entrance of the column due to development of a surface seal (or surface depositional layer) resulting from settling of particles in pores and on the soil surface. These changes were responsible for the loss of nearly all drainable macropores in the soil, which was evidenced by the considerable reduction in cumulative infiltration amounts and rates (Table 4.2; Appendix A; Figures 4.1a – c; 4.2a – d). The increase in bulk density resulted from the occurrence of pore clogging (i.e. compaction) during the formation of the surface seal (Moss, 1991). The ensuing reduction in hydraulic conductivity was also the reason for the substantial reduction in infiltration, and moisture content after infiltration.

These changes suggest that formation of surface seals can result in considerable damage of soil structure in agricultural fields. Under field conditions, erosion may set in (Zejun *et al.*, 2002) resulting in a decrease in water use efficiency. This ultimately reduces rainfall and irrigation water storage for crop use. However, it is worthy to note that seal formation is not always accompanied by decrease of total porosity, hydraulic conductivity and soil water content (Castilho *et al.*, 2011) as evidenced by the surface deposition of 10 and 20 g fine sand.

4.2 Infiltration

The infiltration characteristics were determined in terms of the cumulative infiltration amount and infiltration rate. Cumulative infiltration is the total quantity of water that enters the soil in a given time, whereas, infiltration rate is a measure of the speed at which soil is able to absorb water (from rainfall or irrigation). Thus, infiltration rate and cumulative infiltration are two parameters commonly used in evaluating the infiltration characteristics of soil. A summary of the measured infiltration parameters for the different sediment suspensions and their respective concentrations is presented in Table 4.2. Additionally, detailed statistical results for the various infiltration parameters considered in this study (i.e. cumulative infiltration amount, infiltration rate and steady state infiltrability) are presented in Appendix B. The experimental data for cumulative infiltration (I) with time (t) for clear water and the different sediment suspensions, and their concentrations are presented in Figures 4.1a – c and 4.2a – d. In all the tests, lower infiltration was recorded for the sediment suspensions after 60 minutes (Table 4.2; Appendix B).

The results clearly showed that infiltration was highly dependent on the characteristics of soil and fluid. Relatively, the saturated conditions (high soil water contents) created in this study inhibited the higher infiltrabilities commonly observed when soils are unsaturated. This resulted in the lower and more equal infiltration rates for and within each sediment suspension (Appendix B2.1 – B2.2). The trends of the cumulative infiltration amount curves (Figures 4.1a – c and 4.2a – d) also suggest that the process could best be described by a quasi-steady state regime, since, infiltration decreased slowly with time. However, field observations of infiltration into natural soils reported by Tuffour *et al.* (2014 a, b) and Khalid *et al.* (2014)

exhibited dissimilar patterns, where, infiltration rates were described by two distinct regimes: a transient regime and a quasi-steady state regime. In these cases, infiltration rates decreased rapidly with time in the transient regime and slowly in the quasisteady state regime.

KNUST



Table 4.2: Summary of infiltration characteristics following the interactions among the various fluids and their concentrations

Infiltration property	Fluid												
	Clear water	Clay suspension†				Silt suspension†				Fine sand suspension†			
		10	20	30	40	10	20	30	40	10	20	30	40
I (mm)	409.67	403.31	181.93	75.06	73.79	424.94	222.65	138.68	129.77	436.39	358.78	181.93	173.03
i (mm s ⁻¹)	0.114	0.112	0.051	0.021	0.020	0.118	0.062	0.039	0.036	0.121	0.100	0.051	0.048
K_o (mm s ⁻¹)	0.116	0.115	0.055	0.026	0.024	0.119	0.066	0.047	0.046	0.122	0.104	0.060	0.059

†Mass of sediment particles in suspension (g); I = Cumulative infiltration amount (mm); i = Cumulative infiltration rate (mm s⁻¹); K_o = Steady state infiltrability (mm s⁻¹)

4.2.1 Effect of sediment size on infiltration

Close observations of the cumulative infiltration amount curves (Figs. 4.1a – c and 4.2a – d) revealed that the type (i.e. size) of sediment particle present in the infiltrating water had significant impact on infiltration. The main characteristics of the sediments that influenced infiltration were the size, the concentration, and the settling velocity, which influenced the viscosity of the moving water. According to Poiseuille (1846), in the Law of laminar water flow through a cylindrical soil pore (Hillel, 1998), flow in soil pores is inversely proportional to water viscosity, hence, the presence of soil sediments tended to reduce infiltration and conductivity of muddy water through the soil. This observation, thus, supports earlier reports that the presence of soil sediments in ponded and flowing water can drastically reduce infiltration (Trout *et al.*, 1995; Bouwer *et al.*, 2001).

The smooth, slick seal that was visually obvious on the soil surface following infiltration was the main reason for the reduction in infiltration. This layer was created from the capture of sediments within the pore spaces and at the soil surface, partly due to direct interception, and size exclusion. In all the columns, the sediment concentration in water decreased with time, indicating that the transported sediment continued to deposit at the column perimeter. This observation suggests that the assumption of constant sediment concentration was overly simplified.

The differences in particle sizes of sediments in the depositional layers resulted in differences in the hydraulic properties (e.g. permeability and infiltrability) across the seal-soil layer interface. Significant reductions in hydraulic conductivity were observed due to the deposition of sediment particles transported by water through the

soil. Thus, the accumulation and deposition of suspended sediments, especially clay and silt ultimately led to the clogging of pores. However, the seal layer resulting from the deposition of sand particles recorded very high K_s at low concentrations. This was mainly because deposition of the sand particles created preferential flow paths through fingering, funneling and large connected void spaces in the depositional layer. On the other hand, the fine sediments (i.e. clay) moved into the large pores, attached to other soil particles, filled pore spaces, and thus, reduced porosity and K_s . However, K_s of the seal layer resulting from the fine sand particles was lower than that of the original soil surface at higher concentrations (30 – 40 g). This low conductivity of the surface seal limited the downward movement of water (i.e. infiltration) and held the infiltrating water in the finer pores by capillary forces.

The data presented in Table 4.2 indicates that 96% to 99% reduction in conductivity reduced the final cumulative infiltration by 1.55% to 82% for the clay seal. Similarly, a reduction of 20% to 98% in K_s resulted in 3.73% to 68.32% in the final cumulative infiltration for the silt seal. However, 10 g sand sediment suspension resulted in a 100% increase in K_s , but resulted in only about 6.52% increase in the final cumulative infiltration. It is evident that, infiltration was directly related to the conductivity of the seal as presented in equation (3.17). However, the relationship was not proportional in this study, as might be assumed from a cursory analysis. The relative infiltration would be 1.0 when the resistance is equal to zero (no effect of the seal on infiltration) and will asymptotically approach zero as the resistance becomes large. The presented graphs (Figures 4.1a – c and 4.2a – d) demonstrate the relatively larger increase in resistance required to decrease infiltration.

Under field conditions, the water stored temporarily in these pores may ultimately be removed by evaporation, lateral drainage (if the event occurs on a slope), or percolation (breakthrough into the lower layer). From these observations, it is clear that even with the occurrence of significant aggregate slaking, dispersed clay is mainly responsible for decreased infiltration. In respect of these observations, it was perfect to note that the structure and characteristics of the seal depended on the mechanical properties (i.e. granulometric texture) of the sediment particle in the infiltrating water.

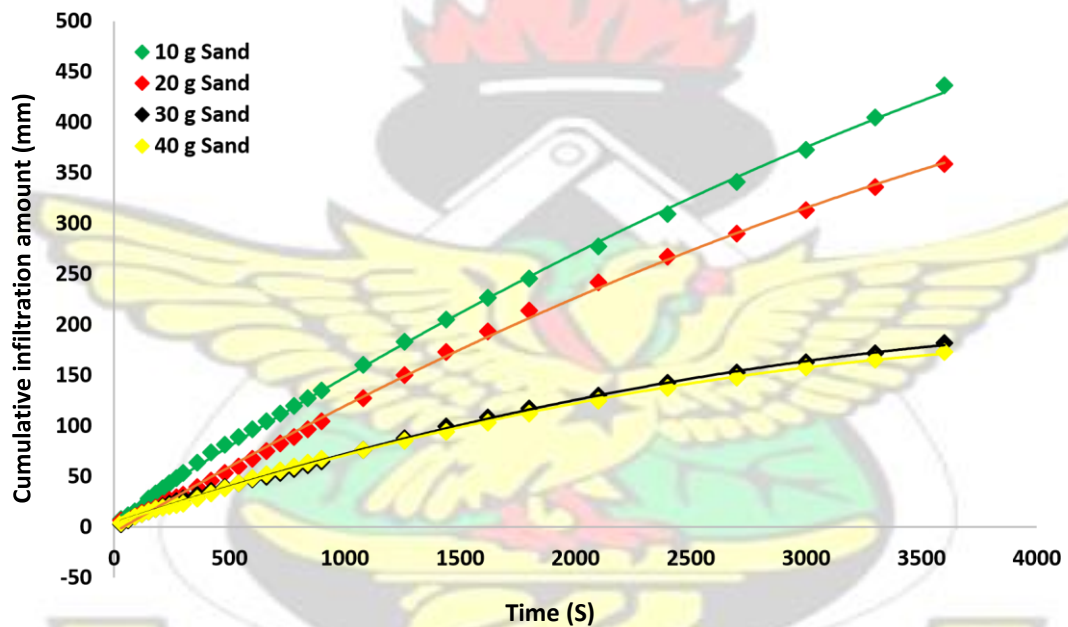


Figure 4.1a: Cumulative infiltration amount with time for sand suspension at different concentrations

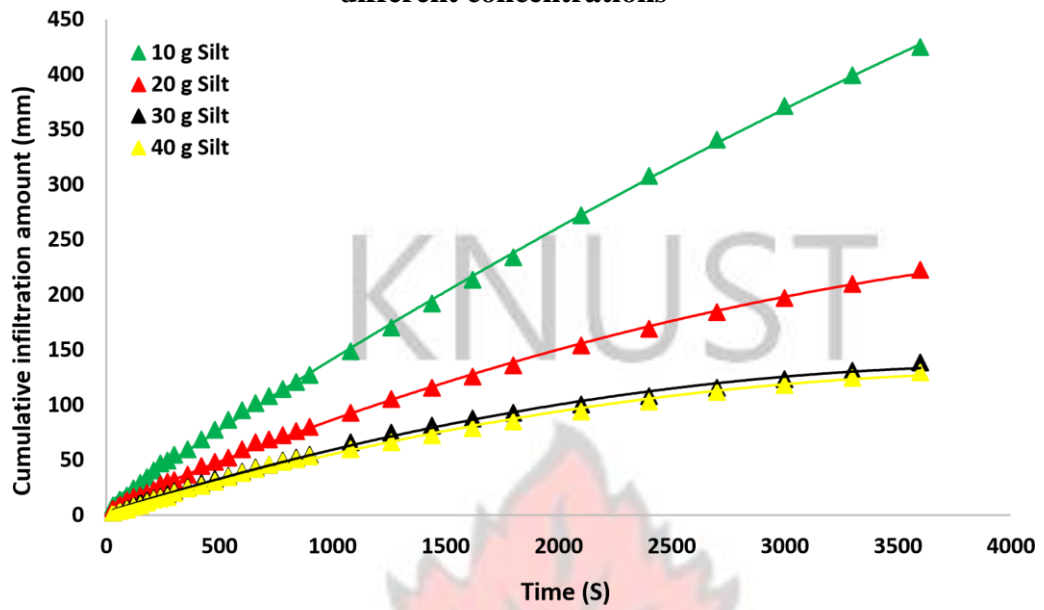


Figure 4.1b: Cumulative infiltration amount with time for silt suspension at different concentrations

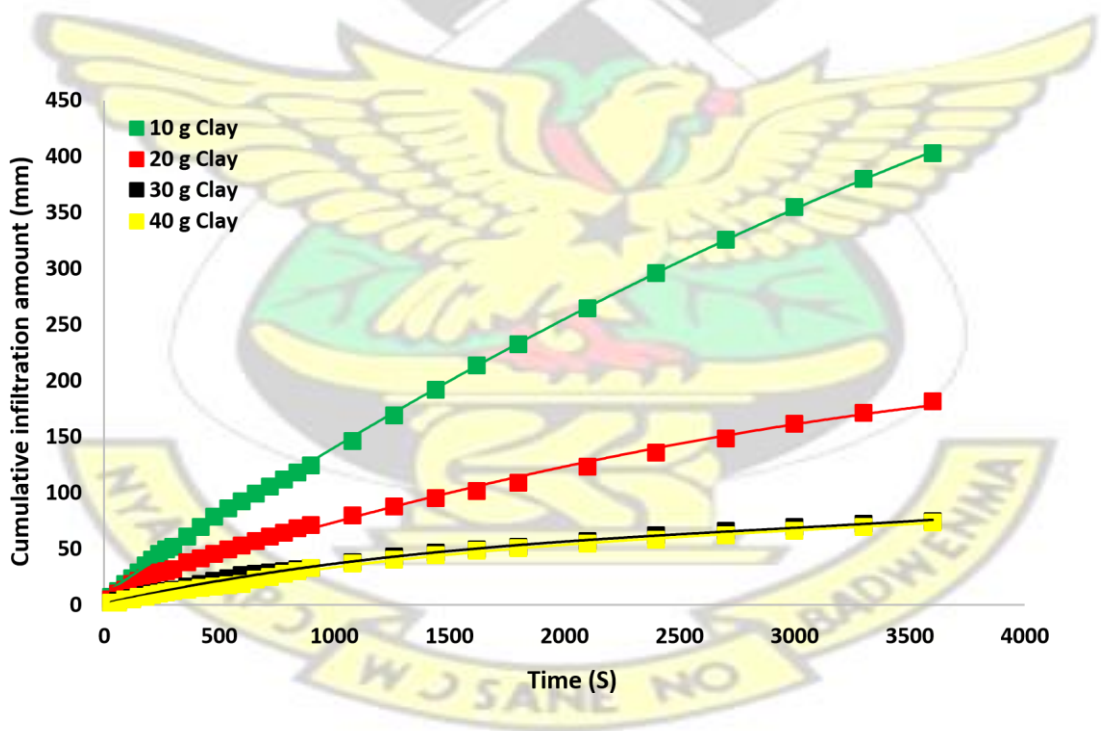


Figure 4.1c: Cumulative infiltration amount with time for clay suspension at different concentrations

With increasing infiltration opportunity time, the differences in cumulative infiltration among the various fluids changed appreciably. Thus, the differences in infiltration were significantly distinguishable following the significant changes in the initial physical and hydraulic conditions of the soil columns. Further, the slopes of the various cumulative infiltration curves (i.e. infiltration rates) decreased with increasing sediment concentration. This indicated that the average soil water suctions at the wetting front decreased with increasing sediment concentration in the infiltrating water.

Equation (3.17) differs from the original Green and Ampt equation in terms of soil water suction, conductivity (i.e. saturated hydraulic conductivity of the seal), fluid viscosity, and sediment type and concentration. It is, however, applicable to clear water infiltration by making the sediment concentration zero. The observed infiltration process can be used to explain the formation of a definable surface layer with a significantly lower permeability (surface seal). It is thus, evident from the results that the smaller the sediment diameter, the lower the infiltration.

4.2.2 Effect of sediment concentration on infiltration

Generally, the saturated hydraulic conductivity and infiltration decreased with increasing sediment concentration, in the order: clay, silt and sand, respectively. From the results, as shown in Table 4.2, final infiltration rate was highest with clear water (0.114 mm s^{-1}) and lowest for clay suspension with 40 g clay particles (0.020 mm s^{-1}) after 60 minutes. Additionally, clear water recorded the highest final cumulative infiltration amount of 409.67 mm, whereas clay suspension with 40 g clay particles recorded the lowest of 73.79 mm in 60 minutes. Thus, 40 g clay

suspension resulted in approximately 82% drop in the final cumulative infiltration amount with regards to clear water. At lower concentration (i.e. 10 g), it appeared that texture had no significant effect on infiltration (Fig. 4.2a). From the experimental results, it was evident that the effect of increasing sediment concentration on infiltration differed for the different sediment particles.

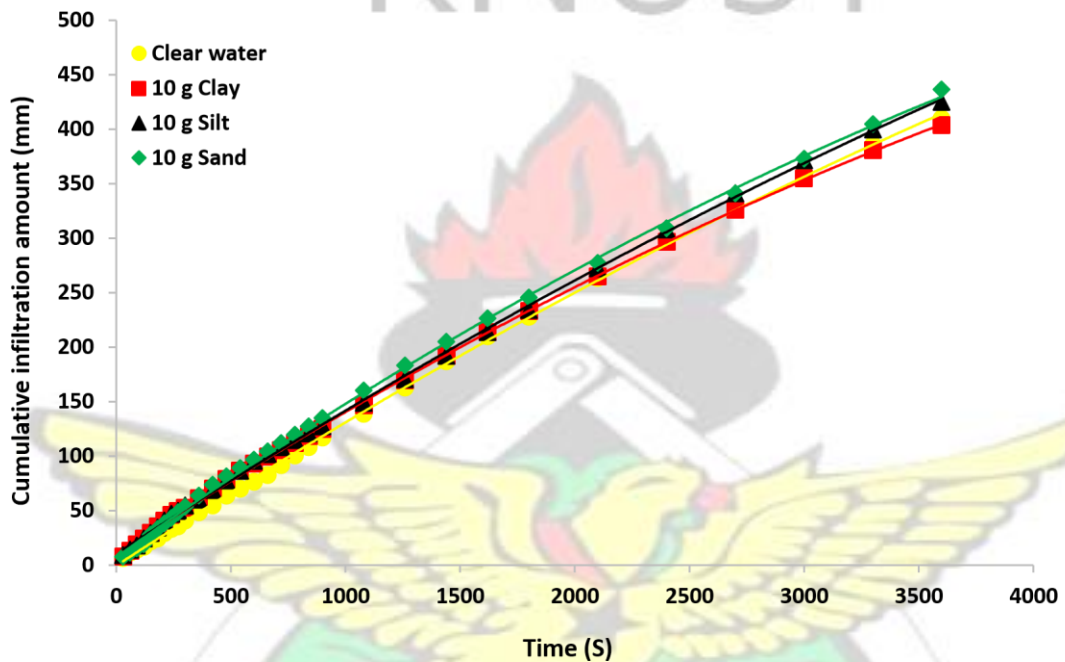


Figure 4.2a: Cumulative infiltration of clear water and 10 g soil particles in suspension

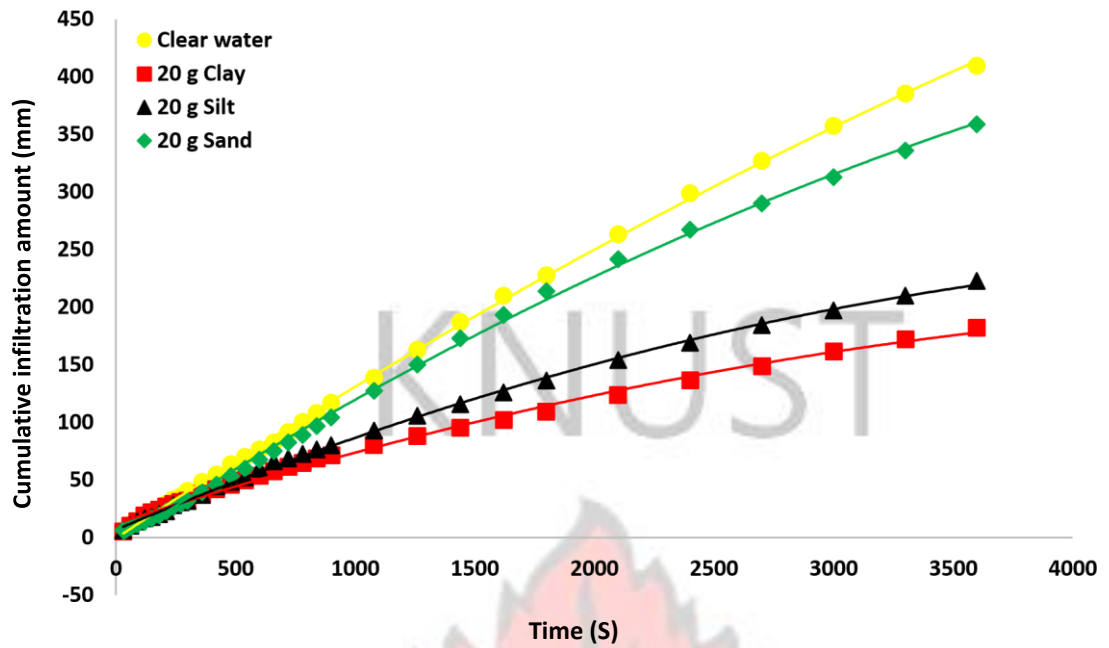


Figure 4.2b: Cumulative infiltration of clear water and 20 g soil particles in suspension

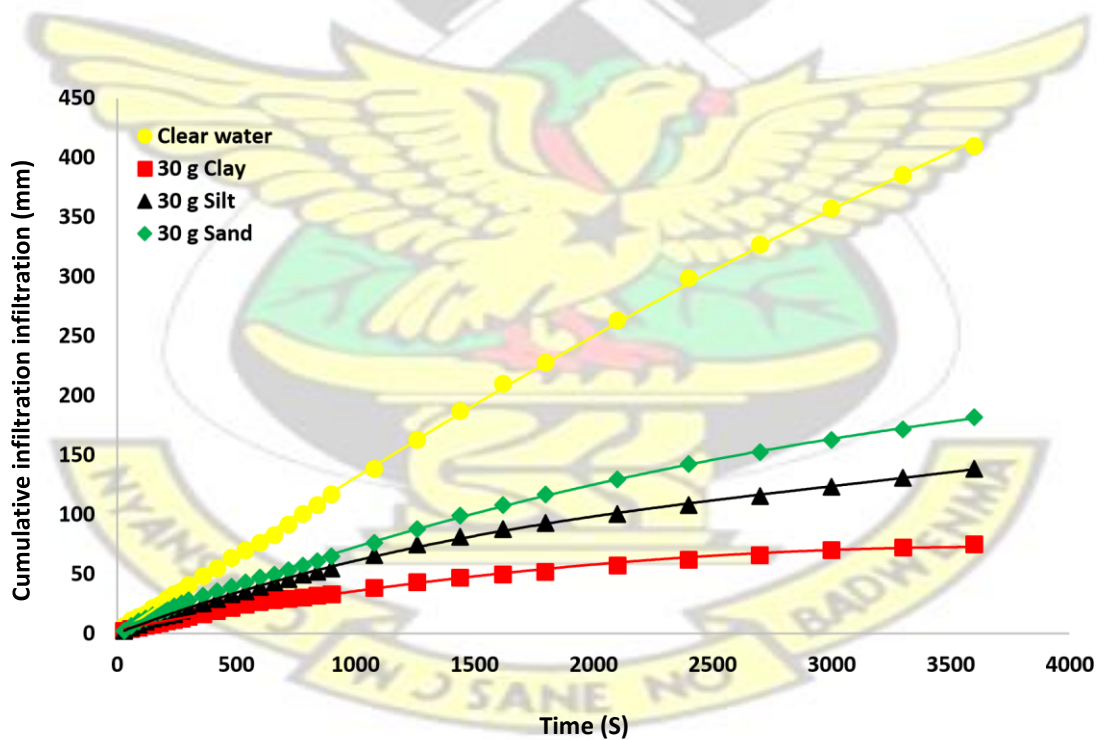


Figure 4.2c: Cumulative infiltration of clear water and 30 g soil particles in suspension

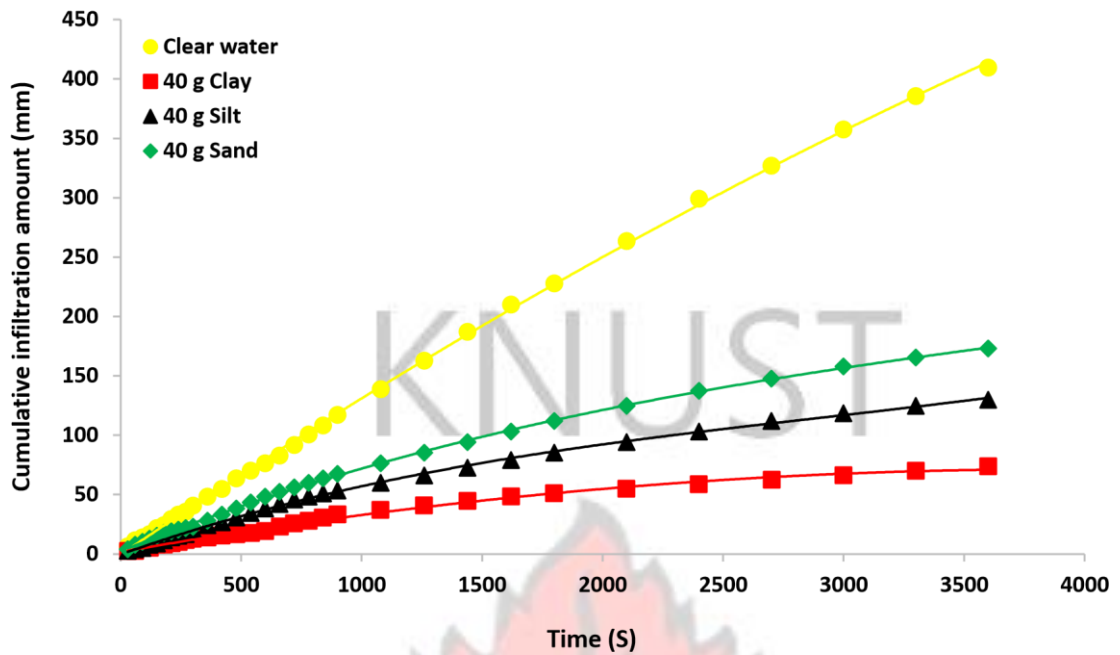


Figure 4.2d: Cumulative infiltration of clear water and 40 g soil particles in suspension

Cumulative infiltration rate and infiltration amount of clear water were significantly greater ($p < 0.05$) than those of the muddy water (sand, silt and clay suspensions) (Appendix B1.1 – B2.1). The presence of dispersed soil particles may have caused the sealing of the soil pores, which led to the lowered infiltration of muddy water. It was also evident that the differences among the cumulative infiltration amounts of the various muddy suspensions and clear water were large except for suspensions containing 10 g sediment particles (Figs. 4.2a – d). A relative decrease in infiltration thus, required a larger relative increase in the seal hydraulic resistance, which is dependent on its thickness (Segeren and Trout, 1991). This explains the reason for the insignificant differences among the cumulative infiltration of fluids at low concentrations (i.e. 10 g), even though seal conductivities showed high variations with respect to sediment particle diameter.

From the data, it was clear that the higher the sediment concentration, the lower the infiltration (Figs. 4.2a – d), due to the increase in sediment deposition at the soil surface, resulting in a rise of its thickness. Additionally, increasing sediment concentration in water increased the viscosity of the suspension, which was clearly observable from the flow measurements taken during the infiltration test. However, the cumulative infiltration amount for sediment concentration of 30 g was almost the same as that of 40 g. This indicates that there is an upper limit for the effects of the sediment concentration on infiltration process. The effect of sediment concentration on infiltration could be attributed mainly to the average soil water suction at the wetting front. Besides, the data points depicted in Figs. 4.1a – c and 4.2a – d appeared to follow the same curves, even though the soil conductivities varied with respect to the surface condition. This indicates that the seal had the same relative effect on infiltration regardless of the hydraulic conductivity of the sub-seal soil. However, it is imperative to note that this tendency would be emphasised by error in the assumption that the seal has a constant hydraulic conductivity.

4.3 Surface sealing

The experimental results on the soil physical and hydraulic properties, as well as the infiltration data showed that sediment particles were trapped in the interstices of the top few millimetres of the soil column and formed a seal layer that impeded the infiltration of water. This observation showed that sediment infiltration occurred to a limited depth within the soil as seen from the thickness of the seal layer (Table 4.3). The seal thickness was expected to increase with time during the infiltration process, but its evaluation was difficult, even after infiltration had ended. Due to this

difficulty, the most direct method to describe the process of soil surface sealing was by equation (3.22).

The study also revealed the possibility that, with sediment movement and surface seal formation, physical changes may have occurred below the thin surface layer. For instance, processes such as consolidation and 'washing-in' of sediments may have been responsible for the reduced conductivity below the seal. The effects of these processes reflected in the computed cumulative infiltration amount values. For different sediments at equal concentrations, statistical results showed no clear differences among seal thickness (Appendix C). However, significant differences existed among different sediments particles at different concentrations. Additionally, one sample t-test analysis revealed considerable variations among seal thickness with respect to time for each sediment concentration (Appendix D).

These results discredit earlier assumptions that seal thickness remains constant during formation, in that, seal thickness was highly variable with time. However, it supports the earlier assumption by Segeren and Trout (1991) that the hydraulic resistance of the seal is the only soil hydraulic parameter that changes after the start of the infiltration. This assumption required all soil characteristics that affect infiltration to be constant for the underlying soil. Thus, the net effect of surface seal on infiltration was a function of the ratio of the seal conductivity to its thickness. Hence, the hydraulic resistance can be regarded as a more practical and useful parameter than hydraulic conductivity to characterize the effects of seal on infiltration. It was also obvious that the presence of surface seal, rather than the water content of the soil profile controlled the reduction in infiltration. This may ultimately

result in the advanced rate of overland flow and soil erosion on sloping land, or surface ponding when the land is relatively flat and horizontal under field conditions.

KNUST



Table 4.3: Estimated seal thickness for the different sediment particles at various concentrations in suspension

Time (S)	Seal thickness (mm)											
	Clay suspension†				Silt suspension†				Sand suspension†			
	10	20	30	40	10	20	30	40	10	20	30	40
30	1.875E-3	3.750E-3	5.625E-3	7.500E-3	1.875E-3	3.751E-3	5.626E-3	7.502E-3	3.750E-3	7.500E-3	1.125E-2	1.500E-2
300	1.875E-2	3.750E-2	5.625E-2	7.500E-2	1.876E-2	3.751E-2	5.626E-2	7.502E-2	3.750E-2	7.500E-2	1.125E-1	1.500E-1
600	3.750E-2	7.500E-2	1.125E-1	1.500E-1	3.751E-2	7.502E-2	1.125E-1	1.500E-1	7.500E-2	1.500E-1	2.250E-1	3.000E-1
900	5.625E-2	1.125E-1	1.688E-1	2.250E-1	5.626E-2	1.125E-1	1.688E-1	2.251E-1	1.125E-1	2.250E-1	3.375E-1	4.500E-1
1800	1.125E-1	2.250E-1	3.375E-1	4.500E-1	1.125E-1	2.251E-1	3.376E-1	4.501E-1	2.250E-1	4.500E-1	6.750E-1	9.000E-1
2100	1.313E-1	2.625E-1	3.938E-1	5.250E-1	1.313E-1	2.626E-1	3.939E-1	5.251E-1	2.625E-1	5.250E-1	7.875E-1	1.0500
2700	1.688E-1	3.375E-1	5.063E-1	6.750E-1	1.688E-1	3.376E-1	5.064E-1	6.752E-1	3.375E-1	6.750E-1	1.0125	1.350
3000	1.875E-1	3.750E-1	5.625E-1	7.500E-1	1.876E-1	3.751E-1	5.626E-1	7.502E-1	3.750E-1	7.500E-1	1.125	1.500
3600	2.250E-1	4.500E-1	6.750E-1	9.000E-1	2.251E-1	4.501E-1	6.752E-1	9.002E-1	4.500E-1	9.000E-1	1.350	1.800

†Mass of sediments in suspension (g)

KNUST

104



In the event of seal formation, loose sediment particles from the suspensions were deposited on the wetted perimeter or transported by infiltration through the upper soil layer, and filled the inter-aggregate voids of the undisturbed soil below the surface (i.e. when flowing through the soil, the particles were brought in contact with retention sites, where they were fixed). These processes resulted in the creation of a compacted layer at the soil surface by reducing the porosity. This also changed the pore size distribution of the surface layer to those of narrower pores. Thus, the reduction in infiltration amount (Figures 4.2a – c) was due to surface seal formation, which acted like a valve at the soil surface. The deposition layer (i.e. surface seal) observed in this study was different from the seal layer that would form as a result of raindrop impact, in that the surface seal resulted from the redistribution of dispersed finer fragments and/or primary particles on the surface or within the top few millimetres of the soil columns.

It is clear from Table 4.3 that, increasing the concentration of sediment particles, irrespective of their characteristic physical diameter (or size) would increase the thickness of the surface seal. In addition, the larger (coarser) the sediment particle, the thicker the surface seal, even at relatively short time intervals. For instance, at 30 seconds, the seal thickness was estimated as 1.875×10^{-3} mm for 10 g clay and silt, and 3.750×10^{-3} mm for sand. These observations clearly showed that at equal concentrations, silt and clay fractions produced surface seals of similar thickness. Thus, the type of sediment particle present in the suspension had considerable influence on seal formation, even though statistical results showed no significant differences among them, where they had similar concentrations in suspension

(Appendix C). Thus, the extent of surface sealing is highly dependent on soil texture, with the content of the finer fraction (i.e. clay and silt) being good indicators of the soil's susceptibility to surface sealing.

In detail, larger particles (i.e. fine sand) filled or covered larger pores, whereas smaller suspended sediment particles (clay) were filtered out at the surface as the water infiltrated and was kept in place by the negative water-phase pressure below the soil surface (Brown *et al.*, 1988). This explains why fine soil particles that would otherwise remain suspended in water adhered to the wetted perimeter upon contact. Additionally, high concentrations of suspended sediment, irrespective of its characteristic diameter appeared to promote sealing capacity. However, the sealing capacity increased with decreasing sediment diameter. Thus, the process of surface sealing is related to the geometrical properties of the soil column and the suspended sediments.

Hydrodynamic forces (Chauveteau *et al.*, 1998) and the effects of the location where the particles were deposited also greatly influenced the mechanisms that led to the decrease in conductivity caused by surface sealing. Other studies have also indicated that the rate of particle blockage within saturated porous media is related to the ratio of particle diameter to sand-grain diameter, the surface roughness of the soil matrix, particle size non uniformity, pore-scale hydrodynamics and pore water chemistry (Xu *et al.*, 2006; Bradford *et al.*, 2007; Porubcan and Xu, 2011). In view of these assertions, flow of suspended particles through soil could be described as mechanical filtration for the sand and silt particles and a physico-chemical filtration for clay particles. The filtration process could thus, be explained as a phase transition of the

sediments from the flowing fluid phase into a solid phase at and below the soil surface. This was responsible for the changes in the physical and hydraulic parameters at the soil surface.

Emphatically, the major factors that influenced the complex sediment sealing process were the size distribution of solids present in the water, the concentration of the sediment in the water, and the flow velocity of water moving vertically toward the soil surface. Thus, the nature (i.e. size) of the suspended sediment greatly influenced the development and physical characteristics of the seal. Again, dispersed clay produced high bulk density seal, whereas the sand particles formed a more porous seal, owing to the random orientation of the particles. In addition, the tension that developed below the seal caused consolidation of the seal and the sub-seal layers, which resulted in the reduction of the conductivity (Trout, 1990). This was responsible for the great reduction in the infiltrability of the soil. Thus, the sealing process had two main effects: an increase in the soil bulk density, and the thickening of the affected zone, creating a disturbed layer at the vicinity of the soil surface.

The physical processes involved in the formation of the seal also involved gravitational settling of suspended sediment, which produced a horizontally extensive depositional layer above the soil surface. This layer was subjected to compressive forces from the soil layer's own mass and that of the overlying water (Bouwer *et al.*, 2001). Retardation of infiltration by this layer, thus, relied upon the force of gravity to cause the deposition, accumulation, and adherence of sediment layers onto the original soil surface. Another mechanism involved infiltrating water sweeping suspended particles into surface soil pores. Gravitational forces caused the

particles to be deposited on the upper surfaces and ledges of soil particles within the matrix, filling in crevices and concavities on the particles. This mechanism, referred to as “washing in”, has been identified in sands and soils subjected to raindrop impact (McIntyre, 1958; Greene *et al.*, 1990; Bresson and Cadot, 1992), and in this study, ponding of turbid water. Thus, in the event of formation, suspended sediments were carried to the wetted perimeter in the flowing water and to some extent by gravitational settling, which led to the formation of a thin, continuous, lowconductivity depositional seal on the original soil surface.

In natural fields, this phenomenon of sealing during rainfall or irrigation is a very complex process and is influenced by many factors, including intensity and energy of rainfall, slope, stability of aggregates and soil texture. Thus, management practices such as irrigation (i.e. sprinkler and surface), and application of polymeric substances may result in surface sealing (Pachepsky and Timlin, 1996). Although local by nature, these changes in the disturbed soil layer can affect its mean physical properties. These observations indicate that under field conditions, prolonged irrigation would be required to ‘wet up’ the root zone, which may eventually result in greater runoff and erosion than would otherwise occur without the presence of a surface seal.

Therefore, the effects of the exposure to muddy water infiltration on the soil structure could be characterized in terms of changes in the mean physical and hydraulic properties of the disturbed layer of the soil. These processes suggest that surface sealing is not solely dominated by rainfall, but some physico-chemical soil properties, as well as the nature of flowing water. The common aspect of these

properties is the cohesive power between the soil particles, which is related to the mechanical, chemical and hydraulic conditions of the soil system, an expression of the soil's resistance to destruction. These observations suggest that, in dealing with sand and mud (clay and silt) mixtures, differential settling is likely to occur.

4.4 Time-to-incipient ponding

Infiltration under rainfall and/or irrigation is a two-phase process. In the course of the first phase, the potential infiltration rate is greater than the rainfall rate. The actual infiltration rate is equal to the rainfall rate because the water can only enter the soil at the application rate. At a certain time, referred to as the time-to-ponding, the potential infiltration rate equals the rainfall rate and water begins to pond on the soil surface. Green and Ampt (1911) defined time-to-incipient ponding (t_p) as the time elapsed between the beginning of rainfall/irrigation and when water begins to pond on the soil surface.

Given a constant rainfall flux, incipient ponding can be defined as the state in which the rainfall rate is equal to the infiltration rate and free water begins to form at the soil surface when the land is horizontal and relatively flat. In this study, the definition of incipient ponding was expanded to include the beginning of runoff on sloping land. The effect of sediment diameter and its concentration on time-to-incipient ponding was estimated from equation (3.24) for a range of hypothetically selected rainfall rates as shown in Table 4.4. Comprehensive summary of statistical analysis (i.e. one sample t-test) is presented in Appendix E. The condition varied from clear water to muddy water, taking into account the particle diameter and concentration of the sediment particle.

KNUST



Table 4.4: Critical time-to-incipient ponding resulting from the interactions among different sediments and their concentrations

R_r (mm h ⁻¹)	t_p (s)												
	Clear water	Clay suspension†				Silt suspension†				Sand suspension†			
		10	20	30	40	10	20	30	40	10	20	30	40
5	N*	4.36	2.18	1.44	1.074	N*	150.95	56.18	33.96	N*	N*	N*	496.23
10	1005.60	4.20	2.14	1.42	1.065	293.076	67.088	38.51	26.58	N*	1021.44	175.58	96.045
15	266.053	4.15	2.12	1.41	1.062	159.86	56.61	34.85	24.78	N*	270.38	117.83	75.70
20	194.53	4.12	2.12	1.41	1.060	130.26	52.50	33.27	23.97	1996.68	197.70	101.18	68.45
25	168.87	4.11	2.11	1.41	1.060	117.91	50.44	32.44	23.54	776.90	171.62	93.70	64.93
30	154.10	4.10	2.11	1.41	1.058	110.32	49.036	31.87	23.23	538.066	156.61	88.93	62.59

N* = Negative t_p (i.e., no surface ponding within the time interval); †Mass of soil sediments (g)

110
KNUST



The performance of equation 3.24 for the unsealed soil surface (i.e. the event of clear water infiltration) and the case of the sealed surfaces (resulting from muddy water infiltration) showed that not all situations would cause surface ponding at the different rainfall intensities. For instance, unrealistic and invalid (i.e. negative) parameter values were obtained for 10 g sand suspension at rainfall rates ranging from 5 mm h^{-1} to 15 mm h^{-1} . Similar results were observed for suspensions with 10 g silt, and 20 and 30 g sand for R_r of 5 mm h^{-1} . This occurred as a result of the larger hydraulic conductivity values in relation to rainfall rates for the surface layers (i.e. sediment depositional layers, herein, referred to as surface seals), especially sand.

Compared to the clear water, clay suspensions gave the shortest t_p followed by silt and sand, respectively. Since the rainfall rates ($5, 10, 15, 20, 25$ and 30 mm h^{-1}) were higher than the base K_x of the clay seal, the occurrence of surface ponding was highly expected. It can therefore, be inferred from the data (Table 4.4; Appendix E) that clear water would take a longer time to pond than muddy water. The t_p of clear water was similar to that observed for the sand suspensions since the sand particles improved the conductivity at the surface upon deposition. This implies that, among other things, the higher the K_s , the less the likelihood of ponding and runoff problems on the land. Thus, the suspensions with clay sediments would probably have the most severe problem of surface ponding and runoff.

The results also indicated that increases in t_p would result in decreases in both runoff and sediment load during erosion. Thus, as t_p increases, water intake would increase with a consequent decrease in runoff and erosion. As soil water content increases through increase in water intake, slaking would be minimized or the forces of

aggregate destabilization would decrease. However, as slaking of soil aggregates and dispersion of clay increase, surface seal formation and pore clogging will increase, thereby reducing water intake and t_p , and increasing runoff and sediment load under field conditions.

Time-to-ponding is not a routine measurement unless rainfall simulation studies are being conducted. However, the ability to estimate accurately when surface ponding occurs and how much runoff is produced is important in civil and agricultural engineering, and is essential for the proper design of irrigation systems, rain harvesting reservoirs, and hydraulic structures at the level of the watershed.

4.5 Prediction of cumulative infiltration amount by the model

Of more practical interest regarding the behaviour of the infiltration model was the question of the fundamental validity of the uniqueness principle that operates for clear water infiltration. Predictions were made for each of the treatments using the model, and the predicted values were compared with those from the laboratory measurements. Specifically, the values predicted by the model and those measured in the laboratory were plotted against each other and fitted with a linear equation with zero intercept to verify the validity of each prediction. The slope of the line of best fit and its coefficient of determination (R^2) for each model prediction is given in Table 4.5. To check the discrepancies between the predicted and the measured values, paired t-test (Appendix G) and Root Mean Square Error (RMSE) analyses were conducted. The Modified Green-Ampt surface sealing (MGASS) infiltration model provided a good fit to the laboratory infiltration data for the different sediment suspensions at different concentration levels. This good agreement could be

considered as an indication that the soil physical and hydraulic properties and the flow conditions assumed herein were appropriate. In addition, thorough statistical results (i.e. Repeated measured one-way ANOVA and Tukey's multiple comparisons test) for the comparison of treatment means are presented in Appendix F.

KNUST



Table 4.5: Values of the performance indices between the predicted and measured cumulative infiltration for the various fluids and their concentrations.

Index	Fluid												
	Clear water	Clay suspension†				Silt suspension†				Sand suspension†			
		10	20	30	40	10	20	30	40	10	20	30	40
R ²	0.9998	0.9994	0.9992	0.9990	0.9986	0.9995	0.9992	0.9991	0.9989	0.9996	0.9994	0.9992	0.9990
Slope	1.005	1.005	1.008	1.005	1.005	1.009	1.006	1.003	1.003	1.006	1.005	1.002	1.004
RMSE	0.0129	0.0503	0.0335	0.0753	0.0793	0.0212	0.0184	0.00875	0.0117	0.00814	0.0192	0.0106	0.0148
t-test	2.045	0.2369	2.220	2.538	2.041	2.242	2.406	2.762	2.209	1.861	2.476	1.904	2.517

†Mass of sediment particles in suspension (g)

The result of the slopes of the regression forced through the origin showed that the model satisfactorily predicted the cumulative infiltration for the different fluids with values ranging from 1.002 to 1.009. The coefficient of determination (R^2) values also lay between 0.9986 and 0.9998. Statistical results from paired t-test analysis also indicated that the model satisfactorily predicted the cumulative infiltration for all the treatments. From the R^2 , the accuracy of prediction of the cumulative infiltration was in the order $10\text{ g} > 20\text{ g} > 30\text{ g} > 40\text{ g}$ for the different concentration levels.

The R^2 values indicated the degree to which data variations were explained by the model, whereas, the RMSE showed the amount of divergence of the model values from the observed values. Where the model curve closely paralleled the observation curve, R^2 was close to one (1) as in the case of clear water ($R^2 = 0.9998$) and 10 g sand suspension ($R^2 = 0.9996$). However, the fit of the model (based on the R^2) was slightly reduced at higher levels of concentration due to an apparent decrease in final cumulative infiltration with an increase in concentration. The decrease in final cumulative infiltration (seal conductivity) with increasing concentration could be due to a thicker and an increase in surface seal density resulting from higher deposition of sediments at the soil surface and clogging of pores below the surface.

Since the relationship between R^2 and RMSE does not follow a definite pattern, a higher R^2 value did not always correspond to a lower RMSE. For instance, clear water had a high R^2 of 0.9998, but recorded RMSE of 0.0129, while 30 g silt suspension, although having a R^2 (0.9991) had a low RMSE (0.00875). Holistically, the pooled analyses of the entire infiltration test data showed that the model satisfactorily

predicted the laboratory measured infiltration amount as shown by the values of the slope of the line of best fit, R^2 , paired t-test (Appendix G) and RMSE (Table 4.5). These indices indicated that simulated and observed data were close matches of each other, which signifies the accuracy and precision in predictability of the model. Based on the R^2 values, accuracy of the model's prediction of cumulative infiltration amount was in the order: Clear water > Sand suspension > Silt suspension > Clay suspension owing to discrepancies between the measured and predicted values. Therefore, it can be concluded that the laboratory measured cumulative infiltration did not differ from those predicted by the model since the observed difference could be accounted for by experimental error. Additionally, the lower divergence of the prediction from the measured data clearly demonstrated the flexibility and accuracy of the model.

4.6 Applications of the proposed model

It is evident that the relative independence of muddy water infiltration and sediment texture influences many aspects of studies concerned with forecasting and management of water resources, especially in dry areas. For example, it puts in question the use of sediment texture as an index for classifying or scaling land areas in respect to their water entry, transmission and storage potentials.

The modified Green and Ampt surface sealing (MGASS) infiltration model has the ability to predict the thickness of the seal/crust layer formed from different sediment particles at different concentrations at different time intervals. Further studies on the mechanism of formation of sealing/crusting will be of very much importance in

understanding the interrelations of infiltration, runoff, and soil erosion under rainstorms and irrigation.

According to Philip (1998), the Green-Ampt equation is ill-fitted to the analysis of infiltration into crusted soils and there is no convincing way of patching it. However, the MGASS model can be applied to simulate infiltration under either saturated or unsaturated conditions, in the event of sealing/crusting or through sealed/crusted surfaces of different textures. It can also be applied to quantitatively analyse the effect of soil texture on the process of surface sealing/crusting and the seal/crust properties, and represent and evaluate the effect of sediment concentration on infiltration and surface sealing/crusting phenomena. Thus, the application of this equation under verified field conditions would lead to the determination of the appropriate infiltration characteristics for the area that would optimize infiltration simulation, irrigation performance and minimize water wastage. It also will enable a more efficient comparative evaluation of the effect of management practices on surface seal/crust formation.

CHAPTER FIVE

5.0 CONCLUSIONS AND RECOMMENDATIONS

5.1 Conclusions

In this study, the only soil physical change affecting infiltration was noticeable at the soil surface in the form of a thin surface seal. Thus, structural changes to the soils as they got wetted under no, minimum or maximum sediment-deposition conditions had great effect on infiltration so that their effects were difficult to isolate. Thus, this work has revealed the significant features of the effect of surface sealing/crusting on infiltration process.

An equation for the flow of a suspension through porous medium with instantaneous surface sealing has, therefore been developed from the Green and Ampt equation. Modifications to the original GA equation were developed and tested for improving the estimation of soil water infiltration. This method was unique from others, in that, it explicitly specified the physical properties (specifically, viscosity and relative density) of the fluid, and size of the sediment particle present in the suspension, which was responsible for the formation of surface seal. While these data did not constitute an adequate set to define an operational estimating method, they provided a basis for the relative impact, which was expected. The proposed model appears to have a promise for indexing the infiltration potential of agricultural fields for improved irrigation practices.

In addition, a constitutive assumption was made to describe not only flow process, but also phase transformations of fine materials. The presented assumption included material (sediment) properties, D and V_s . By the discussion of the influence of sediment parameters on the homogeneous infiltration process, conclusions about the process in the heterogeneous case could also be made. Thus, it was possible to explain the occurrence of surface sealing. Again, the geometric conditions in the structure of the porous medium and the fluidized fine particles have been taken into account in a more detailed way. It is also suggested that the incorporation of a constant concentration, and occurrence of sedimentation improved the efficiency of the model.

Observations and measurements showed that infiltration was highly dependent on the characteristics of soil and fluid. The type of sediment in the suspension strongly

affected the development of surface seals and infiltration. Again, water-entry suction was affected by the granulometric texture of the sediment. Sediment concentration also greatly affected infiltration. Although, the net effect of surface seals on infiltration is a function of the ratio of the seal conductivity and the seal thickness, singly, hydraulic conductivity has proven to be a practical and useful parameter to characterize the effects of surface seals on infiltration. Hence, the modified Green and Ampt surface sealing (MGASS) equation can be effectively used to describe infiltration.

Among the advantages of the method, besides its simplicity and computational efficiency, are its physical basis, robustness, and ability to provide good results for infiltration. Again, it has universal guiding significance, especially in irrigation. While the MGASS approach was limited in that it assumed a homogeneous soil wetting profile, it provided good agreement with the experimental data. Thus, cumulative infiltration was successfully simulated. The good agreement found between the cumulative infiltration amount predicted by the model and the laboratory measured data, indicate that the proposed model efficiently accounted for the main factors affecting infiltration and surface sealing.

Additionally, cumulative infiltration amount data demonstrated the relationship between seal development and sediment characteristics. These data indicated that the infiltration-limiting seals from coarser textured sediments were less effective in reducing infiltration and time-to-incipient ponding, especially at low concentrations in relation to the finer textured ones. Seal conductivity decreased rapidly with increasing concentration of sediment particles, probably due to the increasing

thickness of the seal. This contributed highly to increasing hydraulic resistance of surface seal. Thus, seal formation was dependent on the particle diameter and concentration of the sediment in suspension.

Again, the formation a surface seal on the soil acted as a throttle on infiltration. The negative potential generated at the seal-soil interface resulted in small moisture contents in the wetted region of the soil, with associated small value of hydraulic conductivity. The outcome was the marked reduction in the infiltration rate and cumulative infiltration amount. These reductions obviously became more severe as the seal became thicker, irrespective of the type of sediment. A further effect of the throttling was the reduction in the penetration depth, but this was much less marked than the reduction of moisture content in the wetted zone. In the field, the greatly reduced level of soil wetting will have the consequence of severely limiting water availability in the plant-root zone. This would have severe implications on irrigated and dry-land agriculture and horticulture.

The study has clearly shown that a surface seal may influence profoundly the dynamics of infiltration. This implies that, the seal is destructive when maximal wetting of the soil is required, but it might be valuable if ponding/runoff intensification is preferred. In either case, the study has provided the physical and quantitative description of how surface seals modify infiltration in soils. The major effect of sealing in increasing runoff and the potential for erosion was, thus, obvious from the study results.

From the statistical analysis, accuracy in terms of the predictability of the model for cumulative infiltration was in the order $10\text{ g} > 20\text{ g} > 30\text{ g} > 40\text{ g}$ for sand suspension and $10\text{ g} > 20\text{ g} > 40\text{ g} > 30\text{ g}$ for silt and clay suspensions. Overall, it was noted that the accurate prediction by the model was directly related to the permeability of the porous medium and the physical characteristics of the fluid. In addition, the findings suggest that a single, parametric relationship, such as that proposed in this study, may provide reasonable estimates for infiltration of muddy water comprising wide range of sediment particles. Thus, the results demonstrate that when the traditional assumptions on which the G-A model was formulated are relaxed, it can still provide reasonable results for regional-scale analysis, and can be amended to account for conditions for which it was not intended.

5.2 Recommendations

This study was based on data collected from laboratory column studies on one test site. It is necessary to obtain a much broader base of data in order to make inferences about the applicability of the equation for different types of soils. Thus, it would be valuable to have data from many different sites, in order to make a stronger assessment of the proposed infiltration model.

Further, it is vital to conduct studies to evaluate the MGASS model either for the purpose of validation or establishing the model parameters for different soil conditions or comparison of model efficiencies and applicability for different soils. The need for continuous and in-depth study of the applicability of the equation for different soils cannot be over emphasized since model parameters and performance may vary for different soils. Hence, experiments are needed in this area in order to

come to a better understanding of the sediment parameters in the presented model. In addition, the infiltration parameter values for this equation must be estimated for any irrigation system.

Moreover, when formulating a simplified but physically based soil-water simulation model, it is desirable that components of the model are established on the same underlying assumptions. This not only ensures physical and numerical consistency of the model, but also can reduce the number of inputs needed by the model and avoid over parameterization issues often found in other models. The MGASS model meets this requirement and can accurately simulate infiltration. Additionally, future model validation efforts will be more useful if more statistical analyses are performed with more details reported on both the measurements and predictions. Prediction uncertainty, inherent in model simulations, needs to be estimated and reported. It is caused by errors due to violation of assumptions implicit in the model and by uncertainty in the model parameters.

REFERENCES

- Abrahams, A. D., Parsons, A. J. and Luk, S. (1988). Hydrologic and sediment responses to simulated rainfall on desert hillslopes in Southern Arizona. *CATENA*, 15: 103-117.
- Abu-Sharar, T. M. and Salameh, A. S. (1995). Reductions in hydraulic conductivity and infiltration rate in relation to aggregate stability and irrigation water turbidity. *Agricultural Water Management*, 29: 53-62.
- Adu, S. V. (1992). Soils of the Kumasi Region, Ashanti Region, Ghana. Soil Research Institute, CSIR, Ghana. Memoir 8: pp. 81-85.
- Agassi, M., Shainberg, I. and Morin, J. (1981). Effect of electrolyte concentration and soil sodicity on the infiltration rate and crust formation. *Soil Science Society of America Journal*, 45: 848-851.

- Ajwa, H. A. and Trout, T. J. (2006). Polyacrylamide and water quality effects on infiltration in sandy loam soils. *Soil Science Society of America Journal*, 70: 643-650.
- Akram, M. and Kemper, W. D. (1979). Infiltration of soils as affected by the pressure and water content at the time of compaction. *Soil Science Society of America Journal*, 43: 1080-1086.
- American Society for Testing Materials. (1985). Standard test method for particle size analysis of soils. D422-63(1972). 1985 Annual Book of ASTM Standards. American Society for Testing and Materials, Philadelphia, 04.08: pp. 117-127.
- Amin, M. (2005). Spatial Variability of infiltration in Watershed. *Journal of Hydrology*, 45: 101-122.
- Argyrokastitis, I. and Kerkides, P. (2003). A note to the variable sorptivity infiltration equation. *Water Resources Management*, 17: 133-145.
- Bagnold, R. A. (1977). Bed load transport by natural rivers. *Water Resources Research*, 13: 303-312.
- Baumhardt, R. L., Wendt, C. W. and Moore, J. (1992). Infiltration in response to water quality, tillage, and gypsum. *Soil Science Society of America Journal*, 56: 261-266.
- Bečvář, M. (2006). Sediment Load and Suspended Sediment Concentration Prediction. *Soil Water Research*, 1: 23-31.
- Ben-Hur, M., Shainberg, I., Bakker, D. and Keren, R. (1985). Effect of soil texture and CaCO₃ content on water infiltration in crusted soil as related to water salinity. *Irrigation Science*, 141: 328-333.
- Ben-Hur, M., Stern, R., van der Merwe, A. J. and Shainberg, I. (1992). Slope and gypsum effects on infiltration and erodibility of dispersive and non-dispersive soils. *Soil Science Society of America Journal*, 56: 1571-1576.
- Betson, R. (1964). What is watershed runoff? *Journal of Geophysical Research*, 69(8): 1541-1552.
- Beven, K. (2004). Robert E. Horton's perceptual model of infiltration processes. *Hydrological Processes*, 18: 3447-3460.
- Bissonris, Y. L., Fox, D. and Bresson, L. -M. (1998). Incorporating crusting processes in erosion models. NATO ASI Series, 155, pp. 237-246. Modelling

soil erosion by water. Eds. J. Boardman and D. Favis-Mortlock. SpringerVerlag Berlin Heideberg, 1998.

- Blake, G. J. (1968). Infiltration at the Puketuru experimental basin. *Journal of Hydrology*, 7(1): 38-46.
- Bloem, A. A. and Laker, M. C. (1994). Criteria for adaptation of the design and management of center-pivot irrigation systems to the infiltrability of soils. *Water SA*, 20(2): 127-132.
- Bonsu, M. (1992). A physically based model for surface sealing of soil. *Journal of Soil Science*, 43: 229-235.
- Bonsu, M. and Laryea, K. B. (1989). Scaling the saturated hydraulic conductivity of an Alfisol. *Journal of Soil Science*, 40: 731-742.
- Bouma, J., Belmans, C. F. M and Dekker, L. W. (1982). Water infiltration and redistribution in a silt loam subsoil with vertical worm channels. *Soil Science Society of America Journal*, 46: 917-921.
- Bouwer, H. (1966). Rapid field measurement of air-entry value and hydraulic conductivity of soil as significant parameters in flow system analysis. *Water Resources Research*, 2: 729-738.
- Bouwer, H. (1969). Infiltration of water into non-uniform soil. *Journal of Irrigation and Drainage Division, ASCE*, 95(IR4): 451-462.
- Bouwer, H. (1976). Infiltration into increasingly permeable soils. *Journal of Irrigation and Drainage Division, ASCE*, 102(IR1): 127-136.
- Bouwer, H. (2002). Artificial recharge of groundwater: hydrogeology and engineering. *Hydrogeology Journal*, 10: 121-142.
- Bouwer, H. and Rice, R. C. (1989). Effect of water depth in groundwater recharge basins on infiltration, *ASCE Journal of Irrigation and Drainage Engineering*, 115(4): 556-567.
- Bouwer, H., Ludke, J. and Rice, R. C. (2001). Sealing pond bottoms with muddy water. *Ecological Engineering*, 18: 233-238.
- Bradford, S. A, Torkzaban, S. and Walter, S. L. (2007). Coupling of physical and chemical mechanisms of colloid straining in saturated porous media. *Water Research*, 41: 3012-3024.
- Brady, N. C. and Weil, R. R. (1999). *The Nature and Properties of Soils*. Upper Saddle River, NJ: Prentice Hall, Inc.

- Brakensiek, D. L. and Rawls W. J. (1983). Agricultural management effects on soil water processes. Part II. Green-Ampt parameters for crusting soils. *Transactions of American Society of Agricultural Engineers*, 26:1753-1757.
- Braud, I., De Condappa, D., Soria, J. M., Haverkamp, R., Angulo-Jaramillo, R., Galle, S. and Vauclin, M. (2005). Use of scaled forms of the infiltration equation for the estimation of unsaturated soil hydraulic properties (the Beerkan method). *European Journal of Soil Science*, 56(3): 361-374.
- Bresson, L. -M. and Cadot, L. (1992). Illuviation and structural crust formation of loamy temperate soil. *Soil Science Society of America Journal*, 56: 1565-1570.
- Brown, M. J., Kemper, W. D., Trout, T. J. and Humpherys, A. S. (1988). Sediment, erosion and water intake in furrows. *Irrigation Science*, 9: 45-55.
- Buchan, G. D., Grewal, K. S. and Robson, A. B. (1993). Improved model of particlesize distribution: an illustration of model comparison techniques. *Soil Science Society of America Journal*, 57: 901-908.
- Cai, Q. G., Wang, G. P. and Chen, Y. Z. (1998). Process and simulation of small watershed soil erosion in Loess Plateau. Beijing: *Science Press*. 1998.
- Caron, J., Kay, B. D. and Stone, J. A. (1992). Improvement of structural stability of a clay loam with drying. *Soil Science Society of America Journal*, 56: 1583-90.
- Carrera, J. and Neuman, S. P. (1986). Estimation of aquifer parameters under transient and steady state conditions: 1. Maximum likelihood incorporating prior information. *Water Resources Research*, 22: 199-210.
- Castilho, S. C. D., Cooper, M. and Juhasz, C. E. P. (2011). Influence of crust formation under natural rain on physical attributes of soils with different textures. *Revista brasileira de ciencia do solo*, 5(6): 1893-1905.
- Chauveteau, G., Nabzar, L. and Coste, P. -J. (1998). Physics and modelling of permeability damage induced by particle deposition. *Society of Petroleum Engineers*, 39463: 409-419.
- Chen, J., Hopmans, J. W. and Grismer, M. E. (1999). Parameter estimation of twofluid capillary pressure saturation and permeability functions. *Advances in Water Research*, 22: 479-493
- Cheng, N. S. (1997). Simplified settling velocity formula for sediment particle. *Journal of Hydraulic Engineering*, 123: 149-152.

- Childs, E. C. and Bybordi, M. (1969). The vertical movement of water in stratified porous material. 1. Infiltration. *Water Resources Research*, 5(2): 446-459.
- Chow, V. T., Maidment, D. R. and Mays, L. W. (1988). *Applied Hydrology*. New York, NY: McGraw-Hill.
- Chunye, L., Greenwald, D. and Banin, A. (2003). Temperature dependence of infiltration rate during large-scale water recharge into soils. *Soil Science Society of America Journal*, 67: 487-493.
- Clausnitzer, V., Hopmans, J. W. and Starr, J. L. (1998). Parameter Uncertainty Analysis of Common Infiltration Models. *Soil Science Society of America Journal*, 62:1477-1487
- Clemmens, A. J. (1983). Infiltration equations for border irrigation models. P266274. *In: Advances in infiltration. Proceedings of National Conference on Advances in Infiltration. Dec. 12-13, 1983. Chicago, Ill. ASAE Pub. 11-83. St. Joseph, Mo.*
- Contreras, S., Canton Y. and Sole-Benet, A. (2008). Sieving crusts and macrofaunal activity control soil water repellency in semiarid environments: Evidences from ES, Spain. *Geoderma*, 145: 252-258.
- Criddle, D. W., Davis, S., Pair, C. H. and Shockley, D. G. (1956). Methods for evaluating irrigation systems. USDA Soil Conservation Service. US Government Printing Office.
- Darcy, H. (1856). *Les Fontaines Publiques de la Ville de Dijon*. Technical report, Dalmont, Paris.
- Davidroff, B. and Selims, H. M. (1986). Goodness of fit for eight water infiltration models. *Soil Science Society of America Journal*, 50: 759-764.
- Dawdy, D. R. and Vanoni. V. A. (1986). Modeling Alluvial Channels. *Water Resources Research*, 22 (9): 712-812.
- Dietrich, W. E. (1982). Settling velocity of natural particles. *Water Resources Research*, 18: 1615-1626.
- Doran, J. W. and Parkin, T. B. (1996). Quantitative indicators of soil quality: a minimum data set. pp. 25-37. *In: J. W. Doran and A. J. Jones (Eds.) Methods for assessing soil quality. Soil Science Society of America Special Publication*, 49. SSSA, Madison, WI.

- Duchene, M., McBean, E.A. and Thomson, N.R. (1992). Modeling of Infiltration from Trenches for Storm-water Control, *ASCE Journal of Water Resources Planning and Management*, 120 (3): 276-293.
- Dunne, T. and Leopold, L. (1978). *Water in Environmental Planning*, Freeman, San Francisco.
- Eder, A., Strauss, P., Krueger, T. and Quinton, J. N. (2010). Comparative calculation of suspended sediment loads with respect to hysteresis effects (in the Petzenkirchen catchment, Austria). *Journal of Hydrology*, 389: 168-176.
- Einstein, H. A. (1968). Deposition of suspended particles in a gravel bed. *Journal of Hydraulic Division of American Society of Civil Engineers*, 94 (HY5): 11971205.
- El-Morsy, E. A., Malik, M. and Letey, J. (1991). Interaction between water quality and polymer treatment on infiltration rate and clay migration. *Soil Technology*, 4: 221-231.
- Faning, D., Yunhe, L., Junqiang, C., Zhongan, Z. and Zhouyu, W. (2006). Muddy water seepage theory and its application. *Science in China Series E: Technological Sciences*, 49(4): 476-484.
- FAO-UNESCO. (1988). Soil map of the world, 1:5,000,000. Revised Legend. 4th draft.
- Feng, G. L., Letey, J. and Wu, L. (2002). The influence of two surfactants on infiltration into a water repellent soil. *Soil Science Society of America Journal*, 66: 361-367.
- Ferguson, B. K. (1994). *Storm water Infiltration*, CRC Press, Inc.
- Foster, G. R., Meyer, L. D. and Onstad, C. A. (1977). A runoff erosivity factor and variable slope lengths exponents for soil loss estimates. *Transactions of American Society of Agricultural Engineers*, 20: 683-687.
- Freebairn, D. M., Gupta, S. C. and Rawls, W. J. (1991). Influence of aggregate size and microrelief on development of surface soil crusts. *Soil Science Society of America Journal*, 55: 188-195.
- Fuentes, C., Haverkamp, R. and Parlange, J. -Y. (1992). Parameter constraints on closed-form soil water relationships. *Journal of Hydrology*, 134(1): 117-142.
- Gardner, W. (1986). Water Content pp. 493-544. In: A. Klute (ed.) *Methods of Soil Analysis. Part 1*, 2nd ed. Soil Science Society of America, Madison, WI.

- Ghorbani Dashtaki, S., Homaei, M., Mahdian, M. and Kouchakzadeh, M. (2009). Site-dependence performance of infiltration models. *Water Resources Management*, 23: 2777-2790.
- Gifford, G. F. (1976). Applicability of some infiltration formulae to rangeland infiltrometer data. *Journal of Hydrology*, 28: 1-11.
- Gomez, J. A., Giraldez, J. V. and Fereres, E. (2001). Analysis of infiltration and runoff in an olive orchard under no-till. *Soil Science Society of America Journal*, 65: 291-299.
- Green, P. E. and Carroll, J. D. (1978). Analyzing multivariate data. New York (NY): John Wiley & Sons.
- Green, V. S., Stott, D. E., Norton, L. D. and Graveel, J. G. (2000). Polyacrylamide molecular weight and charge effects on infiltration under simulated rainfall. *Soil Science Society of America Journal*, 64: 1786-1791.
- Green, W. H. and Ampt, G. (1911). Studies of Soil Physics, Part 1. The flow of air and water through soils. *Journal of Agricultural Science*, 4: 1-24.
- Greene, R. S. B., Chartres, C. J. and Hodgkinson, K. C. (1990). The effects of fire on the soil in a degraded semi-arid woodland. I. Cryptogam cover and physical and micromorphological properties. *Australian Journal of Soil Research*, 28: 755-777.
- Greener, M. (2001) Incorporating sediment transport competence into existing soil erosion models. Ph.D. thesis, University of Leicester.
- Hadas, A., and Frenkel, H. (1982). Infiltration as affected by long term use of sodic saline water for irrigation. *Soil Science Society of America Journal*, 46: 524-530.
- Haggard, B. E., Moore Jr., P. A. and Brye, K. R. (2005). Effect of Slope on Runoff from a Small Variable-Slope Box. *Journal of Environmental Hydrology*, 13(25). <http://hydroweb.com>. (Accessed: 18/03/2013).
- Haverkamp, R., Parlange, J. -Y., Starr, J. L., Schmitz, G. and Fuentes, C. (1990). Infiltration under ponded conditions: 3. A predictive equation. *Soil Science*, 149: 292-300.
- Haverkamp, R., Rendon, L. and Vachaud, G. (1987). Infiltration equations and their applicability for predictive use, 142-152. In: Y. -S. Fok (ed.) *Infiltration Development and Application*. Honolulu, Hawaii.
- Haverkamp, R., Ross, P., Smettem, K. and Parlange, J. -Y. (1994). Three-

dimensional analysis of infiltration from the disc infiltrometer: 2. Physically based infiltration equation. *Water Resources Research*, 30(11): 2931-2935.

Hillel, D. (1971). *Soil and Water: Physical Principles and Processes*. Academic Press, New York, NY.

Hillel, D. (1980). *Applications of soil physics*. Academic Press, New York.

Hillel, D. (1998). *Environmental Soil Physics*. Academic Press, San Diego, CA.

Hillel, D. and Gardner, W. R. (1970). Transient infiltration into crust topped profiles. *Soil Science*, 109: 69-76.

Holtan, H. N. (1961). A concept for infiltration estimates in watershed engineering. *USDA, Agricultural Research Service Publication*: 41-51.

Holtan, H. N. and Creitz, N. R. (1967). Influence of soils, vegetation and geomorphology on elements of the flood hydrograph. Symposium on floods and their computation, Leningrad, Russia.

Holtan, H. N., and Lopez, N. C. (1971). USDAHL-70 model of watershed hydrology. *USDA-ARS Technical Bulletin*, 1435, Agricultural Research Station, Beltsville, Md.

Horton, R. E. (1938). The interpretation and application of runoff plot experiments with reference to soil erosion problems. *Soil Science Society of America Journal*, 3: 340-349.

Horton, R. E. (1939). Analysis of runoff plot experiments with varying infiltration capacity. *Transactions of the American Geophysicists*. Union, Part IV: 693694.

Horton, R. E. (1940). An approach towards a physical interpretation of infiltration capacity. *Soil Science Society of America*, 5: 399-417.

Huat, B. B. K., Ali, F. H. J. and Low, T. H. (2006). Water infiltration characteristics of unsaturated soil slope and its effect on suction and stability *Geotechnical and Geological Engineering*, 24: 1293-1306.

Huggins, L. F. and Monke, E. I. (1966). The mathematical simulation of the hydrology of small watersheds. Technical Report No. 1 Purdue Water Resources Research Centre, Lafayette.

Hwang, S., Lee, K. P., Lee, D. S. and Powers, S. E. (2002). Models for estimating soil particle-size distributions. *Soil Science Society of America Journal*, 66: 1143-1150.

- Igbadun, H. E. and Idris, U. D. (2007). Performance Evaluation of Infiltration Models in a Hydromorphic Soil. *Nigerian Journal of Soil and Environmental Research*, 7: 53-59.
- Israelson, O. W. and Hansen, V. E. (1967). *Irrigation Principles and Practices* pp. 198-200 .John Wiley, New Delhi.
- Jungerius, P. D. and Van der Meulen, F. (1988). Erosion processes in a dune landscape along the Dutch coast. *CATENA*, 15: 217-228.
- Jury, W. A., Gardner, W. R. and Gardner, W. H. (1991). *Soil Physics*. 5th ed. New York (NY): John Wiley & Sons.
- Kazman, Z., Shainberg, I. and Cal, M. (1983). Effect of low levels of exchangeable Na applied phosphogypsum on the infiltration rate of various soils. *Soil Science*, 135: 184-192.
- Khalid, A. A., Tuffour, H. O. and Bonsu M. (2014). Influence of Poultry Manure and NPK Fertilizer on Hydraulic Properties of a Sandy Soil in Ghana. *International Journal of Scientific Research in Agricultural Sciences*, 1(2): 16-22.
- Khatri, K. L. and Smith R. J. (2005). Evaluation of methods for determining infiltration parameters from irrigation advance data. *Irrigation and Drainage*, 54: 467-482.
- Kirkham D. and Powers W. L. (1972). *Advanced Soil Physics*. Wiley, New York, NY.
- Klute, A. and Dirksen, C. (1986). Hydraulic conductivity and diffusivity: Laboratory methods. *In: Methods of Soil Analysis, Part 1 Physical and Mineralogical Methods*. Second Edition, ASA, Madison, Wisconsin, USA.
- Kostiakov, A. N. (1932). On the dynamics of the coefficient of water-percolation in soils and on the necessity for studying it from a dynamic point of view for purposes of amelioration. *Transactions Congress International Society for Soil Science*, 6th, Moscow, Part A: 17-21.
- Kozak, J. A. and Ahuja, L. R. (2005). Scaling of infiltration and redistribution of water across soil textural classes. *Soil Science Society of America Journal*, 69:816-827.
- Krammer, C. and Strauss, P. (2014). Land use induced change of suspended sediment loads in the Petzenkirchen catchment, Lower Austria. 15th Biennial Conference of the EuroMediterranean Network of Experimental and

Representative Basins. Advances in Hydrologic Research on Pristine, Rural and Urban Small Basins. 9-13 September, 2014, Coimbra, Portugal.

- Lado, M. and Ben-Hur, M. (2004). Soil mineralogy effects on seal formation, runoff and soil loss. *Applied Clay Science*, 24: 209-224.
- Le Bissonnais, Y. and Bruand, A. (1993). Crust micromorphology and runoff generation on silty soil materials during different seasons. In: Poesen, J. W. A. and Nearing, M. A. (Eds.) *Soil Surface Sealing and Crusting. Catena Supplement*, 24: 1-16.
- Le Bissonnais, Y., Benkhadra, H., Chaplot, V., Fox, D., King, D. and Daroussin, J. (1998). Crusting, runoff and sheet erosion on silty loamy soils at various scales and upscaling from m² to small catchments. *Soil Tillage Research*, 46(1-2): 69-80.
- Le Bissonnais, Y., Renaux, B. and Delouche, H. (1995). Interactions between soil properties and moisture content in crust formation, runoff and interrill erosion from tilled loess soils. *Catena*, 25(1-4): 33-46.
- Le Van Phuc and Morel-Seytoux, H. J. (1972). Effect of soil air movement and compressibility on infiltration rates. *Soil Science Society of America Proceedings*, 36: 237-241.
- Levy, G. J., and Van Der Watt, H. v. H. (1990). Effect of exchangeable potassium on the hydraulic conductivity and infiltration rate of some South African soils. *Soil Science*, 149: 69-77.
- Levy, G. J., Levin, J. L. and Shainberg, I. (1994). Seal formation and interrill soil erosion. *Soil Science Society of America Journal*, 58: 203-209.
- Lewis, J. (1996). Turbidity-controlled suspended sediment sampling for runoff-event load estimation. *Water Resources Research*, 32(7): 2299-2310.
- Lili, M., Bralts, V. F., Yinghua, P., Han, L. and Tingwu, L. (2008). Methods for measuring soil infiltration: State of the art. *International Journal of Agricultural and Biological Engineering*, 1(1): 22-30.
- Loch, R. J. and Foley, J. L. (1994). Measurement of aggregate breakdown under rain: Comparison with tests of water stability and relationships with field measurements of infiltration. *Australian Journal of Soil Research*, 32: 701-720.
- Machiwal, D., Madan Kumar, J. H. A. and Mal, B. C. (2006). Modelling infiltration and quantifying spatial soil variability in a watershed of Kharagpur. *Indian Biosystems Engineering*, 95: 569-582.

- Mallows, C. L. (1973). Some comments on Cp. *Technometrics*, 15: 661-675.
- Maryland Department of the Environment and Centre for Watershed Protection (2000). Maryland Storm water Design Manual, Volumes I and II. Maryland Department of the Environment, Baltimore, Maryland.
- Massmann, J. W. (2003). Implementation of Infiltration ponds research. Technical report for the Washington State Transportation Commission, Department of Transportation in cooperation with U.S. Department of Transportation, Federal Highway Administration.
- Mbagwu, J. S. C. (1993). Testing the goodness of fit of selected infiltration models on soils with different land use histories. International Centre for Theoretical Physics. Trieste, Italy.
- McDowell-Boyer, L. M., Hunt, J. L. and Sitar, N. (1986). Particle transport through porous media. *Water Resources Research*, 22: 1901-1921.
- McIntyre, D. S. (1958). Permeability measurements of soil crust formed by raindrop impact. *Soil Science*, 85: 185-189.
- McNeal, B. L., Layfield, D. A., Norvell, W. A. and Rhoades, J. S. (1968). Factors influencing hydraulic conductivity of soils in the presence of mixed salt solutions. *Soil Science Society of America Proceedings*, 32: 187-190.
- Mein, R. G. and Larson, C. L. (1973). Modelling infiltration during a steady rain. *Water Resources Research*, 9(2): 384-394.
- Messing, I., Iwald, J., Lindgren, D., Lindgren, K., Nguyen, L. and Hai, T. S. (2005). Using pore sizes as described in soil profile descriptions to estimate infiltration rate and saturated hydraulic conductivity. *Soil Use and Management*, 21: 376-277.
- Mezencev, V. J. (1948). Theory of formation of the surface runoff. *Meteorologiae Hidrologia*, 3: 33-40.
- Minasny, B., McBratney, A. B. and Bristow, K. L. (1999). Comparison of different approaches to the development of pedotransfer functions for water-retention curves. *Geoderma*, 93: 225-253.
- Mirzaee, S., Zolfaghari, A. A., Gorji, M., Dyck, M. and Ghorbani Dashtaki, S. (2013). Evaluation of infiltration models with different numbers of fitting in different soil texture classes. *Archives of Agronomy and Soil Science*, 2013: 1-13.

- Mishra, S. K. and Singh, V. P. (1999). Another look at the SCS-CN method. *Journal of Hydrological Engineering*, 4: 257-264.
- Mishra, S. K. and Singh, V. P. (2003). Soil Conservation Service Curve Number (SCS-CN) Methodology. 1st Edn. Kluwer Academic Publishers, Dordrecht, The Netherlands, ISBN-13: 978-1402011320.
- Mishra, S. K., Kumar, S. R. and Singh, V. P. (1999). Calibration and validation of a general infiltration model. *Hydrological Processes*, 13: 1691-1718.
- Mishra, S. K., Tyagi, J. V. and Singh, V. P. (2003). Comparison of infiltration models. *Hydrological Processes*, 17: 2629-2652.
- Mitchell, A. R. (1986). Polyacrylamide application in irrigation water to increase infiltration. *Soil Science*, 141: 353-358.
- Moore, I. D. (1981a). Effects of surface sealing on infiltration. *Transactions of American Society of Agricultural Engineers*, 24: 1546-1552.
- Moore, I. D. (1981b). Infiltration equations modified for surface effects. *Journal of Irrigation and Drainage Division of American Society of Civil Engineers*, 107(IR1): 71-86.
- Moore, I. D., Larson, C. L., Slack, D. C., Wilson, B. N., Idike, F. and Hirschi, M. C. (1981). Modeling infiltration: A measureable parameter approach. *Journal of Agricultural Engineering Research*, 26(1): 21-32.
- Morel-Seytoux, H. J. and Khanji, J. (1974). Derivation of an equation of infiltration. *Water Resources Research*, 10(4): 795-800.
- Morel-Seytoux, H. J., Meyer, P. D. Nachabe, M. Touma, J. van Genuchten, M. Th. and Lenhard, R. J. (1996). Parameter equivalence for the Brooks-Corey and van Genuchten soil characteristics: Preserving the effective capillary drive. *Water Resources Research*, 32(5): 1251-1258.
- Morin, J. and Benyamini, Y. (1977). Rainfall infiltration into bare soils. *Water Resources Research*, 13: 813-817.
- Morin, J., Benyamini, Y. and Michaeli, A. (1981). The dynamics of soils crusting by rainfall impact and the water movement in the soil profile. *Journal of Hydrology*, 52: 321-335.
- Morris, G. L. and Fan, J. (1998). Reservoir sedimentation handbook, McGraw-Hill Book Co., New York.

- Moss, A. J. (1991). Rain-impact soil crust. I. Formation on a Granite-derived soil. *Australian Journal of Soil Research*, 29: 271-289.
- Moss, A. J., Walker, P. H. and Hutka, J. (1980). Movement of loose, sandy detritus by shallow water flows: an experimental study. *Sedimentary Geology*, 25: 4366.
- Motsara, M. R. and Roy, R. N. (2008). Guide to laboratory establishment for plant nutrient analysis. *FAO Fertilizer and Plant Nutrition Bulletin*, 19: 31-33.
- Naeth, M. A., Chanasyk, D. S. and Bailey, A. W. (1991). Applicability of the Kostiakov equation to mixed prairie and fescue grasslands of Alberta. *Journal of Range Management* 44 (1): 18-21.
- Nash, J. E. and Sutcliffe, J. V. (1970). River flow forecasting through conceptual models, Part I-A discussion of principles. *Journal of Hydrology*, 10: 282-290.
- Norton, L. D. (1987). Micromorphological study of surface seals developed under simulated rainfall. *Geoderma*, 40: 127-140.
- Novotny, V., and Olem, H. (1994). *Water Quality: Prevention, Identification, and Management of Diffuse Pollution*. New York, NY: Van Nostrand Reinhold.
- Oram, B. (2005). *Hydrological Cycle. Watershed Assessment, Education, Training, Monitoring Resources in Northeastern Pennsylvania*. Wilkes University. Environmental Engineering and Earth Sciences Department. Wilkes-Barre, PA. http://www.water_research.net/watershed/hydrological_cycle (Accessed 31/05/2014).
- Oster, J. D., Singer, M. J., Fulton, A., Richardson, W. and Prichard, T. (1992). *Water penetration problems in California soils: Prevention, diagnoses, and solutions*. Kearney Foundation of Soil Science, Div. of Agriculture and Natural Resources, University of California.
- Overton, D. E. (1964). *Mathematical refinement of an infiltration equation for watershed engineering*. ARS 41-49, US Department of Agricultural Services, Washington, DC., USA.
- Pachepsky, Y. A. and Timlin, D. (1996). Infiltration into a layered soil covered by a depositional seal. *International Agrophysics*, 10: 21-30.
- Parhi, P. K. (2014). Another look at Kostiakov, modified Kostiakov and revised modified Kostiakov infiltration models in water resources applications. *International Journal of Agricultural Sciences*, 4(3): 138-142.

- Parhi, P. K., Mishra, S. K. and Singh, R. (2007). A Modification to Kostiakov and Modified Kostiakov Infiltration Model, *Water Resources Management*, Kluwer Academic Publishers, 21: 1973-1989.
- Parlange, J. -Y. (1971). "Theory of water movement in soils: 1. One-dimensional absorption", *Soil Science*, 111: 134-137.
- Parlange, J. -Y. (1975). On solving the flow equation in unsaturated soils by optimization: Horizontal infiltration. *Soil Science Society of America Journal*, 39(3): 415-418.
- Philip, J. R. (1954). An infiltration equation with physical significance. *Soil Science*, 77: 153-157.
- Philip, J. R. (1957a). The theory of infiltration: 1. The infiltration equation and its solution. *Soil Science*, 83: 345-357.
- Philip, J. R. (1957b). The theory of infiltration: 4. Sorptivity and algebraic infiltration equations. *Soil Science*, 84: 257-264.
- Philip, J. R. (1957c). The theory of infiltration: 5. The influence of initial water content. *Soil Science*, 84: 329-339.
- Philip, J. R. (1969). Theory of Infiltration: *Advances in Hydrosience*. Chow V. T. (Ed.). Academic Press, New York, USA. pp. 215-296.
- Philip, J. R. (1990). Inverse solution for one-dimensional infiltration, and the ratio a/K_1 . *Water Resources Research*, 26(9): 2023-2027.
- Philip, J. R. (1998). Infiltration into crusted soils. *Water Resources Research*, 34(8): 1919-1927.
- Pierson, T. C. (2005). Hyper-concentrated flow – transitional process between water flow and debris flow. Edited by Debris-flow hazards and related phenomena (159-202). Springer Berlin Heidelberg.
- Poesen, J. W. A. (1984). The influence of slope angle on infiltration rate and Hortonian overland flow. *Geomorphology*, 2(49): 117-131.
- Poiseuille, J. L. M. 1846). Recherches experimentales sur le mouvement des liquids dans les tubes de tres-petits diametres. *In: Memoires presentes par divers savants a l'Academie Royale des Sciences de l'Institut de France*, IX: 433544.
- Porubcan, A. A. and Xu, S. P. (2011). Colloid straining within saturated heterogeneous porous media. *Water Research*, 45: 1796-1806.

- Potter, M. and Wiggart, D. C. (2008). Fluid Mechanics, Schuam's outlines, McGraw Hill (USA), 2008, ISBN 978-0-07-148781-8.
- Rasiah, V., Kay, B. D. and Martin, T. (1992). Variation of structural stability with water content: Influence of selected soil properties. *Soil Science Society of America Journal*, 56: 1604-1609.
- Rawls, W. J., Ahuja, L. R., Brakensiek, D. L. and Shirmohammadi, A. (1993). Infiltration and soil water movement. *In: Handbook of Hydrology*. McGrawHill, Inc.
- Rawls, W. J., Ahuja, L. R., Brakensiek, D. L., Shirmohammadi, A. and Maidment, D. (1992). Infiltration and Soil Water Movement, McGraw-Hill Inc., N.Y.
- Rawls, W. J., Brakensiek, D. L. and Miller, N. (1983). "Green-Ampt Infiltration Parameters from Soils Data". *Journal of Hydraulic Engineering*, 109(1): 6270.
- Rehg, K. J., Packman, A. I. and Ren, J. (2005). Effects of suspended sediment characteristics and bed sediment transport on streambed clogging. *Hydrological Processes*, 19:413-427.
- Remley, P. A. and Bradford, J. M. (1989). Relationship of soil crust morphology to interrill erosion parameters. *Soil Science Society of America Journal*, 53: 1215-1221.
- Richards, L. A. (1931). Capillary conduction through porous mediums. *Physics*, 1: 313-318.
- Römken, M. J. M., Baumhardt, R. L., Parlange, J. -Y., Whisler, F. D. and Prasad, S. N. (1985). Effect of rainfall characteristics on seal hydraulic conductance. *In: Callebaut et al. (eds.), Proceedings of the Symposium on the assessment of Soil Surface Sealing and Crusting*. State University of Ghent, Belgium.
- Sadat-Helbar, S. M., Amiri-Tokaldany, E., Darby, S. and Shafaie, A. (2009). Fall Velocity of Sediment Particles. Proceedings of the 4th IASME / WSEAS Int. Conference on Water resources, Hydraulics and Hydrology (WHH '09).
- Schuh, W. M. (1990) Seasonal Variation of Clogging of an Artificial Recharge Basin in a Northern Climate. *Journal of Hydrology*. 120(1-4): 193-215.
- Segeren, A. G. and Trout, T. J. (1991). Hydraulic resistance of soil surface seals in irrigated furrows. *Soil Science Society of America Journal*, 55: 640-646.

- Shirmohammadi, A. and Skaggs, R. W. (1984). Effect of soil surface conditions on infiltration for shallow water table soils. *Transactions of American Society of Agricultural Engineers*, 27(6): 1780-1787.
- Shirmohammadi, A. and Skaggs, R. W. (1985). Predicting infiltration for shallow water table conditions. *Transactions of American Society of Agricultural Engineers*, 28(6): 1829-1837.
- Shukla, K., Lal, R. and Unkefer, P. (2003). Experimental evaluation of infiltration models for different land use and soil management systems. *Soil Science*, 168(3): 178–191.
- Simons, D. B. and Senturk. F. (1992). *Sediment Transport Technology*. Water Resources Publications, Littleton, Colorado.
- Šimuněk, J., Jarvis, N. J. and van Genuchten, M. Th. (2003). Review and comparison of models for describing non-equilibrium and preferential flow and transport in the vadose zone. *Journal of Hydrology*, 272: 14-35.
- Singer, M. J. and Oster, J. D. (1984). Water penetration problems in California soils. Land, Air, and Water Resources Paper No. 10011, Dep. of Land, Air, and Water Resources, University of California, Davis.
- Singh, V. P. and Yu, F. X. (1990). Derivation of infiltration equation using systems approach. *Journal of Irrigation and Drainage Engineering*, 116: 837-857.
- Siyal, A. G., Oad, F. C., Sarno, M. A., Hassan, Z. and Oad, N. L. (2002). Effect of compactions on infiltration characteristics of soil. *Asian Journal of Plant Sciences*, 1: 3-4.
- Skaggs, R. W. and Khaleel, R. (1982). Chapter 4: Infiltration. *In: Hydrology of Small Watersheds*. St Joseph, Michigan, *American Society of Agricultural Engineers*.
- Skaggs, R. W., Huggins, L. E., Monke, E. J. and Foster, G. R. (1969). Experimental Evaluation of Infiltration Equations. *Transactions of American Society of Agricultural Engineers*. Paper No. 3425: 822- 828.
- Smettem, K. R., Ross, P., Haverkamp, R. and Parlange, J. -Y. (1995). Threedimensional analysis of infiltration from the disk infiltrometer: 3. Parameter estimation using a double-disk tension infiltrometer. *Water Resources Research*, 31(10): 2491-2495.
- Smiles, D. and Knight, J. (1976). A note on the use of the Philip infiltration equation. *Soil Research*, 14(1): 103-108.

- Smith, R. E. (1972). The infiltration envelope: results from a theoretical infiltrometer. *Journal of Hydrology*, 17: 1-21.
- Smith, R. E. (1976). Approximations for vertical infiltration patterns. *Transactions of the American Society of Civil Engineers*, 19(3): 505-509.
- Smith, R. E. and Parlange, J. -Y. (1978). A parameter-efficient hydrologic infiltration model. *Water Resources Research*, 14(3): 533-538.
- Soil Conservation Service (1972). Estimation of direct runoff from storm rainfall National Engineering Handbook, Section 4: Hydrology, pp. 10.1-10.24. Washington, DC: USDA.
- Soil Science Society of America (1975). Glossary of soil science terms: Madison, Wisconsin, Soil Science Society of America.
- Stewart, R. D., Rupp, D. E., Abou Najm, M. R. and Selker, J. S. (2013). Modeling effect of initial soil moisture on sorptivity and infiltration. *Water Resources Research*, 49: 7037-7047.
- Sullivan, M., Warwick, J. J. and Tyler, S. W. (1996). Quantifying and delineating spatial variations of surface infiltration in a small watershed.
- Swartzendruber, D. (1968). The applicability of Darcy's Law. *Soil Science Society of America Proceedings*, 32: 11-18.
- Swartzendruber, D. (1987). A quasi-solution of Richard's equation for the downward infiltration of water into soil. *Water Resources Research*, 23: 809-817.
- Swartzendruber, D. (1997). Exact mathematical derivation of a two-term infiltration equation. *Water Resources Research*, 33: 491-496.
- Swartzendruber, D. (2000). Derivation of a two-term infiltration equation from the Green-Ampt model. *Journal of Hydrology*, 236: 247-251.
- Swartzendruber, D. and Hogarth, W. L. (1991). Water infiltration into soil in response to ponded-water head. *Soil Science Society of America Journal*, 55: 1511-1515.
- Swartzendruber, D. and Youngs, E. G. (1974). A comparison of physically based infiltration equations. *Soil Science*, 117: 165-167.
- Talsma, T. (1969). *In situ* measurement of sorptivity. *Australian Journal of Soil Research*, 7: 269-276.

- Touma, J., Voltz, M. and Albergel, J. (2007). Determining soil saturated hydraulic conductivity and sorptivity from single ring infiltration tests. *European Journal of Soil Science*, 58(1): 229-238.
- Trout, T. J. (1990). Surface seal influence on surge flow furrow infiltration. *Transactions of American Society of Agricultural Engineers*, 35: 1583-1589.
- Trout, T. J., Sojka, R. E. and Lentz, R. D. (1995). Polyacrylamide effect on furrow erosion and infiltration. *Transactions of American Society of Agricultural Engineers*, 38: 761-765.
- Tuffour, H. O., Bonsu, M. and Khalid, A. A. (2014a). Assessment of soil degradation due to compaction resulting from cattle grazing using infiltration parameters. *International Journal of Scientific Research in Environmental Sciences*, 2(4): 139-149.
- Tuffour, H. O., Bonsu, M., Khalid, A. A. and Adjei-Gyapong, T. (2014b). Scaling approaches to evaluating spatial variability of saturated hydraulic conductivity and cumulative infiltration of an Acrisol. *International Journal of Scientific Research in Knowledge*, 2(5): 224-232.
- Turner, E. R. (2006). Comparison of infiltration equations and their field validation with rainfall simulation. M.Sc. Thesis, University of Maryland, College Park.
- Ulag, F. (2005). Concentrations and Transport of Suspended sediment in Slovene Rivers. *RMZ – Materials and Geoenvironment*, 52(1): 131-135.
- Valentin, C. (1991). Surface crusting in two alluvial soils of northern Niger. *Geoderma*, 48: 201-222.
- Vandervaere, J. P., Vauclin, M. and Elrick, D. E. (2000). Transient flow from tension infiltrometers: I. The Two-Parameter Equation, *Soil Science Society of America Journal*, 64(4): 1263-1272.
- Vanoni, V. A. (1975). *Sedimentation Engineering*. ASCE, New York.
- Vereecken, H., Maes, J., Feyen, J. and Darius, P. (1989). Estimating the soil moisture retention characteristic from texture, bulk density, and carbon content. *Soil Science*, 148: 389-403.
- Viessman, W. and Lewis, G. L. (2003). *Introduction to Hydrology*. 5th edition. Prentice Hall, Upper Saddle River, New Jersey.
- Wang, Q., Shao, M. and Horton, R. (1999). Modified Green and Ampt Models for layered soil infiltration and muddy water infiltration. *Soil Science*, 164(4): 445-453.

- Wangeman, S. G., Kohl, R. A. and Molumeli, P. A. (2000). Infiltration and percolation influenced by antecedent soil water content and air entrapment. *American Society of Agricultural Engineers*, 43(6): 1517-1523.
- Whisler, F. D. and Bouwer, H. (1970). Comparison of methods for calculating vertical drainage and infiltration for soils. *Journal of Hydrology*, 10(1): 1-19.
- White, I. and Perroux, K. (1987). Use of sorptivity to determine field soil hydraulic properties. *Soil Science Society of America Journal*, 51(5): 1093-1101.
- White, I. and Perroux, K. (1989), Estimation of unsaturated hydraulic conductivity from field sorptivity measurements. *Soil Science Society America Journal*, 53: 324-329.
- White, I. and Sully, M. (1987). Macroscopic and microscopic capillary length and time scales from field infiltration. *Water Resources Research*, 23(8): 1514-1522.
- White, I., Sully, M. and Perroux, K. (1992). Measurement of surface-soil hydraulic properties: Disk permeameters, tension infiltrometers, and other techniques, in *Advances in Measurement of Soil Physical Properties: Bringing Theory into Practice*, pp. 69-103. Soil Science Society of America, Madison, Wisconsin.
- Witter, J. V., Jungerius, P. D. and ten Harkel, M. J. (1991). Modelling water erosion and the impact of water repellency. *CATENA*, 18: 115-124.
- Wooding, R. (1968). Steady infiltration from a shallow circular pond, *Water Resources Research*, 4: 1259-1273.
- Xu, C. Y. (2003). Approximate infiltration models. Section 5.3. In: *Hydrologic Models*. Uppsala University Department of Earth, Air and Water Sciences. Uppsala, Sweden.
- Xu, S. P., Gao, B. and Saiers, J. E. (2006). Straining of colloidal particles in saturated porous media. *Water Resources Research*, 42: 12-16.
- Yalin, M. S. (1977). *Mechanics of sediment transport*, Pergamon Press, Oxford, pp. 80-87.
- Yang, C. T. (1973). Incipient Motion and Sediment Transport. *Journal of Hydraulics Division, ASCE*, 99 (10): 1679-1704.
- Yang, C. T. (1979). Unit Stream Power Equations for Total Load. *Journal of Hydrology*, 40: 123-138.

- Yang, C. T. (1984). Unit Stream Power Equation for Gravel. *Journal of Hydraulics Division, ASCE*, 110 (HY12): 1783-1798.
- Yang, C. T. (1996). *Sediment Transport: Theory and Practice*. McGraw-Hill, New York.
- Yang, C. T., Huang, J. V. and Greimann, B. P. (2004). User Manual for GSTAR-1D 1.0 (Generalized Sediment Transport for Alluvial Rivers – One Dimensional, Version 1.0). U. S. Bureau of Reclamation Technical Service Center, Denver, CO, 80225.
- Yang, C. T., Molinas, A., and Song, C. C. S. (1989). “GSTARS – Generalized Stream Tube model for Alluvial River Simulation”, Twelve Selected Computer Stream Sedimentation Models Developed in the United States, U. S. Interagency Subcommittee Report on Sedimentation, (Ed.) S. S. Fan, Federal Energy Regulatory Commission, Washington, D. C. pp. 148-178.
- Yang, C. T., Treviño, M. A., and Simões, F. J. M. (1998). User’s Manual for GSTARS 2.0 (Generalized Stream Tube model for Alluvial River Simulation version 2.0), U. S. Bureau of Reclamation Technical Service Center, Denver, CO, 80225.
- Yang, C. T. (1983). Rate of Energy Dissipation and River Sedimentation. pp. 575-585, 2nd International Symposium on River Sedimentation, Nanjing, China.
- Young, I. M. and Mullins, C. E. (1991). Water-suspendible solids and structural stability. *Soil Tillage Research*, 19: 89-94.
- Youngs, E. G. (1968). An estimation of sorptivity for infiltration studies from water movement considerations. *Soil Science*, 106: 157-163.
- Zejun, T., Tingwu, L., Qingwen, Z. and Jun, Z. (2002). The sealing process and crust formation at soil surface under the impacts of raindrops and polyacrylamide. Paper presented to 12th ISCO Conference, Beijing.
- Zolfaghari, A. A., Mirzaee, S. and Gorji, M. (2012). Comparison of different models for estimating cumulative infiltration. *International Journal of Soil Science*, 7: 108-115.
- Zumr, D., Devaty, J., Klipa, V., Kavka, P., Dusek, J. and Dosta, T. (2014). Rainfall, Runoff and Soil Erosion Processes on Small Arable Catchment. 15th Biennial Conference of the EuroMediterranean Network of Experimental and Representative Basins. Advances in Hydrologic Research on Pristine, Rural and Urban Small Basins. 9-13 September, 2014, Coimbra, Portugal.

APPENDICES

APPENDIX A: Repeated Measures one-way ANOVA analysis with Tukey's

Multiple Comparisons test for Hydro-physical properties

KNUST



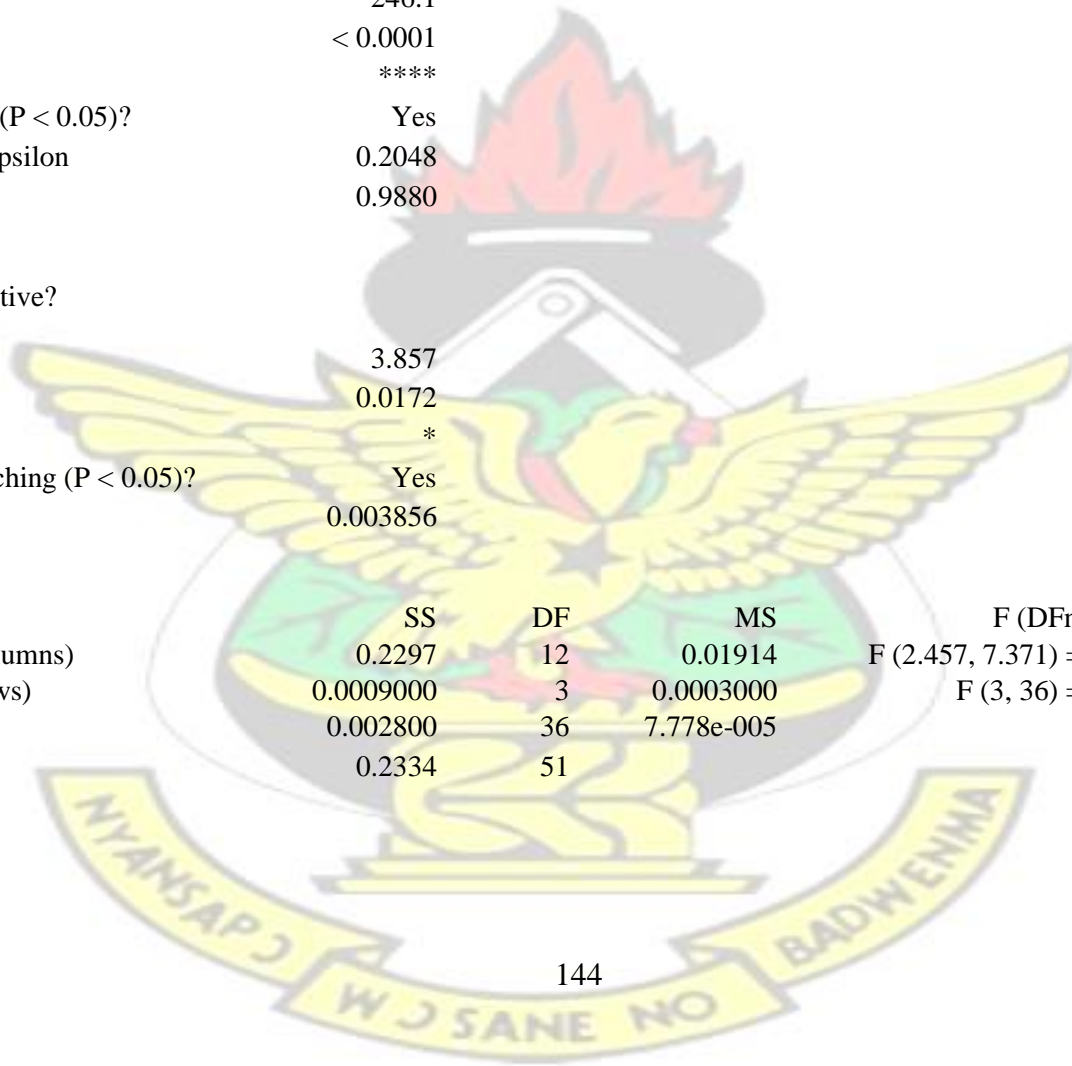
Appendix A1.1: Repeated Measures one-way ANOVA analyses for Bulk density

Assume sphericity?	No
F	246.1
P value	< 0.0001
P value summary	****
Statistically significant (P < 0.05)?	Yes
Geisser-Greenhouse's epsilon	0.2048
R square	0.9880

Was the matching effective?

F	3.857
P value	0.0172
P value summary	*
Is there significant matching (P < 0.05)?	Yes
R square	0.003856

ANOVA table	SS	DF	MS	F (DFn, DFd)	P value
Treatment (between columns)	0.2297	12	0.01914	F (2.457, 7.371) = 246.1	P < 0.0001
Individual (between rows)	0.0009000	3	0.0003000	F (3, 36) = 3.857	P = 0.0172
Residual (random)	0.002800	36	7.778e-005		
Total	0.2334	51			



Appendix A1.2: Tukey's multiple comparisons test summary for Bulk density

Number of comparisons per family 78
 Alpha 0.05

Tukey's multiple comparisons test	Mean Diff.	95% CI of diff.	Significant?	Summary
clear water vs. 10 g clay	-0.02500	-0.07135 to 0.02135	No	Ns
clear water vs. 20 g clay	-0.1075	-0.1527 to -0.06232	Yes	**
clear water vs. 30 g clay	-0.1850	-0.2313 to -0.1387	Yes	**
clear water vs. 40 g sand	-0.2050	-0.2409 to -0.1691	Yes	***
clear water vs. 10 g Silt	-0.02000	-0.04931 to 0.009314	No	Ns
clear water vs. 20 g silt	-0.08500	-0.1314 to -0.03865	Yes	**
clear water vs. 30 g silt	-0.1325	-0.2005 to -0.06454	Yes	**
clear water vs. 40 g silt	-0.1750	-0.2213 to -0.1287	Yes	**
clear water vs. 10 g sand	-0.007500	-0.06882 to 0.05382	No	Ns
clear water vs. 20 g sand	-0.06500	-0.1272 to -0.002815	Yes	*
clear water vs. 30 g sand	-0.09750	-0.1155 to -0.07955	Yes	***

KNUST

clear water vs. 40 g sand	-0.1275	-0.1814 to -0.07365	Yes	**
10 g clay vs. 20 g clay	-0.08250	-0.1005 to -0.06455	Yes	***
10 g clay vs. 30 g clay				
10 g clay vs. 40 g sand	-0.1800	-0.2093 to -0.1507	Yes	****
10 g clay vs. 10 g Silt	0.005000	-0.03090 to 0.04090	No	Ns
10 g clay vs. 20 g silt	-0.0600	-0.1108 to -0.009226	Yes	*
10 g clay vs. 30 g silt	-0.1075	-0.1688 to -0.04618	Yes	*
10 g clay vs. 40 g silt	-0.1500	-0.2008 to -0.09923	Yes	**
10 g clay vs. 10 g sand	0.01750	-0.03635 to 0.07135	No	Ns
10 g clay vs. 20 g sand	-0.04000	-0.09863 to 0.01863	No	Ns
10 g clay vs. 30 g sand	-0.07250	-0.1069 to -0.03813	Yes	**
10 g clay vs. 40 g sand	-0.1025	-0.1638 to -0.04118	Yes	*
20 g clay vs. 30 g clay	-0.07750	-0.09545 to -0.05955	Yes	**
20 g clay vs. 40 g sand	-0.09750	-0.1155 to -0.07955	Yes	***
20 g clay vs. 10 g Silt	0.08750	0.05313 to 0.1219	Yes	**
20 g clay vs. 20 g silt	0.02250	-0.02268 to 0.06768	No	Ns
20 g clay vs. 30 g silt	-0.02500	-0.09375 to 0.04375	No	Ns
20 g clay vs. 40 g silt	-0.06750	-0.1127 to -0.02232	Yes	*
20 g clay vs. 10 g sand	0.1000	0.03445 to 0.1655	Yes	*
20 g clay vs. 20 g sand	0.04250	-0.01882 to 0.1038	No	Ns
20 g clay vs. 30 g sand	0.01000	-0.01931 to 0.03931	No	Ns

20 g clay vs. 40 g sand	-0.02000	-0.07077 to 0.03077	No	Ns
30 g clay vs. 40 g sand	-0.02000	-0.04931 to 0.009314	No	Ns
30 g clay vs. 10 g Silt	0.1650	0.1291 to 0.2009	Yes	***
30 g clay vs. 20 g silt	0.1000	0.04923 to 0.1508	Yes	**
30 g clay vs. 30 g silt	0.05250	-0.008815 to 0.1138	No	Ns
30 g clay vs. 40 g silt	0.01000	-0.04077 to 0.06077	No	Ns
30 g clay vs. 10 g sand	0.1775	0.1236 to 0.2314	Yes	**
30 g clay vs. 20 g sand	0.1200	0.06137 to 0.1786	Yes	**
30 g clay vs. 30 g sand	0.08750	0.05313 to 0.1219	Yes	**
30 g clay vs. 40 g sand	0.05750	-0.003815 to 0.1188	No	Ns
40 g sand vs. 10 g Silt	0.1850	0.1643 to 0.2057	Yes	****
40 g sand vs. 20 g silt	0.1200	0.09069 to 0.1493	Yes	**
40 g sand vs. 30 g silt	0.07250	0.01118 to 0.1338	Yes	*
40 g sand vs. 40 g silt	0.0300	0.0006857 to 0.05931	Yes	*
40 g sand vs. 10 g sand	0.1975	0.1362 to 0.2588	Yes	**
40 g sand vs. 20 g sand	0.1400	0.08923 to 0.1908	Yes	**
40 g sand vs. 30 g sand	0.1075	0.08955 to 0.1255	Yes	***
40 g sand vs. 40 g sand	0.07750	0.04313 to 0.1119	Yes	**
10 g Silt vs. 20 g silt Yes **	-0.0650	-0.08573 to -0.04427	Yes **	10 g Silt vs. 30 g silt -0.1125
				-0.1577 to -0.06732
10 g Silt vs. 40 g silt	-0.1550	-0.1757 to -0.1343	Yes	****
10 g Silt vs. 10 g sand	0.01250	-0.03268 to 0.05768	No	Ns
10 g Silt vs. 20 g sand	-0.04500	-0.08090 to -0.009097	Yes	*
10 g Silt vs. 30 g sand	-0.07750	-0.09545 to -0.05955	Yes	**
10 g Silt vs. 40 g sand	-0.1075	-0.1419 to -0.07313	Yes	**
20 g silt vs. 30 g silt	-0.04750	-0.09268 to -0.002324	Yes	*
20 g silt vs. 40 g silt	-0.09000	-0.09000 to -0.09000	Yes	****
20 g silt vs. 10 g sand	0.07750	0.02365 to 0.1314	Yes	*
20 g silt vs. 20 g sand	0.02000	-0.009314 to 0.04931	No	Ns

20 g silt vs. 30 g sand	-0.01250	-0.04687 to 0.02187	No	Ns
20 g silt vs. 40 g sand	-0.04250	-0.06045 to -0.02455	Yes	**
30 g silt vs. 40 g silt	-0.04250	-0.08768 to 0.002676	No	Ns
30 g silt vs. 10 g sand	0.1250	0.1043 to 0.1457	Yes	***
30 g silt vs. 20 g sand	0.06750	0.04955 to 0.08545	Yes	**
30 g silt vs. 30 g sand	0.03500	-0.02718 to 0.09718	No	Ns
30 g silt vs. 40 g sand	0.005000	-0.05718 to 0.06718	No	Ns
40 g silt vs. 10 g sand	0.1675	0.1136 to 0.2214	Yes	**
40 g silt vs. 20 g sand	0.1100	0.08069 to 0.1393	Yes	**
40 g silt vs. 30 g sand	0.07750	0.04313 to 0.1119	Yes	**
40 g silt vs. 40 g sand	0.04750	0.02955 to 0.06545	Yes	**
10 g sand vs. 20 g sand	-0.05750	-0.09187 to -0.02313	Yes	*
10 g sand vs. 30 g sand	-0.09000	-0.1486 to -0.03137	Yes	*
10 g sand vs. 40 g sand	-0.1200	-0.1918 to -0.04820	Yes	*
20 g sand vs. 30 g sand	-0.03250	-0.08635 to 0.02135	No	Ns
20 g sand vs. 40 g sand	-0.06250	-0.1077 to -0.01732	Yes *	
30 g sand vs. 40 g sand	-0.03000	-0.07146 to 0.01146	No	Ns

Appendix A2.1: Repeated Measures one-way ANOVA analyses Total porosity

Assume sphericity?	No
F	257.8
P value	< 0.0001
P value summary	****
Statistically significant (P < 0.05)?	Yes
Geisser-Greenhouse's epsilon	0.1717

R square

0.9885

Was the matching effective?

F

1.231

P value

0.3126

P value summary

ns

Is there significant matching ($P < 0.05$)?

No

R square

0.001179

ANOVA table

Treatment (between columns)

Individual (between rows)

Residual (random)

Total

SS

DF

MS

F (DFn, DFd)

P value

306.2

12

25.52

F (2.060, 6.180) = 257.8

P < 0.0001

0.3656

3

0.1219

F (3, 36) = 1.231

P = 0.3126

3.564

36

0.09899

310.2

51

Appendix A2.2: Tukey's multiple comparisons test summary for Total porosity

Number of families

1

KNUST

Number of comparisons per family

78

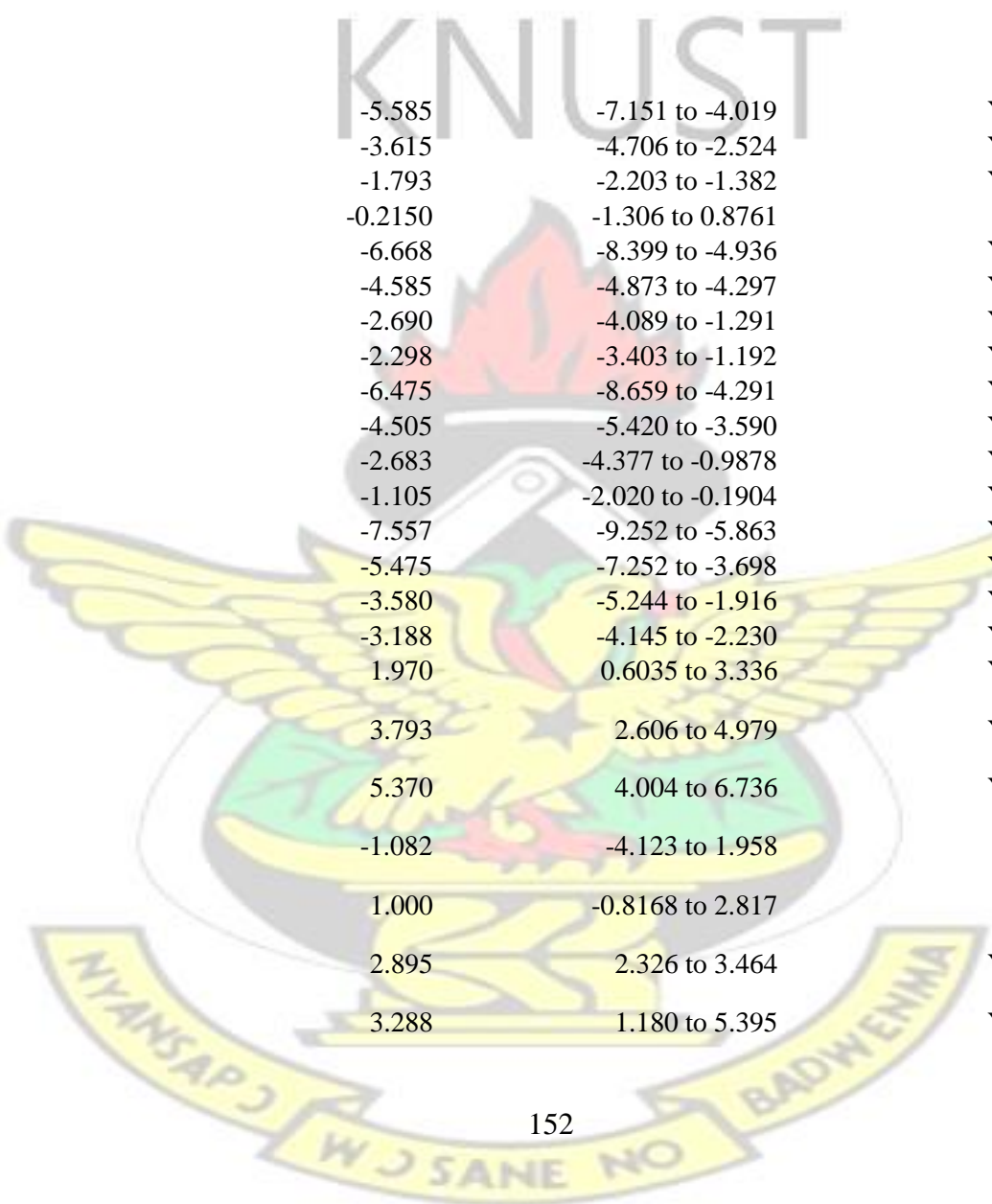
Alpha

0.05

Tukey's multiple comparisons test

	Mean Diff.	95% CI of diff.	Significant?	Summary
clear water vs. 10 g clay	0.1550	-1.700 to 2.010	No	Ns
clear water vs. 20 g clay	3.705	2.039 to 5.371	Yes	**
clear water vs. 30 g clay	6.223	3.697 to 8.748	Yes	**
clear water vs. 40 g sand	7.113	6.439 to 7.786	Yes	****
clear water vs. 10 g Silt	0.6375	-2.051 to 3.326	No	Ns
clear water vs. 20 g silt	2.607	1.063 to 4.152	Yes	*
clear water vs. 30 g silt	4.430	2.077 to 6.783	Yes	**
clear water vs. 40 g silt	6.008	4.463 to 7.552	Yes	**
clear water vs. 10 g sand	-0.4450	-2.592 to 1.702	No	Ns
clear water vs. 20 g sand	1.637	-0.8108 to 4.086	No	Ns
clear water vs. 30 g sand	3.533	1.366 to 5.699	Yes	*
clear water vs. 40 g sand	3.925	2.333 to 5.517	Yes	**

10 g clay vs. 20 g clay	3.550	1.818 to 5.282	Yes	**
10 g clay vs. 30 g clay	6.068	5.099 to 7.036	Yes	****
10 g clay vs. 40 g sand	6.958	5.716 to 8.199	Yes	***
10 g clay vs. 10 g Silt	0.4825	-0.9721 to 1.937	No	Ns
10 g clay vs. 20 g silt	2.452	1.903 to 3.002	Yes	***
10 g clay vs. 30 g silt	4.275	3.530 to 5.020	Yes	***
10 g clay vs. 40 g silt	5.853	5.303 to 6.402	Yes	****
10 g clay vs. 10 g sand	-0.6000	-2.464 to 1.264	No	Ns
10 g clay vs. 20 g sand	1.482	0.4509 to 2.514	Yes	*
10 g clay vs. 30 g sand	3.378	2.390 to 4.365	Yes	**
10 g clay vs. 40 g sand	3.770	2.803 to 4.737	Yes	**
20 g clay vs. 30 g clay	2.518	0.05957 to 4.975	Yes	*
20 g clay vs. 40 g sand	3.407	1.838 to 4.977	Yes	**
20 g clay vs. 10 g Silt	-3.068	-4.680 to -1.455	Yes	**
20 g clay vs. 20 g silt	-1.098	-2.569 to 0.3736	No	Ns
20 g clay vs. 30 g silt	0.7250	-1.357 to 2.807	No	Ns
20 g clay vs. 40 g silt	2.302	0.8314 to 3.774	Yes	*
20 g clay vs. 10 g sand	-4.150	-7.301 to -0.9987	Yes	*
20 g clay vs. 20 g sand	-2.068	-4.640 to 0.5045	No	Ns
20 g clay vs. 30 g sand	-0.1725	-1.411 to 1.066	No	Ns
20 g clay vs. 40 g sand	0.2200	-1.987 to 2.427	No	Ns
30 g clay vs. 40 g sand	0.8900	-0.9621 to 2.742	No	Ns



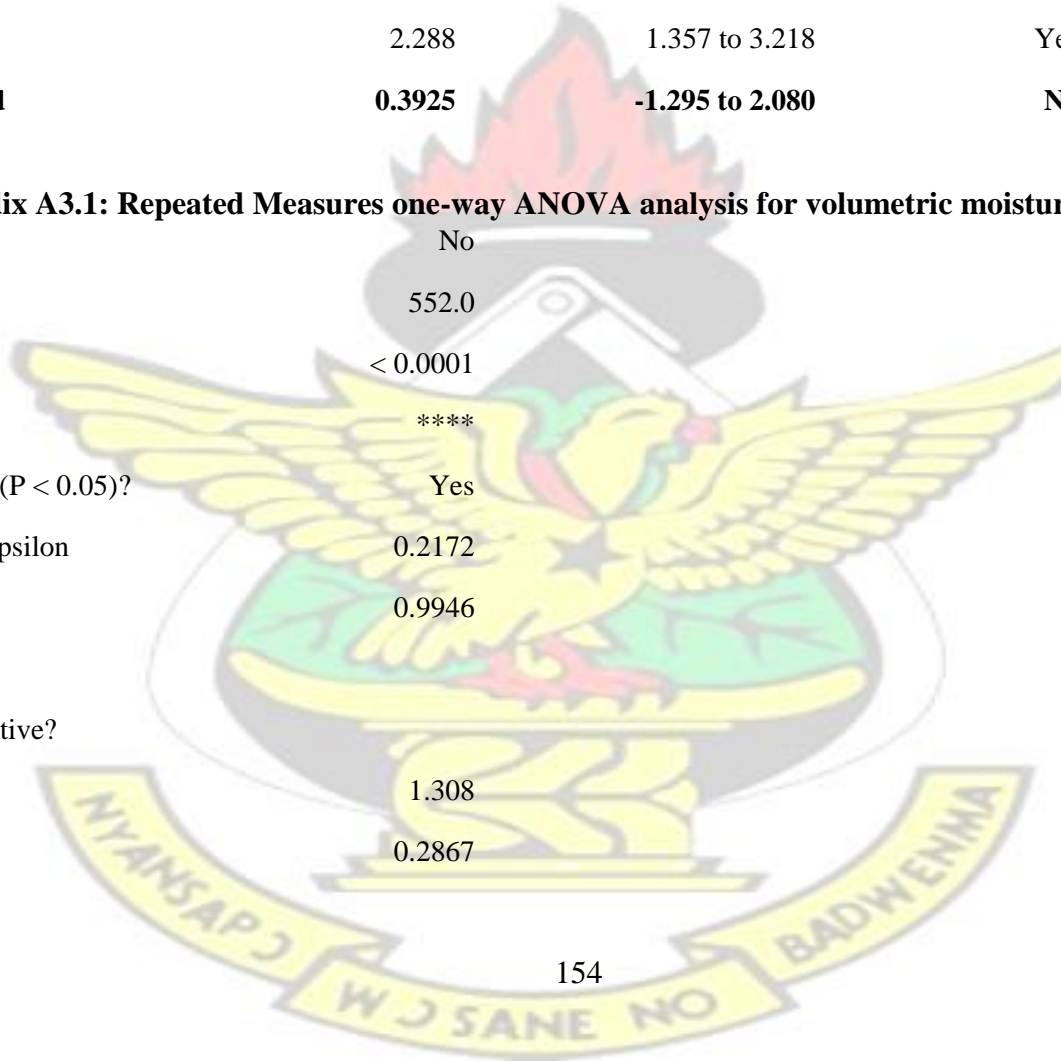
30 g clay vs. 10 g Silt	-5.585	-7.151 to -4.019	Yes	**
30 g clay vs. 20 g silt	-3.615	-4.706 to -2.524	Yes	**
30 g clay vs. 30 g silt	-1.793	-2.203 to -1.382	Yes	**
30 g clay vs. 40 g silt	-0.2150	-1.306 to 0.8761	No	Ns
30 g clay vs. 10 g sand	-6.668	-8.399 to -4.936	Yes	**
30 g clay vs. 20 g sand	-4.585	-4.873 to -4.297	Yes	****
30 g clay vs. 30 g sand	-2.690	-4.089 to -1.291	Yes	**
30 g clay vs. 40 g sand	-2.298	-3.403 to -1.192	Yes	**
40 g sand vs. 10 g Silt	-6.475	-8.659 to -4.291	Yes	**
40 g sand vs. 20 g silt	-4.505	-5.420 to -3.590	Yes	***
40 g sand vs. 30 g silt	-2.683	-4.377 to -0.9878	Yes	*
40 g sand vs. 40 g silt	-1.105	-2.020 to -0.1904	Yes	*
40 g sand vs. 10 g sand	-7.557	-9.252 to -5.863	Yes	***
40 g sand vs. 20 g sand	-5.475	-7.252 to -3.698	Yes	**
40 g sand vs. 30 g sand	-3.580	-5.244 to -1.916	Yes	**
40 g sand vs. 40 g sand	-3.188	-4.145 to -2.230	Yes	**
10 g Silt vs. 20 g silt	1.970	0.6035 to 3.336	Yes	*
10 g Silt vs. 30 g silt	3.793	2.606 to 4.979	Yes	**
10 g Silt vs. 40 g silt	5.370	4.004 to 6.736	Yes	**
10 g Silt vs. 10 g sand	-1.082	-4.123 to 1.958	No	Ns
10 g Silt vs. 20 g sand	1.000	-0.8168 to 2.817	No	Ns
10 g Silt vs. 30 g sand	2.895	2.326 to 3.464	Yes	***
10 g Silt vs. 40 g sand	3.288	1.180 to 5.395	Yes	*

20 g silt vs. 30 g silt	1.822	0.9968 to 2.648	Yes	**
20 g silt vs. 40 g silt	3.400	3.400 to 3.400	Yes	****
20 g silt vs. 10 g sand	-3.052	-4.878 to -1.227	Yes	*
20 g silt vs. 20 g sand	-0.9700	-2.104 to 0.1642	No	Ns
20 g silt vs. 30 g sand	0.9250	0.04289 to 1.807	Yes	*
20 g silt vs. 40 g sand	1.318	0.4815 to 2.154	Yes	*
30 g silt vs. 40 g silt	1.578	0.7518 to 2.403	Yes	**
30 g silt vs. 10 g sand	-4.875	-6.832 to -2.918	Yes	**
30 g silt vs. 20 g sand	-2.793	-3.433 to -2.152	Yes	**
30 g silt vs. 30 g sand	-0.8975	-1.886 to 0.09112	No	Ns
30 g silt vs. 40 g sand	-0.5050	-1.654 to 0.6444	No	Ns
40 g silt vs. 10 g sand	-6.452	-8.278 to -4.627	Yes	**
40 g silt vs. 20 g sand	-4.370	-5.504 to -3.236	Yes	**
40 g silt vs. 30 g sand	-2.475	-3.357 to -1.593	Yes	**
40 g silt vs. 40 g sand	-2.083	-2.919 to -1.246	Yes	**
10 g sand vs. 20 g sand	2.082	0.6284 to 3.537	Yes	*
10 g sand vs. 30 g sand	3.977	1.317 to 6.638	Yes	*

10 g sand vs. 40 g sand	4.370	3.381 to 5.359	Yes	***
20 g sand vs. 30 g sand	1.895	0.2946 to 3.495	Yes	*
20 g sand vs. 40 g sand	2.288	1.357 to 3.218	Yes	**
30 g sand vs. 40 g sand	0.3925	-1.295 to 2.080	No	Ns

Appendix A3.1: Repeated Measures one-way ANOVA analysis for volumetric moisture content (FC)

Assume sphericity?	No
F	552.0
P value	< 0.0001
P value summary	****
Statistically significant (P < 0.05)?	Yes
Geisser-Greenhouse's epsilon	0.2172
R square	0.9946
Was the matching effective?	
F	1.308
P value	0.2867



KNUST

clear water vs. 20 g clay	3.405	3.228 to 3.582	Yes	****
clear water vs. 30 g clay	5.220	4.183 to 6.257	Yes	***
clear water vs. 40 g sand	6.260	5.065 to 7.455	Yes	***
clear water vs. 10 g Silt	0.9425	0.7205 to 1.165	Yes	**
clear water vs. 20 g silt	2.215	2.028 to 2.402	Yes	****
clear water vs. 30 g silt	3.505	3.053 to 3.957	Yes	****
clear water vs. 40 g silt	4.595	4.020 to 5.170	Yes	****
clear water vs. 10 g sand	0.1900	-0.2952 to 0.6752	No	Ns
clear water vs. 20 g sand	1.308	1.204 to 1.411	Yes	****
clear water vs. 30 g sand	3.023	2.717 to 3.328	Yes	****
clear water vs. 40 g sand	3.733	3.217 to 4.248	Yes	****
10 g clay vs. 20 g clay	1.915	0.6574 to 3.173	Yes	*
10 g clay vs. 30 g clay	3.730	1.883 to 5.577	Yes	**
10 g clay vs. 40 g sand	4.770	3.396 to 6.144	Yes	**
10 g clay vs. 10 g Silt	-0.5475	-1.764 to 0.6691	No	Ns
10 g clay vs. 20 g silt	0.7250	-0.5106 to 1.961	No	Ns
10 g clay vs. 30 g silt	2.015	0.8611 to 3.169	Yes	*

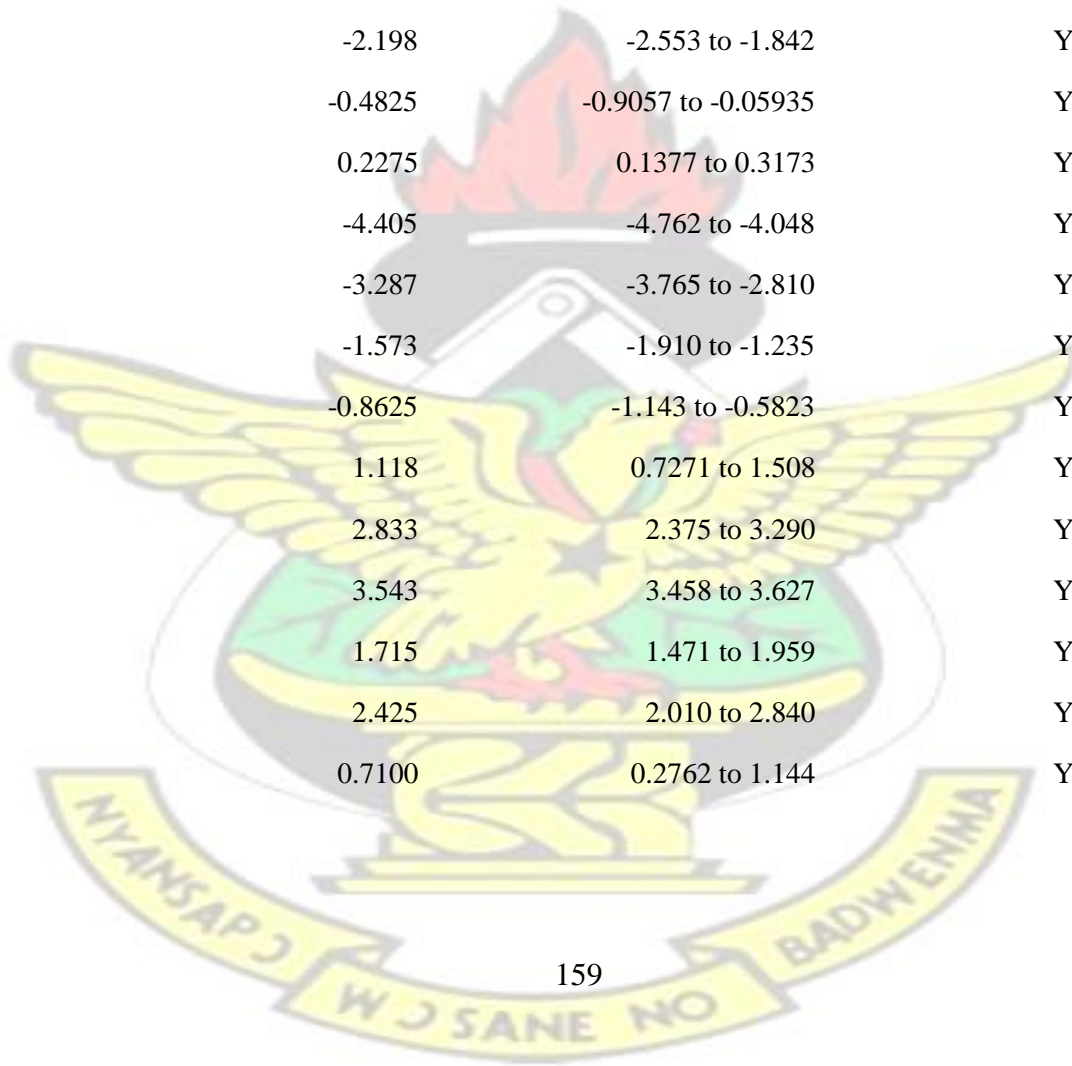
KNUST

10 g clay vs. 40 g silt	3.105	2.251 to 3.959	Yes	**
10 g clay vs. 10 g sand	-1.300	-2.452 to -0.1481	Yes	*
10 g clay vs. 20 g sand	-0.1825	-1.505 to 1.140	No	Ns
10 g clay vs. 30 g sand	1.533	0.4073 to 2.658	Yes	*
10 g clay vs. 40 g sand	2.243	1.175 to 3.310	Yes	**
20 g clay vs. 30 g clay	1.815	0.6701 to 2.960	Yes	*
20 g clay vs. 40 g sand	2.855	1.700 to 4.010	Yes	**
20 g clay vs. 10 g Silt	-2.463	-2.508 to -2.417	Yes	****
20 g clay vs. 20 g silt	-1.190	-1.327 to -1.053	Yes	****
20 g clay vs. 30 g silt	0.1000	-0.1917 to 0.3917	No	Ns
20 g clay vs. 40 g silt	1.190	0.7817 to 1.598	Yes	**
20 g clay vs. 10 g sand	-3.215	-3.542 to -2.888	Yes	****
20 g clay vs. 20 g sand	-2.098	-2.172 to -2.023	Yes	****
20 g clay vs. 30 g sand	-0.3825	-0.6006 to -0.1644	Yes	*
20 g clay vs. 40 g sand	0.3275	-0.01733 to 0.6723	No	Ns
30 g clay vs. 40 g sand	1.040	-0.3919 to 2.472	No	Ns
30 g clay vs. 10 g Silt	-4.278	-5.449 to -3.106	Yes	**
30 g clay vs. 20 g silt	-3.005	-4.024 to -1.986	Yes	**
30 g clay vs. 30 g silt	-1.715	-3.142 to -0.2884	Yes	*
30 g clay vs. 40 g silt	-0.6250	-1.951 to 0.7008	No	Ns
30 g clay vs. 10 g sand	-5.030	-6.492 to -3.568	Yes	**
30 g clay vs. 20 g sand	-3.912	-5.011 to -2.814	Yes	**
30 g clay vs. 30 g sand	-2.198	-3.222 to -1.173	Yes	**
30 g clay vs. 40 g sand	-1.487	-2.942 to -0.03345	Yes	*
40 g sand vs. 10 g Silt	-5.318	-6.465 to -4.170	Yes	***
40 g sand vs. 20 g silt	-4.045	-5.158 to -2.932	Yes	**

40 g sand vs. 30 g silt	-2.755	-3.974 to -1.536	Yes	**
40 g sand vs. 40 g silt	-1.665	-2.762 to -0.5676	Yes	*
40 g sand vs. 10 g sand	-6.070	-7.304 to -4.836	Yes	***
40 g sand vs. 20 g sand	-4.953	-6.122 to -3.783	Yes	**
40 g sand vs. 30 g sand	-3.238	-4.312 to -2.163	Yes	**
40 g sand vs. 40 g sand	-2.528	-3.732 to -1.323	Yes	**
10 g Silt vs. 20 g silt	1.273	1.119 to 1.426	Yes	****
10 g Silt vs. 30 g silt	2.563	2.305 to 2.820	Yes	****
10 g Silt vs. 40 g silt	3.653	3.287 to 4.018	Yes	****
10 g Silt vs. 10 g sand	-0.7525	-1.046 to -0.4588	Yes	**
10 g Silt vs. 20 g sand	0.3650	0.2459 to 0.4841	Yes	**
10 g Silt vs. 30 g sand	2.080	1.871 to 2.289	Yes	****
10 g Silt vs. 40 g sand	2.790	2.485 to 3.095	Yes	****
20 g silt vs. 30 g silt	1.290	0.8828 to 1.697	Yes	**
20 g silt vs. 40 g silt	2.380	1.961 to 2.799	Yes	***
20 g silt vs. 10 g sand	-2.025	-2.468 to -1.582	Yes	***
20 g silt vs. 20 g sand	-0.9075	-1.043 to -0.7720	Yes	****
20 g silt vs. 30 g sand	0.8075	0.6889 to 0.9261	Yes	****
20 g silt vs. 40 g sand	1.518	1.075 to 1.960	Yes	**

KNUST

30 g silt vs. 40 g silt	1.090	0.7469 to 1.433	Yes	**
30 g silt vs. 10 g sand	-3.315	-3.351 to -3.279	Yes	****
30 g silt vs. 20 g sand	-2.198	-2.553 to -1.842	Yes	****
30 g silt vs. 30 g sand	-0.4825	-0.9057 to -0.05935	Yes	*
30 g silt vs. 40 g sand	0.2275	0.1377 to 0.3173	Yes	**
40 g silt vs. 10 g sand	-4.405	-4.762 to -4.048	Yes	****
40 g silt vs. 20 g sand	-3.287	-3.765 to -2.810	Yes	****
40 g silt vs. 30 g sand	-1.573	-1.910 to -1.235	Yes	***
40 g silt vs. 40 g sand	-0.8625	-1.143 to -0.5823	Yes	**
10 g sand vs. 20 g sand	1.118	0.7271 to 1.508	Yes	**
10 g sand vs. 30 g sand	2.833	2.375 to 3.290	Yes	****
10 g sand vs. 40 g sand	3.543	3.458 to 3.627	Yes	****
20 g sand vs. 30 g sand	1.715	1.471 to 1.959	Yes	****
20 g sand vs. 40 g sand	2.425	2.010 to 2.840	Yes	***
30 g sand vs. 40 g sand	0.7100	0.2762 to 1.144	Yes	*



Appendix A4.1: Repeated Measures one-way ANOVA analyses saturated moisture content

Assume sphericity?	No				
F	142.4				
P value	< 0.0001				
P value summary	****				
Statistically significant (P < 0.05)?	Yes				
Geisser-Greenhouse's epsilon	0.1630				
R square	0.9794				
Was the matching effective?					
F	0.3427				
P value	0.7946				
P value summary	Ns				
Is there significant matching (P < 0.05)?	No				
R square	0.0005887				
ANOVA table	SS	DF	MS	F (DFn, DFd)	P value

Treatment (between columns)	198.0	12	16.50	F (1.956, 5.867) = 142.4	P < 0.0001
Individual (between rows)	0.1191	3	0.03970	F (3, 36) = 0.3427	P = 0.7946
Residual (random)	4.170	36	0.1158		
Total	202.3	51			

Appendix A4.2: Tukey's multiple comparisons test summary for saturated moisture content

Number of families	1			
Number of comparisons per family	78			
Alpha	0.05			
Tukey's multiple comparisons test	Mean Diff.	95% CI of diff.	Significant?	Summary
clear water vs. 10 g clay	3.175	2.887 to 3.463	Yes	****
clear water vs. 20 g clay	4.215	2.438 to 5.992	Yes	**
clear water vs. 30 g clay	5.830	5.197 to 6.463	Yes	****
clear water vs. 40 g sand	7.090	4.502 to 9.678	Yes	**
clear water vs. 10 g Silt	1.772	1.132 to 2.413	Yes	**

KNUST

clear water vs. 20 g silt	2.440	1.306 to 3.574	Yes	**
clear water vs. 30 g silt	3.587	1.615 to 5.560	Yes	**
clear water vs. 40 g silt	4.540	3.406 to 5.674	Yes	**
clear water vs. 10 g sand	0.7050	-0.8954 to 2.305	No	Ns
clear water vs. 20 g sand	1.197	-1.168 to 3.563	No	Ns
clear water vs. 30 g sand	3.095	1.479 to 4.711	Yes	**
clear water vs. 40 g sand	4.378	2.583 to 6.172	Yes	**
10 g clay vs. 20 g clay	1.040	-0.8121 to 2.892	No	Ns
10 g clay vs. 30 g clay	2.655	1.999 to 3.311	Yes	**
10 g clay vs. 40 g sand	3.915	1.450 to 6.380	Yes	*
10 g clay vs. 10 g Silt	-1.402	-1.813 to -0.9917	Yes	**
10 g clay vs. 20 g silt	-0.7350	-1.826 to 0.3561	No	Ns
10 g clay vs. 30 g silt	0.4125	-1.308 to 2.133	No	Ns
10 g clay vs. 40 g silt	1.365	0.2739 to 2.456	Yes	*
10 g clay vs. 10 g sand	-2.470	-3.869 to -1.071	Yes	*
10 g clay vs. 20 g sand	-1.978	-4.402 to 0.4473	No	Ns
10 g clay vs. 30 g sand	-0.08000	-1.973 to 1.813	No	Ns
10 g clay vs. 40 g sand	1.203	-0.3044 to 2.709	No	Ns

20 g clay vs. 30 g clay	1.615	0.4187 to 2.811	Yes	*
20 g clay vs. 40 g sand	2.875	1.233 to 4.517	Yes	*
20 g clay vs. 10 g Silt	-2.443	-4.137 to -0.7477	Yes	*
20 g clay vs. 20 g silt	-1.775	-2.690 to -0.8604	Yes	**
20 g clay vs. 30 g silt	-0.6275	-2.881 to 1.626	No	Ns
20 g clay vs. 40 g silt	0.3250	-0.5896 to 1.240	No	Ns
20 g clay vs. 10 g sand	-3.510	-5.174 to -1.846	Yes	**
20 g clay vs. 20 g sand	-3.018	-3.610 to -2.425	Yes	***
20 g clay vs. 30 g sand	-1.120	-2.881 to 0.6411	No	Ns
20 g clay vs. 40 g sand	0.1625	-2.518 to 2.843	No	Ns
30 g clay vs. 40 g sand	1.260	-0.7439 to 3.264	No	Ns
30 g clay vs. 10 g Silt	-4.057	-4.628 to -3.487	Yes	****
30 g clay vs. 20 g silt	-3.390	-3.903 to -2.877	Yes	****
30 g clay vs. 30 g silt	-2.242	-3.930 to -0.5554	Yes	*
30 g clay vs. 40 g silt	-1.290	-1.803 to -0.7772	Yes	**
30 g clay vs. 10 g sand	-5.125	-6.310 to -3.940	Yes	**
30 g clay vs. 20 g sand	-4.633	-6.401 to -2.864	Yes	**
30 g clay vs. 30 g sand	-2.735	-4.379 to -1.091	Yes	*
30 g clay vs. 40 g sand	-1.452	-3.230 to 0.3247	No	Ns
40 g sand vs. 10 g Silt	-5.318	-7.400 to -3.235	Yes	**
40 g sand vs. 20 g silt	-4.650	-6.150 to -3.150	Yes	**
40 g sand vs. 30 g silt	-3.503	-4.986 to -2.019	Yes	**
40 g sand vs. 40 g silt	-2.550	-4.050 to -1.050	Yes	*
40 g sand vs. 10 g sand	-6.385	-7.597 to -5.173	Yes	***
40 g sand vs. 20 g sand	-5.893	-7.471 to -4.314	Yes	**
40 g sand vs. 30 g sand	-3.995	-7.301 to -0.6887	Yes	*
40 g sand vs. 40 g sand	-2.713	-4.959 to -0.4659	Yes	*
10 g Silt vs. 20 g silt	0.6675	-0.1582 to 1.493	No	Ns

KNUST

10 g Silt vs. 30 g silt	1.815	0.4827 to 3.147	Yes	*
10 g Silt vs. 40 g silt	2.768	1.942 to 3.593	Yes	**
10 g Silt vs. 10 g sand	-1.068	-2.056 to -0.07888	Yes	*
10 g Silt vs. 20 g sand	-0.5750	-2.805 to 1.655	No	Ns
10 g Silt vs. 30 g sand	1.323	-0.7919 to 3.437	No	Ns
10 g Silt vs. 40 g sand	2.605	1.361 to 3.849	Yes	**
20 g silt vs. 30 g silt	1.148	-0.3139 to 2.609	No	Ns
20 g silt vs. 40 g silt	2.100	2.100 to 2.100	Yes	****
20 g silt vs. 10 g sand	-1.735	-2.617 to -0.8529	Yes	**
20 g silt vs. 20 g sand	-1.242	-2.655 to 0.1702	No	Ns
20 g silt vs. 30 g sand	0.6550	-1.299 to 2.609	No	Ns
20 g silt vs. 40 g sand	1.938	0.1582 to 3.717	Yes	*
30 g silt vs. 40 g silt	0.9525	-0.5089 to 2.414	No	Ns
30 g silt vs. 10 g sand	-2.883	-3.475 to -2.290	Yes	***
30 g silt vs. 20 g sand	-2.390	-4.947 to 0.1674	No	Ns
30 g silt vs. 30 g sand	-0.4925	-3.822 to 2.837	No	Ns
30 g silt vs. 40 g sand	0.7900	0.0001410 to 1.580	Yes	*

40 g silt vs. 10 g sand	-3.835	-4.717 to -2.953	Yes	**
40 g silt vs. 20 g sand	-3.343	-4.755 to -1.930	Yes	**
40 g silt vs. 30 g sand	-1.445	-3.399 to 0.5093	No	Ns
40 g silt vs. 40 g sand	-0.1625	-1.942 to 1.617	No	Ns
10 g sand vs. 20 g sand	0.4925	-1.507 to 2.492	No	Ns
10 g sand vs. 30 g sand	2.390	-0.4099 to 5.190	No	Ns
10 g sand vs. 40 g sand	3.673	2.538 to 4.807	Yes	**
20 g sand vs. 30 g sand	1.898	-0.3158 to 4.111	No	Ns
20 g sand vs. 40 g sand	3.180	0.08418 to 6.276	Yes	*
30 g sand vs. 40 g sand	1.283	-2.073 to 4.638	No	Ns

Appendix A5.1: Repeated Measures one-way ANOVA analysis for saturated hydraulic conductivity

Assume sphericity?	No
F	40.03
P value	0.0011
P value summary	**
Statistically significant ($P < 0.05$)?	Yes

KNUST

Geisser-Greenhouse's epsilon 0.1342
R square 0.9303

Was the matching effective?

F 1.649
P value 0.1952

P value summary

ns

Is there significant matching ($P < 0.05$)?

No

R square 0.009489

ANOVA table	SS	DF	MS	F (DFn, DFd)	P value
Treatment (between columns)	0.0001004	12	8.368e-006	F (1.610, 4.830) = 40.03	P = 0.0011
Individual (between rows)	1.034e-006	3	3.447e-007	F (3, 36) = 1.649	P = 0.1952
Residual (random)	7.525e-006	36	2.090e-007		
Total	0.0001090	51			

Appendix A5.2: Tukey's multiple comparisons test summary for saturated hydraulic conductivity

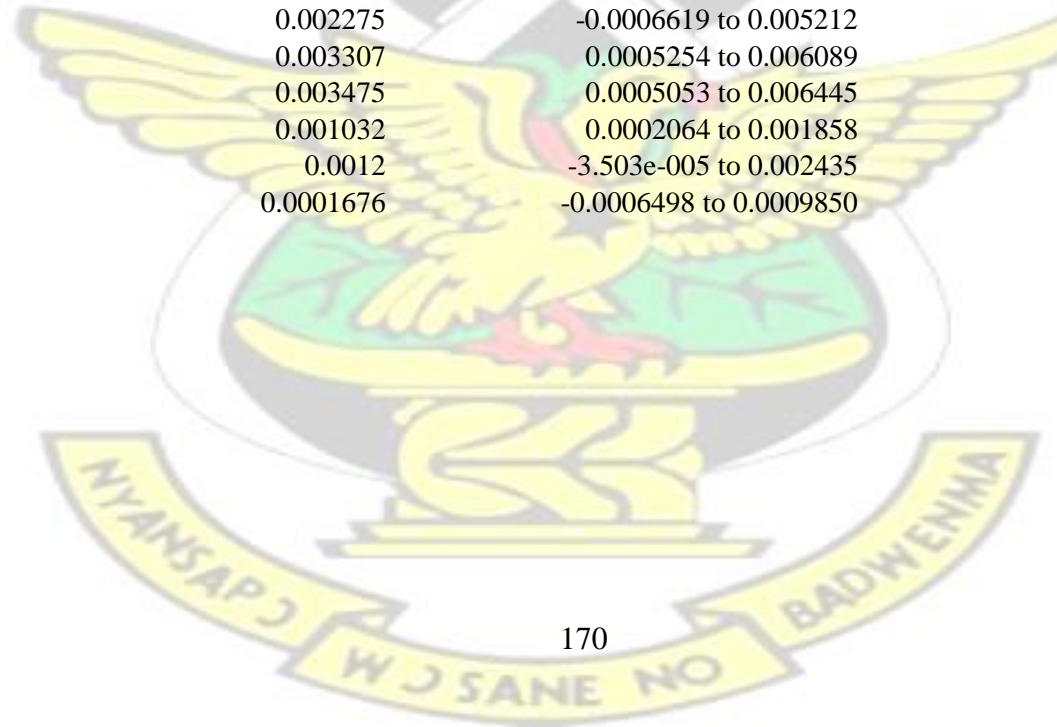
Number of families	1
Number of comparisons per family	78
Alpha	0.05

Tukey's multiple comparisons test	Mean Diff.	95% CI of diff.	Significant?	Summary
clear water vs. 10 g clay	0.0024	0.001624 to 0.003176	Yes	**
clear water vs. 20 g clay	0.002498	0.001872 to 0.003123	Yes	**
clear water vs. 30 g clay	0.002516	0.001893 to 0.003140	Yes	**
clear water vs. 40 g sand	0.002523	0.001910 to 0.003135	Yes	**
clear water vs. 10 g Silt	0.0006000	-0.0003722 to 0.001572	No	Ns
clear water vs. 20 g silt	0.0005500	-0.003939 to 0.005039	No	Ns
clear water vs. 30 g silt	0.001852	0.001091 to 0.002614	Yes	**
clear water vs. 40 g silt	0.0020	0.001224 to 0.002776	Yes	**
clear water vs. 10 g sand	-0.00245	-0.005300 to 0.0003997	No	Ns
clear water vs. 20 g sand	-0.000175	-0.001592 to 0.001242	No	Ns

clear water vs. 30 g sand	0.0008574	0.0001751 to 0.001540	Yes	*
clear water vs. 40 g sand	0.001025	0.0004669 to 0.001583	Yes	**
10 g clay vs. 20 g clay	9.750e-005	-0.0002436 to 0.0004386	No	Ns
10 g clay vs. 30 g clay	0.0001164	-0.0002456 to 0.0004784	No	Ns
10 g clay vs. 40 g sand	0.0001228	-0.0002346 to 0.0004801	No	Ns
10 g clay vs. 10 g Silt	-0.0018	-0.002215 to -0.001385	Yes	**
10 g clay vs. 20 g silt	-0.00185	-0.006940 to 0.003240	No	Ns
10 g clay vs. 30 g silt	-0.0005476	-0.001025 to -7.059e-005	Yes	*
10 g clay vs. 40 g silt	-0.0004	-0.0004000 to -0.0004000	Yes	****
10 g clay vs. 10 g sand	-0.00485	-0.007496 to -0.002204	Yes	**
10 g clay vs. 20 g sand	-0.002575	-0.003315 to -0.001835	Yes	**
10 g clay vs. 30 g sand	-0.001543	-0.001716 to -0.001369	Yes	****
10 g clay vs. 40 g sand	-0.001375	-0.002236 to -0.0005141	Yes	*
20 g clay vs. 30 g clay	1.893e-005	-2.275e-006 to 4.012e-005	No	Ns
20 g clay vs. 40 g sand	2.525e-005	6.168e-006 to 4.433e-005	Yes	*
20 g clay vs. 10 g Silt	-0.001898	-0.002251 to -0.001544	Yes	***
20 g clay vs. 20 g silt	-0.001948	-0.007025 to 0.003130	No	Ns
20 g clay vs. 30 g silt	-0.0006451	-0.0008652 to -0.0004249	Yes	**
20 g clay vs. 40 g silt	-0.0004975	-0.0008386 to -0.0001564	Yes	*
20 g clay vs. 10 g sand	-0.004948	-0.007864 to -0.002031	Yes	*
20 g clay vs. 20 g sand	-0.002673	-0.003604 to -0.001741	Yes	**

20 g clay vs. 30 g sand	-0.001640	-0.001807 to -0.001473	Yes	****
20 g clay vs. 40 g sand	-0.001473	-0.002281 to -0.0006642	Yes	**
30 g clay vs. 40 g sand	6.325e-006	-6.763e-006 to 1.941e-005	No	Ns
30 g clay vs. 10 g Silt	-0.001916	-0.002275 to -0.001558	Yes	***
30 g clay vs. 20 g silt	-0.001966	-0.007045 to 0.003113	No	Ns
30 g clay vs. 30 g silt	-0.0006640	-0.0008731 to -0.0004549	Yes	**
30 g clay vs. 40 g silt	-0.0005164	-0.0008784 to -0.0001544	Yes	*
30 g clay vs. 10 g sand	-0.004966	-0.007902 to -0.002031	Yes	*
30 g clay vs. 20 g sand	-0.002691	-0.003635 to -0.001748	Yes	**
30 g clay vs. 30 g sand	-0.001659	-0.001847 to -0.001471	Yes	****
30 g clay vs. 40 g sand	-0.001491	-0.002301 to -0.0006816	Yes	**
40 g sand vs. 10 g Silt	-0.001923	-0.002291 to -0.001555	Yes	***
40 g sand vs. 20 g silt	-0.001973	-0.007040 to 0.003094	No	Ns
40 g sand vs. 30 g silt	-0.0006703	-0.0008890 to -0.0004517	Yes	**
40 g sand vs. 40 g silt	-0.0005228	-0.0008801 to -0.0001654	Yes	*
40 g sand vs. 10 g sand	-0.004973	-0.007900 to -0.002046	Yes	*
40 g sand vs. 20 g sand	-0.002698	-0.003644 to -0.001751	Yes	**
40 g sand vs. 30 g sand	-0.001665	-0.001849 to -0.001482	Yes	****
40 g sand vs. 40 g sand	-0.001498	-0.002298 to -0.0006974	Yes	**
0.005467 to 0.005367 No	Ns	** 10 g Silt vs. 20 g silt	-5.000e-005	-
10 g Silt vs. 30 g silt	0.001252	0.0008961 to 0.001609	Yes	**
10 g Silt vs. 40 g silt	0.0014	0.0009854 to 0.001815	Yes	**
10 g Silt vs. 10 g sand	-0.00305	-0.006003 to -9.667e-005	Yes	*
10 g Silt vs. 20 g sand	-0.0007750	-0.001571 to 2.109e-005	No	Ns
10 g Silt vs. 30 g sand	0.0002574	-8.710e-005 to 0.0006019	No	Ns
10 g Silt vs. 40 g sand	0.0004250	-0.0006961 to 0.001546	No	Ns
20 g silt vs. 30 g silt	0.001302	-0.003875 to 0.006479	No	Ns
20 g silt vs. 40 g silt	0.00145	-0.003640 to 0.006540	No	Ns
20 g silt vs. 10 g sand	-0.0030	-0.008077 to 0.002077	No	Ns

20 g silt vs. 20 g sand	-0.0007250	-0.006212 to 0.004762	No	Ns
20 g silt vs. 30 g sand	0.0003074	-0.004774 to 0.005388	No	Ns
20 g silt vs. 40 g sand	0.0004750	-0.003899 to 0.004849	No	Ns
30 g silt vs. 40 g silt	0.0001476	-0.0003294 to 0.0006246	No	Ns
30 g silt vs. 10 g sand	-0.004302	-0.007412 to -0.001193	Yes	*
30 g silt vs. 20 g sand	-0.002027	-0.002901 to -0.001154	Yes	**
30 g silt vs. 30 g sand	-0.000995	-0.001323 to -0.0006673	Yes	**
30 g silt vs. 40 g sand	-0.0008274	-0.001676 to 2.077e-005	No	Ns
40 g silt vs. 10 g sand	-0.00445	-0.007096 to -0.001804	Yes	*
40 g silt vs. 20 g sand	-0.002175	-0.002915 to -0.001435	Yes	**
40 g silt vs. 30 g sand	-0.001143	-0.001316 to -0.0009689	Yes	****
40 g silt vs. 40 g sand	-0.000975	-0.001836 to -0.0001141	Yes	*
10 g sand vs. 20 g sand	0.002275	-0.0006619 to 0.005212	No	Ns
10 g sand vs. 30 g sand	0.003307	0.0005254 to 0.006089	Yes	*
10 g sand vs. 40 g sand	0.003475	0.0005053 to 0.006445	Yes	*
20 g sand vs. 30 g sand	0.001032	0.0002064 to 0.001858	Yes	*
20 g sand vs. 40 g sand	0.0012	-3.503e-005 to 0.002435	No	Ns
30 g sand vs. 40 g sand	0.0001676	-0.0006498 to 0.0009850	No	Ns



**APPENDIX B: Repeated Measures one-way ANOVA analysis with Tukey's
Multiple Comparisons test for infiltration parameters**

KNUST



KNUST



Appendix B1.1: Repeated measures ANOVA summary for cumulative infiltration amount of different fluids

Assume sphericity?	No
F	87622
P value	< 0.0001
P value summary	****
Statistically significant (P < 0.05)?	Yes
Geisser-Greenhouse's epsilon	0.1647
R square	1.000

Was the matching effective?	
F	0.7324
P value	0.5744
P value summary	ns
Is there significant matching (P < 0.05)?	No
R square	2.786e-006

ANOVA table	SS	DF	MS	F (DFn, DFd)	P value
Treatment (between columns)	1.165e+006	12	97053	F (1.976, 7.906) = 87622	P < 0.0001
Individual (between rows)	3.245	4	0.8112	F (4, 48) = 0.7324	P = 0.5744
Residual (random)	53.17	48	1.108		
Total	1.165e+006	64			

Appendix B1.2: Tukey's multiple comparisons test summary for cumulative infiltration amount for different fluids

Number of families	1
--------------------	---

Number of comparisons per family
Alpha

78
0.05

Tukey's multiple comparisons test

	Mean Diff.	95% CI of diff.	Significant?	Summary
clear water vs. 10 g clay	6.845	0.4343 to 13.26	Yes	*
clear water vs. 20 g clay	228.1	225.4 to 230.9	Yes	****
clear water vs. 30 g clay	336.1	330.4 to 341.8	Yes	****
clear water vs. 40 g clay	343.2	338.9 to 347.6	Yes	****
clear water vs. 10 g Silt	-14.00	-16.53 to -11.48	Yes	***
clear water vs. 20 g silt	187.3	184.3 to 190.4	Yes	****
clear water vs. 30 g silt	271.1	269.2 to 273.1	Yes	****
clear water vs. 40 g silt	280.1	277.5 to 282.7	Yes	****
clear water vs. 10 g Sand	-26.41	-28.93 to -23.88	Yes	****
clear water vs. 20 g sand	51.18	48.42 to 53.94	Yes	****
clear water vs. 30 g sand	227.9	225.8 to 230.1	Yes	****
clear water vs. 40 g sand	236.2	233.6 to 238.9	Yes	****

KNUST

10 g clay vs. 20 g clay	221.3	216.2 to 226.4	Yes	****
10 g clay vs. 30 g clay	329.3	325.6 to 333.0	Yes	****
10 g clay vs. 40 g clay	336.4	326.4 to 346.3	Yes	****
10 g clay vs. 10 g Silt	-20.85	-26.56 to -15.13	Yes	***
10 g clay vs. 20 g silt	180.5	176.0 to 185.0	Yes	****
10 g clay vs. 30 g silt	264.3	259.4 to 269.1	Yes	****
10 g clay vs. 40 g silt	273.2	269.4 to 277.1	Yes	****
10 g clay vs. 10 g Sand	-33.25	-37.89 to -28.62	Yes	****
10 g clay vs. 20 g sand	44.34	39.77 to 48.90	Yes	****
10 g clay vs. 30 g sand	221.1	216.4 to 225.8	Yes	****
10 g clay vs. 40 g sand	229.4	225.3 to 233.4	Yes	****
20 g clay vs. 30 g clay	108.0	102.9 to 113.2	Yes	****
20 g clay vs. 40 g clay	115.1	108.0 to 122.2	Yes	****
20 g clay vs. 10 g Silt	-242.1	-245.9 to -238.4	Yes	****
20 g clay vs. 20 g silt	-40.78	-43.08 to -38.49	Yes	****
20 g clay vs. 30 g silt	42.98	40.44 to 45.52	Yes	****
20 g clay vs. 40 g silt	51.96	49.59 to 54.32	Yes	****
20 g clay vs. 10 g Sand	-254.5	-257.1 to -252.0	Yes	****
20 g clay vs. 20 g sand	-176.9	-180.6 to -173.3	Yes	****
20 g clay vs. 30 g sand	-0.1760	-3.358 to 3.006	No	Ns
20 g clay vs. 40 g sand	8.105	5.475 to 10.74	Yes	***
30 g clay vs. 40 g clay	7.088	-1.593 to 15.77	No	Ns

30 g clay vs. 10 g Silt	-350.1	-353.9 to -346.4	Yes	****
30 g clay vs. 20 g silt	-148.8	-152.7 to -144.9	Yes	****
30 g clay vs. 30 g silt	-65.03	-69.21 to -60.85	Yes	****
30 g clay vs. 40 g silt	-56.06	-59.78 to -52.33	Yes	****
30 g clay vs. 10 g Sand	-362.5	-366.3 to -358.8	Yes	****
30 g clay vs. 20 g sand	-285.0	-289.2 to -280.7	Yes	****
30 g clay vs. 30 g sand	-108.2	-112.2 to -104.2	Yes	****
30 g clay vs. 40 g sand	-99.91	-104.4 to -95.47	Yes	****
40 g clay vs. 10 g Silt	-357.2	-362.3 to -352.2	Yes	****
40 g clay vs. 20 g silt	-155.9	-162.9 to -148.9	Yes	****
40 g clay vs. 30 g silt	-72.12	-77.81 to -66.43	Yes	****
40 g clay vs. 40 g silt	-63.15	-69.59 to -56.70	Yes	****
40 g clay vs. 10 g Sand	-369.6	-375.9 to -363.4	Yes	****
40 g clay vs. 20 g sand	-292.0	-297.5 to -286.6	Yes	****
40 g clay vs. 30 g sand	-115.3	-120.6 to -110.0	Yes	****
40 g clay vs. 40 g sand	-107.0	-113.4 to -100.6	Yes	****
10 g Silt vs. 20 g silt	201.3	198.2 to 204.5	Yes	****
10 g Silt vs. 30 g silt	285.1	282.9 to 287.3	Yes	****
10 g Silt vs. 40 g silt	294.1	291.5 to 296.7	Yes	****
10 g Silt vs. 10 g Sand	-12.41	-14.87 to -9.944	Yes	***
10 g Silt vs. 20 g sand	65.18	62.93 to 67.43	Yes	****
10 g Silt vs. 30 g sand	242.0	240.1 to 243.8	Yes	****
10 g Silt vs. 40 g sand	250.2	247.0 to 253.4	Yes	****

KNUST

20 g silt vs. 30 g silt	83.77	82.38 to 85.15	Yes	****
20 g silt vs. 40 g silt	92.74	91.23 to 94.26	Yes	****
20 g silt vs. 10 g Sand	-213.7	-214.5 to -213.0	Yes	****
20 g silt vs. 20 g sand	-136.2	-139.5 to -132.8	Yes	****
20 g silt vs. 30 g sand	40.61	38.19 to 43.03	Yes	****
20 g silt vs. 40 g sand	48.89	47.04 to 50.74	Yes	****
30 g silt vs. 40 g silt	8.972	7.878 to 10.07	Yes	****
30 g silt vs. 10 g Sand	-297.5	-298.2 to -296.8	Yes	****
30 g silt vs. 20 g sand	-219.9	-222.2 to -217.6	Yes	****
30 g silt vs. 30 g sand	-43.16	-44.39 to -41.93	Yes	****
30 g silt vs. 40 g sand	-34.88	-36.22 to -33.54	Yes	****
40 g silt vs. 10 g Sand	-306.5	-307.7 to -305.3	Yes	****
40 g silt vs. 20 g sand	-228.9	-230.9 to -226.9	Yes	****
40 g silt vs. 30 g sand	-52.13	-53.43 to -50.84	Yes	****
40 g silt vs. 40 g sand	-43.85	-44.73 to -42.97	Yes	****
10 g Sand vs. 20 g sand	77.59	74.82 to 80.35	Yes	****
10 g Sand vs. 30 g sand	254.4	252.6 to 256.1	Yes	****

10 g Sand vs. 40 g sand	262.6	261.1 to 264.2	Yes	****
20 g sand vs. 30 g sand	176.8	175.6 to 177.9	Yes	****
20 g sand vs. 40 g sand	185.0	182.8 to 187.3	Yes	****
30 g sand vs. 40 g sand	8.281	6.689 to 9.873	Yes	***

Appendix B2.1: Repeated measures ANOVA summary for cumulative infiltration rate of different fluids

Assume sphericity?	No
F	1.538
P value	0.3406
P value summary	ns
Statistically significant ($P < 0.05$)?	No
Geisser-Greenhouse's epsilon	0.08361
R square	0.4348

Was the matching effective?

F	2.281
P value	0.1239
P value summary	ns
Is there significant matching ($P < 0.05$)?	No
R square	0.09703

ANOVA table

SS	DF	MS	F (DFn, DFd)	P value
----	----	----	--------------	---------

Treatment (between columns)	0.3164	12	0.02637	F (1.003, 2.007) = 1.538	P = 0.3406
Individual (between rows)	0.07821	2	0.03910	F (2, 24) = 2.281	P = 0.1239
Residual (random)	0.4114	24	0.01714		
Total	0.8060	38			

Appendix B2.2: Tukey's multiple comparisons test summary for cumulative infiltration rate for different fluids

Number of families	1
Number of comparisons per family	78
Alpha	0.05

Tukey's multiple comparisons test	Mean Diff.	95% CI of diff.	Significant?	Summary
clear water vs. 10 g clay	0.002253	-0.01179 to 0.01630	No	Ns
clear water vs. 20 g clay	-0.1112	-1.964 to 1.742	No	Ns
clear water vs. 30 g clay	0.09547	0.07377 to 0.1172	Yes	***
clear water vs. 40 g sand	0.08783	0.03950 to 0.1362	Yes	*
clear water vs. 10 g Silt	0.003143	-0.04093 to 0.04722	No	Ns
clear water vs. 20 g silt	0.05383	0.03687 to 0.07080	Yes	**
clear water vs. 30 g silt	0.0818	0.04387 to 0.1197	Yes	*
clear water vs. 40 g silt	0.08363	0.05358 to 0.1137	Yes	**
clear water vs. 10 g sand	-0.007833	-0.03743 to 0.02176	No	Ns
clear water vs. 20 g sand	-0.2322	-2.622 to 2.158	No	Ns
clear water vs. 30 g sand	0.06017	0.001220 to 0.1191	Yes	*
clear water vs. 40 g sand	0.0691	0.02206 to 0.1161	Yes	*
10 g clay vs. 20 g clay	-0.1134	-1.979 to 1.752	No	Ns

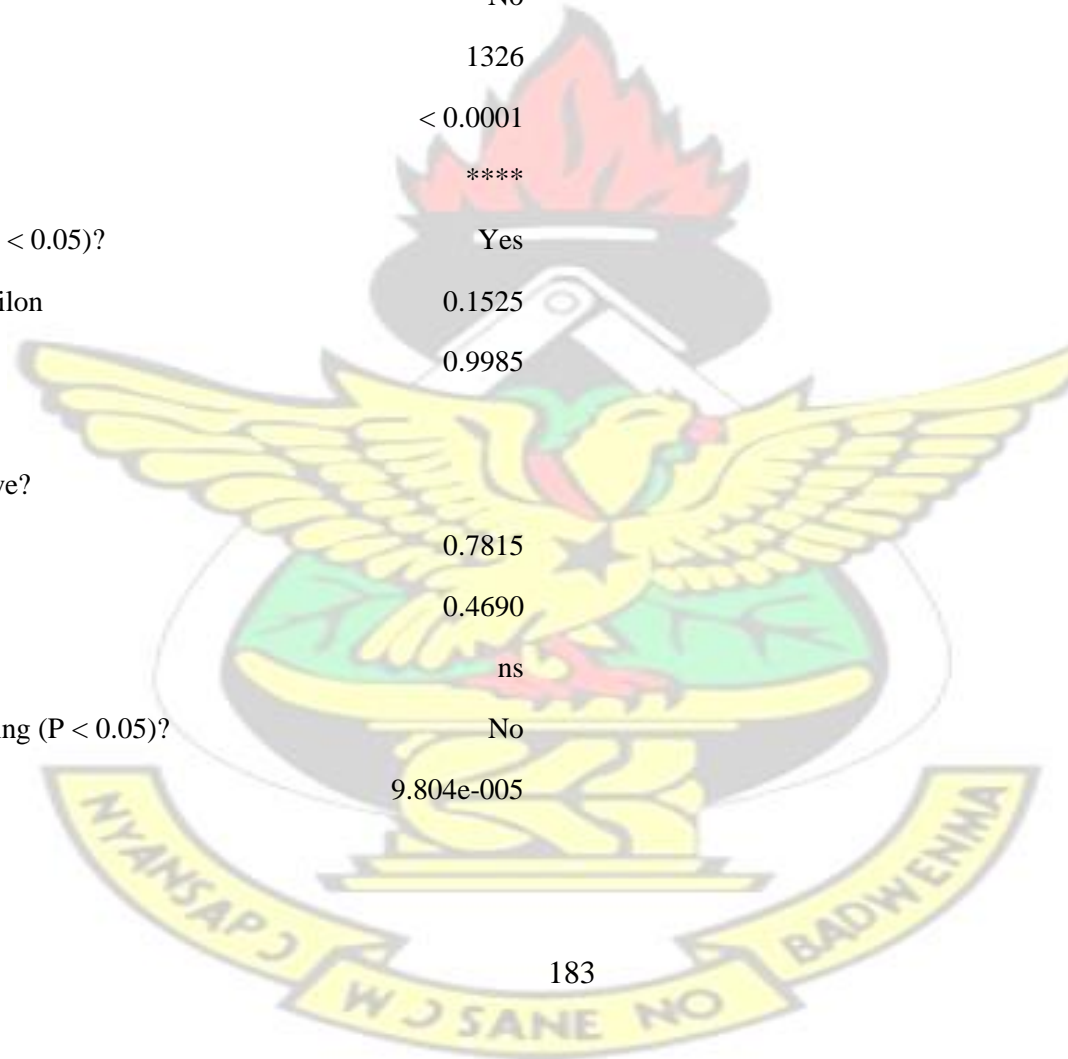
10 g clay vs. 30 g clay	0.09321	0.08096 to 0.1055	Yes	****
10 g clay vs. 40 g sand	0.08558	0.04518 to 0.1260	Yes	*
10 g clay vs. 10 g Silt	0.0008900	-0.03676 to 0.03854	No	Ns
10 g clay vs. 20 g silt	0.05158	0.02249 to 0.08067	Yes	*
10 g clay vs. 30 g silt	0.07955	0.03656 to 0.1225	Yes	*
10 g clay vs. 40 g silt	0.08138	0.04959 to 0.1132	Yes	*
10 g clay vs. 10 g sand	-0.01009	-0.02643 to 0.006252	No	Ns
10 g clay vs. 20 g sand	-0.2344	-2.637 to 2.168	No	Ns
10 g clay vs. 30 g sand	0.05791	-0.01493 to 0.1308	No	Ns
10 g clay vs. 40 g sand	0.06685	0.006869 to 0.1268	Yes	*
20 g clay vs. 30 g clay	0.2066	-1.668 to 2.081	No	Ns
20 g clay vs. 40 g sand	0.1990	-1.669 to 2.067	No	Ns
20 g clay vs. 10 g Silt	0.1143	-1.777 to 2.006	No	Ns
20 g clay vs. 20 g silt	0.1650	-1.681 to 2.011	No	Ns
20 g clay vs. 30 g silt	0.1930	-1.669 to 2.055	No	Ns
20 g clay vs. 40 g silt	0.1948	-1.674 to 2.063	No	Ns
20 g clay vs. 10 g sand	0.1033	-1.773 to 1.979	No	Ns
20 g clay vs. 20 g sand	-0.1210	-0.6714 to 0.4294	No	Ns
20 g clay vs. 30 g sand	0.1713	-1.625 to 1.967	No	Ns
20 g clay vs. 40 g sand	0.1803	-1.643 to 2.004	No	Ns
30 g clay vs. 40 g sand	-0.007633	-0.05714 to 0.04188	No	Ns
30 g clay vs. 10 g Silt	-0.09232	-0.1177 to -0.06690	Yes	**
30 g clay vs. 20 g silt	-0.04163	-0.07292 to -0.01034	Yes	*
30 g clay vs. 30 g silt	-0.01367	-0.05023 to 0.02290	No	Ns
30 g clay vs. 40 g silt	-0.01183	-0.03576 to 0.01209	No	Ns
30 g clay vs. 10 g sand	-0.1033	-0.1246 to -0.08199	Yes	***
30 g clay vs. 20 g sand	-0.3276	-2.740 to 2.084	No	Ns
30 g clay vs. 30 g sand	-0.0353	-0.1147 to 0.04413	No	Ns

30 g clay vs. 40 g sand	-0.02637	-0.08775 to 0.03501	No	Ns
40 g sand vs. 10 g Silt	-0.08469	-0.1569 to -0.01246	Yes	*
40 g sand vs. 20 g silt	-0.0340	-0.09919 to 0.03119	No	Ns
40 g sand vs. 30 g silt	-0.006033	-0.08938 to 0.07732	No	Ns
40 g sand vs. 40 g silt	-0.004200	-0.07628 to 0.06788	No	Ns
40 g sand vs. 10 g sand	-0.09567	-0.1248 to -0.06656	Yes	**
40 g sand vs. 20 g sand	-0.3200	-2.722 to 2.082	No	Ns
40 g sand vs. 30 g sand	-0.02767	-0.1218 to 0.06642	No	Ns
40 g sand vs. 40 g sand	-0.01873	-0.1123 to 0.07485	No	Ns
10 g Silt vs. 20 g silt	0.05069	0.004880 to 0.09650	Yes	*
10 g Silt vs. 30 g silt	0.07866	0.04538 to 0.1119	Yes	*
10 g Silt vs. 40 g silt	0.08049	0.05722 to 0.1038	Yes	**
10 g Silt vs. 10 g sand	-0.01098	-0.05412 to 0.03216	No	Ns
10 g Silt vs. 20 g sand	-0.2353	-2.665 to 2.194	No	Ns
10 g Silt vs. 30 g sand	0.05702	-0.03833 to 0.1524	No	Ns
10 g Silt vs. 40 g sand	0.06596	-0.003654 to 0.1356	No	Ns
20 g silt vs. 30 g silt	0.02797	0.001328 to 0.05461	Yes	*
20 g silt vs. 40 g silt	0.0298	0.005069 to 0.05453	Yes	*
20 g silt vs. 10 g sand	-0.06167	-0.1071 to -0.01626	Yes	*
20 g silt vs. 20 g sand	-0.2860	-2.670 to 2.098	No	Ns

20 g silt vs. 30 g sand	0.006333	-0.04345 to 0.05612	No	Ns
20 g silt vs. 40 g sand	0.01527	-0.01566 to 0.04620	No	Ns
30 g silt vs. 40 g silt	0.001833	-0.01115 to 0.01482	No	Ns
30 g silt vs. 10 g sand	-0.08963	-0.1470 to -0.03231	Yes	*
30 g silt vs. 20 g sand	-0.3140	-2.715 to 2.087	No	Ns
30 g silt vs. 30 g sand	-0.02163	-0.09053 to 0.04726	No	Ns
30 g silt vs. 40 g sand	-0.0127	-0.05111 to 0.02571	No	Ns
40 g silt vs. 10 g sand	-0.09147	-0.1365 to -0.04643	Yes	*
40 g silt vs. 20 g sand	-0.3158	-2.723 to 2.091	No	Ns
40 g silt vs. 30 g sand	-0.02347	-0.09641 to 0.04948	No	Ns
40 g silt vs. 40 g sand	-0.01453	-0.06090 to 0.03183	No	Ns
10 g sand vs. 20 g sand	-0.2243	-2.637 to 2.188	No	Ns
10 g sand vs. 30 g sand	0.0680	-0.01889 to 0.1549	No	Ns
10 g sand vs. 40 g sand	0.07693	0.0006901 to 0.1532	Yes	*
20 g sand vs. 30 g sand	0.2923	-2.042 to 2.627	No	Ns
20 g sand vs. 40 g sand	0.3013	-2.062 to 2.664	No	Ns
30 g sand vs. 40 g sand	0.008933	-0.02526 to 0.04313	No	Ns

Appendix B3.1: Repeated measures ANOVA summary for steady state infiltrability of different fluids

Assume sphericity?	No
F	1326
P value	< 0.0001
P value summary	****
Statistically significant (P < 0.05)?	Yes
Geisser-Greenhouse's epsilon	0.1525
R square	0.9985
Was the matching effective?	
F	0.7815
P value	0.4690
P value summary	ns
Is there significant matching (P < 0.05)?	No
R square	9.804e-005



ANOVA table	SS	DF	MS	F (DFn, DFd)	P value
Treatment (between columns)	0.04857	12	0.004047	F (1.830, 3.659) = 1326	P < 0.0001
Individual (between rows)	4.769e-006	2	2.385e-006	F (2, 24) = 0.7815	P = 0.4690
Residual (random)	7.323e-005	24	3.051e-006		
Total	0.04865	38			

Appendix B3.2: Tukey's multiple comparisons test summary for steady state infiltrability for different fluids

Number of families	1
Number of comparisons per family	78
Alpha	0.05

Tukey's multiple comparisons test	Mean Diff.	95% CI of diff.	Significant?	Summary
clear water vs. 10 g clay	0.002333	-0.001223 to 0.005890	No	Ns
clear water vs. 20 g clay	0.0600	0.04768 to 0.07232	Yes	***
clear water vs. 30 g clay	0.08900	0.07833 to 0.09967	Yes	****
clear water vs. 40 g sand	0.0910	0.07470 to 0.1073	Yes	****
clear water vs. 10 g Silt	-0.003000	-0.003000 to -0.003000	Yes	****
clear water vs. 20 g silt	0.0490	0.03270 to 0.06530	Yes	**
clear water vs. 30 g silt	0.06767	0.05826 to 0.07708	Yes	****
clear water vs. 40 g silt	0.07067	0.06126 to 0.08008	Yes	****
clear water vs. 10 g sand	-0.006667	-0.01949 to 0.006156	No	Ns
clear water vs. 20 g sand	0.009667	-0.009151 to 0.02848	No	Ns

Comparison	Mean	Lower Bound	Upper Bound	Significance	Significance Code
clear water vs. 30 g sand	0.05433	0.04492	0.06374	Yes	****
clear water vs. 40 g sand	0.07033	0.06092	0.07974	Yes	****
10 g clay vs. 20 g clay	0.05767	0.04484	0.07049	Yes	***
10 g clay vs. 30 g clay	0.08667	0.07244	0.1009	Yes	****
10 g clay vs. 40 g sand	0.08867	0.07317	0.1042	Yes	****
10 g clay vs. 10 g Silt	-0.005333	-0.008890	-0.001777	Yes	*
10 g clay vs. 20 g silt	0.04667	0.03117	0.06217	Yes	**
10 g clay vs. 30 g silt	0.06533	0.05251	0.07816	Yes	****
10 g clay vs. 40 g silt	0.06833	0.05551	0.08116	Yes	****
10 g clay vs. 10 g sand	-0.009000	-0.02132	0.003319	No	Ns
10 g clay vs. 20 g sand	0.007333	-0.01247	0.02713	No	Ns
10 g clay vs. 30 g sand	0.0520	0.04584	0.05816	Yes	****
10 g clay vs. 40 g sand	0.0680	0.06184	0.07416	Yes	****
20 g clay vs. 30 g clay	0.0290	0.01270	0.04530	Yes	*
20 g clay vs. 40 g sand	0.0310	0.02484	0.03716	Yes	****
20 g clay vs. 10 g Silt	-0.0630	-0.07532	-0.05068	Yes	****
20 g clay vs. 20 g silt	-0.0110	-0.01716	-0.004840	Yes	*
20 g clay vs. 30 g silt	0.007667	-0.01011	0.02545	No	Ns
20 g clay vs. 40 g silt	0.01067	-0.007115	0.02845	No	Ns
20 g clay vs. 10 g sand	-0.06667	-0.07022	-0.06311	Yes	****
20 g clay vs. 20 g sand	-0.05033	-0.05745	-0.04322	Yes	****

20 g clay vs. 30 g sand	-0.005667	-0.02345 to 0.01211	No	Ns
20 g clay vs. 40 g sand	0.01033	-0.007448 to 0.02811	No	Ns
30 g clay vs. 40 g sand	0.0020	-0.02021 to 0.02421	No	Ns
30 g clay vs. 10 g Silt	-0.0920	-0.1027 to -0.08133	Yes	****
30 g clay vs. 20 g silt	-0.0400	-0.06221 to -0.01779	Yes	*
30 g clay vs. 30 g silt	-0.02133	-0.02489 to -0.01778	Yes	****
30 g clay vs. 40 g silt	-0.01833	-0.02189 to -0.01478	Yes	****
30 g clay vs. 10 g sand	-0.09567	-0.1145 to -0.07685	Yes	****
30 g clay vs. 20 g sand	-0.07933	-0.09913 to -0.05953	Yes	**
30 g clay vs. 30 g sand	-0.03467	-0.05447 to -0.01487	Yes	*
30 g clay vs. 40 g sand	-0.01867	-0.03847 to 0.001134	No	Ns
40 g sand vs. 10 g Silt	-0.0940	-0.1103 to -0.07770	Yes	****
40 g sand vs. 20 g silt				
40 g sand vs. 30 g silt	-0.02333	-0.04665 to -1.344e-005	Yes	*
40 g sand vs. 40 g silt	-0.02033	-0.04365 to 0.002987	No	Ns
40 g sand vs. 10 g sand	-0.09767	-0.1012 to -0.09411	Yes	****
40 g sand vs. 20 g sand	-0.08133	-0.09074 to -0.07192	Yes	****

KNUST

40 g sand vs. 30 g sand	-0.03667	-0.05548 to -0.01785	Yes	*
40 g sand vs. 40 g sand	-0.02067	-0.03948 to -0.001849	Yes	*
10 g Silt vs. 20 g silt	0.0520	0.03570 to 0.06830	Yes	**
10 g Silt vs. 30 g silt	0.07067	0.06126 to 0.08008	Yes	****
10 g Silt vs. 40 g silt	0.07367	0.06426 to 0.08308	Yes	****
10 g Silt vs. 10 g sand	-0.003667	-0.01649 to 0.009156	No	Ns
10 g Silt vs. 20 g sand	0.01267	-0.006151 to 0.03148	No	Ns
10 g Silt vs. 30 g sand	0.05733	0.04792 to 0.06674	Yes	****
10 g Silt vs. 40 g sand	0.07333	0.06392 to 0.08274	Yes	****
20 g silt vs. 30 g silt	0.01867	-0.004653 to 0.04199	No	Ns
20 g silt vs. 40 g silt	0.02167	-0.001653 to 0.04499	No	Ns
20 g silt vs. 10 g sand	-0.05567	-0.05922 to -0.05211	Yes	****
20 g silt vs. 20 g sand	-0.03933	-0.04874 to -0.02992	Yes	***
20 g silt vs. 30 g sand	0.005333	-0.01348 to 0.02415	No	Ns
20 g silt vs. 40 g sand	0.02133	0.002515 to 0.04015	Yes	*
30 g silt vs. 40 g silt	0.0030	0.003000 to 0.003000	Yes	****
30 g silt vs. 10 g sand	-0.07433	-0.09413 to -0.05453	Yes	**
30 g silt vs. 20 g sand	-0.0580	-0.08021 to -0.03579	Yes	**
30 g silt vs. 30 g sand	-0.01333	-0.03111 to 0.004448	No	Ns
30 g silt vs. 40 g sand	0.002667	-0.01511 to 0.02045	No	Ns
40 g silt vs. 10 g sand	-0.07733	-0.09713 to -0.05753	Yes	**
40 g silt vs. 20 g sand	-0.0610	-0.08321 to -0.03879	Yes	**
40 g silt vs. 30 g sand	-0.01633	-0.03411 to 0.001448	No	Ns
40 g silt vs. 40 g sand	-0.0003333	-0.01811 to 0.01745	No	Ns
10 g sand vs. 20 g sand	0.01633	0.006924 to 0.02574	Yes	*
10 g sand vs. 30 g sand	0.0610	0.04470 to 0.07730	Yes	**
10 g sand vs. 40 g sand	0.0770	0.06070 to 0.09330	Yes	***

KNUST

20 g sand vs. 30 g sand
 20 g sand vs. 40 g sand
 30 g sand vs. 40 g sand

0.04467 0.01977 to 0.06956
 0.06067 0.03577 to 0.08556
 0.0160 0.01600 to 0.01600

Yes *
 Yes *
 Yes ****



**APPENDIX C: Repeated Measures one-way ANOVA analysis with Tukey's
Multiple Comparisons test for seal thickness**

KNUST



KNUST



C1.1: Repeated Measures one way ANOVA analyses of seal thickness for different concentrations of clay suspension

Assume sphericity?	No				
F	15.37				
P value	0.0044				
P value summary	**				
Statistically significant ($P < 0.05$)?	Yes				
Geisser-Greenhouse's epsilon	0.09091				
R square	0.6577				
Was the matching effective?					
F	31.44				
P value	< 0.0001				
P value summary	****				
Is there significant matching ($P < 0.05$)?	Yes				
R square	0.4945				
ANOVA table	SS	DF	MS	F (DFn, DFd)	P value

Appendix

-

KNUST

Treatment (between columns)	4.574	11	0.4158	F (1.000, 8.000) = 15.37	P = 0.0044
Individual (between rows)	6.803	8	0.8504	F (8, 88) = 31.44	P < 0.0001
Residual (random)	2.380	88	0.02705		
Total	13.76	107			

Appendix C1.2: Tukey's multiple comparisons test of seal thickness for different concentrations of clay suspension

Number of families

1

Number of comparisons per family

6

Alpha

0.05

Tukey's multiple comparisons test

10.00 vs. 20.00

10.00 vs. 30.00

Mean Diff.

95% CI of diff.

Significant?

Summary

-0.1044

-0.1896 to -0.01922

Yes

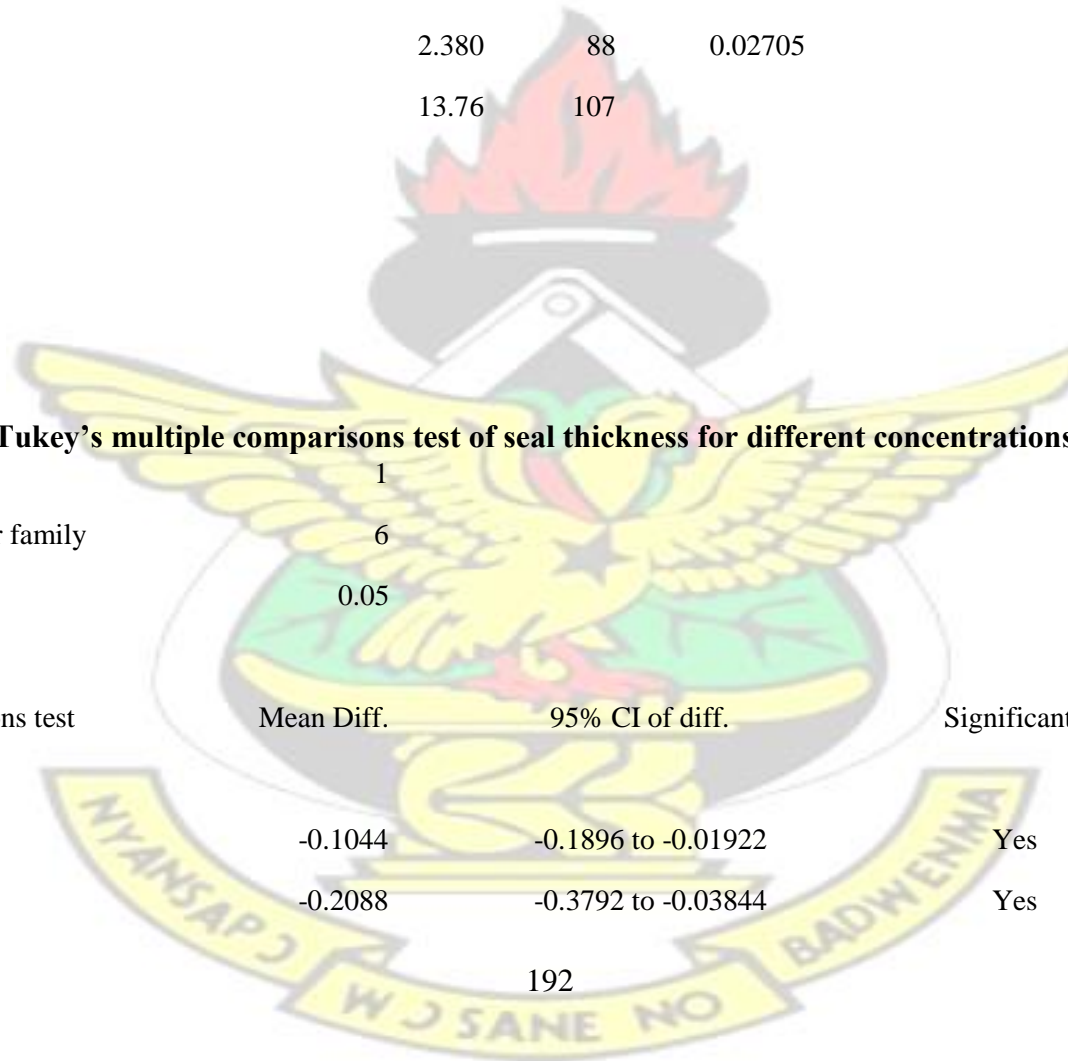
*

-0.2088

-0.3792 to -0.03844

Yes

*



10.00 vs. 40.00	-0.3130	-0.5687 to -0.05735	Yes	*
20.00 vs. 30.00	-0.1044	-0.1896 to -0.01922	Yes	*
20.00 vs. 40.00	-0.2086	-0.3790 to -0.03813	Yes	*
30.00 vs. 40.00	-0.1042	-0.1894 to -0.01891	Yes	*

C2.1: Repeated Measures one way ANOVA analyses of seal thickness for different concentrations of silt suspension

Assume sphericity?	No
F	15.37
P value	0.0044
P value summary	**
Statistically significant ($P < 0.05$)?	Yes
Geisser-Greenhouse's epsilon	0.3333
R square	0.6577
Was the matching effective?	
F	15.00
P value	< 0.0001

Appendix

KNUST

P value summary

Is there significant matching ($P < 0.05$)?

Yes

R square

0.6312

ANOVA table

	SS	DF	MS	F (DFn, DFd)	P value
Treatment (between columns)	1.960	3	0.6534	F (1.000, 8.000) = 15.37	P = 0.0044
Individual (between rows)	5.102	8	0.6377	F (8, 24) = 15.00	P < 0.0001
Residual (random)	1.020	24	0.04251		
Total	8.082	35			

Appendix C2.2: Tukey's multiple comparisons test of seal thickness for different concentrations of silt suspension

Number of families

1

Number of comparisons per family

6

Alpha

0.05

Tukey's multiple comparisons test

Mean Diff.

95% CI of diff.

Significant?

Summary

10.00 vs. 20.00	-0.1044	-0.1896 to -0.01922	Yes	*
10.00 vs. 30.00	-0.2088	-0.3792 to -0.03844	Yes	*
10.00 vs. 40.00	-0.3130	-0.5687 to -0.05735	Yes	*
20.00 vs. 30.00	-0.1044	-0.1896 to -0.01922	Yes	*
20.00 vs. 40.00	-0.2086	-0.3790 to -0.03813	Yes	*
30.00 vs. 40.00	-0.1042	-0.1894 to -0.01891	Yes	*

C3.1: Repeated Measures one way ANOVA analyses of seal thickness for different concentrations of sand suspension

Repeated measures ANOVA summary

Assume sphericity?	No
F	15.37
P value	0.0044
P value summary	**
Statistically significant (P < 0.05)?	Yes
Geisser-Greenhouse's epsilon	0.3333
R square	0.6577

Was the matching effective?

F	15.00
P value	< 0.0001
P value summary	****

Appendix

-

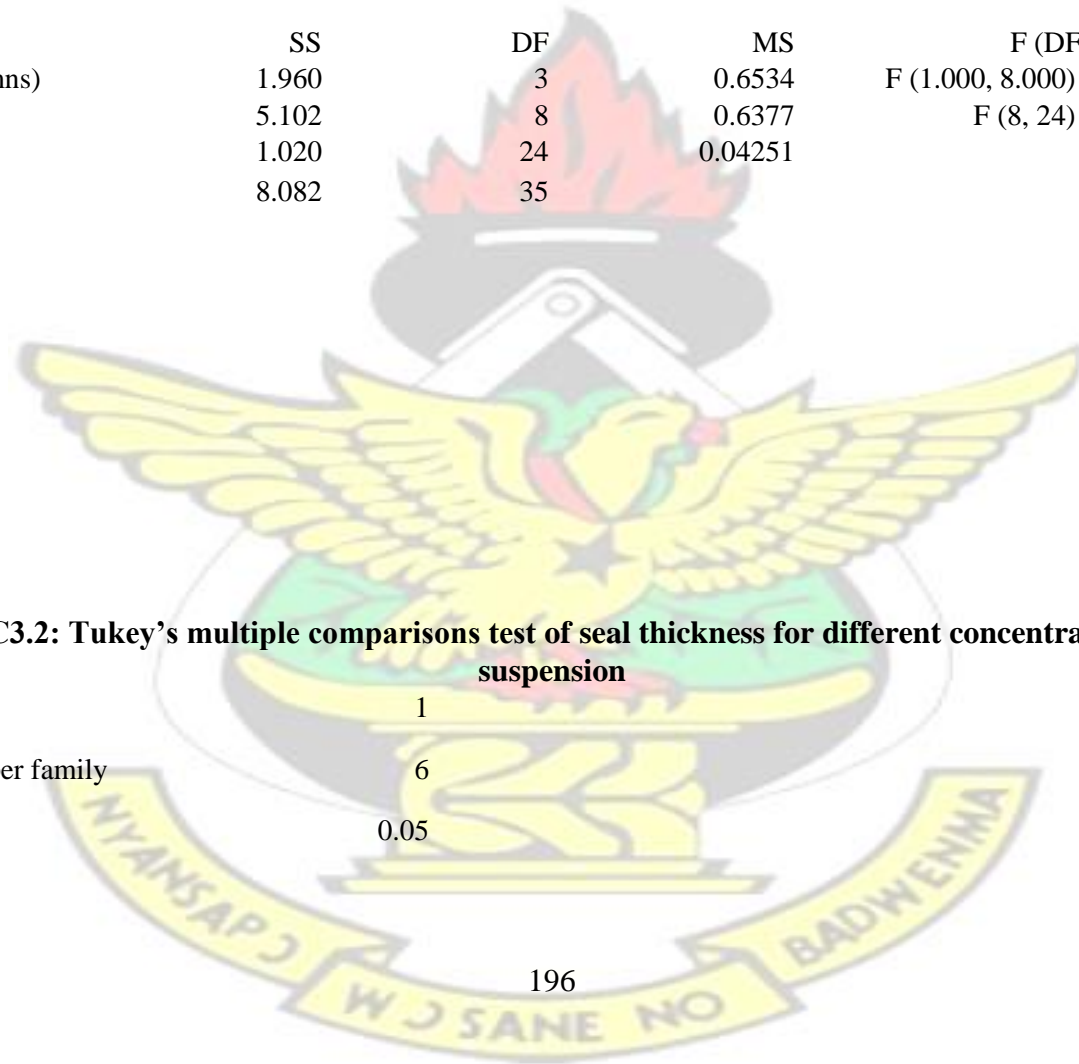
KNUST

Is there significant matching ($P < 0.05$)? Yes
 R square 0.6312

ANOVA table	SS	DF	MS	F (DFn, DFd)	P value
Treatment (between columns)	1.960	3	0.6534	F (1.000, 8.000) = 15.37	P = 0.0044
Individual (between rows)	5.102	8	0.6377	F (8, 24) = 15.00	P < 0.0001
Residual (random)	1.020	24	0.04251		
Total	8.082	35			

Appendix C3.2: Tukey's multiple comparisons test of seal thickness for different concentrations of sand suspension

Number of families 1
 Number of comparisons per family 6
 Alpha 0.05



Tukey's multiple comparisons test	Mean Diff.	95% CI of diff.	Significant?	Summary
10.00 vs. 20.00	-0.2086	-0.3790 to -0.03813	Yes	*
10.00 vs. 30.00	-0.4175	-0.7584 to -0.07666	Yes	*
10.00 vs. 40.00	-0.6261	-1.138 to -0.1147	Yes	*
20.00 vs. 30.00	-0.2089	-0.3793 to -0.03853	Yes	*
20.00 vs. 40.00	-0.4175	-0.7585 to -0.07652	Yes	*
30.00 vs. 40.00	-0.2086	-0.3792 to -0.03799	Yes	*

C4.1: Repeated Measures one way ANOVA analyses of seal thickness for interactions among the different treatments

Repeated measures ANOVA summary

Assume sphericity?

No

F

15.37

P value

0.0044

P value summary

**

Statistically significant ($P < 0.05$)?

Yes

Geisser-Greenhouse's epsilon

0.09091

Appendix

-

KNUST

R square 0.6577

Was the matching effective?

F 31.44

P value < 0.0001

P value summary ****

Is there significant matching (P < 0.05)? Yes

R square 0.4945

ANOVA table	SS	DF	MS	F (DFn, DFd)	P value
Treatment (between columns)	4.574	11	0.4158	F (1.000, 8.000) = 15.37	P = 0.0044
Individual (between rows)	6.803	8	0.8504	F (8, 88) = 31.44	P < 0.0001
Residual (random)	2.380	88	0.02705		
Total	13.76	107			

Appendix C4.2: Tukey's multiple comparisons test of seal thickness for interactions among the different treatments

KNUST

Number of families 1
 Number of comparisons per family 66
 Alpha 0.05

Tukey's multiple comparisons test	Mean Diff.	95% CI of diff.	Significant?	Summary	
10.00 g vs. 20.00 g	-0.1044	-0.2206 to 0.01176	No	Ns	CLAY-CLAY
10.00 g vs. 30.00 g	-0.2088	-0.4412 to 0.02351	No	Ns	CLAY-CLAY
10.00 g vs. 40.00 g	-0.3130	-0.6616 to 0.03560	No	Ns	CLAY-CLAY
10.00 g vs. 10.00 g					
10.00 g vs. 20.00 g	-0.1044	-0.2206 to 0.01176	No	Ns	CLAY-SILT
10.00 g vs. 30.00 g	-0.2088	-0.4412 to 0.02351	No	Ns	CLAY-SILT
10.00 g vs. 40.00 g	-0.3130	-0.6616 to 0.03560	No	Ns	CLAY-SILT
10.00 g vs. 10.00 g	-0.1044	-0.2206 to 0.01176	No	Ns	CLAY- SAND
10.00 g vs. 20.00 g	-0.3130	-0.6616 to 0.03560	No	Ns	CLAY-SAND
10.00 g vs. 30.00 g	-0.5219	-1.103 to 0.05902	No	Ns	CLAY-SAND

Appendix

-

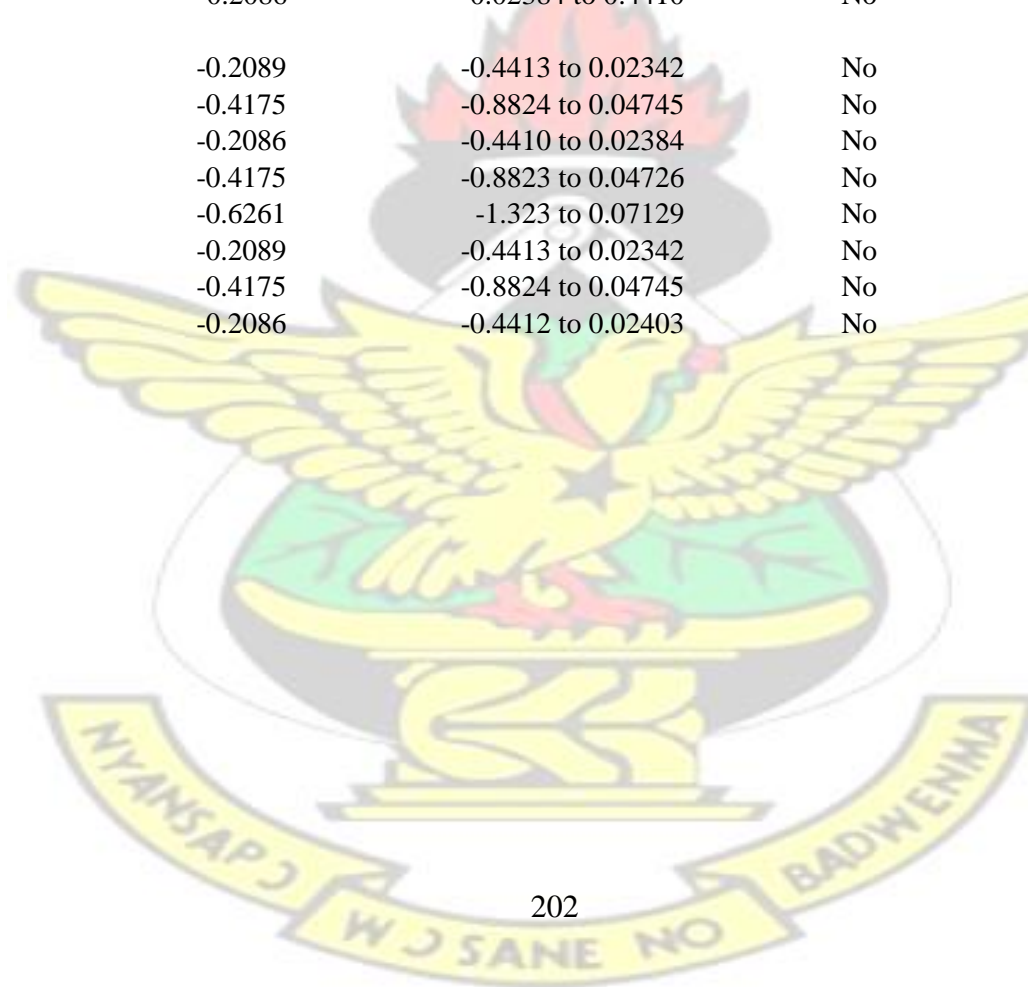
10.00 g vs. 40.00 g	-0.7305	-1.544 to 0.08305	No	Ns	CLAY-SAND
20.00 g vs. 30.00 g	-0.1044	-0.2206 to 0.01175	No	Ns	CLAY-CLAY
20.00 g vs. 40.00 g	-0.2086	-0.4410 to 0.02384	No	Ns	CLAY-CLAY
20.00 g vs. 10.00 g	0.1044	-0.01176 to 0.2206	No	Ns	CLAY-SILT
20.00 g vs. 20.00 g					
20.00 g vs. 30.00 g	-0.1044	-0.2206 to 0.01175	No	Ns	CLAY-SILT
20.00 g vs. 40.00 g	-0.2086	-0.4410 to 0.02384	No	Ns	CLAY-SILT
20.00 g vs. 10.00 g					
20.00 g vs. 20.00 g	-0.2086	-0.4410 to 0.02384	No	Ns	CLAY-SAND
20.00 g vs. 30.00 g	-0.4175	-0.8823 to 0.04726	No	Ns	CLAY-SAND
20.00 g vs. 40.00 g	-0.6261	-1.323 to 0.07129	No	Ns	CLAY-SAND
30.00 g vs. 40.00 g	-0.1042	-0.2204 to 0.01210	No	Ns	CLAY-CLAY



30.00 g vs. 10.00 g	0.2088	-0.02351 to 0.4412	No	Ns	CLAY-SILT
30.00 g vs. 20.00 g	0.1044	-0.01175 to 0.2206	No	Ns	CLAY-SILT
30.00 g vs. 30.00 g					
30.00 g vs. 40.00 g	-0.1042	-0.2204 to 0.01210	No	Ns	CLAY-SILT
30.00 g vs. 10.00 g	0.1044	-0.01175 to 0.2206	No	Ns	CLAY-SAND
30.00 g vs. 20.00 g	-0.1042	-0.2204 to 0.01210	No	Ns	CLAY-SAND
30.00 g vs. 30.00 g	-0.3131	-0.6617 to 0.03551	No	Ns	CLAY-SAND
30.00 g vs. 40.00 g	-0.5217	-1.103 to 0.05954	No	Ns	CLAY-SAND
40.00 g vs. 10.00 g	0.3130	-0.03560 to 0.6616	No	Ns	CLAY-SILT
40.00 g vs. 20.00 g	0.2086	-0.02384 to 0.4410	No	Ns	CLAY-SILT
40.00 g vs. 30.00 g	0.1042	-0.01210 to 0.2204	No	Ns	CLAY-SILT
40.00 g vs. 40.00 g					
40.00 g vs. 10.00 g	0.2086	-0.02384 to 0.4410	No	Ns	CLAY-SAND
40.00 g vs. 20.00 g					
40.00 g vs. 30.00 g	-0.2089	-0.4413 to 0.02342	No Ns	CLAY-SAND	40.00 g vs. 40.00 g
					-0.4175 -0.8824 to 0.04745 No Ns CLAY-SAND
10.00 g vs. 20.00 g	-0.1044	-0.2206 to 0.01176	No	Ns	SILT-SILT
10.00 g vs. 30.00 g	-0.2088	-0.4412 to 0.02351	No	Ns	SILT-SILT
10.00 g vs. 40.00 g	-0.3130	-0.6616 to 0.03560	No	Ns	SILT-SILT
10.00 g vs. 10.00 g	-0.1044	-0.2206 to 0.01176	No	Ns	SILT-SAND
10.00 g vs. 20.00 g	-0.3130	-0.6616 to 0.03560	No	Ns	SILT-SAND
10.00 g vs. 30.00 g	-0.5219	-1.103 to 0.05902	No	Ns	SILT-SAND
10.00 g vs. 40.00 g	-0.7305	-1.544 to 0.08305	No Ns	SILT-SAND	20.00 g vs. 30.00 g
					-0.1044 -0.2206 to 0.01175 No Ns SILT-SILT
20.00 g vs. 40.00 g	-0.2086	-0.4410 to 0.02384	No	Ns	SILT-SILT
20.00 g vs. 10.00 g					
20.00 g vs. 20.00 g	-0.2086	-0.4410 to 0.02384	No	Ns	SILT-SAND
20.00 g vs. 30.00 g	-0.4175	-0.8823 to 0.04726	No	Ns	SILT-SAND
20.00 g vs. 40.00 g	-0.6261	-1.323 to 0.07129	No	Ns	SILT-SAND
30.00 g vs. 40.00 g	-0.1042	-0.2204 to 0.01210	No	Ns	SILT-SILT

KNUST

30.00 g vs. 10.00 g	0.1044	-0.01175 to 0.2206	No	Ns	SILT-SAND
30.00 g vs. 20.00 g	-0.1042	-0.2204 to 0.01210	No	Ns	SILT-SAND
30.00 g vs. 30.00 g	-0.3131	-0.6617 to 0.03551	No	Ns	SILT-SAND
30.00 g vs. 40.00 g	-0.5217	-1.103 to 0.05954	No	Ns	SILT-SAND
40.00 g vs. 10.00 g	0.2086	-0.02384 to 0.4410	No	Ns	SILT-SAND
40.00 g vs. 20.00 g					
40.00 g vs. 30.00 g	-0.2089	-0.4413 to 0.02342	No	Ns	SILT-SAND
40.00 g vs. 40.00 g	-0.4175	-0.8824 to 0.04745	No	Ns	SILT-SAND
10.00 g vs. 20.00 g	-0.2086	-0.4410 to 0.02384	No	Ns	SAND-SAND
10.00 g vs. 30.00 g	-0.4175	-0.8823 to 0.04726	No	Ns	SAND-SAND
10.00 g vs. 40.00 g	-0.6261	-1.323 to 0.07129	No	Ns	SAND-SAND
20.00 g vs. 30.00 g	-0.2089	-0.4413 to 0.02342	No	Ns	SAND-SAND
20.00 g vs. 40.00 g	-0.4175	-0.8824 to 0.04745	No	Ns	SAND-SAND
30.00 g vs. 40.00 g	-0.2086	-0.4412 to 0.02403	No	Ns	SAND-SAND



APPENDIX D: One-sample t-test analysis of seal thickness for the different sediments suspensions and concentrations with respect to time

KNUST



KNUST



**-sample t-
Appendix D1: One test analysis of variation of seal thickness with time for Clay suspensions**

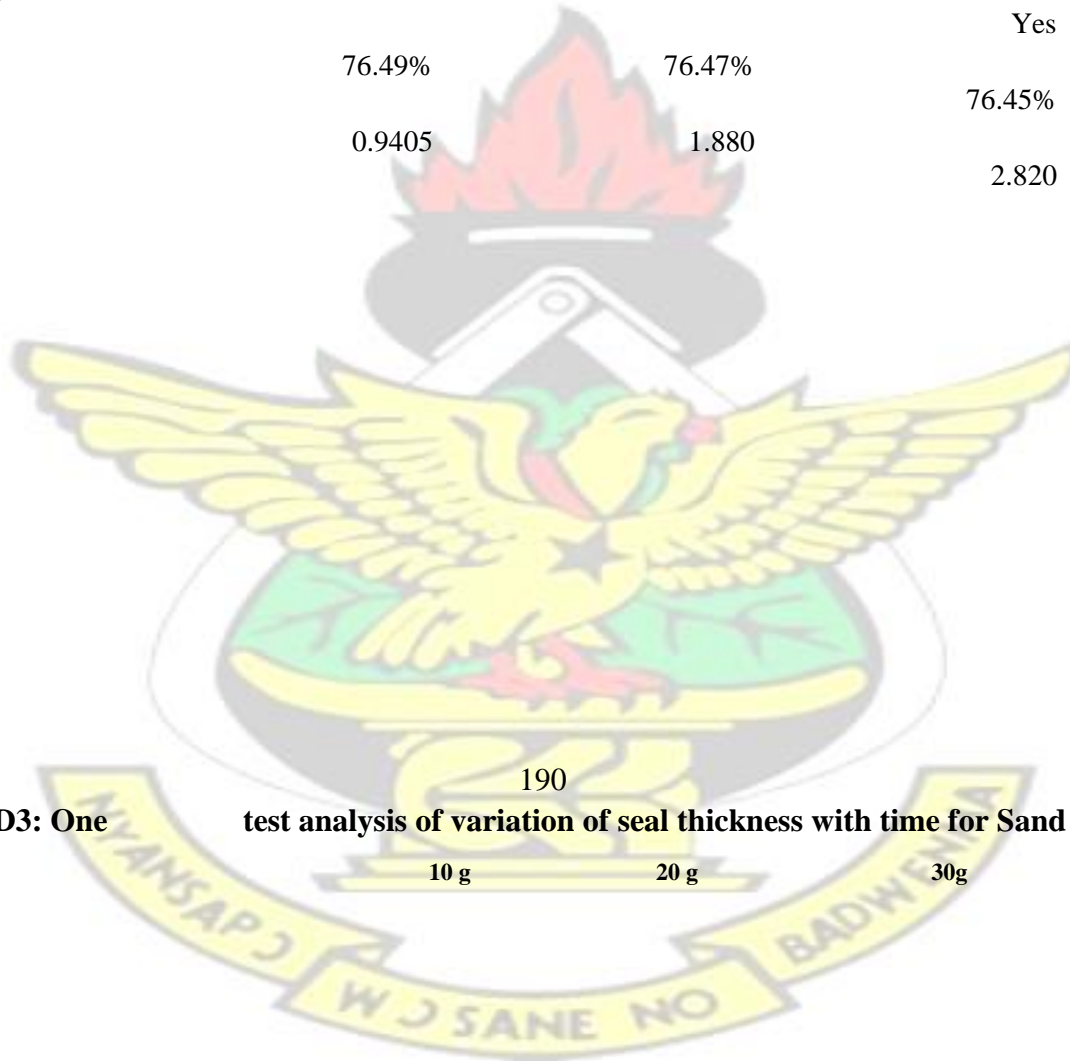
	10 g	20 g	30 g	40 g
Theoretical mean	0.0	0.0	0.0	0.0
Actual mean	0.1045	0.2089	0.3133	0.4175
Discrepancy	-0.1045	-0.2089	-0.3133	-0.4175
95% CI of discrepancy	0.04306 to 0.1659	0.08612 to 0.3317	0.1292 to 0.4975	0.1720 to 0.6630
t, df	t=3.922 df=8	t=3.923 df=8	t=3.924 df=8	t=3.921 df=8
P value (two tailed)	0.0044	0.0044	0.0044	0.0044
Significant (alpha=0.05)?	Yes	Yes	Yes	Yes
Coefficient of variation	76.49%	76.47%	76.45%	76.51%
Sum	0.9405	1.880	2.820	3.758

Appendix D2: One test analysis of variation of seal thickness with time for Silt suspensions

	10 g	20 g	30 g	40 g
Theoretical mean	0.0	0.0	0.0	0.0
Actual mean	0.1045	0.2089	0.3133	0.4175
Discrepancy	-0.1045	-0.2089	-0.3133	-0.4175
95% CI of discrepancy	0.04306 to 0.1659	0.08612 to 0.3317		



	-sample t-			
t, df	t=3.922 df=8	t=3.923 df=8	0.1292 to 0.4975 t=3.924	0.1720 to 0.6630
P value (two tailed)	0.0044	0.0044	df=8	t=3.921 df=8
Significant (alpha=0.05)?	Yes	Yes	0.0044	0.0044
			Yes	Yes
Coefficient of variation	76.49%	76.47%	76.45%	76.51%
Sum	0.9405	1.880	2.820	3.758



190

Appendix D3: One

test analysis of variation of seal thickness with time for Sand suspensions

10 g

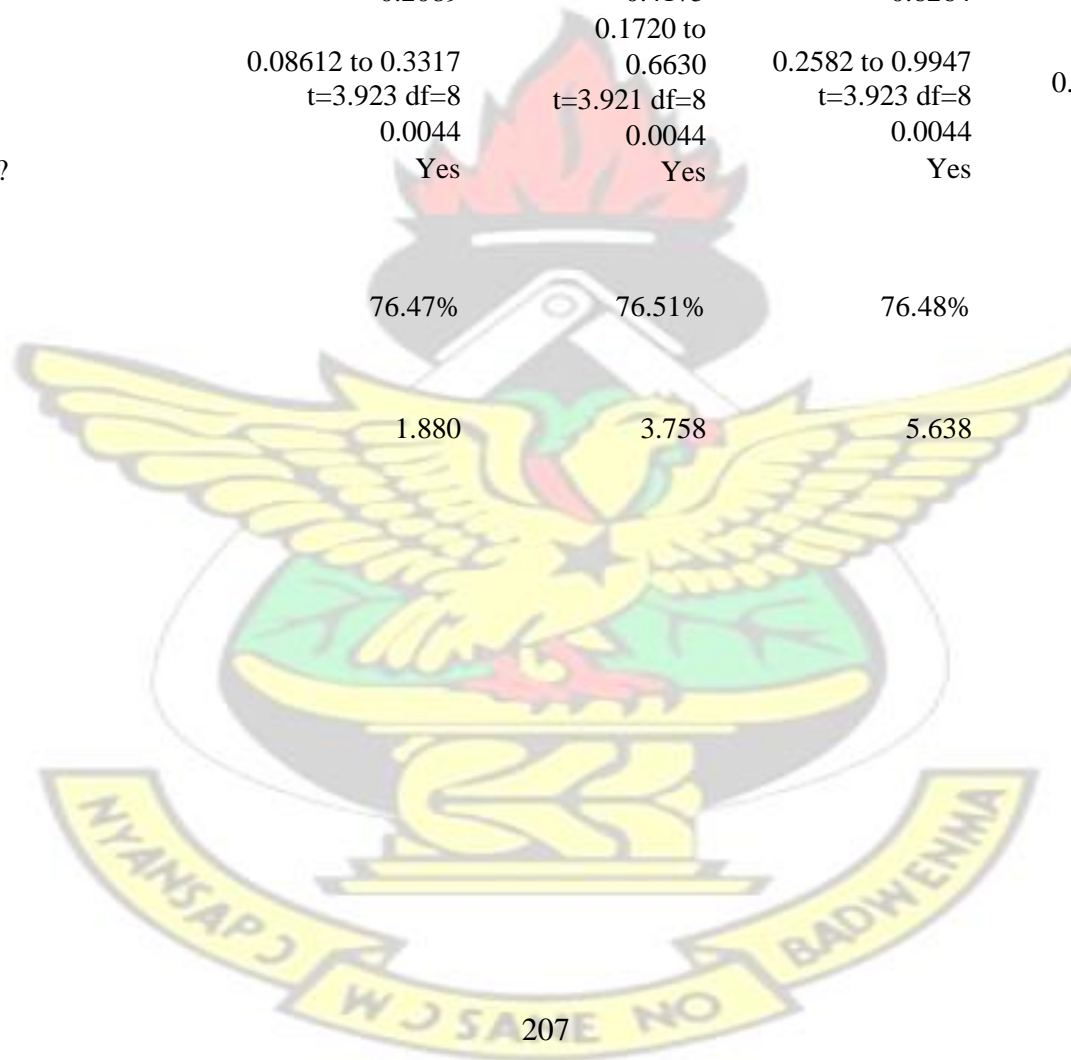
20 g

30g

40 g

KNUST

	-sample t-			
Theoretical mean	0.0	0.0	0.0	0.0
Actual mean	0.2089	0.4175	0.6264	0.8350
Discrepancy	-0.2089	-0.4175	-0.6264	-0.8350
95% CI of discrepancy	0.08612 to 0.3317	0.1720 to 0.6630	0.2582 to 0.9947	0.3439 to 1.326
t, df	t=3.923 df=8	t=3.921 df=8	t=3.923 df=8	t=3.921 df=8
P value (two tailed)	0.0044	0.0044	0.0044	0.0044
Significant (alpha=0.05)?	Yes	Yes	Yes	Yes
Coefficient of variation	76.47%	76.51%	76.48%	76.51%
Sum	1.880	3.758	5.638	7.515



**APPENDIX E: One sample t-test analysis of time-to-incipient ponding in
relation to rainfall rates**

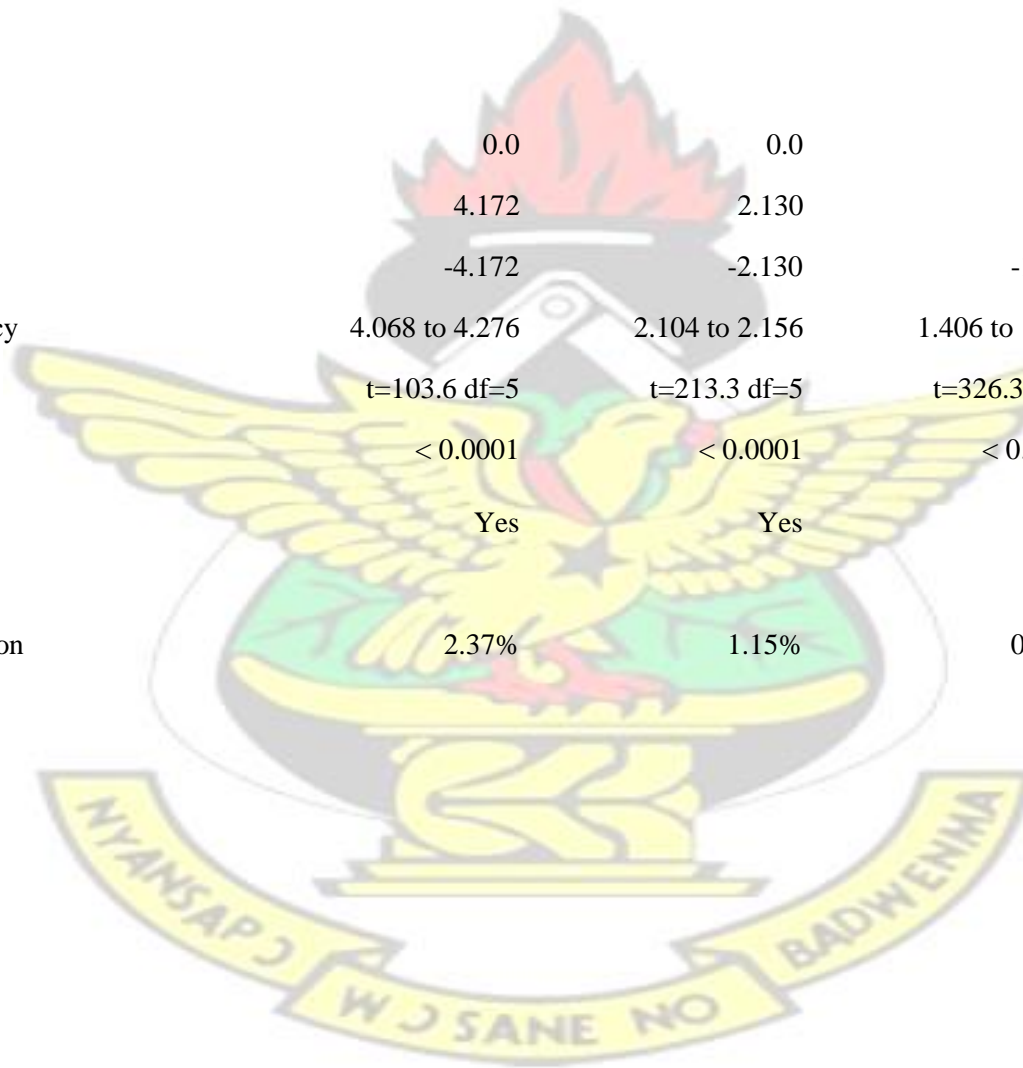
KNUST



KNUST



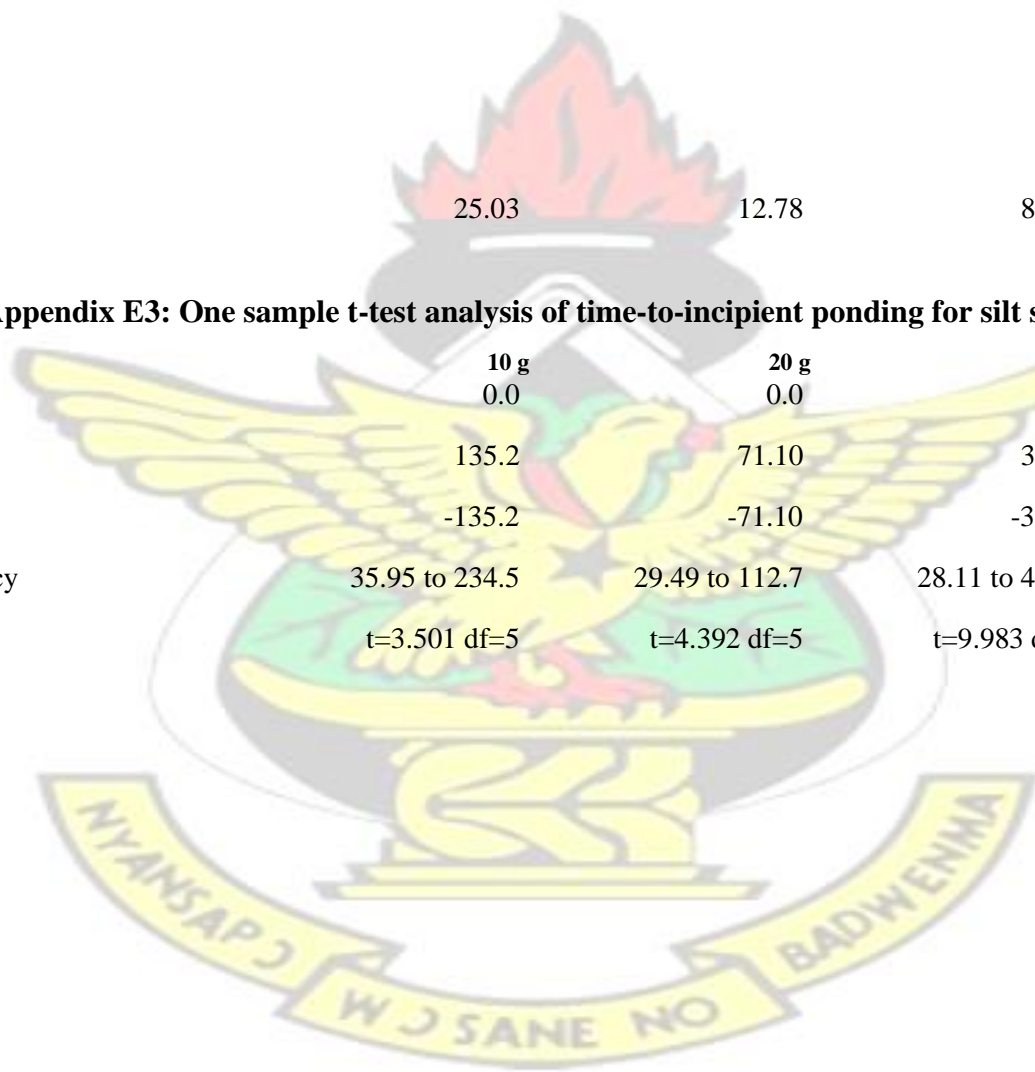
Theoretical mean	0.0	0.0	0.0	0.0
Actual mean	4.172	2.130	1.417	1.063
Discrepancy	-4.172	-2.130	-1.417	-1.063
95% CI of discrepancy	4.068 to 4.276	2.104 to 2.156	1.406 to 1.428	1.057 to 1.069
t, df	t=103.6 df=5	t=213.3 df=5	t=326.3 df=5	t=432.6 df=5
P value (two tailed)	< 0.0001	< 0.0001	< 0.0001	< 0.0001
Significant (alpha=0.05)?	Yes	Yes	Yes	Yes
Coefficient of variation	2.37%	1.15%	0.75%	0.57%



Sum	25.03	12.78	8.501	6.378
-----	-------	-------	-------	-------

Appendix E3: One sample t-test analysis of time-to-incipient ponding for silt suspensions

	10 g	20 g	30 g	40 g
Theoretical mean	0.0	0.0	0.0	0.0
Actual mean	135.2	71.10	37.85	26.01
Discrepancy	-135.2	-71.10	-37.85	-26.01
95% CI of discrepancy	35.95 to 234.5	29.49 to 112.7	28.11 to 47.60	21.74 to 30.29
t, df	t=3.501 df=5	t=4.392 df=5	t=9.983 df=5	t=15.63 df=5



P value (two tailed)	0.0173	0.0071	0.0002	< 0.0001
Significant (alpha=0.05)?	Yes	Yes	Yes	Yes
Coefficient of variation	69.96%	55.77%	24.54%	15.67%
Sum	811.4	426.6	227.1	156.1

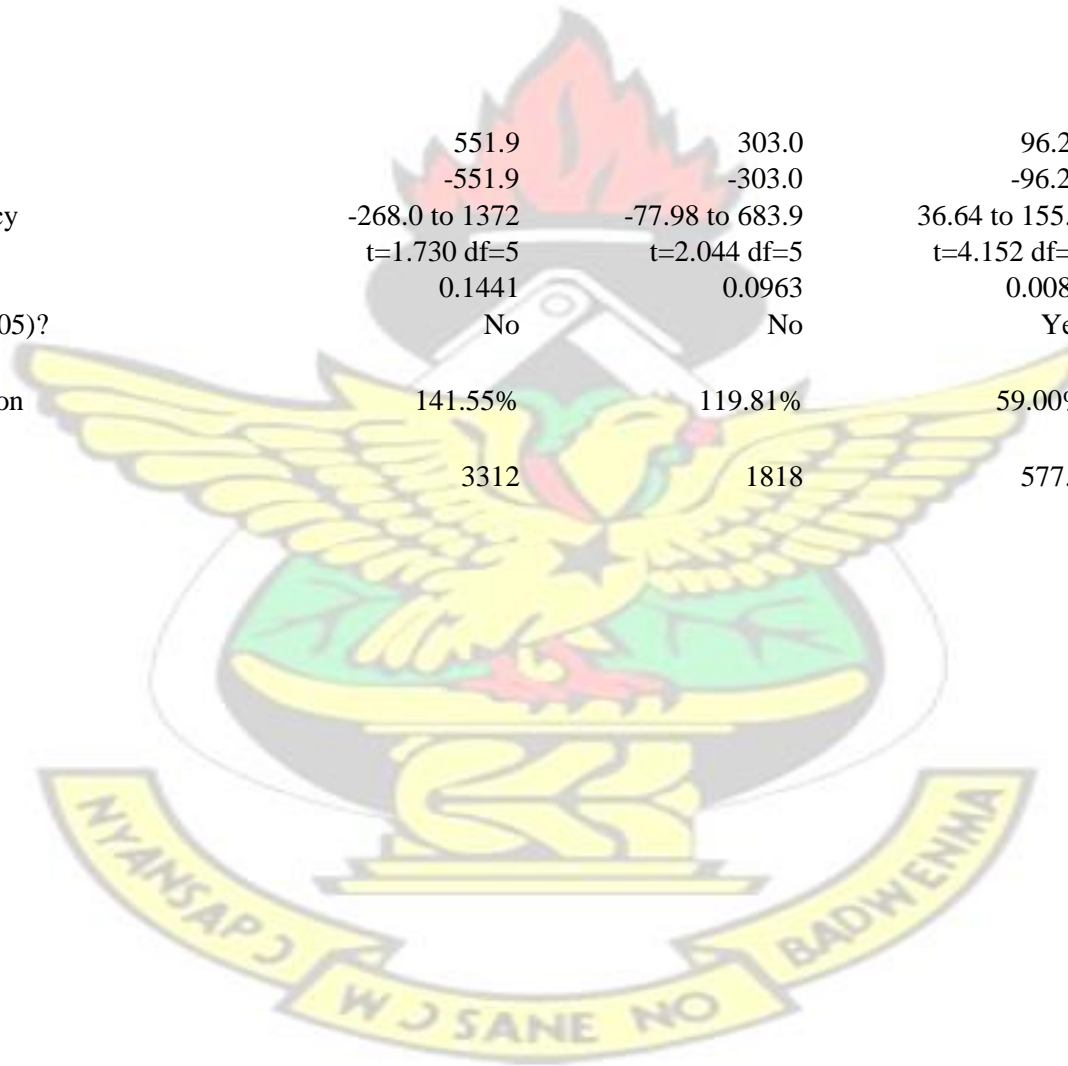
Appendix E4: One sample t-test analysis of time-to-incipient ponding for sand suspensions

	10 g	20 g	30 g	40 g
Theoretical mean	0.0	0.0	0.0	0.0



KNUST

Actual mean	551.9	303.0	96.20	144.0
Discrepancy	-551.9	-303.0	-96.20	-144.0
95% CI of discrepancy	-268.0 to 1372	-77.98 to 683.9	36.64 to 155.8	-37.55 to 325.5
t, df	t=1.730 df=5	t=2.044 df=5	t=4.152 df=5	t=2.039 df=5
P value (two tailed)	0.1441	0.0963	0.0089	0.0970
Significant (alpha=0.05)?	No	No	Yes	No
Coefficient of variation	141.55%	119.81%	59.00%	120.14%
Sum	3312	1818	577.2	863.9



APPENDIX F: Repeated Measures one-way ANOVA analysis and Tukey's

multiple comparisons test of observed and predicted cumulative infiltration amounts

197

KNUST



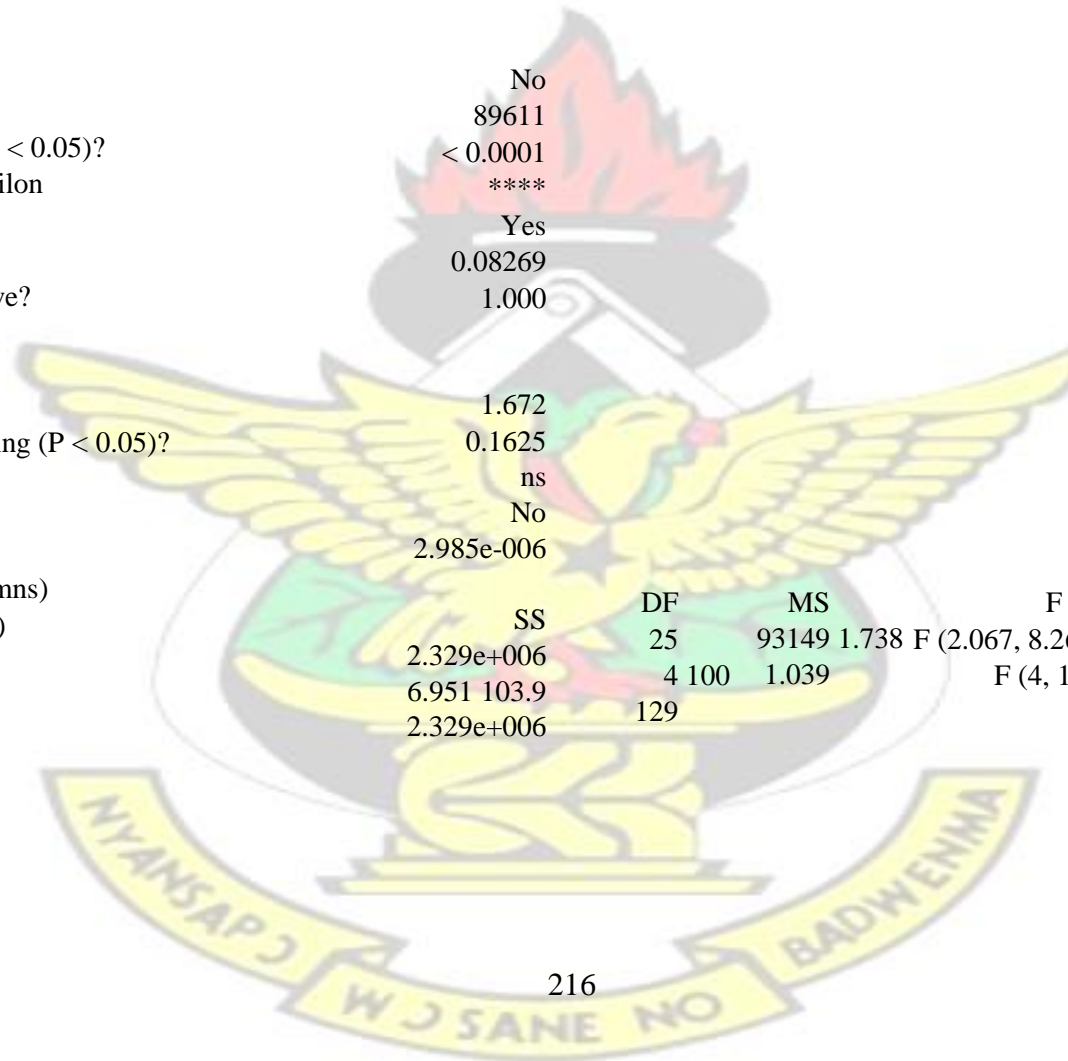
Appendix F1.1: Repeated Measures one-way ANOVA analysis of observed and predicted cumulative infiltration amounts

Repeated measures ANOVA summary Assume sphericity?

F
 P value No
 P value summary 89611
 Statistically significant ($P < 0.05$)? < 0.0001
 Geisser-Greenhouse's epsilon ****
 R square Yes
 0.08269
 Was the matching effective? 1.000

F
 P value
 P value summary 1.672
 Is there significant matching ($P < 0.05$)? 0.1625
 R square ns
 No
 ANOVA table 2.985e-006

Treatment (between columns)	SS	DF	MS	F (DFn, DFd)	P value
Individual (between rows)	2.329e+006	25	93149 1.738	F (2.067, 8.269) = 89611	$P < 0.0001$
Residual (random)	6.951 103.9	4 100	1.039	F (4, 100) = 1.672	$P = 0.1625$
Total	2.329e+006	129			



KNUST

Appendix F1.2: Tukey's Multiple Comparisons test of observed and predicted cumulative infiltration amounts

Number of families 1
 Number of comparisons per family 325
 Alpha 0.05

Tukey's multiple comparisons test	Mean Diff.	95% CI of diff.	Significant?	Summary
10 g sim clay vs. 10 g obs clay	-0.3399	-10.22 to 9.538	No	Ns
10 g sim clay vs. 20 g sim clay	221.9	218.0 to 225.9	Yes	****
10 g sim clay vs. 20 g obs clay	220.9	216.0 to 225.8	Yes	****
10 g sim clay vs. 30 g sim clay	329.4	321.3 to 337.6	Yes	****
10 g sim clay vs. 30 g obs clay	329.0	319.5 to 338.4	Yes	****
10 g sim clay vs. 40 g sim clay	336.5	331.8 to 341.1	Yes	****
10 g sim clay vs. 40 g obs clay	336.0	331.0 to 341.0	Yes	****
10 g sim clay vs. sim clear water	-6.679	-9.814 to -3.544	Yes	**
			Yes	****
			Yes	****
			Yes	****

KNUST

			Yes	****
10 g sim clay vs. obs. clear water	-7.185	-10.08 to -4.286	Yes	**
10 g sim clay vs. 10 g Silt sim	-20.34	-25.23 to -15.45	Yes	***
10 g sim clay vs. 10 g Silt obs.	-21.19	-26.87 to -15.50	Yes	***
10 g sim clay vs. 20 g silt sim	180.8	176.4 to 185.2	Yes	****
10 g sim clay vs. 20 g silt obs.	180.2	174.5 to 185.8	Yes	****
10 g sim clay vs. 30 g silt sim	264.6	260.3 to 268.9	Yes	****
10 g sim clay vs. 30 g silt obs.	263.9	259.2 to 268.7	Yes	****
10 g sim clay vs. 40 g silt sim	273.2	268.3 to 278.1	Yes	****
10 g sim clay vs. 40 g silt obs.	272.9	267.3 to 278.5	Yes	****
10 g sim clay vs. 10 g Sand sim	-33.09	-37.91 to -28.26		
10 g sim clay vs. 10 g Sand obs.	-33.59	-38.89 to -28.29		
10 g sim clay vs. 20 g sand sim	44.65	40.40 to 48.91		
10 g sim clay vs. 20 g sand obs.	44.00	38.11 to 49.89		
10 g sim clay vs. 30 g sand sim	221.2	217.0 to 225.4		
			Yes	****
			Yes	****
			Yes	****

KNUST

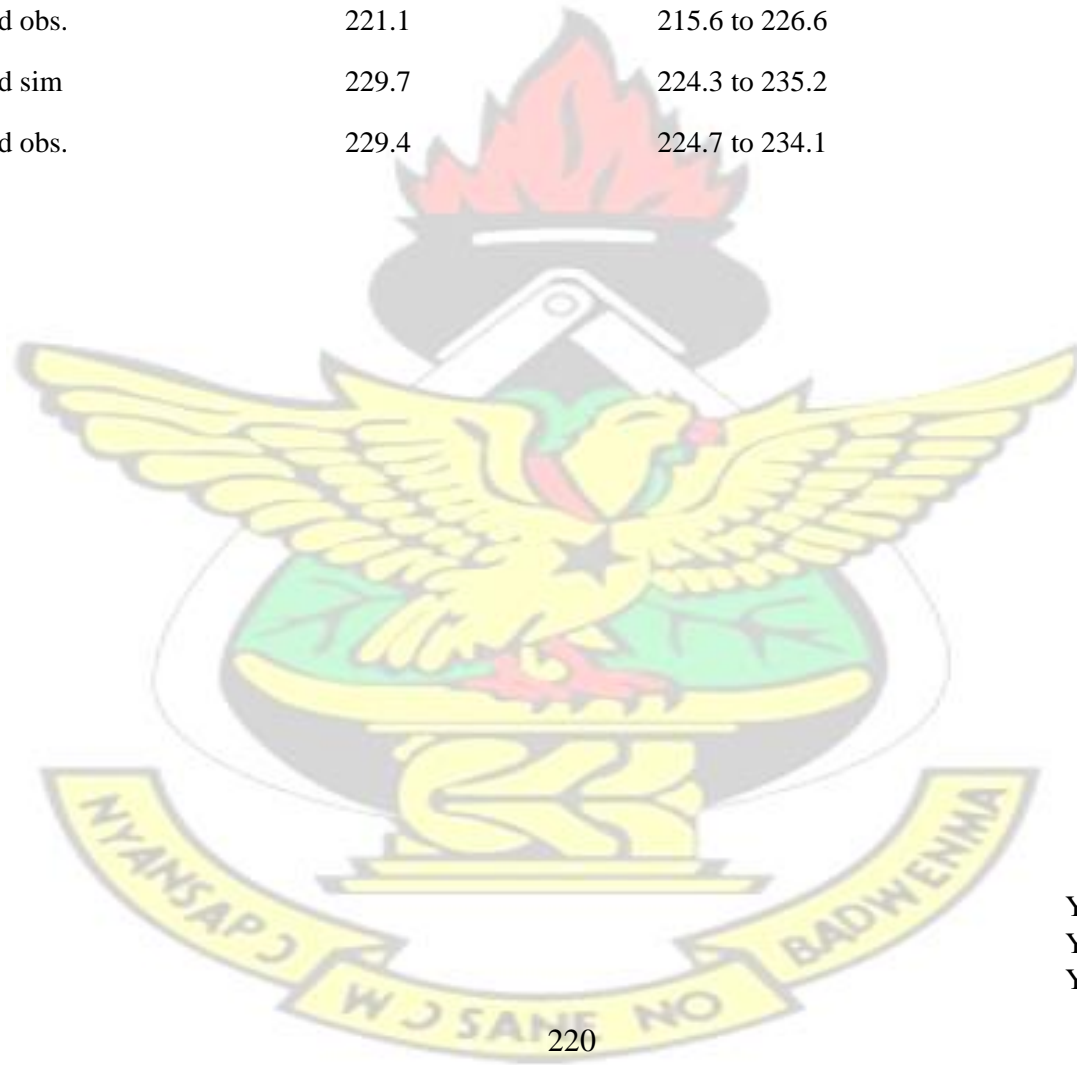
10 g sim clay vs. 30 g sand obs.	220.8	215.5 to 226.0		
10 g sim clay vs. 40 g sand sim	229.4	224.9 to 233.8		
10 g sim clay vs. 40 g sand obs.	229.0	223.7 to 234.4		
10 g obs clay vs. 20 g sim clay	222.3	215.1 to 229.4	Yes	****
10 g obs clay vs. 20 g obs clay	221.3	215.4 to 227.2	Yes	****
10 g obs clay vs. 30 g sim clay	329.8	325.5 to 334.1	Yes	****
10 g obs clay vs. 30 g obs clay	329.3	325.0 to 333.6	Yes	****
10 g obs clay vs. 40 g sim clay	336.8	324.6 to 349.0	Yes	****
10 g obs clay vs. 40 g obs clay	336.4	324.8 to 348.0	Yes	****
10 g obs clay vs. sim clear water	-6.339	-13.76 to 1.085	No	Ns
10 g obs clay vs. obs. clear water	-6.845	-14.30 to 0.6090	No	Ns
10 g obs clay vs. 10 g Silt sim	-20.00	-26.12 to -13.88	Yes	***
10 g obs clay vs. 10 g Silt obs.	-20.85	-27.49 to -14.20	Yes	***
10 g obs clay vs. 20 g silt sim	181.2	174.7 to 187.7	Yes	****
10 g obs clay vs. 20 g silt obs.	180.5	175.3 to 185.7	Yes	****
10 g obs clay vs. 30 g silt sim	264.9	258.7 to 271.2	Yes	****
10 g obs clay vs. 30 g silt obs.	264.3	258.6 to 269.9	Yes	****
10 g obs clay vs. 40 g silt sim	273.5	268.3 to 278.8	Yes	****
10 g obs clay vs. 40 g silt obs.	273.2	268.7 to 277.7	Yes	****
10 g obs clay vs. 10 g Sand sim	-32.75	-38.55 to -26.95	Yes	***
10 g obs clay vs. 10 g Sand obs.	-33.25	-38.65 to -27.86	Yes	****
10 g obs clay vs. 20 g sand sim	44.99	38.74 to 51.24	Yes	****
10 g obs clay vs. 20 g sand obs.	44.34	39.02 to 49.65	Yes	****
			Yes	****
			Yes	****
			Yes	****

KNUST

10 g obs clay vs. 30 g sand sim
 10 g obs clay vs. 30 g sand obs.
 10 g obs clay vs. 40 g sand sim
 10 g obs clay vs. 40 g sand obs.

221.6 215.2 to 227.9
 221.1 215.6 to 226.6
 229.7 224.3 to 235.2
 229.4 224.7 to 234.1

Yes ****
 Yes ****
 Yes ****
 Yes ****
 Yes ****
 Yes ****



Yes ****
 Yes ****
 Yes ****

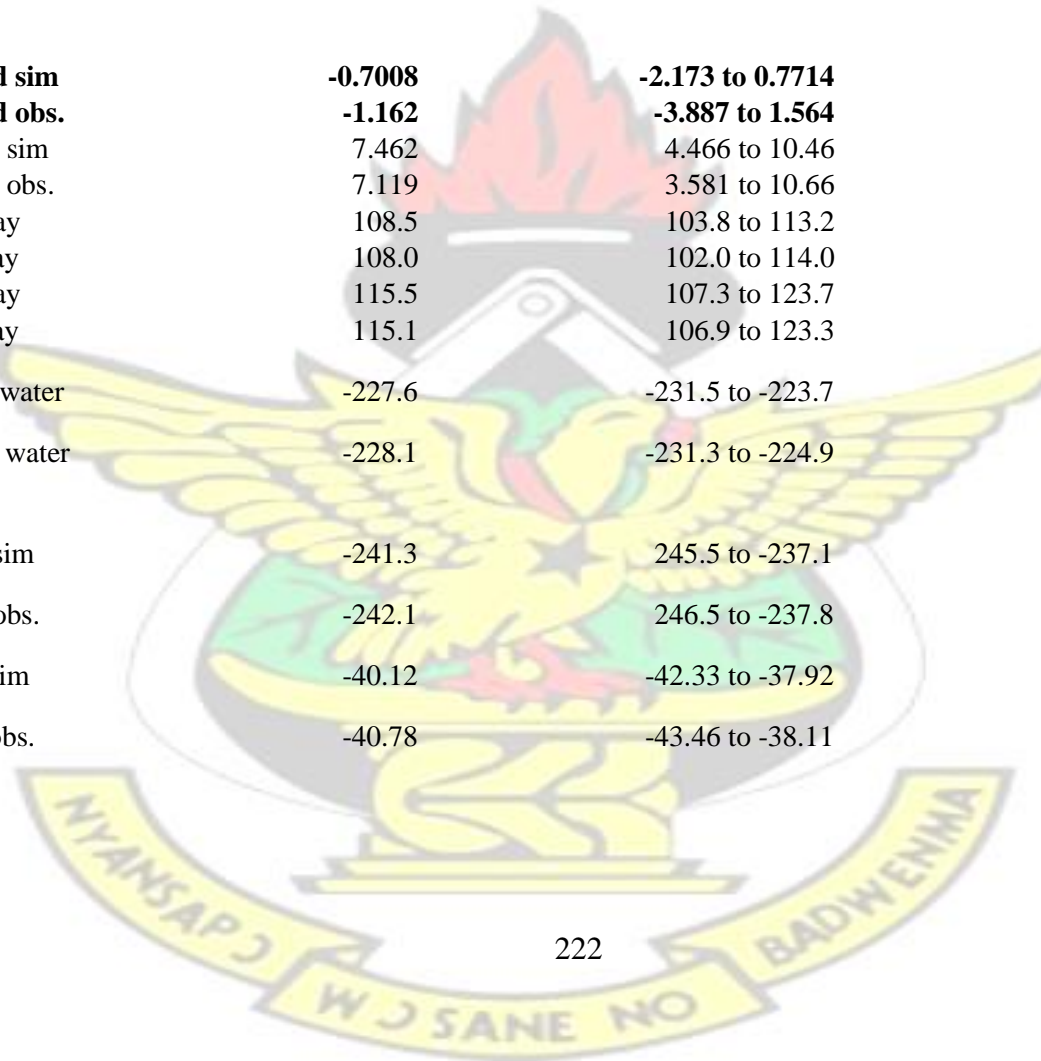
KNUST

	-0.9857	-4.042 to 2.071	No	Ns
20 g sim clay vs. 20 g obs clay				****
20 sim clay vs. 30 sim clay	107.5	102.3 to 112.7	Yes	****
20 sim clay vs. 30 obs clay	107.0	100.6 to 113.4	Yes	****
20 sim clay vs. 40 sim clay	114.5	108.9 to 120.2	Yes	****
20 sim clay vs. 40 obs clay	114.1	108.5 to 119.8	Yes	****
20 sim clay vs. sim clear water	-228.6	-230.7 to -226.5	Yes	****
20 sim clay vs. obs. clear water	-229.1	-230.7 to -227.5	Yes	****
20 sim clay vs. 10 g Silt sim	-242.3	-244.9 to -239.6	Yes	****
20 sim clay vs. 10 g Silt obs.	-243.1	-246.0 to -240.3	Yes	****
20 sim clay vs. 20 g silt sim	-41.11	-45.14 to -37.08	Yes	****
20 sim clay vs. 20 g silt obs.	-41.77	-45.85 to -37.69	Yes	****
20 sim clay vs. 30 g silt sim	42.67	41.21 to 44.13	Yes	****
20 sim clay vs. 30 g silt obs.	42.00	39.01 to 44.98	Yes	****
20 sim clay vs. 40 g silt sim	51.27	48.80 to 53.74	Yes	****
20 sim clay vs. 40 g silt obs.	50.97	47.76 to 54.18	Yes	****
20 sim clay vs. 10 g Sand sim	-255.0	-259.2 to -250.8	Yes	****
20 sim clay vs. 10 g Sand obs.	-255.5	-259.1 to -252.0	Yes	****
20 sim clay vs. 20 g sand sim	-177.3	-179.0 to -175.5	Yes	****
20 sim clay vs. 20 g sand obs.	-177.9	-180.8 to -175.1	Yes	****
			Yes	****
			Yes	****
			Yes	****

KNUST

20 sim clay vs. 30 g sand sim	-0.7008	-2.173 to 0.7714	Yes	****
20 sim clay vs. 30 g sand obs.	-1.162	-3.887 to 1.564	Yes	****
20 sim clay vs. 40 g sand sim	7.462	4.466 to 10.46	Yes	****
20 sim clay vs. 40 g sand obs.	7.119	3.581 to 10.66	Yes	****
20 obs clay vs. 30 sim clay	108.5	103.8 to 113.2	Yes	****
20 obs clay vs. 30 obs clay	108.0	102.0 to 114.0	Yes	****
20 obs clay vs. 40 sim clay	115.5	107.3 to 123.7	Yes	****
20 obs clay vs. 40 obs clay	115.1	106.9 to 123.3	Yes	****
20 obs clay vs. sim clear water	-227.6	-231.5 to -223.7	No	Ns
20 obs clay vs. obs. clear water	-228.1	-231.3 to -224.9	No	Ns
20 obs clay vs. 10 g Silt sim	-241.3	245.5 to -237.1	Yes	**
20 obs clay vs. 10 g Silt obs.	-242.1	246.5 to -237.8	Yes	**
20 obs clay vs. 20 g silt sim	-40.12	-42.33 to -37.92	Yes	****
20 obs clay vs. 20 g silt obs.	-40.78	-43.46 to -38.11	Yes	****

Yes ****
 Yes ****
 Yes ****



KNUST

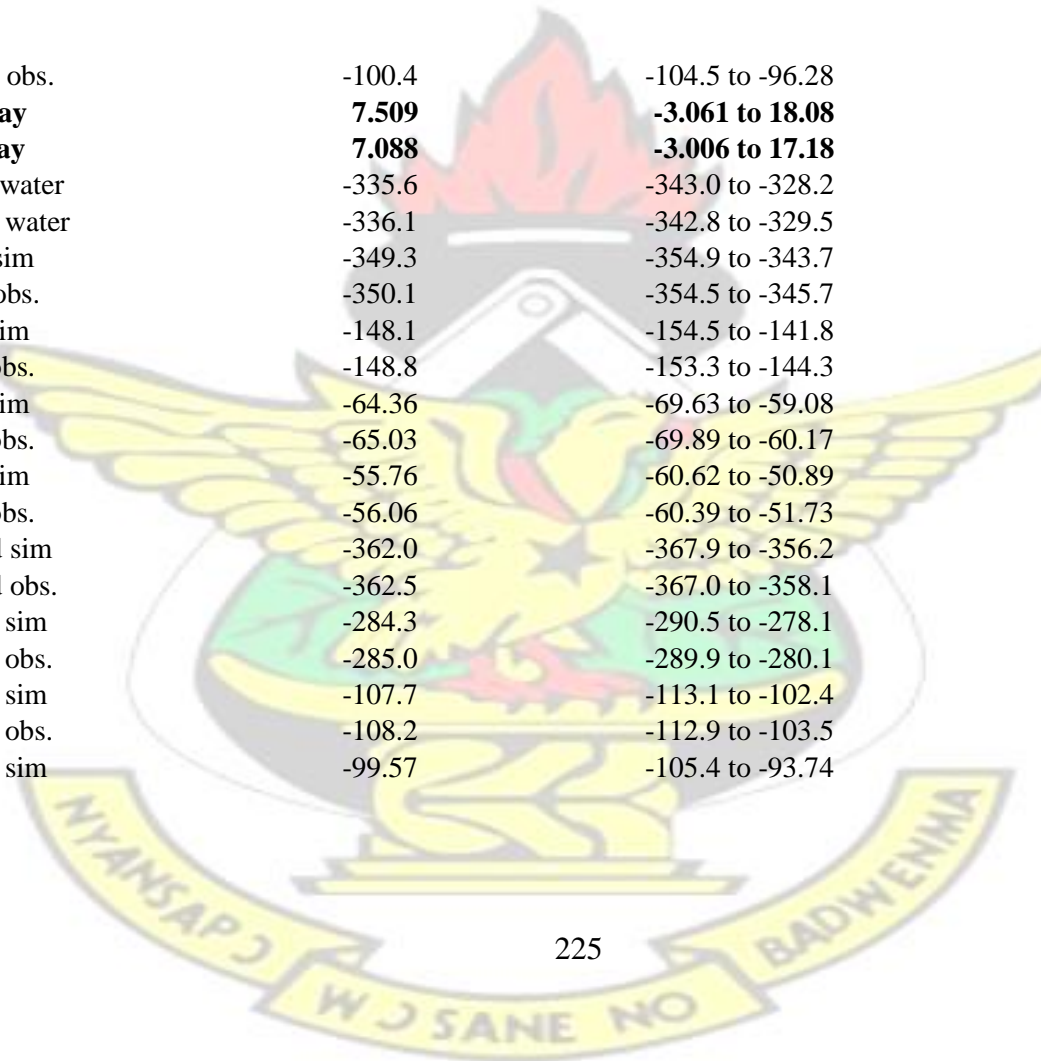
			Yes	****
20 obs clay vs. 30 g silt sim	43.66	41.25 to 46.07		
20 obs clay vs. 30 g silt obs.	42.98	40.03 to 45.94	Yes	****
20 obs clay vs. 40 g silt sim	52.26	50.20 to 54.31	Yes	****
20 obs clay vs. 40 g silt obs.	51.96	49.20 to 54.71	Yes	****
20 obs clay vs. 10 g Sand sim	-254.0	-257.6 to -250.5	Yes	****
20 obs clay vs. 10 g Sand obs.	-254.5	-257.5 to -251.6	Yes	****
20 obs clay vs. 20 g sand sim	-176.3	-179.7 to -172.9	Yes	****
20 obs clay vs. 20 g sand obs.	-176.9	-181.2 to -172.7	Yes	****
20 obs clay vs. 30 g sand sim	0.2850	-2.420 to 2.990	No	Ns
20 obs clay vs. 30 g sand obs.	-0.1760	-3.876 to 3.524	No	Ns
20 obs clay vs. 40 g sand sim	8.448	5.891 to 11.00	Yes	***
20 obs clay vs. 40 g sand obs.	8.105	5.046 to 11.16	Yes	**
30 sim clay vs. 30 obs clay	-0.4846	-1.799 to 0.8300	No	Ns
30 sim clay vs. 40 sim clay	7.024	-2.570 to 16.62	No	Ns
30 sim clay vs. 40 obs clay	6.603	-2.598 to 15.80	No	Ns
30 sim clay vs. sim clear water	-336.1	-342.4 to -329.8	Yes	****
30 sim clay vs. obs. clear water	-336.6	-342.0 to -331.2	Yes	****
30 sim clay vs. 10 g Silt sim	-349.8	-354.4 to -345.1	Yes	****
30 sim clay vs. 10 g Silt obs.	-350.6	-354.1 to -347.2	Yes	****

KNUST

			Yes	****
30 sim clay vs. 20 g silt sim	-148.6	-153.7 to -143.5	Yes	****
30 sim clay vs. 20 g silt obs.	-149.3	-152.6 to -146.0	Yes	****
30 sim clay vs. 30 g silt sim	-64.84	-68.87 to -60.81	Yes	****
30 sim clay vs. 30 g silt obs.	-65.52	-69.20 to -61.83	Yes	****
30 sim clay vs. 40 g silt sim	-56.24	-59.87 to -52.62		
30 sim clay vs. 40 g silt obs.	-56.54	-59.74 to -53.34		
30 sim clay vs. 10 g Sand sim	-362.5	367.4 to -357.7		
30 sim clay vs. 10 g Sand obs.	-363.0	366.3 to -359.8		
30 sim clay vs. 20 g sand sim	-284.8	-289.9 to -279.6		
30 sim clay vs. 20 g sand obs.	-285.4	-289.5 to -281.4		
30 sim clay vs. 30 g sand sim	-108.2	-112.4 to -104.1		
30 sim clay vs. 30 g sand obs.	-108.7	-112.3 to -105.0	Yes	****
30 sim clay vs. 40 g sand sim	-100.1	-104.7 to -95.39	Yes	****
			Yes	****
			Yes	****
			Yes	****

KNUST

30 sim clay vs. 40 g sand obs.	-100.4	-104.5 to -96.28	Yes	****
30 obs clay vs. 40 sim clay	7.509	-3.061 to 18.08	Yes	****
30 obs clay vs. 40 obs clay	7.088	-3.006 to 17.18	Yes	****
30 obs clay vs. sim clear water	-335.6	-343.0 to -328.2	Yes	****
30 obs clay vs. obs. clear water	-336.1	-342.8 to -329.5	Yes	****
30 obs clay vs. 10 g Silt sim	-349.3	-354.9 to -343.7	Yes	****
30 obs clay vs. 10 g Silt obs.	-350.1	-354.5 to -345.7	Yes	****
30 obs clay vs. 20 g silt sim	-148.1	-154.5 to -141.8	Yes	****
30 obs clay vs. 20 g silt obs.	-148.8	-153.3 to -144.3	Yes	****
30 obs clay vs. 30 g silt sim	-64.36	-69.63 to -59.08	Yes	****
30 obs clay vs. 30 g silt obs.	-65.03	-69.89 to -60.17	Yes	****
30 obs clay vs. 40 g silt sim	-55.76	-60.62 to -50.89	Yes	****
30 obs clay vs. 40 g silt obs.	-56.06	-60.39 to -51.73	Yes	****
30 obs clay vs. 10 g Sand sim	-362.0	-367.9 to -356.2	Yes	****
30 obs clay vs. 10 g Sand obs.	-362.5	-367.0 to -358.1	Yes	****
30 obs clay vs. 20 g sand sim	-284.3	-290.5 to -278.1	Yes	****
30 obs clay vs. 20 g sand obs.	-285.0	-289.9 to -280.1	Yes	****
30 obs clay vs. 30 g sand sim	-107.7	-113.1 to -102.4	Yes	****
30 obs clay vs. 30 g sand obs.	-108.2	-112.9 to -103.5	Yes	****
30 obs clay vs. 40 g sand sim	-99.57	-105.4 to -93.74	Yes	****

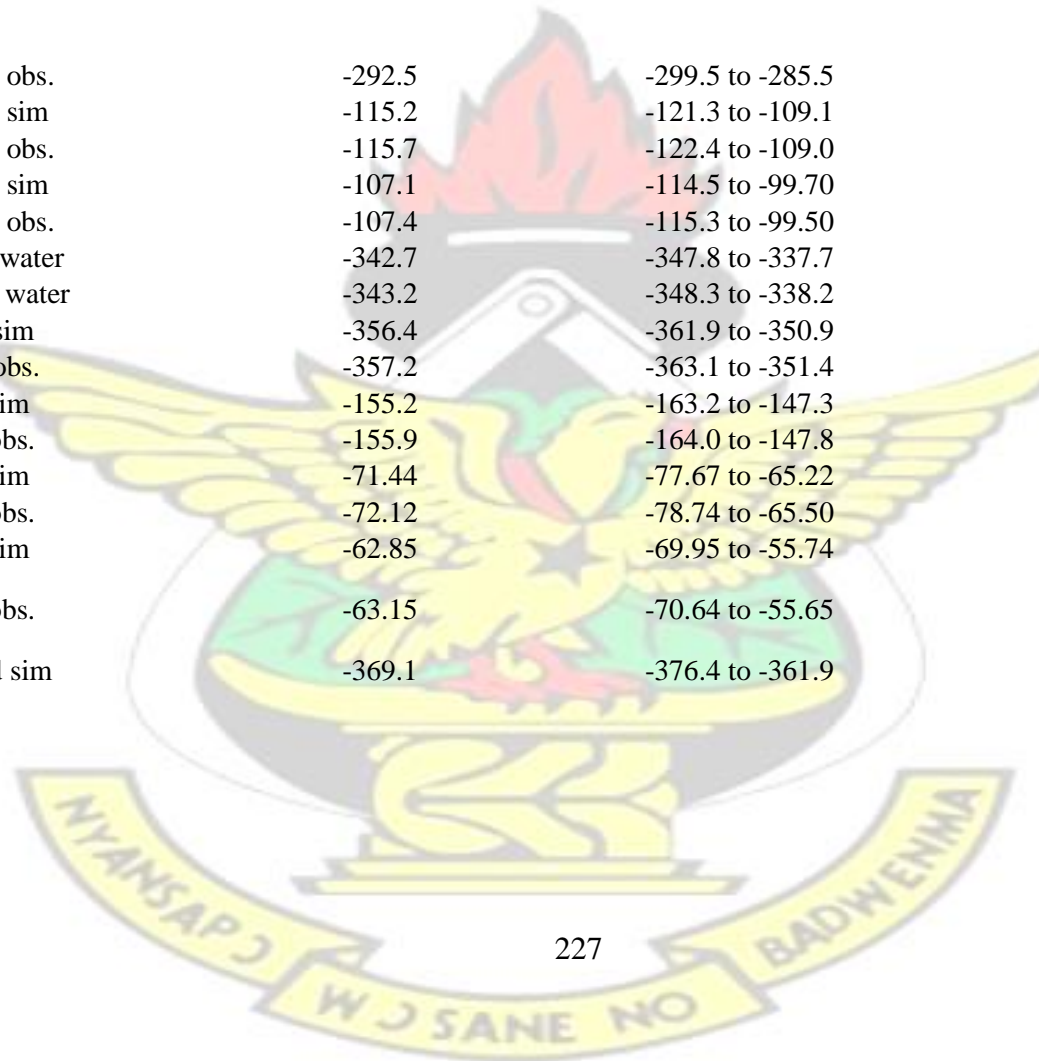


KNUST

			Yes	****
30 obs clay vs. 40 g sand obs.	-99.91	-105.1 to -94.74	Yes	****
40 sim clay vs. 40 obs clay	-0.4206	-1.839 to 0.9978	No	Ns
40 sim clay vs. sim clear water	-343.1	348.5 to -337.8		
40 sim clay vs. obs. clear water	-343.6	348.8 to -338.5		
40 sim clay vs. 10 g Silt sim	-356.8	-362.9 to -350.7		
40 sim clay vs. 10 g Silt obs.	-357.7	-363.8 to -351.5		
40 sim clay vs. 20 g silt sim	-155.6	-163.6 to -147.7		
40 sim clay vs. 20 g silt obs.	-156.3	-164.7 to -147.9	Yes	****
40 sim clay vs. 30 g silt sim	-71.86	-78.24 to -65.49	Yes	****
40 sim clay vs. 30 g silt obs.	-72.54	-79.53 to -65.55	Yes	****
40 sim clay vs. 40 g silt sim	-63.27	-70.64 to -55.90	Yes	****
40 sim clay vs. 40 g silt obs.	-63.57	-71.48 to -55.66	Yes	****
40 sim clay vs. 10 g Sand sim	-369.6	-377.2 to -361.9	Yes	****
40 sim clay vs. 10 g Sand obs.	-370.1	-377.7 to -362.4	Yes	****
40 sim clay vs. 20 g sand sim	-291.8	-298.0 to -285.6	Yes	****
			Yes	****
			Yes	****
			Yes	****

KNUST

			Yes	****
40 sim clay vs. 20 g sand obs.	-292.5	-299.5 to -285.5	Yes	****
40 sim clay vs. 30 g sand sim	-115.2	-121.3 to -109.1	Yes	****
40 sim clay vs. 30 g sand obs.	-115.7	-122.4 to -109.0	Yes	****
40 sim clay vs. 40 g sand sim	-107.1	-114.5 to -99.70	Yes	****
40 sim clay vs. 40 g sand obs.	-107.4	-115.3 to -99.50	Yes	****
40 obs clay vs. sim clear water	-342.7	-347.8 to -337.7	Yes	****
40 obs clay vs. obs. clear water	-343.2	-348.3 to -338.2	Yes	****
40 obs clay vs. 10 g Silt sim	-356.4	-361.9 to -350.9	Yes	****
40 obs clay vs. 10 g Silt obs.	-357.2	-363.1 to -351.4	Yes	****
40 obs clay vs. 20 g silt sim	-155.2	-163.2 to -147.3	Yes	****
40 obs clay vs. 20 g silt obs.	-155.9	-164.0 to -147.8	Yes	****
40 obs clay vs. 30 g silt sim	-71.44	-77.67 to -65.22	Yes	****
40 obs clay vs. 30 g silt obs.	-72.12	-78.74 to -65.50	Yes	****
40 obs clay vs. 40 g silt sim	-62.85	-69.95 to -55.74	Yes	****
40 obs clay vs. 40 g silt obs.	-63.15	-70.64 to -55.65		
40 obs clay vs. 10 g Sand sim	-369.1	-376.4 to -361.9		



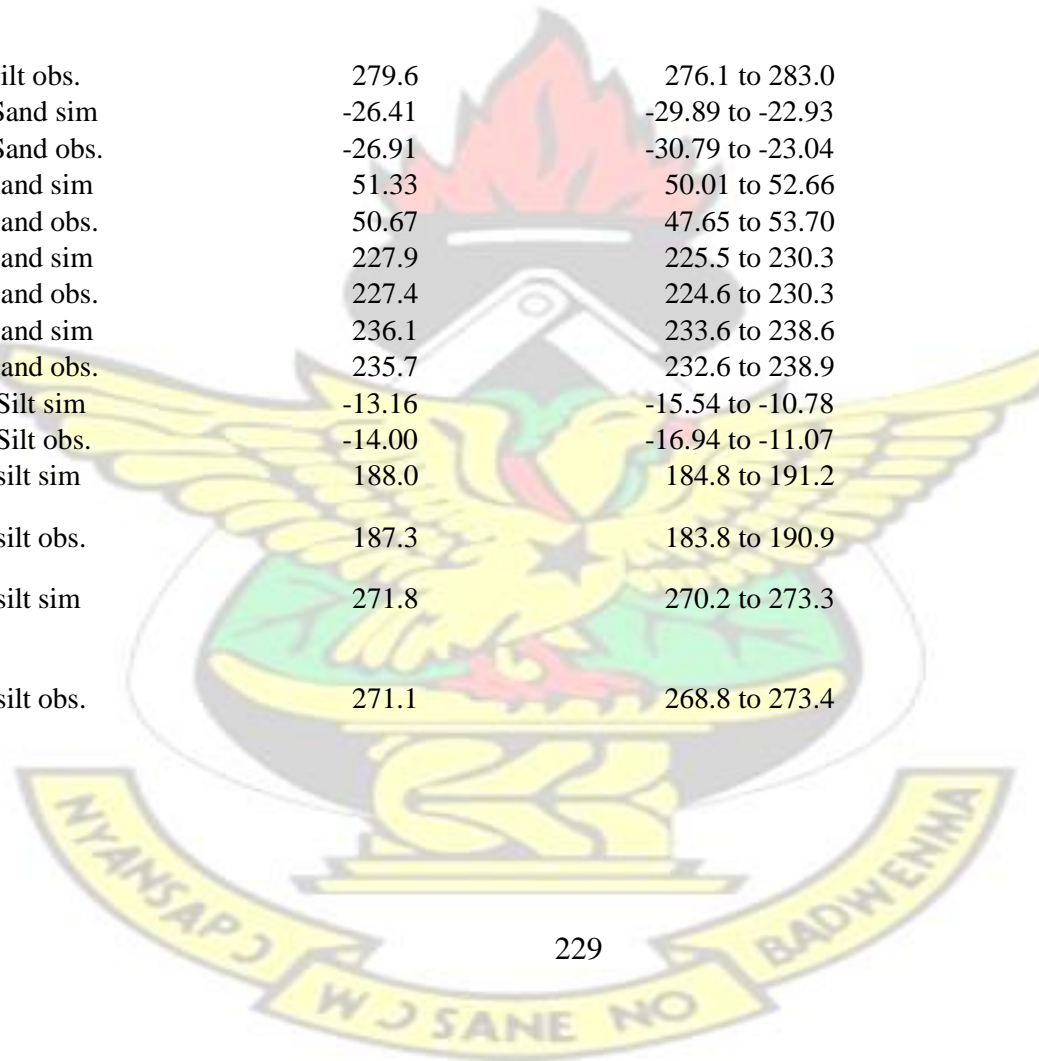
KNUST

			Yes	****
40 obs clay vs. 10 g Sand obs.	-369.6	376.9 to -362.3		
40 obs clay vs. 20 g sand sim	-291.4	297.2 to -285.6		
40 obs clay vs. 20 g sand obs.	-292.0	-298.4 to -285.7		
40 obs clay vs. 30 g sand sim	-114.8	-120.7 to -108.9		
40 obs clay vs. 30 g sand obs.	-115.3	-121.5 to -109.1		
40 obs clay vs. 40 g sand sim	-106.7	-113.7 to -99.64	Yes	****
40 obs clay vs. 40 g sand obs.	-107.0	-114.4 to -99.57	Yes	****
sim clear water vs. obs. clear water	-0.5057	-2.208 to 1.196	No	Ns
sim clear water vs. 10 g Silt sim	-13.66	-15.86 to -11.47	Yes	****
sim clear water vs. 10 g Silt obs.	-14.51	-18.48 to -10.54	Yes	***
sim clear water vs. 20 g silt sim	187.5	183.4 to 191.6	Yes	****
sim clear water vs. 20 g silt obs.	186.8	182.4 to 191.3	Yes	****
sim clear water vs. 30 g silt sim	271.3	268.7 to 273.9	Yes	****
sim clear water vs. 30 g silt obs.	270.6	267.5 to 273.7	Yes	****
sim clear water vs. 40 g silt sim	279.9	276.9 to 282.8	Yes	****
			Yes	****
			Yes	****
			Yes	****

KNUST

sim clear water vs. 40 g silt obs.	279.6	276.1 to 283.0	Yes	****
sim clear water vs. 10 g Sand sim	-26.41	-29.89 to -22.93	Yes	****
sim clear water vs. 10 g Sand obs.	-26.91	-30.79 to -23.04	Yes	****
sim clear water vs. 20 g sand sim	51.33	50.01 to 52.66	Yes	****
sim clear water vs. 20 g sand obs.	50.67	47.65 to 53.70	Yes	****
sim clear water vs. 30 g sand sim	227.9	225.5 to 230.3	Yes	****
sim clear water vs. 30 g sand obs.	227.4	224.6 to 230.3	Yes	****
sim clear water vs. 40 g sand sim	236.1	233.6 to 238.6	Yes	****
sim clear water vs. 40 g sand obs.	235.7	232.6 to 238.9	Yes	****
obs. clear water vs. 10 g Silt sim	-13.16	-15.54 to -10.78	Yes	***
obs. clear water vs. 10 g Silt obs.	-14.00	-16.94 to -11.07	Yes	***
obs. clear water vs. 20 g silt sim	188.0	184.8 to 191.2		
obs. clear water vs. 20 g silt obs.	187.3	183.8 to 190.9		
obs. clear water vs. 30 g silt sim	271.8	270.2 to 273.3		
obs. clear water vs. 30 g silt obs.	271.1	268.8 to 273.4		

Yes ****
 Yes ****
 Yes ****



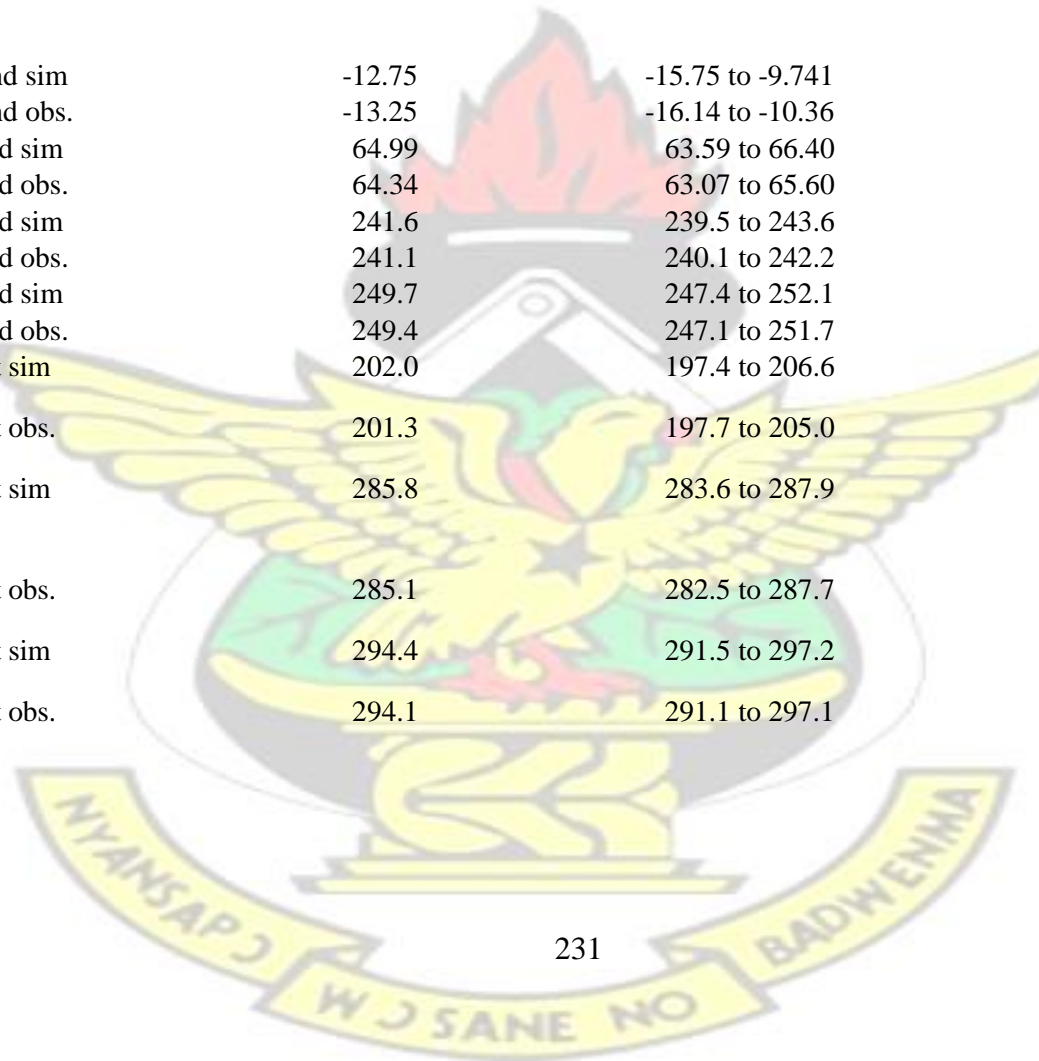
KNUST

			Yes	****
obs. clear water vs. 40 g silt sim	280.4	278.0 to 282.7		
obs. clear water vs. 40 g silt obs.	280.1	277.0 to 283.1		
obs. clear water vs. 10 g Sand sim	-25.90	-29.08 to -22.73		
obs. clear water vs. 10 g Sand obs.	-26.41	-29.34 to -23.47		
obs. clear water vs. 20 g sand sim	51.84	49.90 to 53.78	Yes	****
obs. clear water vs. 20 g sand obs.	51.18	47.97 to 54.39	Yes	****
obs. clear water vs. 30 g sand sim	228.4	227.1 to 229.7	Yes	****
obs. clear water vs. 30 g sand obs.	227.9	225.5 to 230.4	Yes	****
obs. clear water vs. 40 g sand sim	236.6	234.1 to 239.0	Yes	****
obs. clear water vs. 40 g sand obs.	236.2	233.1 to 239.3	Yes	****
10 g Silt sim vs. 10 g Silt obs.	-0.8449	-3.439 to 1.749	No	Ns
10 g Silt sim vs. 20 g silt sim	201.2	196.9 to 205.5	Yes	****
10 g Silt sim vs. 20 g silt obs.	200.5	196.8 to 204.2	Yes	****
10 g Silt sim vs. 30 g silt sim	284.9	282.7 to 287.2	Yes	****
10 g Silt sim vs. 30 g silt obs.	284.3	282.1 to 286.4	Yes	****
10 g Silt sim vs. 40 g silt sim	293.5	291.2 to 295.9	Yes	****
10 g Silt sim vs. 40 g silt obs.	293.2	290.9 to 295.6	Yes	****
			Yes	****
			Yes	****
			Yes	****

KNUST

10 g Silt sim vs. 10 g Sand sim	-12.75	-15.75 to -9.741	Yes	****
10 g Silt sim vs. 10 g Sand obs.	-13.25	-16.14 to -10.36	Yes	****
10 g Silt sim vs. 20 g sand sim	64.99	63.59 to 66.40	Yes	****
10 g Silt sim vs. 20 g sand obs.	64.34	63.07 to 65.60	Yes	****
10 g Silt sim vs. 30 g sand sim	241.6	239.5 to 243.6	Yes	****
10 g Silt sim vs. 30 g sand obs.	241.1	240.1 to 242.2	Yes	****
10 g Silt sim vs. 40 g sand sim	249.7	247.4 to 252.1	Yes	****
10 g Silt sim vs. 40 g sand obs.	249.4	247.1 to 251.7	Yes	****
10 g Silt obs. vs. 20 g silt sim	202.0	197.4 to 206.6		
10 g Silt obs. vs. 20 g silt obs.	201.3	197.7 to 205.0		
10 g Silt obs. vs. 30 g silt sim	285.8	283.6 to 287.9		
10 g Silt obs. vs. 30 g silt obs.	285.1	282.5 to 287.7		
10 g Silt obs. vs. 40 g silt sim	294.4	291.5 to 297.2		
10 g Silt obs. vs. 40 g silt obs.	294.1	291.1 to 297.1		

Yes ****
 Yes ****
 Yes ****

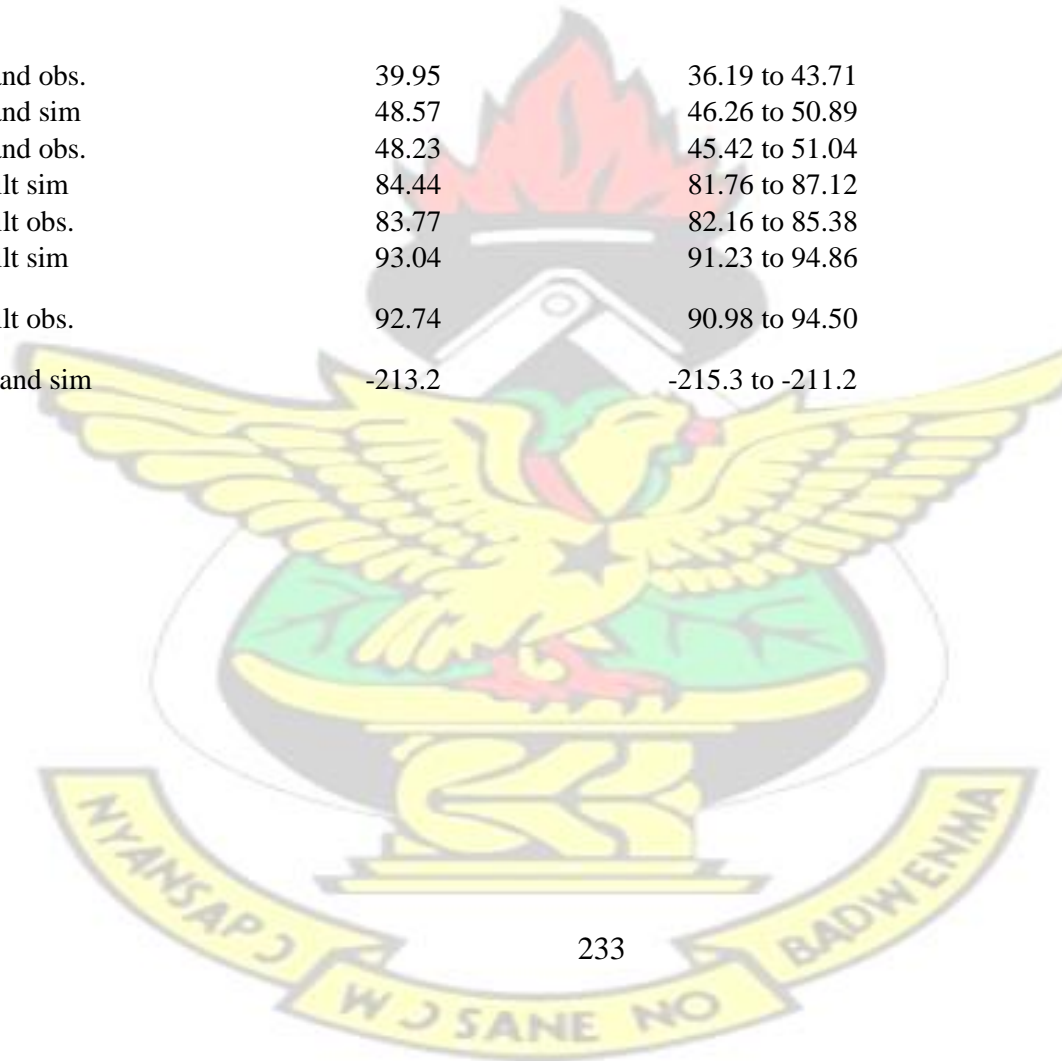


KNUST

			Yes	****
10 g Silt obs. vs. 10 g Sand sim	-11.90	-16.12 to -7.682		***
10 g Silt obs. vs. 10 g Sand obs.	-12.41	-15.27 to -9.543		***
10 g Silt obs. vs. 20 g sand sim	65.84	62.63 to 69.05	Yes	****
10 g Silt obs. vs. 20 g sand obs.	65.18	62.57 to 67.80	Yes	****
10 g Silt obs. vs. 30 g sand sim	242.4	240.4 to 244.4	Yes	****
10 g Silt obs. vs. 30 g sand obs.	242.0	239.9 to 244.1	Yes	****
10 g Silt obs. vs. 40 g sand sim	250.6	246.8 to 254.4	Yes	****
10 g Silt obs. vs. 40 g sand obs.	250.2	246.5 to 254.0	Yes	****
20 g silt sim vs. 20 g silt obs.	-0.6596	-2.547 to 1.228	No	Ns
20 g silt sim vs. 30 g silt sim	83.78	80.77 to 86.80	Yes	****
20 g silt sim vs. 30 g silt obs.	83.11	80.67 to 85.55	Yes	****
20 g silt sim vs. 40 g silt sim	92.38	89.94 to 94.82	Yes	****
20 g silt sim vs. 40 g silt obs.	92.08	89.19 to 94.97	Yes	****
20 g silt sim vs. 10 g Sand sim	-213.9	-216.2 to -211.6	Yes	****
20 g silt sim vs. 10 g Sand obs.	-214.4	-216.7 to -212.1	Yes	****
20 g silt sim vs. 20 g sand sim	-136.2	-140.1 to -132.2	Yes	****
20 g silt sim vs. 20 g sand obs.	-136.8	-141.6 to -132.0	Yes	****
20 g silt sim vs. 30 g sand sim	40.41	37.31 to 43.51	Yes	****
			Yes	****
			Yes	****
			Yes	****

KNUST

20 g silt sim vs. 30 g sand obs.	39.95	36.19 to 43.71	Yes	****
20 g silt sim vs. 40 g sand sim	48.57	46.26 to 50.89	Yes	****
20 g silt sim vs. 40 g sand obs.	48.23	45.42 to 51.04	Yes	****
20 g silt obs. vs. 30 g silt sim	84.44	81.76 to 87.12	Yes	****
20 g silt obs. vs. 30 g silt obs.	83.77	82.16 to 85.38	Yes	****
20 g silt obs. vs. 40 g silt sim	93.04	91.23 to 94.86	Yes	****
20 g silt obs. vs. 40 g silt obs.	92.74	90.98 to 94.50		
20 g silt obs. vs. 10 g Sand sim	-213.2	-215.3 to -211.2		



Yes ****
 Yes ****
 Yes ****

KNUST

			Yes	****
20 g silt obs. vs. 10 g Sand obs.	-213.7	-214.7 to -212.8		
20 g silt obs. vs. 20 g sand sim	-135.5	-139.3 to -131.7		
20 g silt obs. vs. 20 g sand obs.	-136.2	-140.1 to -132.2		
20 g silt obs. vs. 30 g sand sim	41.07	38.30 to 43.84		
20 g silt obs. vs. 30 g sand obs.	40.61	37.79 to 43.43		
20 g silt obs. vs. 40 g sand sim	49.23	46.93 to 51.53	Yes	****
20 g silt obs. vs. 40 g sand obs.	48.89	46.74 to 51.04	Yes	****
30 g silt sim vs. 30 g silt obs.	-0.6743	-2.355 to 1.007	No	Ns
30 g silt sim vs. 40 g silt sim	8.598	7.346 to 9.850	Yes	****
30 g silt sim vs. 40 g silt obs.	8.298	6.276 to 10.32	Yes	***
30 g silt sim vs. 10 g Sand sim	-297.7	-300.8 to -294.6	Yes	****
30 g silt sim vs. 10 g Sand obs.	-298.2	-300.3 to -296.0	Yes	****
30 g silt sim vs. 20 g sand sim	-219.9	-221.9 to -218.0	Yes	****
30 g silt sim vs. 20 g sand obs.	-220.6	-223.1 to -218.1	Yes	****
30 g silt sim vs. 30 g sand sim	-43.37	-43.73 to -43.01	Yes	****

KNUST

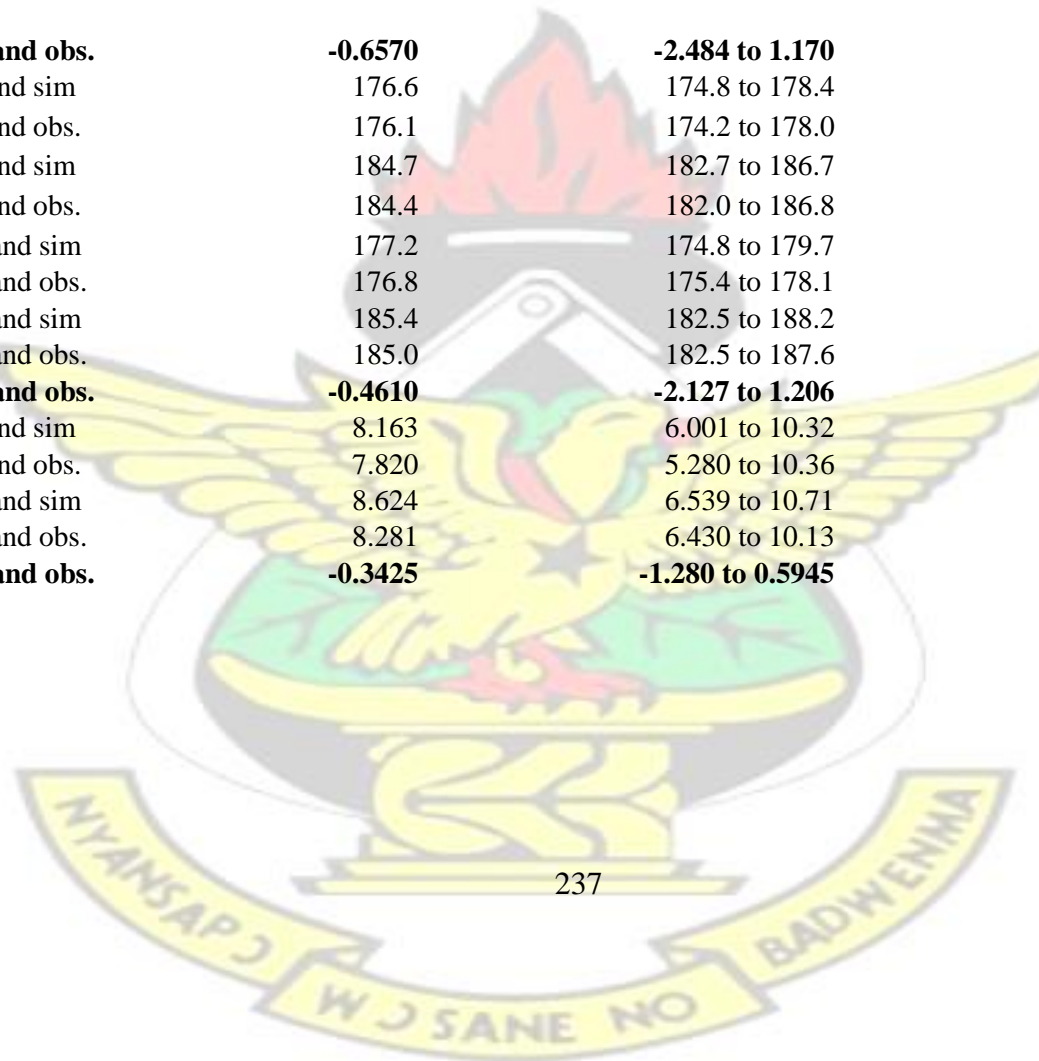
			Yes	****
30 g silt sim vs. 30 g sand obs.	-43.83	-45.67 to -42.00	Yes	****
30 g silt sim vs. 40 g sand sim	-35.21	-37.39 to -33.04	Yes	****
30 g silt sim vs. 40 g sand obs.	-35.55	-38.11 to -33.00	Yes	****
30 g silt obs. vs. 40 g silt sim	9.272	8.110 to 10.43	Yes	****
30 g silt obs. vs. 40 g silt obs.	8.972	7.700 to 10.24	Yes	****
30 g silt obs. vs. 10 g Sand sim	-297.0	-298.7 to -295.3	Yes	****
30 g silt obs. vs. 10 g Sand obs.	-297.5	-298.3 to -296.7	Yes	****
30 g silt obs. vs. 20 g sand sim	-219.3	-221.8 to -216.8	Yes	****
30 g silt obs. vs. 20 g sand obs.	-219.9	-222.6 to -217.2	Yes	****
30 g silt obs. vs. 30 g sand sim	-42.70	-44.28 to -41.12	Yes	****
30 g silt obs. vs. 30 g sand obs.	-43.16	-44.58 to -41.73	Yes	****
30 g silt obs. vs. 40 g sand sim	-34.54	-36.09 to -32.98	Yes	****
30 g silt obs. vs. 40 g sand obs.	-34.88	-36.44 to -33.32	Yes	****
40 g silt sim vs. 40 g silt obs.	-0.2996	-1.233 to 0.6342	No	Ns
40 g silt sim vs. 10 g Sand sim	-306.3	-308.6 to -304.0		
40 g silt sim vs. 10 g Sand obs.	-306.8	-308.2 to -305.3		
40 g silt sim vs. 20 g sand sim	-228.5	-230.7 to -226.4		
40 g silt sim vs. 20 g sand obs.	-229.2	-231.7 to -226.7		
40 g silt sim vs. 30 g sand sim	-51.97	-53.36 to -50.58		

KNUST

40 g silt sim vs. 30 g sand obs.	-52.43	-54.11 to -50.75	Yes	****
40 g silt sim vs. 40 g sand sim	-43.81	-45.13 to -42.49	Yes	****
40 g silt sim vs. 40 g sand obs.	-44.15	-45.63 to -42.67	Yes	****
40 g silt obs. vs. 10 g Sand sim	-306.0	-308.1 to -303.9	Yes	****
40 g silt obs. vs. 10 g Sand obs.	-306.5	-307.9 to -305.1	Yes	****
40 g silt obs. vs. 20 g sand sim	-228.2	-230.7 to -225.8	Yes	****
40 g silt obs. vs. 20 g sand obs.	-228.9	-231.2 to -226.6	Yes	****
40 g silt obs. vs. 30 g sand sim	-51.67	-53.76 to -49.59	Yes	****
40 g silt obs. vs. 30 g sand obs.	-52.13	-53.64 to -50.62	Yes	****
40 g silt obs. vs. 40 g sand sim	-43.51	-45.01 to -42.01	Yes	****
40 g silt obs. vs. 40 g sand obs.	-43.85	-44.87 to -42.83	Yes	****
10 g Sand sim vs. 10 g Sand obs.	-0.5041	-2.369 to 1.361	No	Ns
10 g Sand sim vs. 20 g sand sim	77.74	74.53 to 80.96	Yes	****
10 g Sand sim vs. 20 g sand obs.	77.08	73.39 to 80.78	Yes	****
10 g Sand sim vs. 30 g sand sim	254.3	251.3 to 257.3	Yes	****
10 g Sand sim vs. 30 g sand obs.	253.9	251.2 to 256.5	Yes	****
10 g Sand sim vs. 40 g sand sim	262.5	261.0 to 264.0	Yes	****
10 g Sand sim vs. 40 g sand obs.	262.1	260.6 to 263.6	Yes	****
10 g Sand obs. vs. 20 g sand sim	78.25	75.04 to 81.45	Yes	****
10 g Sand obs. vs. 20 g sand obs.	77.59	74.37 to 80.80	Yes	****
10 g Sand obs. vs. 30 g sand sim	254.8	252.7 to 257.0	Yes	****
10 g Sand obs. vs. 30 g sand obs.	254.4	252.4 to 256.4	Yes	****
10 g Sand obs. vs. 40 g sand sim	263.0	261.0 to 265.0	Yes	****
10 g Sand obs. vs. 40 g sand obs.	262.6	260.8 to 264.5	Yes	****

KNUST

			Yes	****
20 g sand sim vs. 20 g sand obs.	-0.6570	-2.484 to 1.170	No	Ns
20 g sand sim vs. 30 g sand sim	176.6	174.8 to 178.4	Yes	
20 g sand sim vs. 30 g sand obs.	176.1	174.2 to 178.0	Yes	
20 g sand sim vs. 40 g sand sim	184.7	182.7 to 186.7	Yes	
20 g sand sim vs. 40 g sand obs.	184.4	182.0 to 186.8	Yes	
20 g sand obs. vs. 30 g sand sim	177.2	174.8 to 179.7	Yes	****
20 g sand obs. vs. 30 g sand obs.	176.8	175.4 to 178.1	Yes	****
20 g sand obs. vs. 40 g sand sim	185.4	182.5 to 188.2	Yes	****
20 g sand obs. vs. 40 g sand obs.	185.0	182.5 to 187.6	Yes	****
30 g sand sim vs. 30 g sand obs.	-0.4610	-2.127 to 1.206	No	Ns
30 g sand sim vs. 40 g sand sim	8.163	6.001 to 10.32	Yes	***
30 g sand sim vs. 40 g sand obs.	7.820	5.280 to 10.36	Yes	***
30 g sand obs. vs. 40 g sand sim	8.624	6.539 to 10.71	Yes	***
30 g sand obs. vs. 40 g sand obs.	8.281	6.430 to 10.13	Yes	***
40 g sand sim vs. 40 g sand obs.	-0.3425	-1.280 to 0.5945	No	Ns



KNUST



**APPENDIX G: Paired t-test analysis of measured vs predicted cumulative
infiltration amount**

Appendix : Summary of paired t-test analyses of cumulative infiltration

Table Analyzed

KNUST

**G1
amount for observed clear water vs. model predicted value**

	Paired t test data
Column J	clear water: Observed
vs.	vs.
Column I	clear water: Simulated
Paired t test	
P value	0.1103
P value summary	ns
Significantly different? (P < 0.05)	No
One- or two-tailed P value?	Two-tailed
t, df	t=2.045 df=4
Number of pairs	5
How big is the difference?	
Mean of differences	0.5057

Appendix : Summary of paired t-test analyses of cumulative infiltration

Table Analyzed

KNUST

SD of differences	0.5529
SEM of differences	0.2473
95% confidence interval	-0.1808 to 1.192
R squared	0.5112
How effective was the pairing?	
Correlation coefficient (r)	0.7961
P value (one tailed)	0.0536
P value summary	ns
Was the pairing significantly effective?	No

**G2
amount for observed 10 g clay suspension vs. model predicted value**

	Paired t test data
Column B	10g clay: Observed
vs.	vs.

Appendix : Summary of paired t-test analyses of cumulative infiltration

Table Analyzed

KNUST

Column A	10 g clay: Simulated
Paired t test	
P value	0.8244
P value summary	Ns
Significantly different? (P < 0.05)	No
One- or two-tailed P value?	Two-tailed
t, df	t=0.2369 df=4
Number of pairs	5
How big is the difference?	
Mean of differences	0.3399
SD of differences	3.209
SEM of differences	1.435
95% confidence interval	-3.644 to 4.324
R squared	0.01383

Appendix : Summary of paired t-test analyses of cumulative infiltration

Table Analyzed

KNUST

How effective was the pairing?

Correlation coefficient (r)	-0.8424
P value (one tailed)	0.0367
P value summary	*
Was the pairing significantly effective?	Yes

G3

amount for observed 20 g clay suspension vs. model predicted value

	Paired t test data
Column D	20 g clay: Observed
vs.	vs.
Column C	20 g clay: Simulated
Paired t test	
P value	0.0906
P value summary	ns
Significantly different? (P < 0.05)	No

Appendix : Summary of paired t-test analyses of cumulative infiltration

Table Analyzed

KNUST

One- or two-tailed P value?	Two-tailed
t, df	t=2.220 df=4
Number of pairs	5
How big is the difference?	
Mean of differences	0.9857
SD of differences	0.9928
SEM of differences	0.4440
95% confidence interval	-0.2469 to 2.218
R squared	0.5520
How effective was the pairing?	
Correlation coefficient (r)	0.4831
P value (one tailed)	0.2049
P value summary	ns
Was the pairing significantly effective?	No

Appendix : Summary of paired t-test analyses of cumulative infiltration

Table Analyzed

KNUST

**G4
amount for observed 30 g clay suspension vs. model predicted value**

	Paired t test data
Column F	30 g clay: Observed
vs.	vs.
Column E	30 g clay: Simulated
Paired t test	
P value	0.0641
P value summary	Ns
Significantly different? ($P < 0.05$)	No
One- or two-tailed P value?	Two-tailed
t, df	t=2.538 df=4
Number of pairs	5
How big is the difference?	

Appendix : Summary of paired t-test analyses of cumulative infiltration

Table Analyzed

KNUST

Mean of differences	0.4846
SD of differences	0.4270
SEM of differences	0.1910
95% confidence interval	-0.04557 to 1.015
R squared	0.6169
How effective was the pairing?	
Correlation coefficient (r)	0.9881
P value (one tailed)	0.0008
P value summary	***
Was the pairing significantly effective?	Yes

**G5
amount for observed 40 g clay suspension vs. model predicted value**

Paired t test data

Column H 40 g clay: Observed vs. vs.

Appendix : Summary of paired t-test analyses of cumulative infiltration

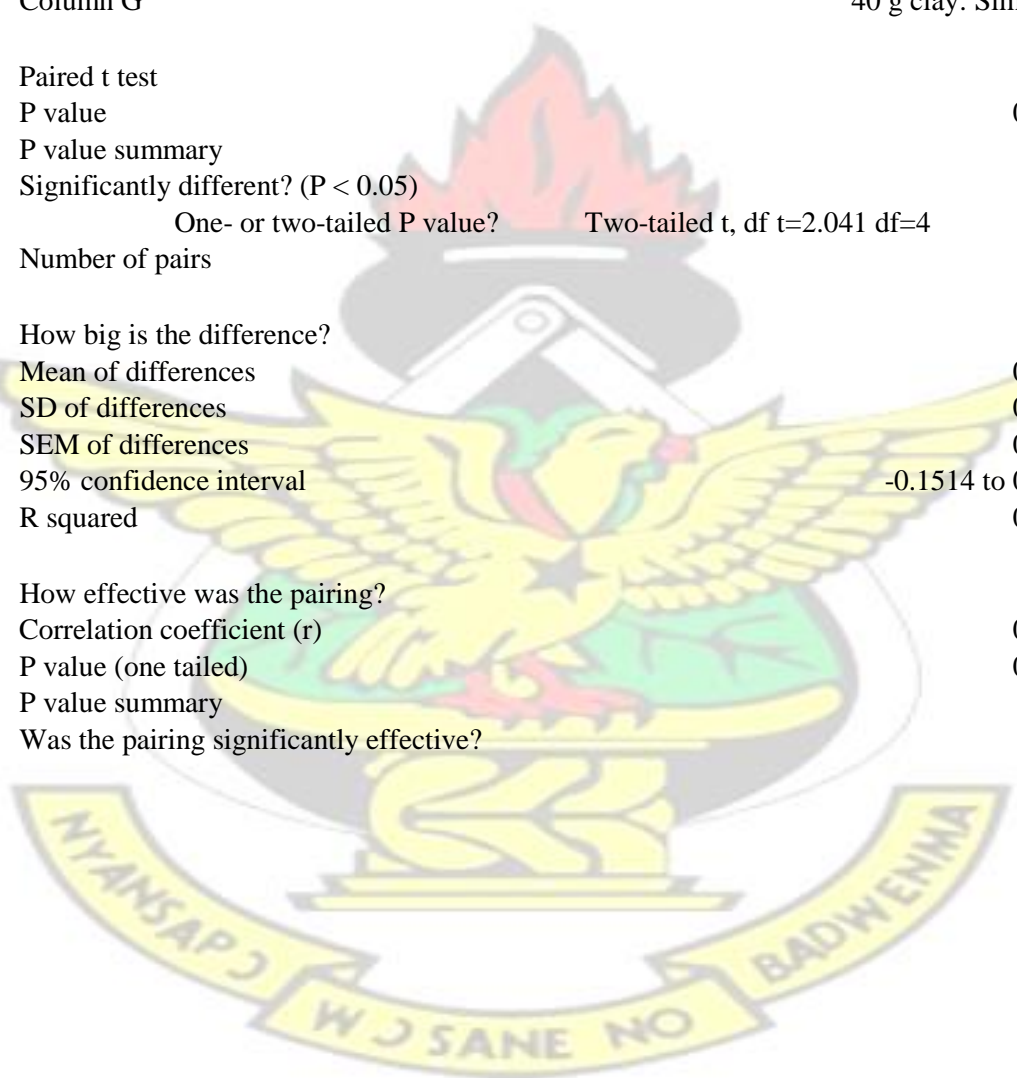
Table Analyzed

KNUST

Column G

40 g clay: Simulated

Paired t test	
P value	0.1108
P value summary	Ns
Significantly different? (P < 0.05)	No
One- or two-tailed P value?	Two-tailed t, df t=2.041 df=4
Number of pairs	5
How big is the difference?	
Mean of differences	0.4206
SD of differences	0.4607
SEM of differences	0.2060
95% confidence interval	-0.1514 to 0.9926
R squared	0.5102
How effective was the pairing?	
Correlation coefficient (r)	0.9801
P value (one tailed)	0.0017
P value summary	**
Was the pairing significantly effective?	Yes



Appendix : Summary of paired t-test analyses of cumulative infiltration

Table Analyzed

KNUST

**G6
amount for observed 10 g silt suspension vs. model predicted value**

	Paired t test data
Column L	10 g Silt: Observed
vs.	vs.
Column K	10 g Silt: Simulated
Paired t test	
P value	0.0884
P value summary	ns
Significantly different? (P < 0.05)	No
One- or two-tailed P value?	Two-tailed
t, df	t=2.242 df=4
Number of pairs	5
How big is the difference?	
Mean of differences	0.8449

Appendix : Summary of paired t-test analyses of cumulative infiltration

Table Analyzed

KNUST

SD of differences	0.8426
SEM of differences	0.3768
95% confidence interval	-0.2014 to 1.891
R squared	0.5569
How effective was the pairing?	
Correlation coefficient (r)	0.3612
P value (one tailed)	0.2752
P value summary	ns
Was the pairing significantly effective?	No

G7
amount for observed 20 g silt suspension vs. model predicted value

Paired t test data

Column N

20 g silt: Observed

Appendix : Summary of paired t-test analyses of cumulative infiltration

Table Analyzed

KNUST

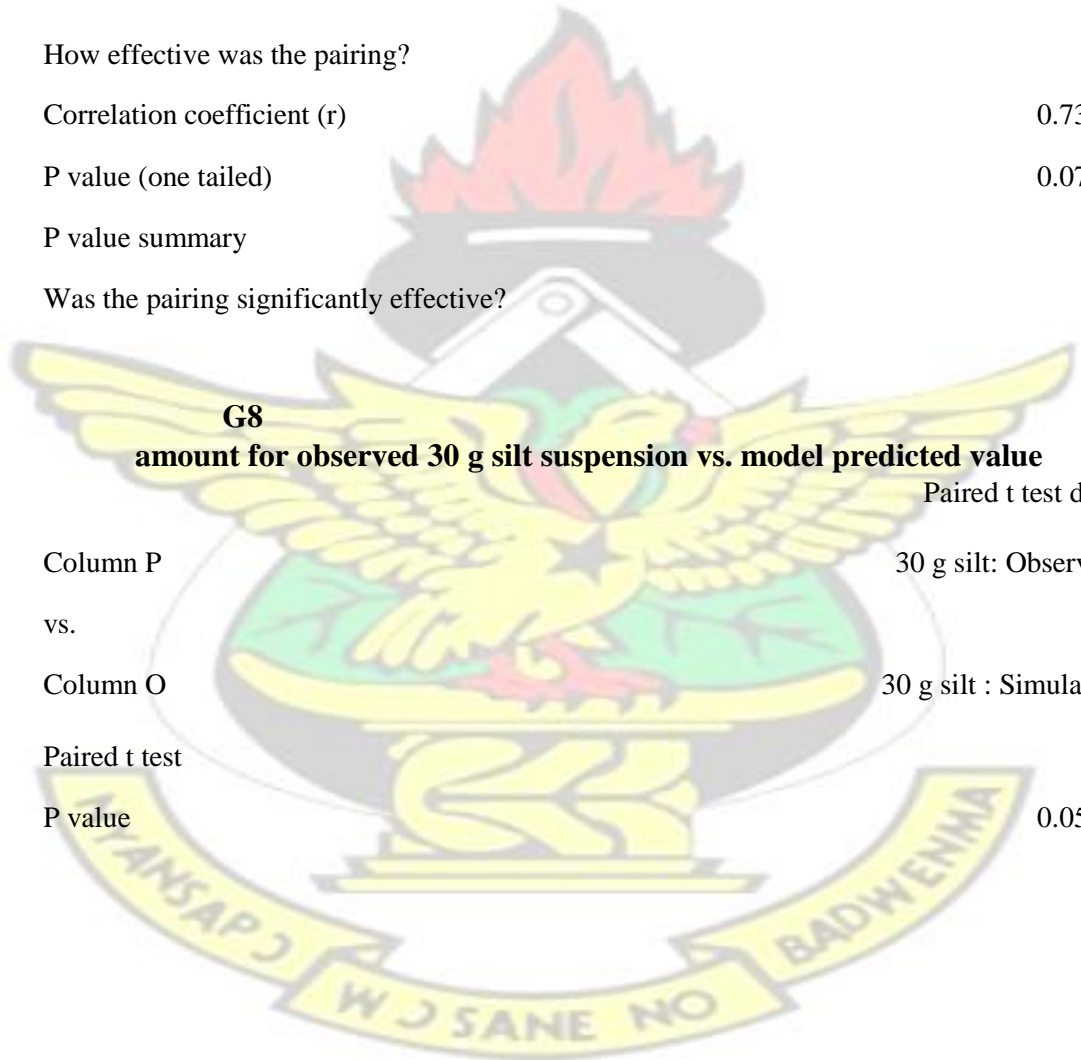
vs.	vs.
Column M	20 g silt : Simulated
Paired t test	
P value	0.0739
P value summary	ns
Significantly different? (P < 0.05)	No
One- or two-tailed P value?	Two-tailed
t, df	t=2.406 df=4
Number of pairs	5
How big is the difference?	
Mean of differences	0.6596
SD of differences	0.6131
SEM of differences	0.2742
95% confidence interval	-0.1017 to 1.421

Appendix : Summary of paired t-test analyses of cumulative infiltration

Table Analyzed

KNUST

R squared	0.5913
How effective was the pairing?	
Correlation coefficient (r)	0.7356
P value (one tailed)	0.0783
P value summary	ns
Was the pairing significantly effective?	No



G8 amount for observed 30 g silt suspension vs. model predicted value

	Paired t test data
Column P	30 g silt: Observed
vs.	vs.
Column O	30 g silt : Simulated
Paired t test	
P value	0.0508

Appendix : Summary of paired t-test analyses of cumulative infiltration

Table Analyzed

KNUST

P value summary	Ns
Significantly different? (P < 0.05)	No
One- or two-tailed P value?	Two-tailed
t, df	t=2.762 df=4
Number of pairs	5
How big is the difference?	
Mean of differences	0.6743
SD of differences	0.5459
SEM of differences	0.2441
95% confidence interval	-0.003598 to 1.352
R squared	0.6560
How effective was the pairing?	
Correlation coefficient (r)	0.2725
P value (one tailed)	0.3287

Appendix : Summary of paired t-test analyses of cumulative infiltration

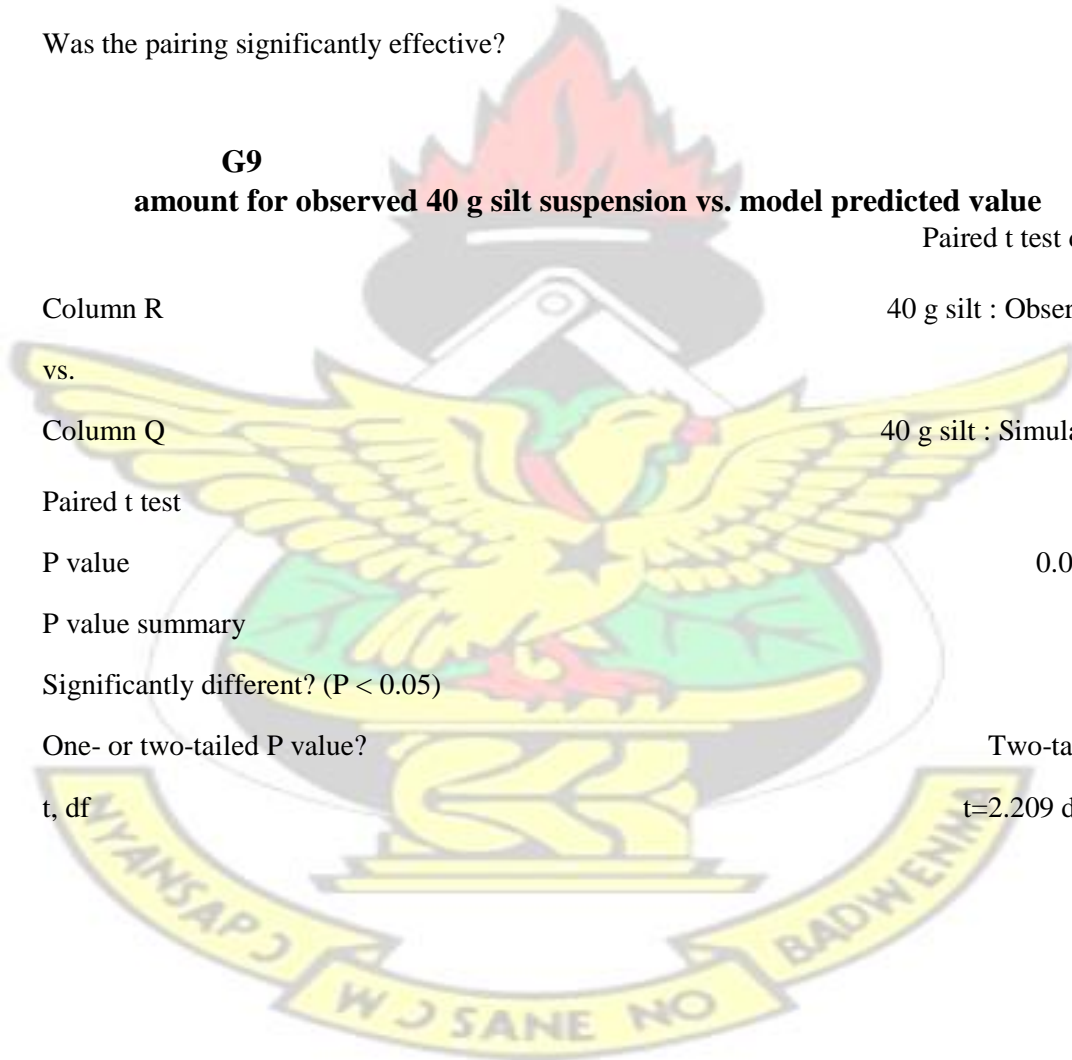
Table Analyzed

KNUST

P value summary ns
 Was the pairing significantly effective? No

**G9
 amount for observed 40 g silt suspension vs. model predicted value**

Paired t test data
 Column R 40 g silt : Observed
 vs. vs.
 Column Q 40 g silt : Simulated
 Paired t test
 P value 0.0918
 P value summary Ns
 Significantly different? (P < 0.05) No
 One- or two-tailed P value? Two-tailed
 t, df t=2.209 df=4



Appendix : Summary of paired t-test analyses of cumulative infiltration

Table Analyzed

KNUST

Number of pairs	5
How big is the difference?	
Mean of differences	0.2996
SD of differences	0.3033
SEM of differences	0.1356
95% confidence interval	-0.07702 to 0.6762
R squared	0.5495
How effective was the pairing?	
Correlation coefficient (r)	0.6538
P value (one tailed)	0.1157
P value summary	ns
Was the pairing significantly effective?	No

G10
amount for observed 10 g sand suspension vs. model predicted value

Appendix : Summary of paired t-test analyses of cumulative infiltration

Table Analyzed

KNUST

	Paired t test data
Column T	10 g Sand: Observed
vs.	vs.
Column S	10 g Sand: Simulated
Paired t test	
P value	0.1363
P value summary	Ns
Significantly different? ($P < 0.05$)	No
One- or two-tailed P value?	Two-tailed
t, df	t=1.861 df=4
Number of pairs	5
How big is the difference?	
Mean of differences	0.5041
SD of differences	0.6057

Appendix : Summary of paired t-test analyses of cumulative infiltration

Table Analyzed

KNUST

SEM of differences	0.2709
95% confidence interval	-0.2480 to 1.256
R squared	0.4640
How effective was the pairing?	
Correlation coefficient (r)	0.2258
P value (one tailed)	0.3575
P value summary	ns
Was the pairing significantly effective?	No

**G11
amount for observed 20 g sand suspension vs. model predicted value**

Paired t test data

Column V	20 g Sand: Observed	vs.	Column U	20 g Sand: Simulated
----------	---------------------	-----	----------	----------------------

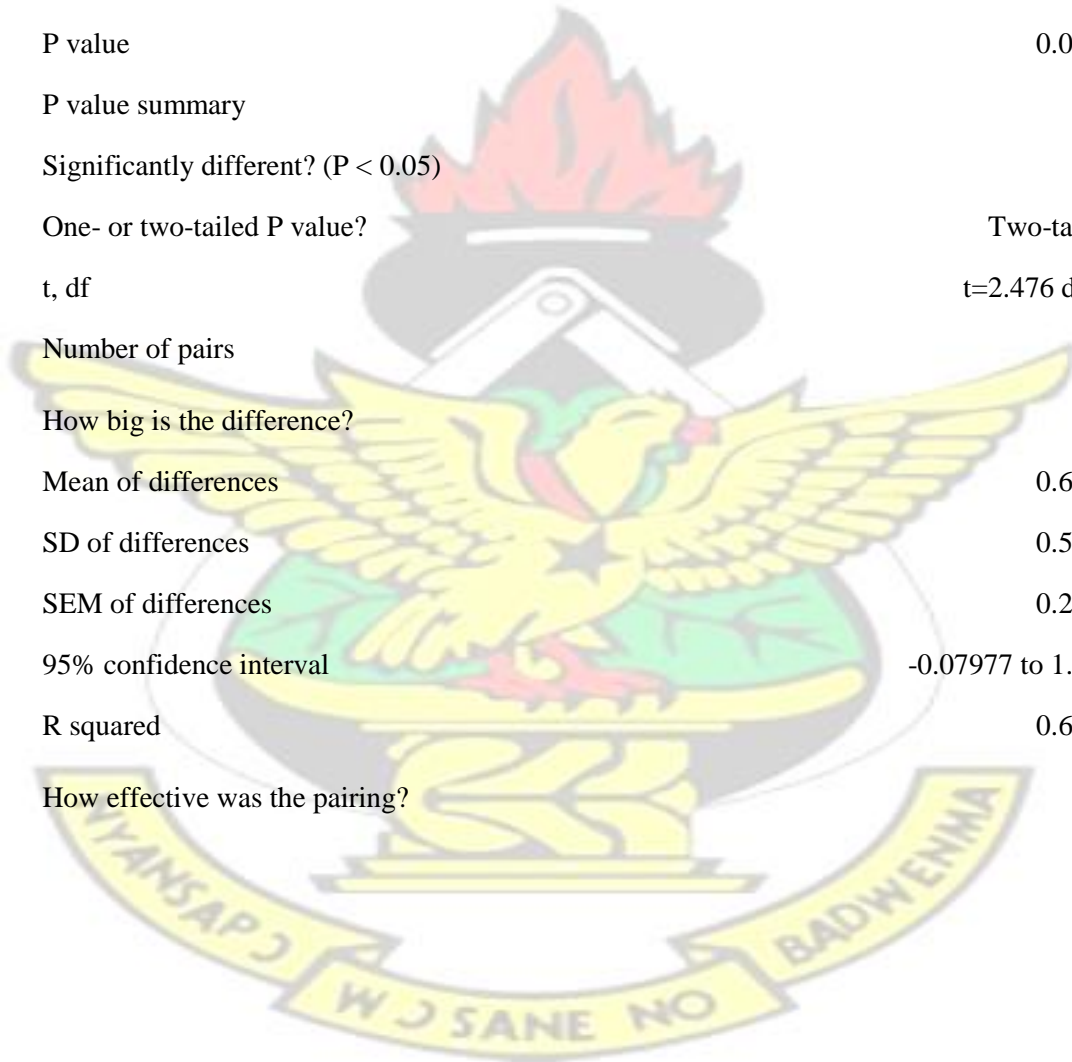
Appendix : Summary of paired t-test analyses of cumulative infiltration

Table Analyzed

KNUST

Paired t test

P value	0.0685
P value summary	Ns
Significantly different? ($P < 0.05$)	No
One- or two-tailed P value?	Two-tailed
t, df	t=2.476 df=4
Number of pairs	5
How big is the difference?	
Mean of differences	0.6570
SD of differences	0.5934
SEM of differences	0.2654
95% confidence interval	-0.07977 to 1.394
R squared	0.6051
How effective was the pairing?	



Appendix : Summary of paired t-test analyses of cumulative infiltration

Table Analyzed

KNUST

Correlation coefficient (r)	0.6433
P value (one tailed)	0.1208
P value summary	ns
Was the pairing significantly effective?	No

**G12
amount for observed 30 g sand suspension vs. model predicted value**

	Paired t test data
Column X	30 g Sand: Observed
vs.	vs.
Column W	30 g Sand: Simulated
Paired t test	
P value	0.1296
P value summary	ns
Significantly different? (P < 0.05)	No

Appendix : Summary of paired t-test analyses of cumulative infiltration

Table Analyzed

KNUST

One- or two-tailed P value?	Two-tailed
t, df	t=1.904 df=4
Number of pairs	5
How big is the difference?	
Mean of differences	0.4610
SD of differences	0.5413
SEM of differences	0.2421
95% confidence interval	-0.2111 to 1.133
R squared	0.4755
How effective was the pairing?	
Correlation coefficient (r)	0.2711
P value (one tailed)	0.3296
P value summary	ns
Was the pairing significantly effective?	No

Appendix : Summary of paired t-test analyses of cumulative infiltration

Table Analyzed

KNUST

G13 amount for observed 40 g sand suspension vs. model predicted value

	Paired t test data
Column Z	40 g Sand: Observed
vs.	vs.
Column Y	40 g Sand: Simulated
Paired t test	
P value	0.0656
P value summary	Ns
Significantly different? ($P < 0.05$)	No
One- or two-tailed P value?	Two-tailed
t, df	t=2.517 df=4
Number of pairs	5
How big is the difference?	

Appendix : Summary of paired t-test analyses of cumulative infiltration

Table Analyzed

KNUST

Mean of differences	0.3425
SD of differences	0.3044
SEM of differences	0.1361
95% confidence interval	-0.03537 to 0.7204
R squared	0.6129
How effective was the pairing?	
Correlation coefficient (r)	0.7289
P value (one tailed)	0.0812
P value summary	ns
Was the pairing significantly effective?	No

